АКАДЕМИЯ НАУК СССР
AKADEMIIA NAUK SSSR

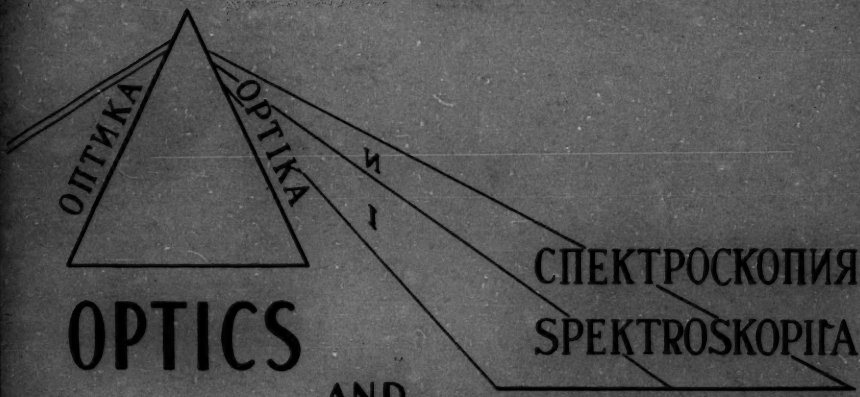

OPTICS AND SPECTROSCOPY

СПЕКТРОСКОПИЯ SPEKTROSKOPIIA

FEBRUARY 1959 - VOL. VI - NO. 2
FEVRAL' 1959 - TOM. VI - VYP. 2

Translated on the Initiative of
THE OPTICAL SOCIETY OF AMERICA, INC.
With a Grant-in-Aid from
THE NATIONAL SCIENCE FOUNDATION
by MORRIS D. FRIEDMAN, INC.

RUSSIAN EDITORIAL STAFF

Editor: S. E. FRISH

Assistant Editor: P. P. FEOFILOV

Corresponding Secretary: L. S. SAZONOV

Associate Editors:

M. M. GUREVICH M. A. EL'IASHEVICH A. A. LEBEDEV V. P. LINNIK
S. L. MANDEL'SHTAM I. V. OBREIMOV V. K. PROKOF'EV
N. N. SOBOLEV A. N. TERENIN A. I. TUDOROVSKII

Translation Editorial Staff

MORRIS D. FRIEDMAN

DR. JAMES R. ARONSON, *Massachusetts Institute of Technology,*
DR. FRED BEHNKE, *Perkin-Elmer Corp.,*
DR. RICHARD DALVEN, *Raytheon Company, Research Division,*
DR. SUMNER P. DAVIS, *University of California,*
DR. CYRUS FELDMAN, *Oak Ridge National Laboratory*
DR. JOHN S. WAUGH, *Massachusetts Institute of Technology,*
DR. ARTHUR W. WINSTON, *National Research Corp.,*

Published semi-monthly by the Optical Society of America, Inc., 121 Lincoln Avenue, Rochester, New York. Business and Editorial office: 33 University Road, Cambridge 38, Mass. Subscriptions for one year to members of the Society: Associates $13.00; Regular members and Fellows $17.00. Subscriptions for non-members of the Society: One Year U. S. and Possessions, $25.00; Foreign $28.00. Back numbers: $3.00 per copy. Lithoprinted in the USA.

Application for 2nd Class mailing privileges pending at Post Office, Boston, Mass.

АКАДЕМИЯ НАУК СССР
AKADEMIIA NAUK SSSR

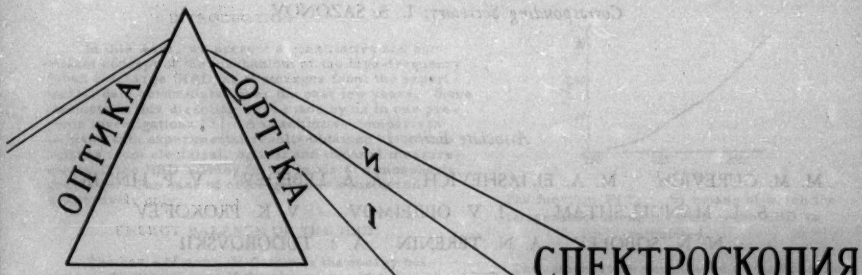

OPTICS AND SPECTROSCOPY

FEBRUARY 1959 - VOL. VI - NO. 2
FEVRAL' 1959 - TOM. VI - VYP. 2

Translated on the Initiative of
THE OPTICAL SOCIETY OF AMERICA, INC.
With a Grant-in-Aid from
THE NATIONAL SCIENCE FOUNDATION
by MORRIS D. FRIEDMAN, INC.

RUSSIAN EDITORIAL STAFF

Editor: S. E. FRISH

Assistant Editor: P. P. FEOFILOV

Corresponding Secretary: L. S. SAZONOV

Associate Editors:

M. M. GUREVICH M. A. EL'IASHEVICH A. A. LEBEDEV V. P. LINNIK
S. L. MANDEL'SHTAM I. V. OBREIMOV V. K. PROKOF'EV
N. N. SOBOLEV A. N. TERENIN A. I. TUDOROVSKII

Translation Editorial Staff

MORRIS D. FRIEDMAN

DR. JAMES R. ARONSON, *Massachusetts Institute of Technology,*
DR. FRED BEHNKE, *Perkin-Elmer Corp.,*
DR. RICHARD DALVEN, *Raytheon Company, Research Division,*
DR. SUMNER P. DAVIS, *University of California,*
DR. CYRUS FELDMAN, *Oak Ridge National Laboratory*
DR. JOHN S. WAUGH, *Massachusetts Institute of Technology,*
DR. ARTHUR W. WINSTON, *National Research Corp.,*

Published semi-monthly by the Optical Society of America, Inc., 121 Lincoln Avenue, Rochester, New York. Business and Editorial office: 33 University Road, Cambridge 38, Mass. Subscriptions for one year to members of the Society: Associates $13.00; Regular members and Fellows $17.00. Subscriptions for non-members of the Society: One Year U. S. and Possessions, $25.00; Foreign $28.00. Back numbers: $3.00 per copy. Lithoprinted in the USA.

Application for 2nd Class mailing privileges pending at Post Office, Boston, Mass.

TOM VI, Vyp. 2 OPTIKA I SPEKTROSKOPIIA Fevral', 1959
VOL. VI. No. 2 OPTICS AND SPECTROSCOPY February, 1959

The Theory of the High-Frequency Brush Discharge

R. GRIGOROVICI and G. CRISTESCU

Abstract: A quantitative model of the mechanism of the high-frequency brush discharge is developed. A comparison is made with the experimental results obtained by various authors studying the electrical, optical, and thermal characteristics of this type of discharge. Satisfactory agreement is obtained.

INTRODUCTION

In this work, we present a quantitative and consistent concept of the mechanism of the high-frequency brush discharge (HBD) as it emerges from the experimental data accumulated over the past few years. Some attempts in this direction were made by us in our previous investigations [1]. A quantitative comparison is made with experimental results obtained by various authors from electrical, optical and thermal measurements of the HBD burning freely in air at atmospheric pressure. The case of other gases is considered qualitatively only.

ENERGY BALANCE OF THE HBD

The basis of our calculation is the energy balance in the discharge. If the phenomena in the luminescent band adjacent to the localizing electrode are neglected, the discharge consists of an intensely luminescent gas, i. e., the brush discharge proper. This gas becomes ionized and glows when the charge carriers are in periodic motion.

The losses due to radiation and ambipolar diffusion may be neglected, because the temperature along the discharge axis is much lower than 7000° K. The portion of energy loss due to convection may be easily estimated. In the case of natural convection, the losses due to heating and dissociation are determined experimentally by measuring the quantity of gas rising in the discharge [2, 3]. This loss amounts to no more than a few percent of the total discharge power. In the case of forced convection, this loss may increase. This means that the only substantial loss of energy is caused by radial heat conduction. For simplicity, let us assume that the brush discharge has a cylindrical shape, which is a good approximation over most of its length. As in the case of an ordinary flame, the length and the diameter of the discharge are determined, principally, by the rising luminescent gases and only to a small degree by field distribution, i. e., by the shape of the electrodes [1c]. We will therefore use the experimentally determined dimensions of the discharge in making our calculations.

The Elenbaas-Heller differential equation will be used here with the following simpifying conditions: the brush discharge has a channel of radius R_1 in which electrical energy is transformed into heat with a constant volume power density P. At the same time, there naturally occurs a radial flow of heat. The channel is surrounded by an envelope of radius R_2, inside of which electrical energy is not transformed into heat.

As follows from [4], under these conditions the channel has the following differential equation

$$-2\lambda\frac{dT}{dr}=rP, \tag{1}$$

and the envelope

$$-2\pi\lambda r\frac{dT}{dr}=\pi R_1^2 P. \tag{2}$$

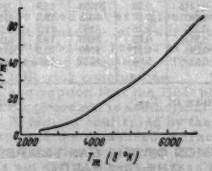

The function $F(T_m)$, by means of which the temperature along the axis of the HBD is calculated.

The temperature dependence of the heat-conductivity of air λ was obtained by generalising the calculations of F. Koppelman for H_2 and N_2 [5]. The data obtained in [6] agree sufficiently well with the results of calculations by Mannkopf [7] if the presently accepted value of the dissociation energy of O_2 molecule (5.08 ev) is substituted in the equation he used. λ may be described, then by the equation

$$\lambda=(5.00\cdot10^{-6}T^{1.4}+6.0\cdot10^{-3}\Phi_1[1.0\cdot10^{-3}(T-4000)]+ \\ +10\cdot10^{-3}\cdot\Phi_1[7.78\cdot10^{-4}(T-7600)]; \tag{3}$$

watt/cm. deg.

where Φ_1 is the Gaussian distribution function. The solution of differential equations (1) and (2) leads to equations (4) and (5), which apply to the channel and envelope, respectively:

$$2.08\cdot10^{-4}(T_m^{3.4}-T_r^{3.4})+6.00\{\Phi[1\cdot10^{-3}(T_m-4000)]- \\ -\Phi[1\cdot10^{-3}(T_r-4000)]\}+12.87\{\Phi[7.78\cdot10^{-4}(T_m-7600)- \\ -\Phi[7.78\cdot10^{-4}(T_r-7600)]\}=P\frac{r^2}{4}. \tag{4}$$

$$2.08\cdot10^{-4}(T_{R_1}^{3.4}-T_r^{3.4})+6.00\{\Phi[1\cdot10^{-3}(T_{R_1}-4000)]- \\ -\Phi[1\cdot10^{-3}(T_r-4000)]\}+12.87\{\Phi[7.78\cdot10^{-4}(T_{R_1}-7600)]- \\ -\Phi[7.78\cdot10^{-4}(T_r-7600)]\}=\frac{PR_1^2}{2}\ln\frac{r}{R_1}, \tag{5}$$

where $\Phi(x_0)=\int_0^{x_0}\Phi_1(x)\,dx$, and T_m, T_{r_1}, and T_r are the temperatures along the axis, at the boundary between the channel and envelope, and at a distance r from the channel axis, respectively. At the edge of the discharge ($r=R_2$; $T_{R_2}=T_0=300^\circ$ K) we obtain the equation

$$F(T_m)=2.08\cdot10^{-4}(T_m^{3.4}-T_0^{3.4})+6.00\{\Phi[1\cdot10^{-3}(T_m- \\ -4000)]+1\}+12.87\{\Phi[7.78\cdot10^{-4}(T_m-7600)]+1\}= \\ =\frac{PR_1^2}{2}\left(\frac{1}{2}\ln\frac{R_2}{R_1}\right), \tag{6}$$

numerical values for which are given in the Figure for various T_m

Table 1

The Calculation of the Temperature of the Gas along the Axis of the High-frequency Brush Discharge.

L (in W)	R_1 (in cm)	R_2 (in cm)	$N = 100$ mc, log $N = 8.000$				$N = 70.8$ mc, log $N = 7.850$				$N = 32.3$ mc, log $N = 7.510$				$N = 12.4$ mc, log $N = 7.094$			
			l (in cm)	P, W/cm³	$F(T_m)$	T_m, °K	l (in cm)	P, W/cm³	$F(T_m)$	T_m, °K	l (in cm)	P, W/cm³	$F(T_m)$	T_m, °K	l (in cm)	P, W/cm³	$F(T_m)$	T_m, °K
20	0.0296	0.1415	0.29	20950	18.9	4270	0.35	17900	16.3	4070	0.51	12710	11.5	3680	0.82	8110	7.32	3220
50	0.0575	0.183	0.57	7035	19.2	4290	0.68	6085	16.7	4100	1.00	4280	11.7	3720	1.62	2720	7.45	3280
75	0.0788	0.215	0.76	4180	19.5	4320	0.91	3625	16.9	4110	1.34	2540	11.8	3730	2.16	1621	8.56	3310
100	0.0976	0.2445	0.93	2950	19.9	4350	1.11	2552	17.2	4130	1.64	1797	12.1	3740	2.65	1259	8.50	3410
150	0.1313	0.298	1.27	1780	20.2	4370	1.51	15550	17.6	4160	2.22	1093	12.4	3760	3.60	769	8.74	3440
200	0.1610	0.338	1.60	1228	19.7	4330	1.90	1072	17.3	4140	2.81	756	12.2	3750	—	—	—	—
Average values of T_m						4322				4118				3732				3332

CALCULATION OF THE GAS TEMPERATURE IN THE DISCHARGE

Calculations were performed, for the values R_1 and R_2 of the radii of the channel and of the envelope resp., and for length l. These quantities were measured photographically for various HBD burning at various frequencies and various powers L, between a point and a flat counter-electrode separated by a 5 cm* gap.

The power absorbed by the HBD was measured under the same conditions. From this, the volume power density P in the channel was found, and another value of $F(T_m)$ then determined from the right-hand side of equation (6). The corresponding values of T_m are shown in the Figure. The results of the calculations are given in Table 1. With regard to these results, the following remarks are in order:

a) In the range 50 watts < L < 200 watts, T_m shows practically no dependence on power, in agreement with measurements by Khokhlov [8].

b) T_m depends on frequency. In the range $10^7 < N < 10^8$, the experimental and calculated values of T_m may be represented by the equations

$$T_m\,(\text{exp.}) = 1150 \lg N + 5050, \tag{7}$$

$$T_m\,(\text{calc.}) = 1150 \lg N + 5225 \tag{8}$$

to a sufficient degree of approximation. As seen from the equations, the temperatures calculated are higher than the measured ones by 175°. This difference is due either to the neglect of certain energy losses or to the approximations made in the calculations. In any case, it shows that the losses are underestimated.

c) The temperatures measured by Cobine and Wilbur [11] and by Mollwo [12] at 915 mc (Table 2) are much lower than the values obtained by extrapolating equation (7). This discrepancy may be explained easily if one takes into account the completely different field distribution and the variation in geometrical form (elongation and contraction of the brush, due to forced convection) used by these authors.)

*It must be emphasized that R_2 and l values are much larger in visual than in photographic observations.

Table 2

Gas Temperature T_m at the Axis of a High-frequency Brush Discharge.

N (in mc)	log N	T_m, °K Calculated	T_m, °K Observed	Method	Ref.
10.0	7.000	—	3000 ± 100	Optical (molecular bands)	[9]
12.4	7.094	3332	—	Same	
22.9	7.380	—	> 2900 **	Longitudinal rise of gas	[3]
32.3	7.510	3732	3610 ± 20***	Optical (molecular bands)	[10]
62.5	7.796	—	3850 ± 100	Same	[1]
70.8	7.849	4118	—	"	
84.5	7.927	—	4100 ± 100	"	[1]
100	8.000	4322	—	"	
915	8.962	6080 *	> 3000 ****	Transverse rise of gas	[11]
915	8.962	6080 *	3800	Optical (molecular bands)	[12]

* Extrapolated using eq. (7)

** Friction was neglected in the calculation of the lower limit.

*** The value of T_m, averaged over 20 measurements with a probable error of ± 20° K. Khokhlov has shown [10], that this temperature is (3450 ± 175)° K. Using this temperature we drew the straight line $T_m = f(\log N)$, (Fig. 3 in [1]), which does not conform with the straight line of eq. (7).

**** This lower limit corresponds to the average temperature of the gas.

THE CALCULATION OF THE CURRENT VS. POWER CHARACTERISTICS

The current vs. power characteristics i = f(L) for the HBD may be calculated by assuming that thermal ionization alone supplies the necessary number of current carriers. In agreement with [1, b, c], there exists the following relationship between the power L, the effective voltage |V|, the effective current |I| flowing through the discharge, and the current i measured by the photoammeter,

$$L = i\,|V| = \frac{|I|}{\sqrt{2}}\,|V|.$$

The discharge current is almost completely dependent on the channel electrons and has the effective value

$$|I| = 2\pi e \int_0^{R_1} nb\,|E|\,r\,dr,$$

where ε is the value of the elemental charge, n is the density and b the mobility of the electrons, and $|E|$ is the effective value of the longitudinal electric field intensity, which is constant over its cross-section. n is determined from Saha's equation, b is assumed to be inversely proportional to the gas density, and $|E|$ is approximately expressed by the average intensity of the longitudinal field

$|E| = \frac{|V| - 280}{d}$, where d is the electrode separation, and 280 V is the voltage drop at the localizing (pointed) electrode of the discharge.

With the aid of these assumptions, we readily obtain the equation

$$(9)\quad \beta = \frac{4.34 \cdot 10^{-2} \varkappa}{\sqrt{2}} \cdot \frac{\varepsilon b_0 \Lambda}{p^{3/2}} \sqrt{\frac{E_i}{g_m}} \frac{L'}{d} \int_0^{R_1} \frac{r^{1.85}}{T_r} e^{-\frac{eV_i}{kT_r}} r\,dr = A_0 \frac{L'}{d} \int_0^{R_1} \psi(r)\,dr,$$

where $b_0 = 2.4\ 10^7 \frac{cm}{sec} / \frac{v}{cm}$ is the mobility of the electrons in air at p = 1 mm Hg and T = 300° K, $\Lambda = 2.865\ 10^{19}\ cm^{-3}$ is the Loschmidt number, p is the pressure (in mm Hg), g_i and g_m are the degrees of degeneracy of the ions and the neutral molecules, respectively, V_i is the ionization potential, and $L' = L\frac{|V| - 280}{|V|}$ is the power delivered exclusively by the brush discharge.

If Saha's equation is applied to a mixture of 21% 0_2 and 79% N_2 at 7000°K, almost all the ionization is due to oxygen, [6] and the effective ionization potential of the mixture is given by the equation

$$V_i = V_{i0_2} - \frac{kT}{\varepsilon} \ln 0.21 = \left[12.5 + 1.343 \cdot 10^{-4}\, T\right] V.$$

On the other hand, the ground state of the 0_2 molecule is [3] $\sum (g_m = 3)$, and that of the 0_2^+ ion, $^2\pi\ (g_i = 2)$. It follows from all of this that $A_0 = 3.88 \cdot 10^2$ amp/V cm deg$^{3/4}$. The value of integral (9) was obtained graphically, while T_r was determined from (4). The values of the current calculated from (9) may be compared to the values measured by us and given in [1, c]. As before, d = 5 cm, the localizing electrode is pointed and the counter-electrode is flat. The results of the calculations are given in Table 3.

Table 3

Comparison of the Calculated and Observed Current vs. Power Characteristics.

N (in mc)	T_m (in K)	V_i (in V)	L (in W)	i (in ma) calculated	i (in ma) measured	$f = \frac{i^2(\text{calc.})}{i^2(\text{meas.})}$
100	4125	13.04	50	27.5	31	0.79
			100	58	64	0.83
			150	84	102	0.85
			200	131	144	0.83
70.6	3975	13.01	50	21	26	0.68
			100	44	53	0.69
			150	70	83	0.71
			200	96	120	0.64
32.3	3600	12.98	50	9.2	19	0.23
			100	20	41	0.24
			150	31	65	0.23
			200	43	95	0.20
12.4	3100	12.91	50	1.56	14.5	0.011
			100	3.25	31.0	0.011
			150	5.15	48.5	0.011

All calculated values turned out to be smaller than the measured ones. In accordance with (9), the deficiency of charge carriers f is equal to the square of the ratio of the calculated current to the measured current. In the case of the maximum frequency the deficiency amounted to only 17%. Due to many simplifying assumptions in our calculations, we cannot claim great accuracy, and consequently cannot attach real significance to this difference.

It must be noted that at a given frequency the value of f is not a function of power in the range $50 < L < 200$ watts, but decreases at an accelerating rate with decreasing frequency. This decrease leads to the following conclusions:

a) The assumption that the HBD plasma in air at atmospheric pressure is isothermal at frequencies higher than 70 Mc, is confirmed by the agreement of the calculated and the measured characteristic curves.

b) At frequencies lower than 30 Mc, thermal ionization is not sufficient in any case to explain the electrical conductivity values obtained in the plasma.

These conclusions are in complete agreement with the numerous electrical and optical phenomena observed by other investigators and by us in the HBD, and conform with the statements made by us in our previous works.

ANISOTHERMY OF THE PLASMA OF THE HIGH-FREQUENCY BRUSH DISCHARGE

If n is the density of the electron gas in the plasma at temperature T_e, the number of collisions between electrons and gas molecules per unit volume per unit time is given by the equation

$$(10)\qquad \nu = \frac{2\pi}{\lambda} \sqrt{\frac{2kT_e}{\pi m}} = \frac{2\pi}{\lambda_0 p} \sqrt{\frac{2kT_e}{\pi m}};$$

the power transferred to a unit volume by the electrons being

$$(11)\qquad P = \frac{3}{2} kT_e \nu \cdot n.$$

In these equations λ_0 is a constant independent of the temperature (for air at atmospheric pressure, $\lambda_0 = 1.26 \cdot 10^{-7}$ cm/deg.) and $\varkappa$ is the fraction of an electron's energy transferred to an air molecule in a single collision. In air, when $T_e = 4000°K$ and $T = 300°K$, $\varkappa = 0.013$ [13]; as T increases, the value of $\varkappa$ should increase noticeably, due to the excitation of the vibrational levels of the N_2 and 0_2 molecules.

The value of $\varkappa$ may be estimated at a gas temperature of approximately 4000° K if it is assumed that thermal equilibrium exists in the HBD plasma at 100 Mc and 200 watts. Then $T_e = T$, $P = 1228$ watts cm^{-3}, as seen from the Table 1, and the value of the electron density may be obtained from Saha's equation. From (10) and (11) we obtain $\varkappa = 0.089$, which is reasonable.

Since $\varkappa$ increases with increasing T_e and T, and since T and T_e vary in different directions, with varying frequency, let us assume that $\varkappa$ is a constant. From Eq. (10) and (11), it then follows that

$$(12)\qquad T_e^{3/2} = 1 \cdot 10^{-2} \frac{PT}{\varkappa \cdot n}.$$

The actual electron density n may be determined by calculating the electron density at thermal equilibrium n' from Saha's equation, and dividing it by the ionization deficiency f taken from Table 3. The value of P is taken from Table 1. The results of calculations made by using (12) are given in Table 4 . Obviously, the temperature in question here is an average electron temperature, which is probably higher at the lower portion of the discharge; i. e., at the localizing electrode.

Table 4

The Electron Temperature T_e in the High-frequency Brush Discharge (in°K)

L (in W)	N=100 mc T_m=4125°K	N=70.6 mc T_m=3975°K	N=32.3 mc T_m=3600°K	N=12.4 mc T_m=3100°K
200	4400	5370	8290	—
150	5830	6880	10600	10800
100	7880	9560	14800	16100
75	9670	12000	18600	18300
50	13200	16500	26200	25500
20	28000	33400	36700	36800

Unfortunately, data on electron temperatures are too scarce and inaccurate to permit a quantitative comparison of calculated and experimental values. Thus, improbably high values of T_e (from 7.8 to 13.4 10^4° K), measured by means of Langmuir probes by Cobine and Wilbur [11], were not confirmed under identical experimental conditions by Mollwo, [12] who showed that the probe greatly distorts the high-frequency field. Mollwo, therefore, determined the average temperature of the noise, and found that at 915 Mc, the temperature of a brush discharge is 9050° K in air and 8050° K in nitrogen while the temperature of the air itself is only 3800° K. Since the noise is caused not only by thermal fluctuations but also by fluctuations of the electron concentration, which are of the same order of magnitude as the thermal fluctuations, Mollwo concludes that the electron temperature is much lower than the noise temperature and that "the existence of thermal equilibrium is very probable". These results conform especially well with the point of departure of our calculations.

The optical behavior of the HBD qualitatively confirms the results of our calculations. In fact, while at high frequencies the brush discharge spectrum changes little over a wide range of power values, the dependence on power becomes significant as the latter is decreased to a certain limiting value, which becomes smaller as the frequency is reduced [1d] : at low power levels, in the channel of a brush discharge in air, there appear difficultly excitable bands (excitation potential = 11.0 V) which correspond to the second positive group of nitrogen. The appearence of these bands distinguishes the channel from the other portion of the discharge and allows one to observe the variation of its color. This is easily explained under the existing conditions (low power levels and frequency) by the fact that the electron temperature is much higher than the gas temperature as seen from Table 4, that is, by the fact that plasma becomes very anisothermal. Thus, Popov and Stolov [14] noticed the bands of the second positive group of N_2 in the channel of the HBD in air at 760 mm Hg and N = 10 Mc, while Khokhlov, [8] under identical experimental conditions except for frequency (which was 32.4 Mc) did not notice these bands until he changed the pressure to 350 mm Hg [10]. This fact, along with others, means that the anisothermy of the plasma increased as the pressure is reduced.

THE HIGH-FREQUENCY BRUSH DISCHARGE IN OTHER GASES

The discharge in molecular gases of low thermal conductivity (N_2, O_2, CO_2), behaves in the same way as in air: the energy received by the electrons from the electric field is transferred to the gases mainly through excitation of the molecular vibrations; χ in Eq. (12) is relatively large, and at atmospheric pressure the electron temperature cannot exceed the temperature of the gas by much. Therefore, the plasma is not in these gases, and is almost in a state of thermal equilibrium.

Similar conditions of energy transfer from the field to the gas exist in molecular gases of high thermal conductivity (H_2 and illuminating gas). The attainment of high temperatures in these gases is difficult because of their high thermal conductivity; electrons cannot act as ionizers, since their average energy cannot exceed the energy of the gas. For this reason, Cobine and Wilbur [11] found it very difficult to sustain the HBD in illuminating gas and could not sustain it at all in H_2.

The inert gases are poor conductors of heat and the transfer of energy from the field to them by means of electrons is made difficult by the fact that there is an absence of easily excited molecular vibrations. χ in Eq. (12) is therefore small, the electron temperature may exceed the temperature of the gas considerably, and the plasma produced will be strongly anisothermal. Thus, according to the data of Cobine and Wilbur [11], the HBD remains "cold", i. e. has a low gas temperature in the pure inert gases (He, Ar) temperature. However, little power is absorbed by the discharge because heat losses are low, and there are no losses in the form of energy dissociation, a fact pointed out by these authors. If as little as 0.3% H_2 is added to the He, it is possible to sustain "hot" discharges, in the spectra of which all He lines disappear, and the discharge emits the spectrum of the impurity only.

CONCLUSION

In our opinion, this paper brings to an end almost all apparent contradictions between experimental results and their different interpretations by various authors, attributing these contradictions solely to differences in experimental conditions. At the same time, it puts the HBD on a quantitative basis for the first time, which may prove to be valuable in the practical application of this discharge.

K. N. Parkhon
University Bucharest October 6, 1958

References

1. G. CRISTESCU, R. GRIGOROVICI: a) Bull. Soc. Roum. Phys., 42, 37 (1941); b) Anal. Acad. R. P. R., Mem., 3 (1949); c) Bul. St. Acad. R.P.R., 4, 419 (1952); d) Comunic. Acad. R.P.R. 5, 515 (1955); e) Revue de Phys., 1, 103 (1956)
2. E. BADAREU, M. GIURGEA, G. GIURGEA: A. T. H. TRUTIA: Colloquium Spectroscopicum Internat., 6, 441, 1956, Amsterdam
3. V. TRUNECEK: Spisy prir. fak. Masarykovy Univ. Brno, No. 384, 1957
4. W. ELENBAAS: Physica, 1, 211 (1934)
5. A. V. ENGEL, M. STEENBECK: Elektrische Gasentladungen, II, 146, Berlin, 1934
6. R. GRIGOROVICI, G. CRISTESCU: Revue de Phys. (In press)
7. R. MANNKOPFF: Z. Phys., 120, 228 (1943)
8. M. Z. KHOKHLOV: Cand. Dissert., Moscow 1954
9. L. V. POPOV, A. L. STOLOV: Uch. Zap. Kazansk. Univ., 113, No. 9, 81 (1953)
10. M. Z. KHOKHLOV: ZETF, 29, 645 (1955) (See Sov. Phys. JETP)
11. J. D. COBINE, D. A. WILBUR: J. Appl. Phys., 22, 835 (1951)
12. L. MOLLWO: Physiker-Tagung, Wiesbaden, 1955
13. L. H. G. HUXLEY, A. A. ZAAZOU: Proc. Roy. Soc. A196, 402 (1949)
14. L. V. POPOV, A. L. STOLOV: Uch. Zap. Kazansk. Univ., 113, No. 9, 53 (1953)

TOM VI, Vyp. 2 OPTIKA I SPEKTROSKOPIIA Fevral' 1959
VOL. VI. No. 2 OPTICS AND SPECTROSCOPY February, 1959

On the Question of the Nature of the Infrared Emission Band Displacement in Flame Spectra

R. B. TAGIROV

Introduction

Paschen [1] noted that the maximum of the intensity of the $\nu_3 = 2349.3\ cm^{-1}$ band of the $C0_2$ molecule has a "red" shift in the infrared emission spectrum of a Bunsen burner flame as compated to its location in the absorption spectrum of atmospheric carbon dioxide. An analogous "red" shift was detected by Julius [2] in the case of the HCl band in the flame spectrum of $H_2 + Cl_2$, the CS_2 and SO_2 bands in the flame spectrum of $CS_2 + 0_2$, etc.

According to Kondrat'ev [3] for the HCl band and, according to Guidon [4] for the CO_2 band, the fundamental reason for such a "red" shift in the flame spectra is the nonequilibrium excitation of the high vibrational levels of the ground electronic state related to the liberation of the reaction energy. Actually, there are statements in [5, 6] on the partial chemical excitation of the CO_2 molecule in a CO flame. On the basis of the statements of Garner and Johnson [7] on the absence of a ground band of the CO_2 molecule $\nu_2 = 667\ cm^{-1}$ in the emission flame spectrum, Gaydon concluded that the excitation of CO_2 in a CO flame is principally chemical in nature.

However, the ground band of the CO_2 molecule $\nu_2 = 667\ cm^{-1}$ was detected both in the infrared spectrum of an electric discharge in CO_2 [8] and in the flame spectrum of $CO + 0_2$ also [9]. Moreover, the temperature of the $CO + 0_2$ flame, measured by means of infrared radiation under the assumption that the radiation is equilibrium, is in good agreement with results existing in the literature [10].

An attempt is made herein to explain the nature of the excitation of the CO_2 molecules in a diffusion flame of CO in oxygen and the reason for the band shift in the emission infrared spectra in comparison with its position in absorption spectra.

1. INFRARED EMISSION SPECTRUM OF A DIFFUSION FLAME OF CO IN O_2

The infrared emission spectrum of a diffusion flame of CO in 0_2 was obtained on the IKS-11 infrared spectrometer for which the loss in the light energy passing through the input slit was made a minimum [11] and a spherical mirror was placed behind the flame at a distance equal to the radius of curvature in order to amplify the radiation intensity. The carbon monoxide was obtained by the reaction between formic and sulfuric acids and was stored in a gasometer over water prior to burning. The gas was then burned without preliminary drying.

The spectral curves obtained without corrections for atmospheric absorption are presented for the 6000-400 cm^{-1} frequency range on Figure 1. Part of the bands shown on Figure 1 was observed by other authors also.

It is seen on figure 1 that the infrared emission spectra of the diffusion flame of $CO + 0_2$ are abundant in bands and lines. A comparison with known results shows that the intensity maximums of certain CO_2 bands are displaced in comparison with their position in the absorption spectrum at room temperature either toward the 'red' or the 'violet'. The intensity maximum of the CO band in emission is displaced toward the shortwavelength relative to absorption (fig. 2).

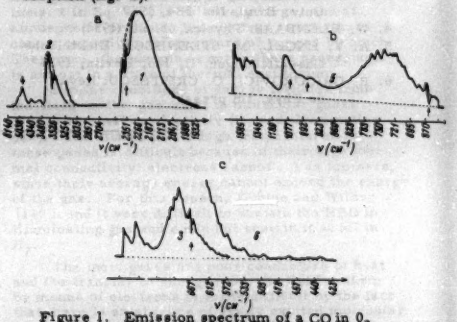

Figure 1. Emission spectrum of a CO in 0_2 diffusion flame. a - LiF prism; b - NaCl prism; c - KBr prism. Slit width Δ (in mm):

2. NATURE OF EXCITATION OF THE CO_2 MOLECULE IN A CO IN O_2 DIFFUSION FLAME

In explaining the nature of the excitation of a CO_2 molecule in a diffusion CO in 0_2 flame, we started from the known and undoubted fact that the excitation of H_20 molecules in hydrogen-oxygen flames is of thermal character [4]. It seems to us that the nature of CO_2 excitation can be established by measuring the dependence of infrared emission on temperature and other parameters for the H_20 and CO_2 molecules, respectively, in diffusion flames of H_2 and CO in 0_2, without relying on direct measurements of the absorption and emission capabilities of flames.

Let us consider how the intensity of the $C0_2$ bands changes in the spectrum of a diffusion CO flame and of the H_20 bands in the spectrum of a diffusion H_2 flame when the air is replaced by oxygen.

The diffusion CO and H_2 flames have a temperature of approximately 2100° K in air and of the order of 3000° K in oxygen. A rise in the flame temperature should lead to an increase in the

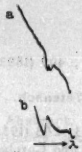

Figure 2
$2\nu_0$ band of the CO molecule in absorption spectra of the cold gas (a) and CO in O_2 flame emission (b).

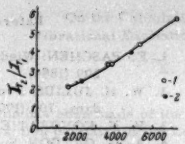

Figure 3
Frequency dependence of the ratio of the band intensities of H_2O and CO_2 molecules at different temperatures T_1 and T_2 in emission spectra of H_2 and CO flames.

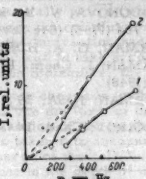

Figure 4
Dependence on pressure of the band intensities of CO_2 (1) and H_2O (2) in the emission spectra of rarefied CO and H_2 in O_2 flames.

population of the higher energy levels and, therefore, the frequency dependence of the ratio of the intensities of the appropriate bands for temperatures of 3000 and 2100° K should be exponential for a thermal nature of the excitation. In the presence of chemiluminescence, the point corresponding to the ratio of the intensities of the band $\nu_3 = 2349.3\ cm^{-1}$ in CO flame spectra, is not plotted on this curve. Presented on figure 3 is an experimental curve of the dependences of the ratio of the intensities of the H_2O band in the H_2 flame spectrum and the CO_2 band in the CO flame spectrum. It is seen from figure 3 that these curves are not only similar for the H_2O and CO_2 molecules but are even superposed within the limits of measurement accuracy. Therefore, the participation of chemiluminescence, if it exists, in the emission of a diffusion CO flame is negligibly slight.

Furthermore, let us analyze how a reduction in the pressure influences the emission intensity of H_2 and CO flames in O_2. Garner and Hall [5] state that if the pressure-emission energy curve intersects the coordinate axis but not at the origin, it indicates the partial chemiluminescent nature of the emission. The experimental curves of pressure versus emission intensity of the fundamental frequencies for the H_2O and CO_2 molecules, respectively, in the H_2 and CO diffusion flames in O_2 are presented in figure 4. As is seen from figure 4, the curves for pressures close to atmospheric are in agreement with a line passing through the origin. They deviate from the line for lower pressures and would intersect the pressure axis at 150 - 200 mm Hg if continued further. Therefore, chemiluminescence starts to play a significant part in diffusion flames only at low pressures, where it also occurs for water molecules in an H_2 flame in O_2.

Measurements were also made of the temperature and emission intensity of H_2O and CO_2 when the air surrounding the burning gas was enriched by oxygen. The complete analogy of the curves for both flames holds in this case also.

The experimental results presented show that the excitation of the CO_2 molecules in flames of moist CO in O_2 or in air is of a thermal nature.

3. NATURE OF THE BAND DISPLACEMENT IN EMISSION SPECTRA

We have established in the preceding paragraphs that 'red' and 'violet' displacements of the CO_2 band are observed in the emission spectra of a CO in O_2 flame; excitation of the latter is of a thermal nature. The CO molecule band has a 'violet' displacement.

The basic reason for the displacement is apparently the asymmetry of the band and the formation of band heads. As an example, let us analyze the absorption band $\nu_3 = 2349.3\ cm^{-1}$ of the CO_2 molecule. In studying the absorption spectra of atmospheric carbon dioxide, it is difficult to draw a conclusion on the formation of band heads on one of the branches although the asymmetry is expressed sufficiently clearly (fig. 5a). An increase in the CO_2 concentration in the chamber of the apparatus permits the formation of a band head from the shortwave side of the band to be established and it is seen that the band as a whole is displaced toward the longer wavelengths (fig. 5b).

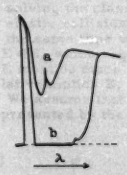

Fig. 5. Absorption band $\nu_3 = 2349.3\ cm^{-1}$ of the CO_2 molecule for low (a) and high (b) concentrations

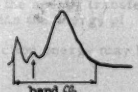

Fig. 6. Emission band of CO_2 at T = 230° C. The arrow points to the Co_2 absorption band $\nu_3 = 2349.3\ cm^{-1}$.

At high temperatures, the intensity maximum of the branches of the band under consideration is displaced because of excitation of the higher rotational levels which (because of the formation of a head on one of the branches) leads to a displacement of the intensity maximum in the opposite direction. This is seen from figure 6 where the emission band

ν_3 = 2349.3 cm^{-1} of CO_2 is presented for a 230 - 250° C temperature. It is not suitable to speak of any kind of part for chemiluminescence in this case. Moreover, higher vibrational levels, the transitions between which can only lead to a 'red' displacement, should be excited at the temperature of hot flames.

In addition to the reasons presented, the displacement of the CO_2 emission band ν_3 = 2349.3 cm^{-1} in the flame spectrum of CO and hydrocarbons depends on the superposition of the sufficiently intense CO band ν= 2142 cm^{-1} whose branches extend from 1900 to 2250 cm^{-1}. The 'violet' displacement of the CO emission band depends, in our opinion, on the asymmetry and temperature broadening of the band.

In conclusion, the author is grateful to V.N. Kondrat'ev and V. V. Voevodskii for discussions.

April 19, 1957

References

1. F. PASCHEN: Wied. Ann., 50, 409 (1893); 52, 209 (1894)
2. W. H. JULIUS: Proc. Akad. Wetensch., Amsterdam, 706 (1907)
3. V. N. KONDRAT'EV: ZETF, 3, 265 (1933)
4. A. G. GAYDON: Spectroscopy and Combustion Theory, London, Chapman-Hall, 1942 (IL, Moscow, 1950)
5. W. E. GARNER, D. A. HALL: J. Chem. Soc., 2037 (1930)
6. R. T. HASLAM, W. G. LOVELL, R. D. HUNNEMAN: Ind. Eng. Chem. Anal., 17, 272 (1925)
7. W. E. GARNER, C. H. JOHNSON: Phil. Mag., Ser. 7, A3, 97 (1927)
8. N. IA. DODONOVA, V. V. SOBOLEV: ZETF, 28, 764 (1955) (See Sov. Phys. JETP)
9. S. SILVERMAN, G. A. HORNBECK, R. C. HERMAN: J. Chem. Phys., 16, No. 2, 155 (1948)
10. S. SILVERMAN: JOSA, 39, 275 (1949)
11. R. B. TAGIROV: Cand. Dissert., Kazan Univ. 1957

TOM VI, Vyp. 2 OPTIKA I SPEKTROSKOPIIA Fevral', 1959
VOL. VI. No. 2 OPTICS AND SPECTROSCOPY February, 1959

On the Calculation of the Probability for Vibrational Excitation of Molecules during Collisions

E. E. NIKITIN

Abstract: A calculation has been made of the cross-section for vibrational excitation in molecular collisions, using an interaction potential of the Lennard-Jones type. A qualitative comparison is made of the dependence of the cross section on the depth of the potential well, describing the attraction betweeen molecules, with experimental results from ultrasonic dispersion and the attenuation of fluorescence.

A calculation of the probability of vibrational excitation of molecules during collisions has been carried out in references [1] and [2] for a one-dimensional model and in reference [3] for the three-dimensional case. It was assumed that the intermolecular interaction at short separations increases exponentially with r (where r is the separation between the colliding molecules). In order to define the interaction radius of the exchange forces a^{-1} and to take account of the attraction between molecules, the constants in the potential Ae^{-ar} are chosen in such a way as to correctly reproduce the form of the Lennard-Jones potential in the region of the turning point; moreover the attraction is taken into account simply by increasing the energy of the colliding particles by an amount ε equal to the depth of the potential well. Hence it is to be expected that even with a solution of the three-dimensional problem, the calculated and experimental transition probabilities will agree only in order of magnitude, since the constants of the Lennard-Jones potential are determined from the phenomena of diffusion and heat conductivity. Nevertheless a qualitative dependence of the transition probability on the transferred energy, the masses of the molecules, the interaction radius of the forces, and the depth of the potential well can be given by such a calculation.

In the present work time-dependent perturbation theory is used to calculate the cross-section for inelastic collisions between diatomic molecules producing vibrational excitation. It is assumed that the energy of the intermolecular intersection will be given by a Lennard-Jones potential and that neglect of the angular dependence of the interaction does not change the order of magnitude of the cross section [3]. This calculation is of interest, in part, because the minimum of the potential well for the interaction used lies rather close to the region of the classical turning-point, rather than at infinity as in reference [3].

The complete Hamiltonian for two colliding molecules A and B, averaged over the electronic wave functions, may be written

$$H = H_A + H_B + H_{AB}$$

where H_A and H_B are the Hamiltonians for the vibrational and rotational motions of the molecules A and B. The energy of interaction W depends on the relative separation $r=r_{AB}$ and on the vibrational coordinates q_A and q_B. We assume, as in reference [2] that the interaction energy does not depend on the relative orientation of the molecules. If the molecular collisions cause transitions only between the lowest vibrational levels, where the amplitude of vibration is small in comparison to the interaction radius of the exchange forces [1], then $W(q_A, q_B, r)$ can be expanded in a series in powers of $q-q_{equ.} = \Delta q$, retaining only the linear term. Then the term linear in Δq can be considered to be a perturbation connecting the Hamiltonians H_A and H_B with the Hamiltonian describing the elastic collision of molecules A and B. Insofar as the majority of the molecules satisfy the conditions for quasi-classical motion, in the region which makes the most important contribution to the inelastic scattering cross section [3], we can treat the vibrational transition probabilities according to time-dependent perturbation theory and consider the molecules to move along definite trajectories.

We assume further that vibrations are excited in only one molecule A, whose vibrational coordinate is $q_A = q$.

In first-order perturbation theory the probability for a transition from the vibrational level n to the level m is given by the formula

$$P_{nm} = \left| \Delta q_{nm} \frac{1}{\hbar} \int_{-\infty}^{\infty} \frac{\partial W(q_{equ}, r)}{\partial q} e^{i\omega_{nm} t} dt \right|^2, \quad (1)$$

in which the time-dependence of r is determined by solving the classical equations of motion for an elastic collision between molecules A and B. At the same time we must satisfy the condition $\Delta E \ll E$, which requires that the energy transfer ΔE must be much smaller than the energy of relative motion E.

We assume that the interaction energy may be represented by the function

$$W(q, r) = 4\varepsilon \left[\left(\frac{r_0}{r} \right)^{2n} - \left(\frac{r_0}{r} \right)^{n} \right], \quad (2)$$

in which r_0 is the Van der Waals collision radius of the molecules and ε is the depth of the potential well. Since the chief contribution to the integral in equation [1] comes from the region near the turning point, we can use simply the first term from equation [2] in differentiating W; i.e.,

$$P_{nm} = \left| \Delta q_{nm} \frac{2n}{r_0} \right|^2 \left| \frac{1}{\hbar} \int_{-\infty}^{\infty} 4\varepsilon \left(\frac{r_0}{r} \right)^{2n} \exp(i\omega t)\, dt \right|^2. \quad (3)$$

To compute this integral we make use of the method of reference [1]. Integration along the real axis is replaced by integration along a

contour l, which extends from $+i\infty$, encircles the singular point of the integrand, and from this point follows a cut in the plane of the complex variable t. In our case the singular point t_1 is determined by the equation $r(t_1)=0$. The dependence of r on t is given by the classical integral of motion

$$t=\int_{r_1}^{r}\frac{dr}{v\sqrt{1-\frac{\rho^2}{r^2}-\frac{4\varepsilon}{E}\left[\left(\frac{r_0}{r}\right)^{2n}-\left(\frac{r_0}{r}\right)^{n}\right]}}. \tag{4}$$

In this expression v is the relative velocity at infinity of the colliding molecules, ρ is the collision parameter, and the lower limit is taken at the turning point. [A different choice for the lower limit would merely change an unessential phase factor in the integral of equation (1)].

As $r\to 0$, equation(4) maybe written in the form

$$t=it-\frac{i}{v}\int_0^r\sqrt{\frac{E}{4\varepsilon}\left(\frac{r}{r_0}\right)^n}\,dr=it-i\sqrt{\frac{E}{4\varepsilon}\left(\frac{r}{r_0}\right)^{n+1}}\frac{r_0}{(n+1)v}, \tag{5}$$

where τ is the collision time and is defined by the integral

$$\tau=\int_0^{t_1}\frac{dr}{v\sqrt{\frac{4\varepsilon}{E}\left[\left(\frac{r_0}{r}\right)^{2n}-\left(\frac{r_0}{r}\right)^{n}\right]+\frac{\rho^2}{r^2}-1}}. \tag{6}$$

From equation (5), when $r\to 0$, we find

$$\left(\frac{r}{r_0}\right)=\left[\frac{(t-is)v(n+1)}{ir_0}\sqrt{\frac{4\varepsilon}{E}}\right]^{2/(n+1)}. \tag{7}$$

During the integration along the imaginary axis from $i\tau$ to $i\infty$ the integrand $\left(\frac{r_0}{r}\right)^{2n}$ varies substantially only over an interval $\sim\tau$, whereas the exponential function varies over the interval $\sim\frac{1}{\omega}$. Since we are considering only the case of nearly adiabatic collisions, we have $\omega\tau\gg 1$ (for inelastic collisions this requirement is usually satisfied). Hence over the whole path of integration along the contour l we can use equation (7) for $\left(\frac{r}{r_0}\right)$. Carrying out the integration, and remembering that

$$\int_l(t-is)^{-\alpha}e^{i\omega t}dt=\frac{2\pi(i\omega)^{\alpha}}{\Gamma(\alpha)}e^{-\omega s},$$

we find

$$P_{nm}=\left|\Delta\varphi_{nm}\frac{2n}{r_0}\right|^2\left(\frac{2\pi\omega Er_0^2}{4\varepsilon v^2(n+1)^2}e^{-\omega s}\right)^2. \tag{8}$$

Here and henceforth we are considering 2n for all practical purposes to be almost always considerably larger than 1; and moreover that the quantity $\left(\frac{4\varepsilon}{E}\right)^{\frac{1}{2n}}$ is approximately equal to 1. (The quantities $\frac{4\varepsilon}{E}$ and E usually differ by less than an order of magnitude).

The inelastic scattering cross section σ_{nm} equals the scattering probability P_{nm} integrated over all collision parameters, i.e.,

$$\sigma_{nm}=2\pi\int_0^{\infty}P_{nm}\rho d\rho. \tag{9}$$

In order to compute the collision time τ from formula (6) we notice that if $\rho\ll r_0$, i.e., under the conditions that the turning-point is determined by the potential W (r) rather than by a centrifugal potential, then the quantity $\frac{\rho^2}{r^2}$ may be replaced by $\frac{\rho^2}{r_0^2}$, since the latter quantity varies much more slowly than W (r). Hence we find

$$\tau\approx\frac{r_0}{vn\sqrt{1-\frac{\rho^2}{r_0^2}}}\left[\frac{\pi}{2}-\operatorname{arc\,tg}\sqrt{\frac{\varepsilon}{E\left(1-\frac{\rho^2}{r_0^2}\right)}}\right],\ \frac{\rho}{r_0}\ll 1. \tag{10}$$

The approximation of formula (10) is not valid for $\rho\approx r_0$. A more exact calculation shows that for $\rho\approx r_0$ τ increases rapidly to the asymptotic value $\frac{\rho}{v}$, characteristic of free flight. Formula 10 gives $\tau\approx\frac{r_0}{v}\sqrt{\frac{2\varepsilon}{E}}$ for $E\ll\varepsilon$ that is, a quantity independent of the collision parameter. For the opposite case $\varepsilon\gg E$ we find

$$\tau\approx\frac{r_0}{vn\sqrt{1-\frac{\rho^2}{r_0^2}}}\left[\frac{\pi}{2}-\sqrt{\frac{\varepsilon}{E}}\cdot\frac{1}{\sqrt{1-\frac{\rho^2}{r_0^2}}}\right] \tag{11}$$

Since P_{nm} decreases rapidly with increasing τ, the integral in equation (9) can be taken between the limits 0 to r_0 and we can use the approximation of equation (11).° This calculation gives

$$\sigma_{nm}=\pi r_0^2\left|\Delta\varphi_{nm}\frac{2n}{r_0}\right|^2\frac{v\pi^2}{\omega r_0\pi}\left(\frac{\mu\omega r_0^3}{\hbar(n+1)^2}\right)^3\exp\left[-\frac{\omega r_0\pi}{nv}\left(1-\frac{2}{\pi}\sqrt{\frac{\varepsilon}{E}}\right)\right]. \tag{12}$$

In this expression v is the velocity of the colliding molecules at infinity. In our computation this quantity is defined with an accuracy given by a small amount Δv, related to the energy change ΔE. The condition that $\Delta E\ll E$ guarantees the fulfillment of the inequality $\Delta v\ll v$. However, a small error in the determination of the velocity may strongly influence σ_{nm} since, as we have assumed, the exponent in the exponential is considerably larger than 1. An exact quantum mechanical calculation of σ_{nm} would lead to an expression in which it is obvious that both the initial and final velocities would appear. When the condition $\Delta E\ll E$ is fulfilled, the quantum mechanical expression for σ_{nm} would approach the classical expression and the quantity v would appear as a function of the initial and the final velocities, i.e., $v=f(v_i, v_f)$. The function f must by symmetric in both arguments, as required by the principle of detailed balancing. Moreover it must satisfy the obvious requirement $f(v_i, v_f)=v_i$. To an accuracy given by the linear term in ΔE, these two requirements are sufficient to express the dependence of v on v_i, or v_f, independent of the form of the function f. In fact,

$$(13)\qquad \begin{aligned} &v = f(v_i', v_f) = f(v_i, v_i) + \frac{\partial f}{\partial v_f'} \cdot \frac{\partial v_f'}{\partial E} \Delta E; \\ &\frac{d}{dv_f'} f(v_f', v_f) = 2 \frac{\partial f}{\partial v_f'} = 1, \; v_f' = v_f; \\ &v = v_i - \frac{1}{2} \cdot \frac{\partial v_i}{\partial E} \Delta E = v_f + \frac{1}{2} \frac{\partial v_f}{\partial E} \Delta E. \end{aligned}$$

It is necessary to introduce this correction only into the largest term in the exponent. Inserting (13) in (12), we find

$$(14)\qquad s_{nm} = \frac{2r_0 \pi}{\omega r_0 \kappa} \left| \Delta q_{nm} \right| \frac{2\pi}{r_0} \left(\frac{\mu \omega r_0^2}{\hbar (n+1)^2} \right)^3 \exp\left[-\frac{\omega r_0 \pi}{\hbar v_i} \left(1 \pm \frac{\hbar \omega}{2 m v_i^2} - \frac{2}{\pi} \sqrt{\frac{\varepsilon}{E}} \right) \right],$$

where a positive sign in front of $\frac{\hbar \omega}{2 m v_i^2}$ corresponds to a de-excitation of vibration, and a negative sign to excitation.

Averaged over the thermal distribution of the colliding molecules, the cross section for inelastic collisions takes the form

$$(15)\qquad s_{nm} = \frac{1}{2} \left(\frac{\mu}{kT} \right)^3 \int_0^\infty s_{nm} v_i^5 \exp\left(-\frac{\mu v_i^2}{2kT} \right) dv_i.$$

where μ is the reduced mass of the colliding molecules. Since the integrand has a sharp maximum for a certain velocity v_i^0, we can perform the average by the method of steepest descent. The position of the point of steepest descent can be determined simply by calculating the maximum of the first term in the exponential term of equation (14). Calculation gives

$$(16)\qquad s_{nm} = 4\pi r_0^2 \left| \Delta q_{nm} \right| \frac{2\pi}{r_0} \sqrt{\frac{\pi}{3}} \varkappa^{\frac{1}{2}} \left(\pi \frac{\hbar \omega}{\varepsilon_0} \right)^3 \exp\left(-3\varkappa \pm \frac{\hbar \omega}{2kT} + \frac{4}{\pi} \sqrt{\varkappa \frac{\varepsilon}{kT}} \right),$$

where $\varkappa = \frac{\mu (v_i^0)^2}{2kT} = \left(\frac{\omega^2 r_0^2 \pi^2 \mu}{n \cdot 8kT} \right)^{-\frac{1}{3}}$ and $\varepsilon_0 = \frac{\hbar^2}{2\mu} \left(\frac{2\pi}{r_0} \right)^2$. The condition for the method of steepest descent to be applicable is $\varkappa \gg 1$, and the condition $\hbar\omega \ll E$ and $\varepsilon \ll E$ may now be written in the form $\hbar\omega \ll E^*$ and $\varepsilon \ll E^*$. These conditions are satisfied over a rather wide range of temperature.

If we identify the quantity $\frac{2\pi}{r_0} = \alpha$ with the reciprocal of the interaction radius of the exchange forces, then as $\varepsilon \to 0$ our quasi-classical expression for σ_{nm} corresponds (except for a factor of 4) with the analogous expression in reference [3], derived from an exact quantum mechanical calculation of the transition probability in an exponential field $e^{-\alpha z}$ for the one-dimensional case. The mistaken absence of the factor of 4 in reference [3] has been noticed earlier [4]. For $\hbar\omega \ll 2kT$ and $\varepsilon \to 0$ the exponential term corresponds exactly to the one obtained by the semi-classical method of reference [1]. This agreement as $\varepsilon \to 0$ is understandable, since as the depth of the well decreases, it becomes increasingly accurate to approximate the function W (r) by an exponential.

For $\varepsilon \neq 0$ formula (16) and the analogous expression in reference [3] differ by a factor which takes account of the presence of attraction between the molecules. In place of our factor $\left(\frac{4}{\pi} \sqrt{\varkappa \frac{\varepsilon}{kT}} \right)$, reference [3] has the factor $\exp\left(\frac{\varepsilon}{kT} \right)$. Since at ordinary temperatures the quantity $\frac{\varepsilon}{kT}$ varies only between limits close to 1, the factor $\exp\left(\frac{\varepsilon}{kT} \right) \approx 1$. In formula (16), however, the factor $\sqrt{\frac{\varepsilon}{kT}}$ increases 3-4 times in the neighborhood of 1, since for various molecules the quantity $\varkappa$ is 5-10 [6]. Hence taking account of the attraction between molecules may increase the cross section by 1-2 orders of magnitude. Qualitatively this corresponds to experimental results on the probability of vibrational de-excitation found by the methods of ultrasonic dispersion (see reference [5]), and the attenuation of fluorescence [6]. The extremely strong dependence of the cross section on the nature of the colliding molecules cannot be explained simply by variations in the reduced mass and the interaction radius of the exchange forces α^{-1} which should be approximately constant for all molecules [5], since it has the role of the characteristic parameter in the Morse potential for the various molecules [7]. The 10-100 fold increase in the cross section for vibrational de-excitation during collisions of strongly attracting molecules (collisions of two polar molecules or collisions which at low temperatures can form a stable system) as compared with the cross section for the analogous process for non-polar molecules or for molecules with saturated bonds, corresponds in our model to an increase in the depth of the potential well by a factor of 2-4.

CONCLUSIONS

1. Using the methods of time-dependent perturbation theory we have calculated the cross section for inelastic collisions between molecules resulting in vibrational excitation. The calculation has taken account of the change in the relative energy of the colliding molecules before and after the collision and it is shown that this has a sizeable effect on the magnitude of the cross section. If one takes account only of the repulsion between the molecules, then our cross section coincides with the one found earlier on the basis of an exact quantum mechanical calculation.

2. The dependence of the cross section on the depth of the potential well, which characterised the attraction between molecules, is shown to be much stronger than found previously in approximate treatments of the attraction. Qualitatively, this corresponds to the strong dependence of the probability of vibrational de-excitation on the nature of the colliding molecules.

In conclusion I wish to express my deep thanks to N. D. Sokolov for reading over this work.

February 6, 1958

References

1. L. LANDAU, E. TELLER: Phys. Z. Sow., 10, 34 (1936)
2. J. M. JACKSON, N. F. MOTT: Proc. Roy. Soc. A137, 703 (1932)
3. R. N. SCHWARTZ, K. F. HERZFELD: J. Chem. Phys., 22, 767 (1954)
4. F. I. TANCZOS: J. Chem. Phys., 25, 439 (1956)
5. J. C. MC COUBREY, W. D. MC GRATH: Quart. Rev., 11, 87 (1957)
6. A. V. KLEINBERG, A. N. TERENIN: DAN USSR, 101, 1031 (1955)
7. G. GEL'MAN: Einfuhrung in die quantenchemie, Leipzig und Wien, F. Deuticke, 1937 (ONTI, Moscow, 1937)

TOM VI, Vyp. 2 OPTIKA I SPEKTROSKOPIIA Fevral', 1959
VOL. VI, No. 2 OPTICS AND SPECTROSCOPY February, 1959

Vibrational Spectra and Rotational Isomerization of 2, 3-Dimethylbutane

R. I. PODLOVCHENKO, L. M. SVERDLOV, AND M. M. SUSHCHINSKII

Abstract: Calculations were made of the normal vibration frequencies of the four rotational isomers of 2, 3-dimethylbutane (trans isomer, gauche isomer, cis-symmetrical and cis unsymmetrical isomers). Experimental data was obtained for Raman spectra and infrared spectra of 2, 3-dimethylbutane, supplementing the literature values. By comparing calculated values with experimental data a conclusion was made concerning the existence in the liquid phase of two rotational isomers: the trans isomer and the unsymmetrical isomer occupying an intermediate position between gauche and cis-symmetric. The characteristic frequencies of the adjacent tertiary carbon atoms were established.

1. The phenomenon of rotational isomers of paraffins was repeatedly studied by the method of vibrational spectra, and it was observed that, in contrast to the normal paraffins, upon cooling and freezing only small changes were observed in the spectra of branched paraffins reducing to an insignificant change of the relative intensity of some lines. The most complete data available is for 2-methylbutane and 2, 3-dimethylbutane, the spectra of which were studied by the authors of the works [1-3]. In the first paper [1] this result was explained as due to the fact that rotational isomers of branched paraffins possess almost equal energy and, consequently, the correlation of their concentration is weakly dependent on temperature. The authors of this work did not, however, rule out the possibility of a second extreme case of a very large difference of energy of isomers, owing to which there is present in the liquid phase only one isomer.

Thus, for a final answer to the question concerning the existence of rotational isomers of branched paraffins, and also for establishment of their geometrical configuration further investigation is needed. The present work is devoted to a theoretical and experimental investigation of the vibrational spectra of 2, 3-dimethylbutane-one of the lower representatives of the branched paraffin hydrocarbons.

2. Calculation of the vibrational frequencies of 2, 3-dimethylbutane was done by the method of El'iashevich and Stepanov [4]. Four configurations of 2, 3-dimethylbutane were considered: symmetric and unsymmetric trans isomers (or else trans and gauche isomer) and symmetric and unsymmetric cis isomers (see fig. 1) In the calculation it was assumed that force constants do not change in going from one isomer to another. Force constants were taken from calculation of ethane and propane [4]. Each of the rotational isomers has 54 normal modes of vibration. The vibrations have the following types of symmetry:

Trans isomer (symmetry C_{2h}):

$$G = 15A_g + 13A_u + 12B_g + 14B_u,$$

cis-symmetrical isomer (symmetry C_{2v}):

$$G = 15A_1 + 13A_2 + 12B_2 + 14B_1,$$

Gauche and cis- asymmetrical isomer (symmetry C_2):

$$G = 28A + 26B.$$

(See figure 2 for the designations of the internal coordinates)*

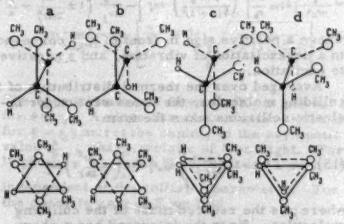

Fig. 1. Configuration of isomers of 2, 3-dimethylbutane. a-trans isomer, b-gauche isomer, c-symmetrical cis isomer, d-asymmetrical cis isomer. Above- general view, below- projection on the plane, perpendicular to the C-C axis.

The secular equations were solved by the method of successive approximations with the help of a BESM electronic computing machine. The calculated frequencies of normal modes of vibration are listed in table 1.

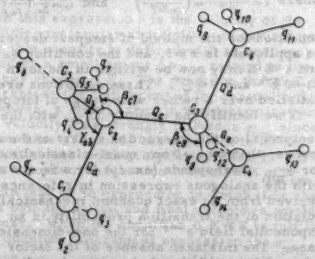

Fig. 2. Internal coordinates of the trans symmetrical isomer of 2, 3-dimethylbutane.

3. Raman and infrared spectra of 2, 3-dimethylbutane were investigated in a series of papers [2, 5, 6], but the existing data are incomplete. Therefore, we carried out some further measurements, in particular, measurement of the extent of depolarization of Raman lines. The methods used to make these measurements are described in the paper [7]. The data obtained are listed in table 2 in comparison with the literature values. Special attention was paid to the region of the spectrum below 500 cm^{-1}, where

* We did not consider coordinates characterizing hindered rotation of the methyl groups.

Table 1

Calculated Vibrational Frequencies of the Rotational Isomers of 2, 3-Dimethylbutane

Coordinates	Trans-asym. $\varphi=0$	Cis-asym. $\varphi=60°$	Trans-asym. ("gauche") $\varphi=120°$	Cis-sym. $\varphi=180°$
	A_2	A	A	A_1
γ (CCC)	270	184	201	210
γ (CCC)	445	451	440	342
Q_1^+ (C—C)	749	751	739	727
Q (C—C)	939	937	935	934
β^- (CCH)	1159	1060	1049	1041
β^- (CCH)	1213	1213	1216	1225
β_{CH}^+ (CCH)	1388	1336	1334	1357
α^+ (HCH)	1379	1380	1381	1382
α^- (HCH)	1467	1466	1465	1465
α^- (HCH)	1490	1492	1486	1487
φ^+ (C—H)	2899	2899	2899	2899
β_{CH}^+ (C—H)	2950	2953	2956	2958
φ^- (C—H)	2977	2977	2977	2977
φ^- (C—H)	2979	2979	2980	2980
	B_2			A_2
γ (CCC)	415	281	306	415
β^- (CCH)	940	939	940	940
β^- (CCH)	963	976	966	963
Q_1^- (C—C)	1179	1165	1174	1179
β_{CH}^- (CCH)	1355	1401	1370	1355
α^+ (HCH)	1382	1382	1386	1382
α^- (HCH)	1460	1460	1460	1460
α^- (HCH)	1470	1469	1469	1470
φ^+ (C—H)	2899	2899	2899	2899
φ^- (C—H)	2975	2975	2975	2975
φ^- (C—H)	2976	2976	2976	2976
	A_2	B	B	B_2
γ (CCC)	175	247	194	175
β^+ (CCH)	937	937	937	937
β^- (CCH)	981	966	976	981
Q_2^- (C—C)	1116	1148	1132	1116
β_{CH}^- (CCH)	1336	1268	1308	1336
α^+ (HCH)	1381	1381	1382	1381
α^- (HCH)	1460	1460	1460	1460
α^- (HCH)	1467	1468	1468	1467
φ^+ (C—H)	2899	2899	2899	2899
φ^- (C—H)	2975	2975	2975	2975
φ^- (C—H)	2976	2976	2976	2976
	B_2			B_1
γ (CCC)	296	351	347	338
γ (CCC)	359	464	511	514
Q_2^+ (C—C)	873	878	866	859
β^- (CCH)	1009	1018	1056	1088
β^- (CCH)	1154	1162	1162	1180
β_{CH}^- (CCH)	1285	1364	1373	1342
α^+ (HCH)	1381	1383	1384	1381
α^- (HCH)	1464	1465	1466	1467
α^- (HCH)	1469	1471	1472	1471
φ^+ (C—H)	2899	2899	2899	2899
φ_{CH}^- (C—H)	2957	2955	2951	2949
φ^- (C—H)	2977	2977	2977	2977
φ^- (C—H)	2980	2979	2979	2979

Note: φ - angle between planes passing through the C-C axis and one of the H atoms (see fig. 1.).

measurements were made with low pressure lamps. Because of the low background of these lamps we succeeded in carrying out more reliable measurements of parameters of Raman lines in this region. The data obtained (see table 2) in some cases differ from the data of other authors. In our measurements we did not observe the frequencies cited in reference [5] at 446(1), 605(0), 657(0), 812(2), 1239(0)* cm^{-1} and those frequencies cited in reference [6] at 819(2), 1106(2)cm^{-1}. These frequencies and also weak lines in the 2600-2800 cm^{-1} region, undoubtedly belonging to overtones are not cited in table 2. On the other hand, we disclosed several new lines.

We also carried out an investigation of the infrared spectra of 2, 3-dimethylbutane. A survey of the spectra was carried out with the aid of a doublebeam infrared spectrometer A-IKS-FIAN-4. In the region from 700 to 1500 cm^{-1} the spectrum was taken with a NaCl prism and a cuvette thickness of 1 mm. In spite of the great thickness of the cuvette, we observed only one new line with frequency of 806 cm^{-1} in comparison to the data of Axford and Rank [2]. We specifically note that in the vicinity of 756 cm^{-1}, where an intensive Raman line is found, we did not succeed in observing any traces of a line in the infrared. In the 700-450 cm^{-1} region the survey was carried out using a KBr prism and a cuvette thickness of 0.5 mm. In this region two weak lines were observed at frequencies of 477 and 542 cm^{-1}.

4. Comparison of the calculated values of vibrational frequencies with experimental values permits, first of all, a settlement of the question of the number of rotational isomers of 2, 3-dimethylbutane. Most significant in this respect is the region of fully symmetrical skeletal vibrations (700-800 cm^{-1}). In this region in the Raman spectrum there are observed two intensive polarized lines at 728 and 756 cm^{-1}. According to the calculation, each isomer has only one line in this region. Thus, two rotational isomers of 2, 3-dimethylbutane must exist in appreciable quantities.

Comparison of the Raman spectra and infrared spectra shows that some intensive Raman lines (505, 756, 943 cm^{-1}) do not appear in the infrared spectrum, while the infrared bands at 921, 991, 1280 cm^{-1} are not observed in the Raman spectra. This shows that the isomer to which the indicated lines belong has a center of symmetry, i.e. it is the trans-symmetric isomer. Settlement of the question of configuration of the second isomer is more difficult, and requires using the calculations of the frequency values.

*In our work and reference [5] one and the same preparation was investigated. Therefore, absence of some lines in spectra obtained by us is not connected with the degree of purity of the material, but is explained, evidently, by the more favorable ratio of the intensity of the lines at 4358, 4348 and 4339 Å in the mercury lamp we used because of which we could eliminate "repetition" from the last two lines more reliably.

Table 2

Raman Spectrum of 2, 3-Dimethylbutane

According to [5]			According to [6]			Results of our measurements*		
Δν (in cm^{-1})	J_0	ρ	Δν (in cm^{-1})	J_0	ρ	Δν (in cm^{-1})	J_0	ρ
—	—	—	271	7	—	267	1	—
282	1	—	280	9	—	283	2	0.32
346	1	—	346	11	—	346	3	0.72
382	1	—	388	11	—	379	2	0.18
—	—	—	—	—	—	395	2	0.58
421	1	—	430	11	—	432	2	0.84
479	7	—	475	21	—	479	7	0.14
505	9	—	506	23	—	505	9	0.07
—	—	—	—	—	—	537	1	—
728	39	0.09	728	100	0.01	728	39	0.05
756	13	0.2	753	30	0.08	756	13	0.11
869	7	0.7	868	11	0.82	869	7	0.78
932	17	0.57	936	53	0.49	932	17	0.48
943	17		946	50		943	17	
957	12	—	955	v. w.	—	957	12	0.7
1034	8	0.7	1033	11	0.82	1034	8	0.81
1151	8	—	1150	5	—	1151	8	—
1163	11	0.62	1161	22	0.79	1163	11	0.52
1195	7	0.5	1196	13	0.48	1195	7	0.53
1301	9	0.7	1301	15	0.91	1301	9	0.56
1326	0	—	—	—	—	1326	1	—
1344	9	0.9	1345	11	0.91	1344	9	0.65
1383	1	—	1381	1	—	1383	2	—
1445	22	0.77	1447	64	0.80	1445	22	0.81
1467	22		1468	66	0.80	1467	22	0.76
2858	70	—	2857	320	0.06	2858	100	0.27
2872	170	—	2874	1000	0.48	2872	160	0.20
2903	110	—	2903	560	—	2903	110	0.30
2926	110	—	2938	830	—	2936	120	0.22
2960	140	—	2963	850	—	2960	150	0.81
2977	60	—	2977	400	—	2977	80	0.78

*In the region above 700 cm^{-1} frequencies and intensity are cited from reference [5].

Table 3

Interpretation of spectra of 2, 3-Dimethylbutane

Trans isomer						Gauche isomer						Cis-asym. isomer
Raman spectrum			IR spectrum		Calc.	Raman spectrum			IR spectrum		Calc.	Calc.
Δν	J_0	ρ	ν	J	ν	Δν	J_0	ρ	ν	J	ν	ν
					A_g						A	A_1
293	2	0.32	—	—	270	267	1	—	—	—	201	210
505	9	0.07	—	—	448	479	7	0.14	477	v	447	342
756	13	0.11	—	—	749	728	39	0.05	728	m	739	727
943	17	0.48	—	—	939	932	17	0.48	—	—	935	934
1151	8	—	—	—	1159	1031	8	0.61	1038	s	1049	1041
1195	7	0.53	—	—	1213	1195	7	0.53	1196	v	1216	1225
1383	2	—	—	—	1388	1326	1	—	—	—	1331	1357
					B_g						A_2	
432	2	0.84	—	—	415	379	2	0.18	—	—	396	415
—	—	—	—	—	940	—	—	—	—	—	960	940
—	—	—	—	—	963	957	12	0.7	958	v	966	963
—	—	—	—	—	1179	1163	11	0.52	—	—	1174	1179
—	—	—	—	—	1355	1344	9	0.65	—	—	1370	1355
					A_u						B	B_2
—	—	—	—	—	175	—	—	—	—	—	194	175
—	—	—	921	m	937	—	—	—	910	s	937	937
—	—	—	991	s	981	—	—	—	—	—	976	981
—	—	—	1066	m	1116	—	—	—	1129	v. s.	1132	1116
—	—	—	1308	w	1330	1301	9	0.56	1297	m	1308	1336
—	—	—	1376	s	1381	—	—	—	1376	s	1382	1381
					B_u						B_1	
—	—	—	—	—	296	346	3	0.72	—	—	347	338
—	—	—	359	—	359	537	1	—	542	w	511	514
—	—	—	870	s	873	869	7	0.78	870	s	864	859
—	—	—	1028	m	1009	—	—	—	—	—	1056	1088
—	—	—	1153	s	1154	—	—	—	—	—	1162	1160
—	—	—	1280	s	1285	—	—	—	—	—	1373	1342

Note: s = strong, v. s. = very strong, m = medium, w = weak

In table 3 are compared the calculated and experimentally found frequencies of 2, 3-dimethylbutane, where we have limited ourselves to frequencies up to 1380 cm^{-1}, since higher frequencies are poorly sensitive to changes of geometrical configuration of the molecule (see table 1). For Raman spectra the data of reference [5] are cited, supplemented by the data of our measurements (see table 2); for infrared spectra, the data of reference [2] are cited for solid 2, 3-dimethylbutane, supplemented in the 450-700 cm^{-1} region by our data.

From table 3 it follows that in the assumption of the existence of one more rotational isomer besides the trans-symmetric, all frequencies in the Raman spectrum except the 395 cm^{-1} frequency may be interpreted as fundamentals. In the infrared spectrum three weak bands at 806, 832, and 1083 cm^{-1} must be interpreted as overtones or combination frequencies. Agreement between calculated and experimental frequencies are satisfactory except for the region of low frequency (lower than 500 cm^{-1}) where discrepancies between them are observed. These discrepancies evidently testify to the fact that the system of force constants established for calculations of normal paraffins demand some revisions on transition to branched paraffins. The inexactitude of force constants, naturally, is most telling in the region of low frequencies.

Some experimentally observed lines might be easiest to explain if we suppose that, besides the two isomers contained in the liquid phase in significant quantity, there is another, a third isomer, in small quantity. This supposition is contradicted by the fact that in the region of fully symmetrical skeletal vibrations, where intensity of lines in the Raman spectrum is greatest, only two narrow and sharp lines are observed. It is possible to assume that in this region of the spectrum two isomers have coinciding frequencies. Calculation shows, however, that in the observed region only the trans-symmetric (749 cm^{-1}) and cis asymmetric (751 cm^{-1}) isomers possess very similar frequencies. For the last isomer the line at 751 cm^{-1} is permitted in the infrared spectrum. In reality, however, this line is not observed in the infrared spectrum, even using cuvettes of great thickness. Consequently, the cis-asymmetric isomer does not exist.

Thus we will proceed from the assumption of the existence of only two rotational isomers of 2, 3-dimethylbutane. The first of these, as was shown above, has the symmetric trans-configuration. For the second isomer the asymmetric trans-configuration might be taken most naturally. Under this assumption, as seen in table 3, not bad agreement between calculated and experimental frequencies exists. If it were to be assumed that the second isomer has the symmetrical cis-configuration, then some

Table 4

Characteristic Frequencies of Adjacent Tertiary Carbon Atoms (in cm^{-1})

Molecule	Asymmetrical isomer									Trans isomer					
	Raman spectrum [5]									Infrared spectrum [8,9]			Raman spectrum [5]		
	ω_1^+ (C–C)	ω_2^- (C–C)	δ_{CH}^+(CCH)	δ_{CH}^-(CCH)	$\delta_{H_3}^-$(CCH)	Q (C–C)	$\delta_{CH_3}^-$(CCH)	ω_3^+ (C–C)	γ_1 (CCC)	ω_4^- (C–C)	$\delta_{CH_3}^+$(CCH)	$\rho_{CH_3}^-$(CCH)	ω_5^+ (C–C)	Q (C–C)	γ_1 (CCC)
2,3-dimethybutane . . .	728 (30)	1163 (11)	1301 (9)	1345 (9)	1195 (7)	932 (17)	1034 (8)	869 (7)	479 (7)	1129 (s.)	1066 (m.)	921 (m.)	756 (13)	943 (17)	432 (2)
2,3-dimethylpentane . .	712 (5)	1162 (10)	1306 (3)	1352 (7)	1189 (6)	916 (12)	1039 (9)	851 (8)	463 (2)	1122 (s.)	1075 (m.)	918 (m.)	752 (15)	955 (9)	427 (3)
2,3-dimethylhexane . . .	719 (6)	1160 (10)	1304 (11)	1353 (3)	1190 (7)	937 (8)	1035 (8)	850 (4)	469 (7)	1127 (s.)	1075 (m.)	919 (m.)	755 (10)	956 (9)	427 (2)
2,3-dimethylheptane . . .	714 (5)	1159 (8)	1304 (2)	1352 (8)	1208 (4)	926 (10)	—	872 (10)	—	1128 (s.)	1080 (m.)	918 (m.)	760 (18)	954 (3)	—
2,3-dimethyloctane . . .	—	—	—	—	—	—	—	—	—	1128 (s.)	1089 (m.)	915 (m.)	—	—	—
3,4-dimethylhexane . . .	729 (10)	1161 (9)	1283 (9)	1360 (8)	1182 (7)	—	1032 (12)	—	462 (1)	1122 (s.)	1071 (m.)	—	762 (8)	953 (7)	434 (11)
3,4-dimethylheptane . . .	730 (5)	1166 (9)	1301 (8)	1359 (4)	—	931 (4)	1035 (12)	—	—	1122 (s.)	1063 (m.)	920 (m.)	751 (10)	—	428 (5)
3,4-dimethyloctane . . .	—	—	—	—	—	—	—	—	—	1124 (s.)	1077 (m.)	919 (m.)	—	—	—
2,2,3-trimethylhexane	731 (9)	1164 (18)	1318 (18)	1346 (17)	1190 (9)	926 (7)	—	884 (8)	459 (9)	—	—	—	763 (23)	957 (20)	428 (12)
2,2,3-trimethylhexane	732 (8)	1160 (19)	1309 (20)	1346 (15)	1190 (12)	926 (9)	1024 (5)	877 (2)	465 (5)	—	—	—	765 (16)	956 (24)	433 (4)
2,3,6-trimethylheptane	727 (7)	1168 (13)	1307 (13)	1344 (16)	—	930 (3)	1047 (4)	875 (4)	462 (4)	—	—	—	766 (18)	953 (12)	422 (5)

Note: s.= strong, m.= medium

lines in the spectrum, for example, the line at 479 cm^{-1}, cannot be interpreted satisfactorily. There are, however, facts which contradict the assumption that the second isomer has the asymmetrical trans-configuration. First of all there is the noticeable polarization of the lines at 869, 346, 1301 cm^{-1}, which, according to the rules of selection, ought to be depolarized. Secondly, the displacement of frequencies in going from the first to the second isomer does not fully agree with the assumption that the latter represents the "gauche" trans isomer. The calculation carried out by us is not, of course, able to claim great exactness in computing the significant frequencies. Nevertheless, the speed of change frequencies in going from one isomer to the other and the approximate size of the frequency jump, it would seem the calculation ought to tell correctly. Here, indeed, we observe (see table 3) that for the most characteristic pairs of lines, 505 and 479, 756 and 728, 1151 and 1034, 432 and 379 cm^{-1} the jump of experimental frequencies does not correspond to the jump in calculated frequencies for the "gauche" isomer, and better corresponds to the jump in frequencies calculated for the cis-symmetric isomer. The latter, however, as already demonstrated, cannot be chosen interpretation of the spectrum as the second isomer. Thus, we arrive at the conclusion that the second isomer in all probability holds a position intermediate between the trans-asymmetric and the cis-symmetric isomers, i. e., it corresponds to an angle of rotation, somewhere between 120° and 180°. If it is assumed that this isomer does not have the elements of symmetry owing to the rotation of the CH_3 group near the C-C axis, then the difficulty with the violation of the selection rules, which was mentioned above, disappears.

The intensity of the lines in the Raman spectrum allows the possibility of getting some idea of the concentration of each of the isomers. In the majority of cases the intensities of corresponding lines in the spectrum are directly between both, from which it might be possible to infer approximate equality of concentration of the isomers. Nevertheless, in the case of lines belonging to fully symmetrical valence vibrations of the skeleton, which are the most reliable for deciding about the concentration of isomers (see [7]), the intensity of the 728 cm^{-1} line of the asymmetrical isomer is significantly greater than the intensity of the 756 cm^{-1} line of the symmetric-trans isomer (see table 3). Upon comparing the integral intensities of the lines the demonstrated increase is not so very great, and comes, according to the data of reference [5], to $I_{728}/I_{756} \approx 1.5$.

Thus, the asymmetrical isomer at a temperature of 300°K, evidently, is present in concentration than the symmetrical trans isomer, i. e. it is more stable.

5. In conclusion we consider the question of the characteristic frequencies of the adjacent tertiary carbon atoms. As the calculation shows, the molecule of 2,3-dimethylbutane has the sum total of frequencies which are characteristic for the groups of coordinates which correspond to the structual element shown. But since this structual group is part of the combination $R\text{-}\underset{CH_3}{CH}\text{-}\underset{CH_3}{CH}\text{-}CH_2\text{-}R_1$, then consequently, molecules of this series will possess approximately the same characteristic frequencies as does 2,3-dimethylbutane. The characteristicness is conditioned by the fact that vibration coordinates corresponding to this group interact very strongly with both and, by comparison, more weakly with coordinates of the radicals R, R_1, adding to the adjacent tertiary atoms. This conclusion is sufficiently well substantiated by experimental results. In table 4 are cited the data on hand for the series of hydrocarbons.

Note in Proof: Recently Dr. N. Sheppard courteously, let us know the data of his measurements in the infrared spectrum of 1,3-dimethylbutane, under conditions of its slow crystallization.*** Lines retained were 870 (m), 920 (m), 958 (w), 988 (s), 1068 (s), 1158 (s), 1282 (m), 1297 (w), 1378 (s), 1460 (s). Moreover, there were observed new lines by comparison with the liquid phase at 1176 (m), 1312 (m). Comparison of these data with the results of our work (table 3) permits the conclusion that the

***We take this opportunity to express sincere thanks to Dr. N. Sheppard for this communication.

isomer which is stable in the solid phase has a configuration close to the symmetrical trans configuration, but not strictly symmetrical, since otherwise difficulty arises in interpretation of two bands at 958 (w), and 1176 (w).

January 21, 1958

References

1. G. J. SZASZ, N. SHEPPARD: J. Chem. Phys., 17, 93 (1949)
2. D. W. E. AXFORD, D. H. RANK: J. Chem. Phys., 18, 51 (1950)
3. J. K. BROWN, N. SHEPPARD: J. Chem. Phys., 19, 976 (1951)
4. M. V. VOL'KENSHTEIN, M. A. EL'IASHEVICH: B. I. STEPANOV: Kolebaniia Molekul (Molecule Vibration), 1951
5. G. S. LANDSBERG, P. A. BAZHULIN, M. M. SUSHCHINSKII: Osnovnye Parametry Spektrov Akad. Nauk Press. Mos. 1956 Kombinatsionnogo Passeianiia Yglevodorodov (Fundamental Parameters ofSpectra of Raman Spectra of Hydrocarbons.)
6. F. F. CLEVELAND, P. PORCELLI: J. Chem. Phys, 18, 1459, (1950)
7. M. M. SUSCHINSKII: Doctoral Dissertation, FIAN, USSR, 1957
8. N. SHEPPARD, D. SIMPSON: Quart. Rev., 7, 19, (1953)
9. MC. MURRY, V. THORNTON: Anal. Chem., 24, 319. (1952)

TOM VI, Vyp. 2 OPTIKA I SPEKTROSKOPIIA Fevral', 1959
VOL. VI. No. 2 OPTICS AND SPECTROSCOPY February, 1959

Calculation of the Vibrational Spectra of the Cyclopentane and Deuterocyclopentane Molecules

R. S. LEBEDEV

Abstract: By a mechanical model a calculation of frequencies and form of normal vibrations of the cyclopentane and deuterocyclopentane molecules were made. Applicability of D_h^5 symmetry was confirmed for them. Derivatives were found from the frequencies according to different parameters and the order of magnitude of the major force constants of C_5H_{10} was estimated.

Cyclopentane and substituted cyclopentanes are found in petroleum oil. Analysis of oil by spectrum has great practical interest [1-6]. Interpretation of the cyclopentane spectrum [7] has not been completed fully; there is a most probable correlation of frequencies with types of vibration of the molecule [8]. The purpose of the present work is the calculation of vibration frequencies of cyclopentane and deuterocyclopentane in accordance with a mechanical model.

The C_5H_{10} structure was investigated by the method of electron diffraction [9-11]. The idea was adopted that the five carbon atoms comprise a flat regular pentagon with very insignificant distortion of planarity within the limits of precision of the electron diffraction method. Evidently it must substantially affect the symmetry of the molecule.

The possibility of D_h^5 symmetry was subjected to discussion. The probability of a flat or almost flat ring is confirmed by good agreement of the electron diffraction results with the representation of a planar ring; by the insignificant deviation of 1°28' of the C-C-C angle from the tetrahedral as against the normal angle in normal paraffins, which ought to correspond to an unstrained ring; by the small number of lines in the Raman spectrum below 1400 cm^{-1}.

According to measurements it is accepted that in the equilibrium configuration the carbon atoms form a regular pentagon with the C-C-C angle equal to 108°, with sides S(C-C) = 1.53Å.*

Every two C-H bonds of length 1.09Å, located symmetrically to the plane of the carbon atoms, are in a plane passing through its center (see figures).

The H-C-H angle = 109°28 is assumed to be tetrahedral. The H-C-C angle = 109° 50' is calculated geometrically. Thus, the calculated model possesses D_{5h} symmetry [12]. In the case of cyclopentane there are 39 normal modes of vibrations.

For the calculation we introduce the following 45 symmetry coordinates: for changes of lengths of bonds C-C q_i x(i=1-5); lengths of bonds C-H q_i x(i=1-10); angles between corresponding C-C bonds: γ_{15}, γ_{12}, γ_{23}, γ_{43}, γ_{45}; angles between C-H bonds: α_{12}, α_{34}, α_{56}, α_{78}, α_{910}.

For changes of angle HCC were introduced the set of twenty equivalent coordinates: β_{11}, β_{23}, β_{35}, β_{47}, β_{59}, β_{12}, β_{24}, β_{36}, β_{48}, $\beta_{5\,10}$, β_{51}, β_{13}, β_{25}, β_{37}, β_{49}, β_{52}, β_{14}, β_{26}, β_{38}, $\beta_{4\,10}$.**

Coordinates for non-planar vibrations of the ring were not introduced because of the absence of corresponding force constants, because of the assumed weak interaction between planar and non-planar forms of movement owing to high symmetry, and because of great calculation difficulties.

Determination of the matrix elements of the kinematic coefficients was done by the method of El'iashevich [12] with the use of corrections for anharmonicity by the method of spectroscopic mass.

The matrix of potential energy coefficients was represented in the usual notations [13].

The following force constants (in units of 10^{-6} cm^{-2}), taken from other molecules [12] are assumed to be different from zero in the calculations: $K_q = 7.84$, $K_Q = 7.02$, $K_\beta = 0.92$, $K_\gamma = 1.1$, $K_\alpha = 0.71$, $A = 0.43$, $a = 0.35$, $l = -0.035$, $n_\gamma = 0.12$, $m_{\beta\gamma} = -0.02$, $n = -0.02$, $m_\beta = 0.12$.

In view of the complexity of the matrices with 45 elements obtained, ***they were not reduced, but all possible interactions between normal vibration coordinates are given in reference [14].

For dependent coordinates, corresponding to changes of angles for each carbon atom, five additional correlations are found by a vector method [12]:

$$1.0202\alpha_{12} + \beta_{11} + \beta_{21} + \beta_{25} + \beta_{15} + 0.9928\gamma_{15} = 0,$$
$$1.0202\alpha_{34} + \beta_{31} + \beta_{32} + \beta_{41} + \beta_{42} + 0.9928\gamma_{12} = 0,$$
$$1.0202\alpha_{56} + \beta_{53} + \beta_{52} + \beta_{62} + \beta_{63} + 0.9928\gamma_{23} = 0,$$
$$1.0202\alpha_{78} + \beta_{74} + \beta_{73} + \beta_{84} + \beta_{83} + 0.9928\gamma_{34} = 0,$$
$$1.0202\alpha_{9\,10} + \beta_{94} + \beta_{95} + \beta_{105} + \beta_{104} + 0.9928\gamma_{45} = 0,$$

The condition of closure of the ring determines two additional correlations:

$$\gamma_{12} + \gamma_{23} + \gamma_{34} + \gamma_{45} + \gamma_{51} = 0$$
$$q_3 - 0.809(q_1 + q_5) + 0.309(q_2 + q_4) - 1.185[\gamma_{15} + 0.309(\gamma_{12} + \gamma_{45}) - 0.809(\gamma_{23} + \gamma_{34})] = 0.$$

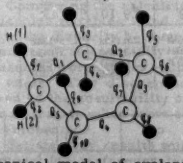

Mechanical model of cyclopentane. Light circles are carbon atoms, dark circles are hydrogen atoms.

*The length of the C-C bond is supposed to be 1.54Å, according to Khassel and Firfol; 1.51Å according to Wierl; 1.52Å according to Pauling and Brockway.

**First subscripts correspond to the number of C-C (Q) bonds, second subscripts to the number of C-H(q) bonds, (see figures).

***Some authors have tried to reduce the order of the matrices so, for example, Tschamler and Voetter considered a five-mass model; Kilpatrick, Pitzer and Spitzer did not consider the C-H frequencies and used a bent ring model with pseudo-rotation.

Matrix of potential energy coefficients is written as :

u	Q_1	β_{11}	q_1
Q_1	K_Q+2H	$4(A_\beta+B_\beta+D_\beta)-7.842B_e$	$4h_Q$
β_{11}	$A_\beta+B_\beta+D_\beta-1.96B_e$	$K_\beta+l_\beta^2+l_\gamma^2+o_\beta+2(r_\beta+P_\beta)+n_\beta+r_\beta+m_\beta+n_\beta-3.92(l_{\pi\beta}+r_{\pi\beta})-1.96[4(l_{\sigma\beta}+r_{\sigma\beta})-3.92A_e]$	$a_\beta+b_\beta+c_\beta+d_\beta-1.96a_e$
q_1	$2h_Q$	$2(a_\beta+b_\beta+c_\beta+d_\beta)-3.92a_e$	$K_\gamma+h$

For the A_2'' symmetry type of vibration the matrices have the form :

T^{-1}	q_1	β_{11}
q_1	1.0604	−0.0870
β_{11}	−0.0435	0.5522

u	q_1	β_{11}
q_1	$K_\gamma-h$	$2(a_\beta+c_\beta-d_\beta-b_\beta)$
β_{11}	$a_\beta+c_\beta-d_\beta-b_\beta$	$K_\beta+2(r_\beta-P_\beta)-l_\beta^2+l_\gamma^2+n_\beta+m_\beta-o_\beta-r_\beta-n_\beta$

Doubly degenerate types of vibration are represented by the matrices :

E_1'' vibration type

T^{-1}	q_9	β_{11}	β_{32}
q_9	1.1208	−0.2329	0.2142
β_{11}	−0.0921	1.8568	−0.1636
β_{32}	0.0786	0.1445	0.8606

u	q_9	β_{11}	β_{32}
q_9	$K_\gamma-h$	$0.618(a_\beta-b_\beta)+1.618(d_\beta-c_\beta)$	$2(b_\beta-a_\beta)+0.618(d_\beta-c_\beta)$
β_{11}	$d_\beta-c_\beta$	$K_\beta-l_\beta^2-l_\gamma^2+o_\beta+0.618(r_\beta-P_\beta-m_\beta+n_\beta+n_\beta-r_\beta)$	$m_\beta-n_\beta+0.618(n_\beta-o_\beta)$
β_{32}	$b_\beta-a_\beta+0.618(d_\beta-c_\beta)$	$n_\beta-r_\beta+0.618(o_\beta+m_\beta-l_\gamma^2-n_\beta)$	$K_\beta-l_\beta^2+l_\gamma^2-o_\beta+0.618(r_\beta-P_\beta-n_\beta+r_\beta+m_\beta-n_\beta)$

E_1' vibration type

T^{-1}	Q_2	q_9	$\alpha_{9\ 10}$	γ_{45}	β_{11}	β_{32}
Q_2	0.1639	0.0094	−0.1408	0.1382	−0.4591	−0.0062
q_9	0.0497	1.0604	−0.0854	0.0421	−0.0405	−0.0454
β_{11}	−0.1277	−0.0371	0.0427	−0.1076	1.9917	−0.0634
β_{32}	−0.0410	−0.0320	0.5556	−0.0346	0.3875	0.5327

u	Q_2	q_9	β_{11}	β_{32}
Q_2	$K_Q+0.618H-0.521C_\gamma+1.364A_\beta-1.327B_e$	$-3.236h_Q$	$4D_\beta+1.236A_\beta+1.960B_e-3.236D_\beta$	$3.236(A_\beta+B_\beta)-1.236D_\beta-6.343B_e$
q_9	$0.82a_\gamma-0.843b_\gamma-0.521d_\gamma-1.618h_Q$	$K_\gamma+h$	$0.618(a_\beta+b_\beta)-1.212a_e-1.618(c_\beta+d_\beta)$	$3.921a_e-2(a_\beta+b_\beta)-0.618(c_\beta+d_\beta)$
$\alpha_{9\ 10}$	$0.82K_{\pi\gamma}-0.843\sigma_{\pi\gamma}-0.521P_{\sigma\gamma}-1.618B_e$	$2a_e$	$1.236l_{\pi\beta}-3.236r_{\pi\beta}-1.212K_\pi$	$3.921K_\pi-4l_{\pi\beta}-1.236r_{\pi\beta}$

E_1' vibration type (continued)

u	Q_2	q_9	β_{11}	β_{32}
γ_{45}	$0.618C_\gamma-1.618A_\gamma-0.843K_\gamma+1.364S_\gamma-0.521m_{\sigma\gamma}+0.507P_{\sigma\gamma}+0.82o_{\sigma\gamma}$	$1.236d_\gamma+2b_\gamma$	$4r_{\pi\beta}-3.236(n_{\pi\beta}+t_{\pi\beta})+1.236l_{\pi\beta}-1.212(P_{\sigma\gamma}+o_{\sigma\gamma})$	$3.921o_{\sigma\gamma}+2.423P_{\sigma\gamma}-1.236(n_{\pi\beta}+r_{\pi\beta})+3.236t_{\beta}-4l_{\pi\beta}$
β_{11}	$0.618(A_\beta-B_\beta)+D_\beta+0.843a_{\beta\beta}+0.521t_{\beta\beta}-0.843r_{\beta\gamma}-0.82\sigma_{\beta\beta}$	$-c_\beta-d_\beta$	$K_\beta+l_\beta^2-l_\gamma^2-o_\beta+0.618(n_\beta+r_\beta+r_\beta+P_\beta-m_\beta-n_\beta)+1.212\sigma_{\beta\beta}$	$m_\beta+n_\beta-3.921r_{\sigma\beta}+0.618(n_\beta+r_\beta)$
β_{32}	$A_\beta+0.618B_\beta+0.843l_{\pi\beta}+0.521(a_{\pi\beta}-t_{\beta\beta})-0.821a_{\beta\beta}-0.507r_{\sigma\beta}$	$-a_\beta-b_\beta-0.618(c_\beta+d_\beta)$	$0.618(m_\beta+n_\beta-o_\beta-l_\gamma^2)+n_\beta+r_\beta+1.212l_{\sigma\beta}+0.749r_{\beta}$	$K_\beta+l_\beta^2+l_\gamma^2+o_\beta+0.618(r_\beta+P_\beta-n_\beta-r_\beta+m_\beta+n_\beta)-3.921l_{\pi\beta}-2.423r_{\pi\beta}$

The highest order have matrices of the E_2^1 vibration type :

T^{-1}	Q_2	q_9	$\alpha_{9\ 10}$	γ_{45}	β_{11}	β_{32}
Q_2	0.2265	−0.0380	0.0538	−0.1382	0.2412	−0.0626
q_9	−0.0190	1.0604	−0.0854	0.1100	−0.0032	0.0218
$\alpha_{9\ 10}$	−0.1382	0.2200	−0.3106	0.4215	−0.0878	0.1028
β_{11}	0.2228	−0.0301	0.0427	−0.1235	1.7191	−0.0790
β_{32}	−0.2009	0.0855	0.4601	0.1253	−0.9889	0.5942

u	Q_2	q_9	γ_{45}	β_{11}	β_{32}
Q_2	$K_Q-1.618H$	$1.232h_Q$	$0.618A_\gamma-1.618c_\gamma-0.601B_e$	$4D_\beta-3.236A_\beta+1.236B_\beta+1.96B_e$	$3.236D_\beta-1.236(A_\beta+B_\beta)+2.423B_e$
q_9	$0.618h_Q$	$K_\gamma+h$	$b_\gamma-1.618d_\gamma-0.973a_e$	$0.618(c_\beta+d_\beta)-1.618(a_\beta+b_\beta)+3.172a_e$	$1.618(c_\beta+d_\beta)+3.921a_e-2(a_\beta+b_\beta)$
$\alpha_{9\ 10}$	$0.618B_e$	$2a_e$	$a_{\pi\gamma}-1.618P_{\sigma\gamma}-0.973K_\pi$	$1.236r_{\pi\beta}-3.236l_{\pi\beta}+3.172K_\pi$	$3.921K_\pi-4l_{\pi\beta}+3.236r_{\pi\beta}$
γ_{45}	$0.618A_\gamma-1.618C_\gamma$	$2b_\gamma-3.236d_\gamma$	$K_\gamma+0.618S_\gamma'-1.618m_\gamma-0.973(o_{\sigma\gamma}-1.618P_{\sigma\gamma})$	$4r_{\pi\beta}-3.236(r_{\pi\beta}+n_{\pi\beta})+1.236(n_{\pi\beta}+1.618o_{\sigma\gamma}-1.618P_{\sigma\gamma})+3.172(o_{\sigma\gamma}-1.618P_{\sigma\gamma})$	$3.236(r_{\pi\beta}+n_{\pi\beta})-1.236l_{\pi\beta}-4l_{\pi\beta}+3.921o_{\sigma\gamma}-1.618P_{\sigma\gamma}$
β_{11}	$1.618(B_\gamma-A_\gamma+D_\gamma)$	$-a_\beta-d_\beta$	$1.618t_{\beta\beta}-n_{\beta\gamma}+0.973r_{\sigma\beta}$	$K_\beta+l_\beta^2-l_\gamma^2-o_\beta+1.618(n_\beta+m_\beta-P_\beta-r_\beta-r_\beta-n_\beta)-3.172r_{\sigma\beta}$	$m_\beta+n_\beta-3.921r_{\sigma\beta}-1.618(n_\beta+r_\beta)$
β_{32}	$A_\beta-1.618B_\beta$	$1.618(c_\beta+d_\beta)-a_\beta-b_\beta$	$1.618a_{\pi\beta}-l_{\pi\beta}-1.618r_{\pi\beta}-0.973(1.618r_{\sigma\beta}-l_{\sigma\beta})$	$1.618(l_\beta^2+o_\beta-m_\beta-n_\beta)+n_\beta+r_\beta+3.172(1.618r_{\sigma\beta}-l_{\sigma\beta})$	$K_\beta+l_\beta^2+l_\gamma^2+o_\beta+1.618(n_\beta+r_\beta-m_\beta-n_\beta-r_\beta-P_\beta)+3.921(1.618r_{\sigma\beta}-l_{\sigma\beta})$

Table 1
Frequencies and Forms of Normal Vibrations of Cyclopentane

Interpretation	Sym.	Experimental frequencies (cm^{-1}) [8] Raman spectrum (gas)	Experimental frequencies (cm^{-1}) [8] I.R. spectrum (gas)	Calculated freq. (cm^{-1})	Form of Vibrations
ν_1 (C—H)	A_1'	2906 (10)	—	2894	$\varphi_1 = 1, Q_1 = -0.12, \beta_{11} = 0.02$
ν_2 (HCH)	A_1'	1453 (4)	—	1488	$\beta_{11} = 1, Q_1 = -0.32, \varphi_1 = 0.06$
ν_3 (C—C)	A_1'	886 (9; 11)	—	859	$Q_1 = 1, \varphi_1 = 0.05, \beta_{11} = 0.04$
ν_4 (C—H)	A_2''	—	2960 (10)	2886	$\varphi_1 = 1, \beta_{11} = -0.02$
ν_5 (CCH)	A_2''	—	964 (3)	754	$\beta_{11} = 1, \varphi_1 = -0.08$
ν_6 (C—H)	E_1''	2966 (9)	—	2937	$\varphi_1 = 1, \beta_{11} = -0.99, \beta_{22} = 0.04$
ν_7 (CCH)	E_1''	1207 (3)	—	1216	$\beta_{11} = 1, \beta_{22} = 0.27, \varphi_1 = 0.01$
ν_8 (CCH)	E_1''	1104 (1)	—	799	$\beta_{22} = 1, \beta_{11} = -0.10, \varphi_1 = 0.08$
ν_9 (C—H)	E_1'	—	2899 (10)	2886	$\varphi_2 = 1, Q_2 = 0.10, \beta_{11} = -0.03, \beta_{22} = -0.01$
ν_{10} (C—C)	E_1'	—	896 (8)	938	$Q_2 = 1, \varphi_2 = -0.01, \beta_{11} = 0.43, \beta_{22} = 0.25$
ν_{11} (HCH)	E_1'	—	1456 (9)	1468	$\beta_{22} = 1, \beta_{11} = 0.23, Q_2 = -0.21, \varphi_2 = -0.07$
ν_{12} (HCC)	E_1'	—	1316 (4)	1310	$\beta_{11} = 1, \beta_{22} = 0.21, Q_2 = -0.32, \varphi_2 = 0.01$
ν_{13} (C—H)	E_2'	2904 (4)	—	2877	$\varphi_2 = 1, Q_2 = -0.04, \beta_{11} = -0.03, \beta_{22} = 0.05, \gamma_{45} = 0.19$
ν_{14} (C—C)	E_2'	1030 (5)	—	1146	$Q_2 = 1, \varphi_2 = 0, \beta_{11} = -1.29, \beta_{22} = 0.94, \gamma_{45} = -0.80$
ν_{15} (HCC)	E_2'	1283 (2)	—	1289	$\beta_{11} = 1, \varphi_2 = 0, Q_2 = 0.33, \beta_{22} = -1.80, \gamma_{45} = -0.25$
ν_{16} (HCH)	E_2'	1453 (4)	—	1440	$\beta_{22} = 1, \beta_{11} = 0.34, \varphi_2 = -0.12, Q_2 = 0.07, \gamma_{45} = -0.01$
ν_{17} (CCC)	E_2'	589 (0)	—	556	$\gamma_{45} = 1, \beta_{22} = 0.22, \beta_{11} = -0.01, Q_2 = 0.09, \varphi_2 = 0.01$

Table 2
Frequencies and Forms of Normal Vibrations of Deuterocyclopentane.

Interpretation	Sym.	Experimental frequencies (cm^{-1}) [8] Raman spectrum (gas)	Experimental frequencies (cm^{-1}) [8] I.R. spectrum (gas)	Calculated freq. (cm^{-1})	Form of Vibrations
ν_1 (C—D)	A_1'	2129 (8)	—	2138	$\varphi_1 = 1, Q_1 = -0.25, \beta_{11} = 0.08$
ν_2 (DCD)	A_1'	1064 (3)	—	1140	$\beta_{11} = 1, Q_1 = -0.89, \varphi_1 = -0.06$
ν_3 (C—C)	A_1'	802 (9)	—	776	$Q_1 = 1, \beta_{11} = 0.24, \varphi_1 = 0.11$
ν_4 (C—D)	A_2''	—	2220 (10)	2100	$\varphi_1 = 1, \beta_{11} = -0.02$
ν_5 (CCD)	A_2''	—	685 (1)	550	$\beta_{11} = 1, \varphi_1 = -0.08$
ν_6 (C—D)	E_1''	2214 (6)	—	2199	$\varphi_2 = 1, \beta_{11} = -0.13, \beta_{22} = 0.10$
ν_7 (CCD)	E_1''	937 (5)	—	893	$\beta_{11} = 1, \varphi_2 = 0.02, \beta_{22} = 0.16$
ν_8 (CCD)	E_1''	778 (1)	—	618	$\beta_{22} = 1, \varphi_2 = 0.06, \beta_{11} = -0.13$
ν_9 (C—D)	E_1'	—	2125 (10)	2124	$\varphi_2 = 1, Q_2 = 0.20, \beta_{11} = -0.08, \beta_{22} = -0.03$
ν_{10} (C—C)	E_1'	—	738 (6)	778	$Q_2 = 1, \varphi_2 = -0.06, \beta_{11} = 1.28, \beta_{22} = -0.04$
ν_{11} (DCD)	E_1'	—	1064 (6)	1113	$\beta_{22} = 1, Q_2 = -0.80, \varphi_2 = -0.06, \beta_{11} = -0.19$
ν_{12} (DCC)	E_1'	—	1155 (3)	1117	$\beta_{11} = 1, Q_2 = 0.66, \beta_{22} = 0.41, \varphi_2 = 0.07$
ν_{13} (C—D)	E_2'	2130 (2)	—	2108	$\varphi_2 = 1, Q_2 = 0.09, \gamma_{45} = 0.39, \beta_{11} = 0.06, \beta_{22} = 0.09$
ν_{14} (C—C)	E_2'	937 (5)	—	1227	$Q_2 = 1, \varphi_2 = 0.03, \gamma_{45} = -0.69, \beta_{11} = 1.27, \beta_{22} = -1.14$
ν_{15} (DCC)	E_2'	1124 (4)	—	861	$\beta_{11} = 1, Q_2 = -0.12, \varphi_2 = 0, \gamma_{45} = 0.16, \beta_{22} = -0.77$
ν_{16} (DCD)	E_2'	1084 (3)	—	1065	$\beta_{22} = 1, Q_2 = -0.13, \varphi_2 = -0.06, \gamma_{45} = -0.73, \beta_{11} = -0.18$
ν_{17} (CCC)	E_2'	(490)	—	525	$\gamma_{45} = 1, Q_2 = 0.09, \varphi_2 = 0, \beta_{11} = -0.04, \beta_{22} = 0.28$

The correctness of the composition of the matrix was checked according to the additional correlation found. Their multiplication was not carried out.

Reduction of matrices of kinetic and potential energy coefficients according to symmetry, and calculation of additional correlations by the method of Maiants [15] defines vibrations of the following types of symmetry: $G = 3A_1' + A_2' + A_1'' + 2A_2'' + 4E_2'' + 3E_1'' + 4E_1' + 5E_2'$.

For allowed types of symmetry, matrices of kinetic T^{-1} and potential energy coefficients Φ emerge in the following way:

Type of Vibration A_1 (fully symmetrical)

T^{-1}	Q_1	β_{11}	φ_1
Q_1	0.1252	—0.1776	—0.1228
β_{11}	—0.0444	0.5834	0.0435
φ_1	—0.0614	0.0870	1.0804

The secular equations of the corresponding types of vibrations in numerical form were obtained in reference [14]. Frequencies and forms of the normal vibrations were determined by the method of iteration [15]. Validity of the calculation of frequencies was tested according to spacing. The matrices of kinetic energy coefficients of allowed types of symmetry were determined for deuterocyclopentane and verification carried out according to the rule of Teller and Redlich.

Correlation of frequencies, given by Tschamler and Voetter [8] for Raman [2, 7, 8, 16-19] and infrared [7] spectra of cyclopentane and deuterocyclopentane, were used by us as the most probable.

Results of the calculation are presented in tables 1 and 2.

Simultaneously with the frequencies, according to the method of Maiants [15], derivatives of the frequencies were calculated according to the force constants. Validity of their determination was tested according to the relationship $\nu = 2\sum_{(ij)} \nu_{ij} K_{ij}$.

The results obtained were published [14].

Comparing the calculated and found frequencies in tables 1 and 2 it is necessary to note the disparity between theory and experiment. It is especially significant for frequencies corresponding to changes of the HCC angle. This discrepancy might be explained by the unsuitability of substituting force constants taken from other molecules for cyclopentane.

Satisfactory results were obtained by our model for α-frequencies.

Comparison of the calculated frequency of 859 cm^{-1} with the frequency of 889 cm^{-1} of the cyclopentane spectrum does not provoke doubts. This turned out lower than expected by 30 cm^{-1}. Derivatives of it according to force constants showed great dependence of

frequency on interaction of the two neighboring C-C bonds, which also corresponds with the conclusion from calculation of the methylcyclopentane molecule [14]. Analogous results were obtained by Tschamler and Voetter by the five-mass model.

However, the combination they proposed of variably operating significant constants for the ring demands verification in the structure we studied. Evidently the force constants of cyclopentane and other naphthenes differ significantly from the corresponding force constants of normal paraffins [6].

In analyzing the discrepancy between obtained and expected frequencies we ought to be convinced of the truth of the interpretation which we initially accepted. The criterion of such correspondence was the fulfillment in our work of the rule of Teller and Redlich. For complete acceptance of the suggestion advanced it is necessary to have agreement of the rule of derivatives with the intensities of bands and establishment of equality between entropies obtained calorimetrically and spectrally.

Miller and Inskeep [7] were not able to demonstrate satisfactorily application of all three criteria to the study of the cyclopentane spectrum.

This led them to the conclusion that cyclopentane definitely did not have D_{5h} symmetry, but that its structure was unknown.

In connection with the contradictions which arose, Tschamler and Voetter extended the analysis of the question being studied and explained the insignificant discrepancy in entropy obtained by some reduction of the degeneracy. But this in turn ought to be explained by the insignificant deviation of the carbon atoms from the planar position and shown spectrally in the appearance of additional lines. The latter in the C_5H_{10} and C_5D_{10} spectrum have insignificant intensity, which speaks of planar or almost planar position of carbon atoms in the ring. Consequently the D_{5h} symmetry is applicable for the cyclopentane and deuterocyclopentane molecules.

The absence of coordinates for the nonplanar vibrations of the ring did not lead to contradictions, for, in the cyclopentane and deuterocyclopentane spectrum between the frequencies of 899 and 290 cm^{-1}, if any lines are there, then they are very weak and have escaped the experimenters.

Full analysis of the cyclopentane and deuterocyclopentane spectrum and problems of characteristic frequencies in the series of cyclopentane and its derivatives [5] can be given after full elucidation of the field forces of the molecule, but this presents special difficulty.

In conclusion I consider it a duty to express my gratitude to L. S. Maiants for suggesting the work, and L. M. Sverdlov for his interest in it.

February 10, 1958

References

1. P. A. BAZHULIN: IAN USSR, Ser. fiz., 5, 2-3, 168 (1941)
2. P. A. BAZHULIN, KH. E. STERIN, T. F. BULANOVA, O. P. SOLOVOVA, M. B. TUROVA-POLIAK, B. A. KAZANSKII: IAN USSR, OKhN, 17, No. 1, 7-18 (1946)
3. G. S. LANDSBERG, B. A. KAZANSKII: IAN USSR OKhN, 2, 100-114 (1951) (For translation see ATS, #RJ-224)
4. G. S. LANDSBERG, P. A. BAZHULIN, M. M. SUSHCHINSKII: IAN USSR, Ser. fiz., 17, 604 (1953)
5. M. M. SUSHCHINSKII: IAN USSR, Ser. fiz., 17, 608 (1953)
6. L. M. SVERDLOV, E. P. KRAINOV: OiS, 3, 54 (1957)
7. F. A. MILLER, R. G. INSKEEP: J. Chem. Phys., 18, 1519 (1950)
8. H. TSCHAMLER, H. VOETTER: Monatsh. Chem., 83, H. 5, 1228 (1952); 83, 302, (1952)
9. L. PAULING, L. O. BROCKWAY: J. Am. Chem. Soc., 59, 1223 (1937)
10. R. WIERL: Ann. d. Phys., 13, H. 4, 453, (1932)
11. J. E. KILPATRICK, K. S. PITZER, R. SPITZER: J. Am. Chem. Soc., 69, 2483 (1947)
12. M. V. VOL'KENSHTEIN, M. A. EL'IASH EVICH, B. I. STEPANOV: Kolebaniia Molekul (Molecule Vibrations) l., GITTL, 1949
13. M. A. EL'IASHEVICH: ZFKh, 15, 847 (1941); UFN, 28, 482 (1946)
14. R. S. LEBEDEV: Uch. Zap. Keremovsk. Ped. Inst., 3 (1958) (In press)
15. L. S. MAIANTS: DAN USSR, 89 (3), 423-426 (1953) (Translation #RT-33, 4 pp.) ZETF, 25, 393 (1953); Tr. FIAN USSR, 5, 63 (1950)
16. K. W. F. KOHLRAUSCH, R. SEKA: Ber. dtsch. Chem. Ges., 69, 729 (1936)
17. A. W. REITZ: Z. phys. Ch., 33, Abt. B, 179 (1936); 38, Abt. B, 38 (1938)
18. E. J. ROSENBAUM, H. F. JACOBSON: J. Am. Chem. Soc., 63, 2841 (1941)
19. M. R. FENSKE, W. G. BRAUN, R. V. WIEGAND, D. QUIGGLE, R. H. MC CORMICK, D. H. RANK: Anal. Chem., 19, 700 (1947)

TOM VI, Vyp. 2 OPTIKA I SPEKTROSKOPIIA Fevral', 1959
VOL. VI. No. 2 OPTICS AND SPECTROSCOPY February, 1959

Interpretation of the Vibration Spectrum of Coronene

N. I. ZHIRNOV

Abstract: On the basis of models of representations concerning the structure of the molecule a qualitative explanation is given of the fact of duplication in the vibrational spectrum of coronene of frequencies analogous to the frequencies which are produced most strongly in the vibrational spectrum of benzene.

1. Up to the present time there has been obtained sufficiently extensive experimental information concerning the vibrational spectrum of the coronene molecule [1-3]. However, interpretation of the spectra obtained is attended by great difficulties. First of all, the most reliable method of attributing vibrational frequencies to one or another type of symmetry, based on the comparison of Raman with infra-red spectra, does not apply in the given case, since the spectra for coronene mentioned have not, at present, been obtained. Under these conditions a single possibility remains: to elicit some information from analogy of the structure of the coronene molecule with that of benzene. Thus, from the one fact of coronene and benzene belonging to one and the same point group of D_{6h} symmetry, and from the selection rules associated with this symmetry group, the completely well defined assignment of the 598 cm^{-1} frequency to the E_g^+ vibrational type results.

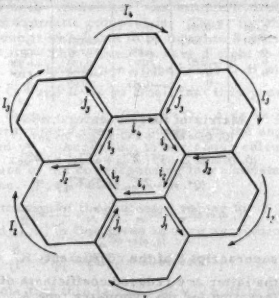

Figure 1. Currents of the π-electrons in coronene molecule.

However, the analogy with benzene goes much farther than it is possible to expect proceeding only from the selection rules for symmetry. This analogy, noticed by Shpol'skii, consists in the fact that very strong frequencies present in the benzene spectrum, are also present in the spectrum of coronene. First of all there is the frequency at 992 cm^{-1} of the fully symmetrical vibration of the benzene ring and the frequency at 3070 cm^{-1} near the 3062 cm^{-1} frequency of the fully symmetrical vibrations of the CH bonds in benzene.

In this article it is shown that the cause of the demonstrated analogy lies in the special role of the internal benzene ring in the coronene $C_{24}H_{12}$ molecule.

2. We shall consider the distribution of currents in the molecule of coronene (fig. 1) which owe their origin to collectivisation of the π electrons, proceeding from a metallic model of the molecule, i. e. consideration of the coronene molecule as a system of locked-in superconductors. It is well known [4] that a current is induced by a magnetic field H = 1, in every such superconductor, the magnitude of which current, with accuracy a constant factor, is determined from the expression similar to Ohm's law,

$$Il = S, \tag{1}$$

where S is the area enclosed by the current contour (in units 1/6th of the area of the benzene ring), l is the length of the contour of the current (in units of length of the C-C bond in benzene, 1.39 Å) and I is the current (in units of the current in the benzene molecule). Applying the Kirchoff rule and Ohm's law in the form (1) to the branching of the currents in the coronene molecule and taking, for simplicity, the length of all the C-C bonds equal to 1, it is possible to write down:

$$I_1 = I_2 + j_1, \tag{2}$$
$$I_2 = I_3 + j_2, \tag{3}$$
$$I_4 = I_3 + j_3, \tag{4}$$
$$i_2 = i_1 + j_1, \tag{5}$$
$$i_2 = i_3 + j_2, \tag{6}$$
$$i_3 = i_4 + j_3, \tag{7}$$
$$3I_1 - i_1 + 2j_1 = 6, \tag{8}$$
$$3I_2 - i_2 - j_1 - j_2 = 6, \tag{9}$$
$$3I_3 - i_3 + j_2 - j_3 = 6, \tag{10}$$
$$3I_4 - i_4 + 2j_3 = 6, \tag{11}$$
$$i_1 + 2i_2 + 2i_3 + i_4 = 6. \tag{12}$$

Solution of the system of equations (2) - (12), as shown in the appendix is :

$$j_1 = j_2 = j_3 = 0,$$
$$i_1 = i_2 = i_3 = i_4 = 1,$$
$$I_1 = I_2 = I_3 = I_4 = \tfrac{7}{3}.$$

Thus, coronene significantly differs from other condensed aromatic compounds by the characteristic of collectivized π-electrons. If, for example, in the naphthalene molecule collectivization of the π-electrons gives a current along the C-C bonds, common for two benzene rings, then in coronene the π-electrons are collectivized in two locked-in circular currents, with currents in one and the same direction.

Such a representation of the molecular currents in coronene is in agreement with the available experimental data. Thus, in accordance with ref. [5], the anisotropy of molar diamagnetic susceptibility of coronene is equal to $465 \cdot 10^{-6}$ per mole, while a calculation analogous to those shown in [4] for naphthalene and anthracene, gives $632 \cdot 10^{-6}$ per mole.

3. The indicated character of the collectivization of π-electrons in the coronene molecule shows that the C-C bonds joining the central benzene ring with the peripheral "coronene" ring, approximate ordinary C-C bonds in their character.

It should be assumed that they are analogous to the C-C bonds joining the two benzene rings in the diphenyl $C_{12}H_{10}$ molecule. Their length, obviously, is close to 1.50 Å [6], to which value, by the way, direct X-ray investigations point [7].

The absence of π-electron bonds between the central benzene ring and peripheral "coronene" rings allows us to consider the force interaction between them as equal to zero. The same may also be said concerning the force of interaction

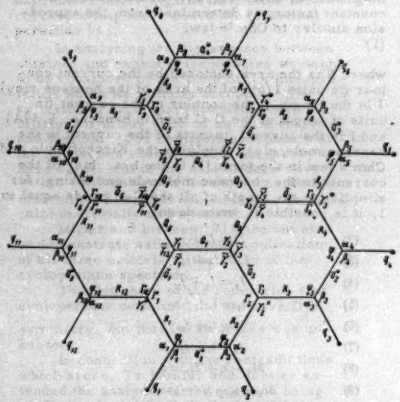

Figure 2. Natural coordinates of coronene (planar vibrations)

of the ordinary bonds Q_1 (see fig. 2) with both rings. The only exception is the kinetic energy coefficients of interaction of the angles Γ_2, Γ_3, with angles γ_2, γ_3, for which, according to [6, 8], it is possible to assume values of $m_\beta = 0.12$ and $n_\beta = 0.02$. The force constant of the inter-ring ordinary bond $K_{Q_1 Q_2}$ may be assumed to be equal to 7.02. Furthermore, owing to the absence of direct force of interaction of the central benzene ring with "the coronene" ring, and the insignificant force of interaction of the rings across the inter-ring bonds Q_1 it is unlikely that the force of interaction in the central benzene ring of the coronene molecule can differ very much from the force of interaction in the ring of the benzene molecule. Therefore, with good enough accuracy it is possible to depict the force of interaction in the central benzene ring by the system of force constants for the benzene molecule, obtained by Kovner [9]. The character of the force of interaction in the "coronene" ring is not known at present.

4. Proceeding from the indicated representation of the character of the force of interaction in the coronene molecule, we shall attempt to elucidate the reason for the presence of the frequencies of 992 and 3070 cm^{-1} in the spectrum of coronene.

For this purpose we shall attempt to make a calculation for the coronene molecule of the six vibrational frequencies of the type A_{1g}. For formulating and solving the corresponding secular equations use was made of the method of Vol'kenshtein, El'iashevich and Stepanov [8]. In figure 2 is represented the designation of 114 natural coordinates, among which there are 45 supplementary relationships. Further, 12 coordinates of symmetry of the type A_{1g} were established with the aid of the table of 16 coefficients of symmetry for the group D_{6h} [8] between which there are 6 supplementary correlations, and, finally the reduced potential energy coefficients (in numerical form) and reduced coefficients of dynamic interaction (in letter form), were calculated. Below are presented the matrices of kinetic energy and force interaction in their final form after calculation of the additional relationships between coordinates of symmetry according to the rule derived in reference [8].

Matrix of Kinetic Energy Interaction

	Q	$\tilde{Q}$	Q*	Γ	β	φ
Q	0.091	−0.091	0	0	0	0
$\tilde{Q}$	−0.091	0.181	0	−0.087	0	0
Q*	0	0	0.181	0.087	−0.111	−0.064
Γ	0	−0.087	0.087	0.139	−0.036	−0.062
β	0	0	−0.111	−0.036	1.091	0
φ	0	0	−0.064	−0.062	0	1.091

Matrix of force of interaction*

$$(Q,\ Q) = \mathcal{K}^s_{QQ} + 2\sqrt{2}\ \mathcal{K}^s_{Q\alpha} + 2\mathcal{K}^s_{\alpha\alpha};$$

$$(\tilde{Q},\ Q) = \mathcal{K}^s_{\tilde{Q}Q} + \sqrt{2}\left(\mathcal{K}^s_{Q\alpha} + \mathcal{K}^s_{\tilde{Q}\alpha}\right) + 2\mathcal{K}^s_{\alpha\alpha};$$

$$(Q^*,\ \varphi) = \mathcal{K}^s_{Q^*\varphi} - \sqrt{2}\ \mathcal{K}^s_{\alpha\varphi};$$

$$(\Gamma,\ \varphi) = \mathcal{K}^s_{\alpha\varphi} - \mathcal{K}^s_{\gamma\varphi} - 2\mathcal{K}^s_{\gamma\alpha} + \frac{\sqrt{3}}{2}\mathcal{K}^s_{\beta\varphi};$$

$$(\varphi,\ \varphi) = \mathcal{K}^s_{\varphi\varphi}$$

The superscript S of the coefficients K^S_{ij} shows that the latter are reduced coefficients of force of interaction for the symmetry type A_{1g}.

Multiplying the matrices written above we find the following expression for diagonal elements of the secular equation, corresponding to coordinates of symmetry Q and q:

$$D_{QQ} = 0.091\left\{\mathcal{K}^s_{QQ} - \mathcal{K}^s_{\tilde{Q}Q} + \sqrt{2}\left(\mathcal{K}^s_{Q\alpha} - \mathcal{K}^s_{\tilde{Q}\alpha}\right)\right\};$$

$$D_{\varphi\varphi} = 1.091\,\mathcal{K}^s_{\varphi\varphi} - 0.064\,(Q^*,\ \varphi) - 0.062\,(\Gamma,\ \varphi).$$

In view of the remarks made above concerning the force of interaction of the benzene ring with the "coronene" ring and their interactions with the inter-ring bonds Q_1, $K^S_{QR} = K^S_{\tilde{Q}\tilde{Q}} = K^S_{\tilde{Q}R} = 0$. From reference [9] we have $K^S_{QQ} = 11.70 \cdot 10^6$ cm^{-2}, from which in the zero approximation

$$\nu_{QQ} = \sqrt{D_{QQ}} = 1031\ cm^{-1},$$

i. e. we really obtain the frequency near the 992 cm^{-1} frequency. We must anticipate that calculation of the small interactions of coordinate Q with other coordinates by means of a more complete and

*We present here only that part of the matrix of force of interaction the knowledge of which is necessary for understanding of the estimation of frequencies carried out below.

more precise system of force constants, the determination of which is coming in the future, ought to reduce the frequency of zero approximation to 992 cm^{-1}. It is appropriate here to observe that even for benzene, in the zero approximation, the frequency of the fully symmetrical vibration of the carbon skeleton is significantly higher than 985 cm^{-1}. Moreover, the correctness of the assignment made by us of the 992 cm^{-1} frequency to type A_{1g} is confirmed also in the fact that in the interval from 365 to 1400 cm^{-1} in the coronene spectrum there are no other lines so intense as the line corresponding to the 992 cm^{-1} frequency; on the other hand, vibrations of the A_{1g} type, as a rule, are very intense.

Further, in the reference [9] it was shown that for benzene, reduction of the kinetic energy coefficients gives $K^S_{qq} = 8.63$ spectroscopic units, as a matter of fact, $K^S_{qq} = K_{q1q1}$, i. e. the force constant of elasticity of the C-H bond. There is no basis for thinking that interaction of the C-H bonds in the coronene molecule can be greatly different from their interactions in the benzene molecule, all the more, since the elasticity constant of the C-H bond varies very little in the transition from simple hydrocarbons to complex aromatic compounds. Thus, for the methyl group it was found to be equal to 8.08, for methane 8.34. Therefore, we have a right to suppose $K_{q1q1} = 8.63$. Interaction of the bonds C-H with carbon bonds Q_i* and R_i is so small that it is possible to disregard them, placing $(Q^*, q) = 0$. Also as small is the interaction of the C-H bonds with the angles α_i, φ_i, and γ_i^*. According to our rough calculation, based on use of the corresponding force constants for benzene, $(\Gamma, q) = 0.25$.

Substitution of the indicated values for K^S_{qq}, (Q^*, q) and (Γ, q) in D_{qq} gives in zero approximation

$$\nu_{qq} = \sqrt{D_{qq}} = 3066 \text{ cm}^{-1}.$$

We may note that this is value of ν_{qq} a little different from the 3066 cm^{-1} also obtained by us by solution of the secular equation by the method of successive approximations under circumstances of very different assumptions concerning the character of the force of interaction in the outer "coronene" ring.

CONCLUSION

The estimations carried out above of some normal vibrations frequencies of the coronene molecule show that the presence in the vibrational spectrum of coronene of bands analogous to the bands which are most strongly represented in the vibrational spectrum of benzene is connected with the basic role of the central benzene ring in the coronene molecule. This ring is very weakly bound dynamically to the remainder of the coronene molecule, and, to a certain extent, is similar to the carbon skeleton of the free benzene molecule. Therefore, it is clear that the frequencies characteristic for the vibrations of the carbon skeleton of the benzene molecule, recur also in the vibrational spectrum of coronene.

Recurrence in the coronene spectrum of frequencies characteristic for vibrations of the C-H bonds in the benzene molecule is connected with the fact that their force of interaction in the coronene molecule does not differ practically from the character of their interactions in the benzene molecule.

In conclusion a debt of gratitude is owed to E. V. Shpol'skii and L. S. Maiants for discussion and constant interest in the work.

SUPPLEMENT

SOLUTION OF THE SYSTEM OF EQUATIONS (2) -(12)

Subtracting equation (9) from (8), (9) from (10), and (10) from (11), and utilizing equations (2) to (7), we obtain the following system of linear homogeneous equations for determination of currents j_1, j_2, and j_3

$$7j_1 + j_2 = 0,$$
$$j_1 + 6j_2 - j_3 = 0,$$
$$j_2 - 7j_3 = 0.$$

The determinant of this system is different from zero, and therefore $j_1 = j_2 = j_3 = 0$. Further solution of the system of equations (2) to (12) is evident.

April 3, 1958

References

1. E. V. SHPOL'SKII, A. A. IL'INA, L. A. KLIMOVA: DAN USSR, 87, 935 (1952)
2. E. V. SHPOL'SKII, L. A. KLIMOVA: DAN USSR, 111, 1227 (1956) (Translation in Sov. Phys. Doklady, 1, 782-6, 1956)
3. E. J. BOWEN, B. BROCKLEHURST: J. Chem. Soc., 3875 (1954); 4320 (1955)
4. M. V. VOL'KENSHTEIN: Stroenie i fizicheskie svoistva molekul (Structure and physical properties of molecules) Akad. Nauk USSR Press, 1955
5. B. PULLMAN, A. PULLMAN: Les theories electronique de la chimie organique. Paris, 1952
6. M. A. KOVNER: OiS, 1, 742 (1956)
7. J. M. ROBERTSON: Organic crystals and molecules. Cornell Univ. Press, Ithaca, N. Y., 1953
8. M. V. VOL'KENSHTEIN, M. A. EL'IASHEVICH, B. I. STEPANOV: Kolebaniia molekul (Vibrations of molecules), vol. 1, GITTL, Moscow, 1949
9. M. A. KOVNER: ZETF, 26, 598 (1954)

TOM VI, Vyp. 2 OPTIKA I SPEKTROSKOPIIA Fevral', 1959
VOL. VI. No. 2 OPTICS AND SPECTROSCOPY February, 1959

On the Simultaneous Absorption of Light in Binary Mixtures

CH. K. MUKHTAROV

Abstract: The question of simultaneous vibrational excitation of two interacting molecules is examined. A formula is obtained which relates the line intensity of simultaneous absorption with the intensity of the characteristic lines in the infrared spectrum and in the Raman spectrum. There is obtained, for the case of molecules possessing a center of symmetry, a simple selection rule which allows one to determine frequencies of lines in the spectrum of simultaneous absorption.

Recently there have appeared several experimental papers [1,2] devoted to a new kind of molecular spectrum which is associated with so-called "simultaneous" absorption in compressed gases and liquids. The outstanding feature of this phenomenon lies in the fact that, under observation of infrared absorption in a mixture of compressed gases or solutions, there appear absorption lines which are absent in the spectra of the pure substances entering into the make-up of the mixture. At the same time, the frequencies ν, corresponding to the absorption lines may be computed, correct to several cm^{-1}, according to the formula

$$\nu = \nu^a \pm \nu^b, \tag{1}$$

where ν^a and ν^b are the fundamental vibrational frequencies of the molecules which are present in the mixture. Such values of frequencies are associated with vibrational excitation of two molecules of different sorts (a and b), which absorb, simultaneously, 1 quantum of radiation of frequency ν.

Unfortunately, we have been unable to find in the literature available, treatment of this absorption, which is associated with intermolecular interaction; hence, an elementary theory of the phenomenon is set forth below.

As is well known, the wave function of a molecule may be approximately represented as a product of electron and vibrational eigenfunctions:

$$\psi_{e,v} = \psi_e(r, q)\,\psi_v(q).$$

The total wave function depends on the normal coordinates, q, of the nuclei, and on the coordinates, r, of all the electrons; e and v are the electron and vibrational quantum numbers; q enters as a parameter in the electron function $\psi_e(r, q)$, pertaining to immobile nuclei which are fixed in location q. $\psi_v(q)$, in the case of small vibrations, appears as a product of wave functions of harmonic oscillators.

We shall investigate the absorption of light by a molecule of sort a. For an isolated molecule, the probability of vibrational transition under the influence of radiation is proportional to the square of the matrix element of the dipole moment $[p^{0a}]_{ee,v'v''}$ between the wave functions of an isolated molecule. Since vibrational transitions will be considered only for a stationary electronic state of a molecule, the subscript ee may be dropped. We then get

$$[p^{0a}]_{v'v''} = \int \psi_{v'}^{0a*}(q_a^0)\, p_j^0(q_a^0)\, \psi_{v''}^{0a}(q_a^0)\, dq_a^0 = \int \psi_{v'}^{0a} p_j^{0a} \psi_{v''}^{0a} dq_a^0, \tag{2}$$

Here

$$p_j^0 = p_j(r, q_a^0) = e_i r_{ij} + e_k z_{kj}^0, \tag{3}$$

$$p_j^{0a} = p_j^0(q_a^0) = \int |\psi_e^0(r, q_a^0)|^2\, p_j^0\, dr, \tag{4}$$

where e_i is the electronic charge, r_{ij} is the j-th component of the coordinate of the i-th electron, and $e_k z_{kj}^0$ is a linear combination of the nuclear charges. In formula (4), as in what follows, the summation is performed over the suppressed subscripts.

In the case which interests us (a gas mixture or a solution) molecule a is not isolated since it is surrounded by interacting neighbors (system b); this leads to a change in the wave function of the molecule, and, consequently, to a change in the transition probability.

In the case of non-interacting systems, simultaneous transitions will not occur because the dipole moments are additive and the matrix elements for transitions of molecule a differ from zero only when transitions in system b are absent.

Let $E^a(q_m^b) = E^a$ be the electric field produced by system b (this may be a single molecule or a group of molecules) at the place where molecule a is located. The energy of the molecule in this field is:

$$\Delta W^a(r, q_a^0, q_m^b) = -p_j^{0a} E_j^a. \tag{5}$$

As is evident from formula (1), the energy of the molecule changes insignificantly; therefore, when calculating the wave functions, we shall take advantage of perturbation theory. In the first approximation for the electronic wave function of molecule a, we get

$$\psi_e(r, q_a^0) = \psi_e^0(r, q_a^0) + E_j^a \psi_j^a, \tag{6}$$

where

$$\psi_j^a = \sum_{e \neq e'} \frac{[p_j^a]_{e'}}{W_e^a - W_{e'}^a} \psi_{e'}^0(r, q_a^0), \tag{7}$$

and W_e^a are electron terms of the isolated molecule a.

When finding $\psi_v(q_k^a)$ in the vibrational Schrödinger equation, the potential energy is increased by

$$[\Delta W^a(r, q_a^0, q_m^b)]_{av} = -p_j^{0a} E_j^a. \tag{8}$$

In the case of small vibrations, p_j^{0a} may be expanded in powers of q_a^k keeping only the linear terms:

$$p_j^{0a} = p_j^{0a}(0) + \left(\frac{\partial p_j^{0a}}{\partial q_a^k}\right)_0 q_a^k + \ldots \tag{9}$$

Hence,

$$[\Delta W^a(r, q_a^0, q_m^b)]_{av} = -p_j^{0a}(0)\, E_j^a - E_j^a \left(\frac{\partial p_j^{0a}}{\partial q_a^k}\right)_0 + \ldots \tag{10}$$

As is well known, the addition of a linear term in q_k^a into Schrödinger's equation for a harmonic oscillator causes the vibrational wave functions to take the form

$$\psi_v(q_a^0) = \psi_v^0(q_a^0 - \gamma_{kj}^a E_j^a), \tag{11}$$

where

$$\gamma_{kj}^a = \frac{1}{m\omega^2}\left(\frac{\partial p_j^{0a}}{\partial q_a^k}\right)_0. \tag{12}$$

Here m and ω are the effective mass and angular frequency of the k-th normal vibration.

The matrix element of the i-th component of the dipole moment of molecule a is:

$$[p_i^{0a}]_{v'v''} = \int \psi_{v'}(q_a^0) \int |\psi_e(r, q_a^0)|^2\, p_i^0\, dr\, \psi_{v''}(q_a^0)\, dq_a^0. \tag{13}$$

Using expressions [6] and [11] for the wave functions and making a substitution of variables:

$$[p_i^{0a}]_{v'v''} = \int \psi_{v'}(q_a^0) \int |\psi_e(r, q_a^0)|^2\, p_i^0\, dr\, \psi_{v''}(q_a^0)\, dq_a^0. \tag{14}$$

where

$$(15)\qquad \alpha^a_{ij}\left(q^a_k\right)=2\int \left|\psi^0_e\left(r,\, q^a_k\right)\varphi^*_j\right| p^a_i\, dr.$$

Expanding $p^0_i\,(q^a_k+\gamma^a_{kj}E^a_j)$ and $\alpha^a_{ij}\,(q^a_k-\gamma^a_{kj}E^a_j)$ in a Taylor series about q^a_k and keeping the terms linear in E^a_j, we find

$$(16)\qquad [\Delta p^a_i]_{v'v''}=[p^{ab}_i-p^{ab}_i]_{v'v''}=E^a_j\int \psi^{ab}_{v'}\left|\gamma^a_{ij}\frac{\partial p^{ab}_i}{\partial q^a_k}+\alpha^a_{ij}\right|\psi^{ab}_{v''}\,dq^a_k.$$

The first term in the braces, associated with the change in the motion of nuclei in an external field, is proportional to the quantity $e^a_k=\left(\partial p^{0a}_i/\partial q^a_k\right)$ the effective charge of the k-th normal vibration. Hence it is determined by the intensity of the corresponding infrared spectral line. The second term corresponds to the electronic polarizability of molecule a as a function of q^a_k; this polarizability, as is well known, is associated with the intensity of the Raman spectrum.

The matrix element of the additional dipole moment of molecule b, induced by molecule a, may be obtained by analogous means:

$$(17)\qquad [\Delta p^b_i]_{v'v''}=E^a_j\int \psi^{ab}_{v'}\left|\gamma^b_{mj}\frac{\partial p^{ab}_i}{\partial q^b_m}+\alpha^b_{ij}\right|\psi^{ab}_{v''}\,dq^b_m.$$

The probability of a simultaneous transition is proportional to the square of the matrix element of the total dipole moment, $[\Delta p^{ab}_i]\,v'u'v''u''$ where

$$(18)\qquad \begin{aligned}[\Delta p^{ab}_i]_{v'u',v''u''}=&\int \psi^{ab}_{v'u'}E^a_j\psi^{ab}_{v''u''}\,dq^a_k\int \psi^{ab}_{v'}\left|\gamma^a_{ij}\frac{\partial p^{ab}_i}{\partial q^a_k}+\alpha^a_{ij}\right|\psi^{ab}_{v''}\,dq^a_k+\\ &+\int \psi^{ab}_{v'u'}E^b_j\psi^{ab}_{v''u''}\,dq^a_k\int \psi^{ab}_{v'}\left|\gamma^b_{mj}\frac{\partial p^{ab}_i}{\partial q^b_m}+\alpha^b_{ij}\right|\psi^{ab}_{v''}\,dq^b_m.\end{aligned}$$

Expanding E^a_j, E^b_j and the expression in the braces in series we will get an integrand in which the linear terms in q alter the transition probability in the infrared spectrum, or if the transition is forbidden, remove that restriction. Terms of the second degree in q are associated with binary transitions in one molecule or, with simultaneous transitions in two molecules. The matrix element corresponding to a simultaneous transition v', $u'\to v''$, u'' is defined by the equation:

$$(19)\qquad \begin{aligned}[\Delta p^{ab}_i]_{v'u',\,v''u''}=&\left[\left(\frac{\partial E^a_j}{\partial q^a_m}\right)_0\left[\gamma^a_{ij}\left(\frac{\partial p^{ab}_i}{\partial q^a_k}\right)_0+\left(\frac{\partial \alpha^a_{ij}}{\partial q^a_k}\right)_0\right]+\right.\\ &\left.+\left(\frac{\partial E^b_j}{\partial q^b_k}\right)_0\left[\gamma^b_{mj}\left(\frac{\partial p^{ab}_i}{\partial q^b_m}\right)_0+\left(\frac{\partial \alpha^b_{ij}}{\partial q^b_k}\right)_0\right]\right][q^a_k]_{v'v''}[q^b_m]_{u'u''}.\end{aligned}$$

For the probability of a simultaneous transition per unit time, w^{ab}, we have

$$(20)\qquad w^{ab}=\frac{2\pi}{\hbar^2}\left|n_i[\Delta p^{ab}_i]_{v'u',\,v''u''}\right|^2\rho(\nu),$$

where n is a unit vector in the direction of the electric field vector of the light wave and $\rho(\nu)$ is the spectral radiation density.

Thus, there exists the possibility of emission and absorption of quanta with energy $h(\nu^a\pm\nu^b)$, so that the probability of transition is related to the value of the inducing field, through $\left(\partial E^a/\partial q^b\right)_0$, and to the electro-optic characteristics, through the derivatives of polarizability and dipole moment with respect to the normal coordinates of molecules. The intensity of lines in simultaneous absorption is determined by means of formula (19) in which one should, naturally, take into consideration the population of the levels; this plays an essential role because the presence of excitation in system b is necessary for the absorption of a quantum $h(\nu^a-\nu^b)$.

For centrally symmetric molecules, in which there occurs a further restriction, formula (19) may be simplified.

In this case, $\gamma^a_{kj}\left(\frac{2\,p^{0a}_i}{q^{a2}_k}\right)_0=0$, since, if the pertinent frequency is forbidden in the infrared spectrum, then $\gamma^a_{kj}=0$, and, if the frequency is forbidden in the Raman spectrum, then $\left(\frac{\partial 2\,p^{0a}_i}{\partial q^{a2}_k}\right)_0=0$.

Therefore, the matrix element of the dipole moment, in this case, equals:

$$(21)\qquad [\Delta p^{ab}_i]_{v'u',\,v''u''}=\left[\left(\frac{\partial E^a_j}{\partial q^a_m}\right)_0\left(\frac{\partial \alpha^a_{ij}}{\partial q^a_k}\right)_0+\left(\frac{\partial E^b_j}{\partial q^b_k}\right)_0\left(\frac{\partial \alpha^b_{ij}}{\partial q^b_m}\right)_0\right][q^a_k]_{v'v''}[q^b_m]_{u'u''}.$$

From this formula it follows that simultaneous absorption is possible not for just any combination of ν^a and ν^b, but only for those such that at least one of the combining frequencies is active in Raman spectrum. Simultaneous absorption does not take place if both combining frequencies are active in the infrared spectrum

If one were to consider that the electric field E^a_j is associated with the dipole moment of a molecule $p^b_m=p^b_m(0)+e^b_m q^b_m$, then

$$(22)\qquad [\Delta p^{ab}]_{v'u',\,v''u''}\sim\frac{e^b_m}{R^3}\left(\frac{\partial \alpha^a}{\partial q^a_k}\right)[q^a_k]_{v'v''}[q^b_m]_{u'u''},$$

where R is the distance between molecules. Consequently, in the spectra of simultaneous absorption of molecules possessing a center of symmetry frequencies may combine only when one is active in the infrared spectrum and the other in the Raman spectrum.

The formulas obtained should certainly not be used for precise quantitative calculations since they are derived from simplified assumptions concerning the character of intermolecular interactions; however, they are useful in that they allow one to determine simply the frequencies at which one may expect simultaneous absorption, and to estimate its intensity.

The author takes pleasure in expressing thanks to I. V. Obreimov for his interest in this work and for a series of valuable suggestions, as well as to S. I. Pekar for helpful discussions.

April 18, 1958

References

1. J. A. A. KETELAAR, F. N. HOOGE: Rec. trav. chim., 76, 529 (1957)
2. J. FAHRENFORT, J. A. A. KETELAAR: J. Chem. Phys., 22, 1631 (1954)

TOM VI, Vyp. 2 OPTIKA I SPEKTROSKOPIIA Fevral', 1959
VOL. VI. No. 2 OPTICS AND SPECTROSCOPY February, 1959

Absorption Spectra of Dye Films in Vacuo

L. A. LYZINA AND A. T. VARTANIAN

Abstract: A method is described for the preparation of solid dye films by sublimation, and the subsequent measurement of their absorption spectra in vacuo. Spectra of films of twelve dyes of six classes are shown. The spectra are compared with spectra of solutions and films obtained by deposition from solution.

INTRODUCTION

The spectral study of dye films obtained by deposition from solution have permitted the determination of the existence of a relation between the state of the dye in solution and of the film obtained from that solution [1, 2]. Since the degree of aggregation of the dye depends on the nature of the solvent and the concentration of the solution, it seemed interesting to study the absorption of the dye films obtained without the use of any solvent. Such a film can be obtained by sublimation of the dye in vacuo. The first attempt at a systematic investigation of solid films of dyes obtained by sublimation in vacuo was made by one of the authors [3]. Absorption spectra of films of more than forty dyes, belonging to many classes, were measured in air. For methylene blue, by means of these spectra the change in the structure of the film due to the influence of atmospheric moisture has been confirmed and spectrophotometrically examined in detail.* It was to be expected that the moisture in the air could affect the structure of films of other dyes.

In order to eliminate the influence of atmospheric moisture on the sublimed film, it was necessary to measure their absorption spectra in vacuo, without exposure to air after sublimation. Such measurements have been already performed for Rhodamine B, Malachite Green, Trypaflavine, Pinacyanole and Methylene Blue by Weigl [6]. However, his method of preparation of films and the interpretation he gave to the results are open to discussion.

The task we undertook was, on one hand, to obtain absorption spectra in vacuo of sublimed films of a large number of dyes, and on the other hand, to follow, by means of the spectra, the changes that take place in the films under the influence of humidity.

In the present article we are concerned only with the first task.**

EXPERIMENTAL PART

In order to obtain sublimed films of dyes and measure their absorption spectra in vacuo, a glass vessel was used as shown in fig. 1, a. The dye intended for sublimation is deposited from solution as a solid layer in the well O (fig. 1, b). A plate P is placed over the well. The vessel, in the horizontal position, is connected to a high vacuum system by means of a glass joint. The dye in the well is heated by a small electric oven placed over the well. After the dye film has been deposited on the plate the stopcock K is closed and the vessel disconnected from the system. Turning the vessel into the vertical position throws the disc with the deposited film into the lower part of the vessel - into a space between parallel quartz windows (fig. 1, c). The latter had a thickness of 2 mm and were glued to the vessel with Piceine.

The size of the vessel was such that it fit precisely to the frame for solid samples on a SF - 4 spectrophotometer.

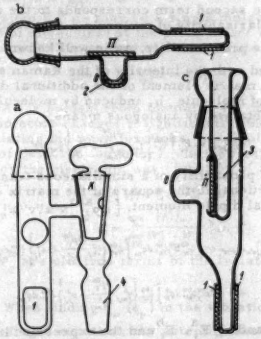

Figure 1. Apparatus for sublimation and measurement of spectra of films of dyes in vacuo. a - general view of the vessel; b and c - variants of the main part.

In order to obtain sublimed films, we generally followed the sublimation temperatures given in paper [3]. Nonetheless, on sublimation of the dye from the well, we encountered some deposits whose mention we consider necessary.

1) For the series of dyes which are easily decomposed by overheating (Crystal Violet, Methylene Blue, etc.) it was necessary that the layer in the well be thin and, if possible, uniform, because dyes in clumps easily undergo changes connected with tarring.

On the other hand for Rhodamine B the thickness of the dye layer in the well should be greater. Otherwise it undergoes the changes described in paper [3].

In order to prevent overheating of the dye, the well should be as short and wide as possible. In order to obtain sublimed films of Methylene Blue and Crystal Violet, we had to give up the use of the well altogether and build up the dye on the

*The change of the absorption spectrum of a film of Methylene Blue with the change in its structure under the influence of humidity has been established previously for films obtained by deposition from a hot alcoholic solution [4]. For films of Crystal Violet and Malachite Green deposited from solution, Dilung and Dain [5] studied the change of their absorption spectra with air pumped out followed by letting it in again.

**An article dealing with the second question will be published later.

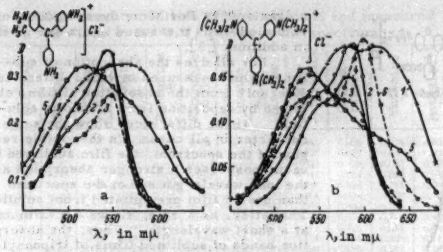

Figure 2. Absortion of triphenylmethane dyes:
a - Fuchsine, b - Crystal Violet
1 - Sublimed film in vacuo, 2 - Dilute aqueous solution, 3 - concentrated aqueous solution 4 - alcoholic solution, 5 - Film obtained by deposition from solution, 6 - benzene solution.

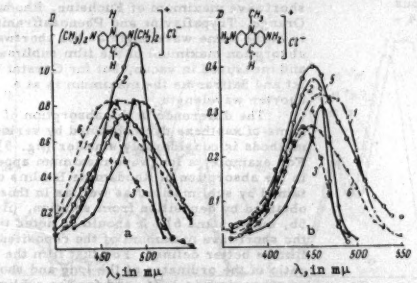

Figure 3. Absorption of acridine dyes:
a - Rhoduline Orange; b - Trypaflavine
1 - Sublimed film in vacuo, 2 - dilute aqueous solution, 3 - concentrated aqueous solution, 4 - alcoholic solution, 5 - sublimed film, measured in air [3], 6 - film deposited from solution.

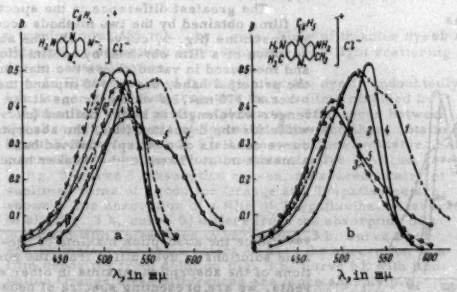

Figure 4. Absorption of azine dyes:
a - Phenosaffranine b - Saffranine O.
1 - Sublimed film in vacuo, 2 - dilute aqueous solution, 3 - concentrated aqueous solution, 4 - alcoholic solution 5 - film deposited from solution, 5 - film deposited from solution, 6 - benzene solution.

wall of the vessel.

We were not able to obtain a film of Malachite Green free of decomposition products in the vessel which was constructed as described above. After heating for 15-20 minutes the dye became completely brown and a colorless substance deposited on the plate. However, using the vessel described in paper [3], the duration of the sublimation could be prolonged to an hour without damage. Therefore, if it is intended to perform the measurement in air, it is better to approach it by the more delicate method described in paper [3], in which the dye is sublimed from a quartz finger placed in a jacket connected to a high vacuum system.

2) At the sublimation point of the dye it is necessary - as a rule - to avoid direct heating of the plate, since at a higher temperature a change of structure can take place, e. g. crystallization. To prevent the heating of the plate one can, e. g., hinge it to the finger with glass hooks attached to a sealed cover. This method of hingeing the plate has the advantage that, by filling the finger with a cool or hot liquid, one can change the temperature of the plate as desired.

3) In all cases a rapid sublimation is preferred. In order to avoid local overheating of the dye, it must not be heated with an open flame. Such overheating apparently took place in Weil's experiments, because, according to the author, a brownish deposit remained after sublimation. In fact, he did not work with films of pure dyes but with a mixture of the dye and its decomposition products. In each experiment the decomposition of the dye could proceed to a different degree and therefore the inconsistency of Weil's data is not surprising.

4) To be sure of the absence of decomposition products in the sublimed film, it is imperative to measure in the ultraviolet region, since it is not always possible to detect such changes in the visible.

In the present article, the results of measurements of twelve dyes belonging to various classes are given. The plates were made of fused quartz discs. The measurements of absorption spectra were performed on a SF-4 spectrophotometer. Since films of some dyes may undergo changes in time, not only in air but also in vacuo, the spectra were measured immediately after the deposition of the film. In figures 2 to 7 the values of optical density are given, since the thickness of films was not determined and no correction for reflection was made.

RESULTS

In figures 2 to 7 absorption spectra of dye films obtained by measurements in vacuo are shown. *** They are compared with absorption spectra of films obtained by deposition from solution and with spectra of the dyes dissolved in water, alcohol and other organic

***In general, the absorption spectra are shown only for the visible region. Data for absorption in the ultraviolet region are given in the table.

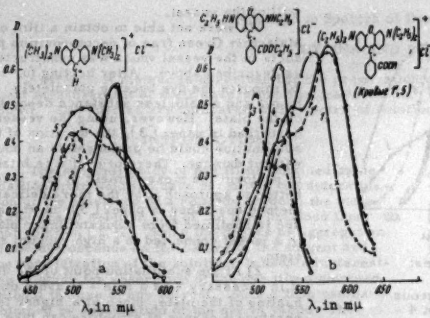

Figure 5. Absorption of xanthene dyes:
a - Pyronine, b - Rhodamine 6G and B.
1 - sublimed film in vacuo, 2 - diluted aqueous solution, 3 - concentrated aqueous solution, 4 - alcoholic solution, 5 - film deposited from solution.

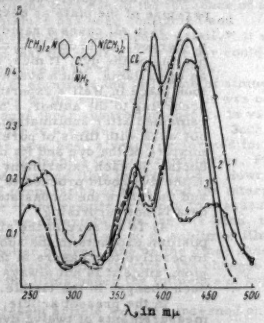

Figure 6. Absorption of Auramine O.
1 - sublimed film in vacuo; 2 - aqueous solution, 3 - alcoholic solution, 4 - film deposited from an alcoholic solution.

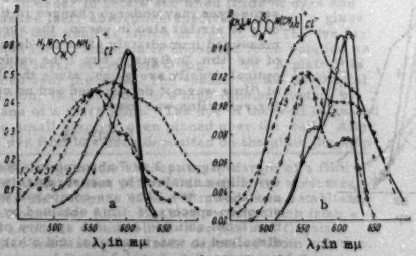

Figure 7. Absorption of thiazine dyes:
a - Thionine, b - Methylene Blue.
1 - sublimed film in vacuo, 2 - dilute aqueous solution, 3 - concentrated aqueous solution, 4 - alcoholic solution, 5 - sublimed film, measured in air.

solvents.**** For some dyes, spectra of sublimed films measured in air are given in addition. [3].

For all dyes the absorption of sublimed films measured in vacuo differs considerably from the absorption of films obtained by deposition from alcoholic solution. These differences show the same character in all cases. In the visible region of the spectrum, the film sublimed in vacuo possesses a stronger absorption at the long wavelength end of the spectrum than does a film precipitated from solution. The latter, as a rule, shows a maximum at a short wavelength. Thus, the absorption bands of sublimed films of triphenylmethane -, acridine - and azine dyes, measured in vacuo, show two maxima of approx. the same height. (figs. 2 to 4, curve 1). Films deposited from solution (figs. 2 to 4, curve 5) show asymmetrical bands and the absorption occurs at the short wavelength end of the spectrum. This shortwave maximum of Fuchsine, Rhoduline Orange, Trypaflavine and Phenosaffranine is at the same wavelength as the shortwave absorption maximum of the film sublimed and measured in vacuo, but for Crystal Violet and Saffranine the maximum is at a shorter wavelength.

The difference in the absorption of films of xanthene dyes obtained by various methods is considerably smaller (fig. 5). For example, a longwave maximum appears in the absorption of Rhodamine B films obtained by sublimation, as well as in those obtained by deposition from solution, (fig. 5b, curve 5 and 6). It should be noted that the shortwave maximum of the deposited film is better defined. For that film the ratio of the ordinates of the long and shortwave maxima is 1.34, and for the sublimed film it is 1.54. The spectra of films of Pyronine G obtained by sublimation and by deposition from solution show a shortwave maximum (fig. 5a, curve 1 and 5), which in the cases examined above, occurs in films deposited from solution.

The greatest difference in the spectra of films obtained by the two methods occurs in Auramine (fig. 6, curve 3, 4). The absorption of a film obtained by sublimation and measured in vacuo shows two maxima in the principal band, one at 430 mμ and the other at 370 mμ, of which the one at the longer wavelength is better defined (curve 3), while for the deposited film, the absorption curve consists of a sharply defined band with a maximum at 390 mμ and a weaker band with

**** Since the absorption maxima of benzene solutions of dyes differ from the positions of the absorption maxima in other solvents, we are presenting spectra of benzene solutions of all dyes for which such solutions could be obtained. The absorption maxima of dye solutions in acetone, chloroform, etc., lie approximately at the same wavelength as the maxima of water and alcohol solutions.

Optical density of films of dyes obtained and measured in vacuo in the U.V. region of the spectrum

(in mμ)	Fuchsine	Crystal Violet	Pyronine G	Rhodamine B	Rhodamine 6 G	Rhodoline Orange	Trypaflavine	Phenosaffranine	Saffranine O	Thionine	Methylene Blue
400	0,025	—	0,085	0,079	0,051	—	—	0,041	0,028	0,074	0,034
390	0,035	—	0,072	0,075	0,056	—	—	0,038	0,022	0,080	0,034
380	0,047	—	0,068	0,075	0,059	—	—	0,037	0,020	0,087	0,036
370	0,060	—	0,061	0,088	0,078	—	—	0,041	0,024	0,093	0,042
360	0,076	0,000	0,066	0,119	0,104	—	—	0,046	0,026	0,111	0,048
350	0,088	0,026	0,072	0,121	0,100	0,079	0,052	0,054	0,035	0,146	0,061
340	0,090	0,011	0,077	0,107	0,087	0,085	0,052	0,064	0,039	0,191	0,075
330	0,080	0,022	0,080	0,097	0,083	0,120	0,063	0,076	0,050	0,248	0,089
320	0,095	0,053	0,091	0,145	0,101	0,222	0,074	0,117	0,126	0,314	0,086
310	0,130	0,065	0,125	0,194	0,146	0,474	0,147	0,154	0,134	0,339	0,112
300	0,184	0,051	0,174	0,201	0,167	0,753	0,231	0,190	0,189	0,397	0,157
290	0,158	0,041	0,214	0,226	0,175	0,854	0,301	0,315	0,338	0,498	0,196
280	0,131	0,043	0,228	0,239	0,178	1,140	0,367	0,490	0,512	0,533	0,191
270	0,116	0,046	0,284	0,301	0,190	1,299	0,472	0,490	0,515	0,510	0,175
260	0,127	0,045	0,405	0,389	0,279	1,130	0,472	0,380	0,460	0,497	0,153
250	0,144	0,040	0,448	0,321	0,380	0,730	0,384	0,266	0,362	0,478	0,146
240	0,150	0,029	0,408	0,387	0,369	0,643	0,262	0,211	0,262	0,490	0,120
230	0,143	0,045	0,274	0,417	0,351	0,814	0,211	0,211	0,242	0,488	0,105
220	0,242	0,105	0,603	0,412	0,334	0,610	0,196	0,224	0,271	0,482	0,115

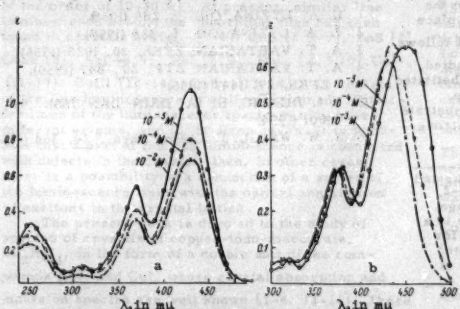

Figure 8. The dependence of the absorption of Auramine O on concentration:
a - alcoholic solution, b - solution in dichlorethane. The curves represent molecular concentrations.

a maximum at 455 mμ. As a rule, films of thiazine dyes obtained by deposition from solutions show light scattering due to crystallization.

In films deposited from solution the dye is undoubtedly in a larger state of aggregation than in films obtained by sublimation. This partly explains the differences between the absorption spectra of deposited films and those obtained by sublimation in vacuo [5]. As shown before, moisture has a considerable influence on the state of a dye in vacuo. ***** In fig. 3 (curve 5) absorption curves, measured in air, of sublimed films of Rhoduline Orange and Trypaflavine are shown. The absorption of a film of Trypaflavine, measured in air (fig. 3 b, curve 5) differs from the absorption of a sublimed film, measured in vacuo (fig. 3 b, curve 1) to approximately the same extent as does the absorption of a film deposited from solution (fig. 3 b, curve 6); with Rhoduline Orange these differences are more sharply pronounced (fig. 3 a, curves 1, 5, 6). A greater difference also occurs for sublimed films of Thionine, one of which was measured in vacuo, and the other in air (fig. 7 a, curves 1 and 5).

***** A detailed discussion of these results will be given in another paper.

This and other differences in absorption of sublimed films, measured in one case in air and in another in vacuo, undoubtedly depends not only on the varying tendency of the dye to change its state under the influence of humidity, but also on the duration of the exposure of the dye to air before the spectrophotometric measurement, the humidity of the air, the thickness of the investigated layer, etc.

Let us compare now the absorption spectra of films obtained and measured in vacuo with the spectra of solutions. The greatest similarity between these spectra occurs in Auramine (fig. 6, curves 1 to 3). Not only do the positions of the maxima coincide, but in addition, the ratio of their ordinates (if the absorption curve of the sublimed film is split into two components - the dotted curves in the figure) is similar. For the film this ratio of the ordinates is 2.14, for the aqueous solution 2.23, and for the alcoholic solution 2.02.

It has been shown experimentally that the absorption bands of Auramine, with maxima at 370 and 430 mμ, are due to two modifications of the dye. This is proved by the fact that in spectra of Auramine solutions of different origin, the ratio of the ordinate of the long wave maximum to the ordinate of the short wave maximum varies in solutions of identical concentration: for one of our specimens, this ratio, in aqueous solution, was of the order of 2.25, in alcohol, 2.00; for the other sample the ratio was 2.45 in water, 2.20 in alcohol.

It was found that the component of the powdered dye which is characterized by absorption at 370 mμ (form II) dissolves in benzene more easily than the other component, which is characterized by absorption at 430 mμ (form I.). The solubility difference is so great that they can be separated. A saturated aqueous solution chromatographed over an Al_2O_3 column showed two yellow rings. We think that form I represents the genuine Auramine. The nature of the form II is not yet clear. It is, however, important to note that under certain definite conditions during process of sublimation of the dye from the well, form I can change to form II.

For Auramine the change of absorption with increasing concentration was observed not only in aqueous solutions but also in such organic solvents as alcohol, acetone and dichlorethane. Figure 8 shows absorption spectra of Auramine solutions in alcohol (fig. 8, a) and dichlorethane (fig. 8, b). On increasing the concentration of the dye in alcohol, a change in the positions and ratio of the maxima was not observed; however, a general decrease in absorption occurs. Such an effect takes place in aqueous solutions of Auramine.

In dilute solutions of Auramine in dichlorethane, the absorption maxima lay at 450 and 378 mμ. At higher concentrations, a shift of both bands towards shorter wavelengths takes place: the maximum of the long wavelength band shifts to 430 mμ, the maximum of the short wavelength band to 370 mμ. An analogous, though weaker,

change is observed for acetone solutions of Auramine. The half width of the absorption band depends on the nature of the solvent****** In ethyl alcohol the half width is ~2500 cm^{-1}, in acetone and dichlorethane ~3000 cm^{-1}, in water solution ~3500 cm^{-1}. For solid films of Auramine the halfwidth of the band reaches 4000-4500 cm^{-1}. An analogous increase of the half-width band with the transition from solutions to solid films takes place also for other dyes. Such a broadening of bands for films means a significant increase of the influence of identical molecules on each other.

The spectra of films measured in vacuo differ from the spectra of solutions by the presence also of additional absorption on the long wavelength side (fig. 2 to 5, 7). We attribute it to the molecules of the dye being bound to the support by absorption forces. This idea has been presented and illustrated by us before [2].

It is noteworthy that for Thionine, Trypaflavine and Fuchsine this additional absorption is shifted more towards longer wavelengths, and is better defined than for Methylene Blue, Rhoduline Orange and Crystal Violet, (fig. 2, 3, 7) which differ from the former by the presence of $N(CH_3)_2$-groups in place of the NH_2-group. From the cited examples it follows that for the pairs of dyes of the same class studied, the bond to the support is stronger for an unsubstituted amino group than for a substituted amino group.

For Auramine, the interaction with the substrate is very weak. For the Rhodamines, it is the strongest.

Since the longwave absorption in the spectra of films obtained by deposition from solutions and of sublimed films exposed to air (influence of moisture), is either almost absent or noticeably weakened in comparison with the absorption of a film sublimed in vacuo, one can assume that in air the bond between the molecules of the dye and the support is weak. Along with the weakening of the bond between the dye molecule and the support, an increase of the degree of aggregation of the dye molecules apparently takes place, since the absorption curve of the film bears resemblance to the absorption curve of a concentrated aqueous solution.

We postpone the discussion of the state of dyes in solid films until the publication of the results of studying the influence of steam on the spectrum of films of dyes sublimed in vacuo.

March 4, 1958

References

1. L. A. LYZINA: OiS, 5, 286 (1958)
2. L. A. LYZINA: OiS, 5, 428 (1958)
3. A. T. VARTANIAN: ZFKh, 30, 1028 (1956)
4. A. T. VARTANIAN: ZTF, 20, 847 (1950); ZFKh, 29, 1447 (1955)
5. I. I. DILUNG, B. IA. DAIN: DAN USSR, 95, 1001 (1954)
6. J. W. WEIGL: J. Chem. Phys., 24, 364 (1956)

****** On changing the concentration of aqueous and alcohol solutions within the limits of 10^{-5} to 10^{-2} mol/l, the half-width of the band does not change. In the case of acetone and dichlorethane, there is a change in the half width of the absorption band for the most concentrated solutions.

TOM VI, Vyp. 2 OPTIKA I SPEKTROSKOPIIA Fevral', 1959
VOL. VI. No. 2 OPTICS AND SPECTROSCOPY February, 1959

Line Luminescence and Reflection Spectra of Copper-Iodo-Mercurate Crystals at Low Temperatures

CHAO HUAN-TSEN

Luminescence spectra of crystals of Cu_2HgI_4 were investigated at T = 4.2°K. A great number of narrow emission lines was observed in the luminescence spectra, and were distributed around the longwave edge of crystal absorption. Diffuse reflection spectra of powdered Cu_2HgI_4 at T = 4.2°K. were obtained in which a line structure around the absorption edge was also detected. The question of the origin of the line structure of the spectra of Cu_2HgI_4 is discussed.

1. Recently a great number of communications have appeared, in which the distinctive luminescence of many inactive crystals, mainly salts, observed at low temperatures is described. The spectrum of this luminescence usually consists of a group of more or less narrow lines, distributed around the longwave absorption edge of the crystal. The absorption edge of a crystal possessing line luminescence has, in all cases, complex line structure, from which is noted the resonance of some of the luminescent lines with the absorption lines (usually there is a Stokes shift of the order of 20-30 Å). At present, similar line luminescence around the absorption edge has been found in crystals of HgI_2 [1-4], CdS [2,5-7], ZnS [2] CdSe [8], AgI [2,9], PbI [2,9], PbI_2 [2,3,10], CuI [11-14], CuCl [12-14], CuBr [13-14]. The origin of the line luminescence is still unexplained. Different lines of the luminescence spectrum may have different origins, and if, in some cases, it is probable that a part of the line luminescence is connected with defects in the crystal, then, in other cases, there is a possibility of a connection of a series of the luminescence lines with the optical annihilation of excitons in the crystal lattice.

The present work is devoted to the study of spectra of crystals of copper-iodo-mercurate, Cu_2HgI_4, in the form of a double salt of the compounds HgI_2 and CuI, whose crystal absorption and emission spectra are well known [1-4, 11-14]. There is reference in the literature to the existence of low temperature line luminescence of Cu_2HgI_4 [3]; in the paper [15] the complex spectral curve of the reflection coefficient of powdered Cu_2HgI_4 at room temperature is also given. In the present work, the luminescence and the diffuse reflection spectra of crystals of Cu_2HgI_4 at low temperatures are subjected to a detailed study.

2. The crystals of Cu_2HgI_4 occur in two modifications. The present work deals with the β-modification of Cu_2HgI_4, which is stable below 70°C. This form has a tetragonal lattice [16] in which it is possible to discern the I layer and, in between, alternately distributed Cu and Hg [17].

The Cu_2HgI_4 was prepared as a fine crystalline powder in several ways: by grinding together equivalent quantities of powdered CuI and HgI_2 in ethyl alcohol (sample I); by chemical reaction of aqueous solutions of $K_2HgI_4 + 2KI + 2CuSO_4 \rightarrow Cu_2HgI_4 + 2K_2SO_4 + 2I$ followed by washing and drying of the precipitated Cu_2HgI_4 (sample II and sample III were prepared with great care); by recrystallizing the powder obtained in the above manner in boiling hydrochloric acid (sample IV); by melting together stoichiometrically equivalent amounts of the components HgI_2 and CuI in vacuo at T = 450°C, followed by slow cooling of the melt and recrystallization in boiling HCl (sample V). In each case a red powder of a different shade was obtained; the shade depended on the manner of preparation. Unlike the others, the powder recrystallized from HCl, showed numerous points of reflected light, which suggests that the crystallites have larger dimensions in this case.*

3. The spectra of powdered Cu_2HgI_4 were photographed using prism spectographs of high dispersion (ISP-51 with a UF-85 camera, giving a dispersion in the investigated region of D~6 Å/mm and with a "Schmidt and Haensch" giving a value of D~5 Å/mm). Low dispersion (ISP-51 with a 270 mm camera, giving D~60 Å/mm) was also used. The excitation of luminescence was effected by the radiation of a mercury lamp SVDSH-250, using an FS filter (i.e., basically by the line λ = 436 mμ); the latter coincides with the intrinsic absorption region of the Cu_2HgI_4 crystals. The diffuse reflection spectra were obtained by illuminating the powder with light from an incandescent lamp using a yellow filter which cuts off the short wave region of the spectrum.

We investigated the luminescence spectra of Cu_2HgI_4 mainly at T = 4.2°K** because the light intensity fell off strongly on heating and was extremely weak even at T = 77°K.

The luminescence spectra of the powdered Cu_2HgI_4 at T = 4.2°K consists of a large number of lines of various intensities lying in the yellow-green part of the spectrum in the region 5450-5700 Å; the emission lines of the crystals of CuI and HgI_2 composing Cu_2HgI_4 lie respectively around 4000 and 5300 Å. The intensity of the luminescence is noticeably different in samples of different origin. While the general character of line emission spectra is retained, there is also a difference in the luminescence spectra for samples of different origin. These differences are in the sharpness of the lines, in their relative intensities and in the presence and absence of specific lines in the spectrum. At the same time, one can discern the invariant elements of structure in the spectra of investigated samples.

The samples III, IV, V show approximately equal intensities of line luminescence, and the emission spectra are also almost the same, differing only in the sharpness of the lines. Figure 1, a shows the emission spectrum of sample IV obtained with the low dispersion instrument and figure 2, b the spectrum of sample V taken using high dispersion. A large

* All samples were synthesized for us in the laboratory of General Chemistry LU. The author takes this opportunity to thank S. M. Aria for this kind favor. The author is also indebted to E. V. Stroganov for the X-ray analysis of the samples.

** For assistance in working with liquid helium the author expresses his gratitude to N. M. Reinov, director of the cryogenic laboratory LFTI.

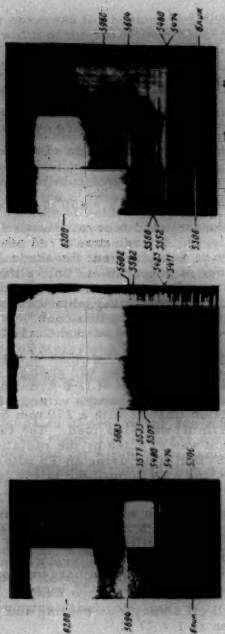

Figure 1. Luminescence spectra (a-c, f, g) and reflection spectra (d, e) of crystals of Cu_2HgI_4 at T=4.2°K, obtained with a spectrograph of low dispersion. Samples: a - IV, b - II, c - I, d - IV, e - II, f - with an excess HgI_2, g - with an excess of CuI.

number of narrow emission lines are visible in the spectrograms; between them the lines with greatest intensities stand out at wavelengths of 5444, 5474, 5480, 5494 (triplet), 5521(triplet) and 5552 Å. It is difficult to detect any general regularity in the distribution of the emission lines. A group of very narrow and weak lines is seen lying between intense ones and appearing in an equidistant series: $\Delta\nu \approx 20\ cm^{-1}$ (fig. 2, b). It is also necessary to mention the existence of a weak shortwave line in the emission spectrum, at 5306 Å, (fig. 1, a) close to the one observed previously [1-4] for the crystals of mercuric iodide HgI_2.

The spectrum of sample II. given in fig. 1,b and 2,a shows considerable differences from the one above. The majority of the lines, especially the strong ones, present in the spectrum of the samples III. IV and V, are also found here, but the relative intensities of some of the lines are different. At the same time, new lines, with noticeable intensity, appear mainly in the longwave part of the spectrum. This new group of longwave lines is plainly visible in the photomicrogram of the spectrum (fig. 3). It includes a narrow line at 5694 Å and several washed out weak lines in the range 5560-5680 Å. In addition, there appears a very strong and wide band ($\Delta\lambda \sim 200$ Å), centered at 6200 Å, (fig. 1 b) determining the observed red color of the luminescence of the sample. The shortwave line at 5306 Å disappears completely. The spectrum of sample I. (fig. 1,c), possessing very weak luminescence contains the most intense lines observed in the spectrum of samples III, IV and V and also contains a strong line at 5306 Å.

When comparing the luminescence spectra of the various samples, it is necessary to stress that they are practically identical for the three samples III, IV, and V, although they have an entirely different history of preparation. This circumstance obviously allows us to consider the luminescence spectra of these samples characteristic of the fine crystalline powder of Cu_2HgI_4. At the same time, for the samples whose method of preparation was not so careful (I and II), this spectrum although basically preserved, undergoes changes involving the weakening and disappearance of certain series of lines and the appearance of new lines, mainly in the longwave region of the spectrum.

In the preliminary investigation of the influence of a magnetic field on the emission spectrum of Cu_2HgI_4, it was observed that the luminescence spectrum of sample V., when brought into a magnetic field of H~30,000-35,000 Oersted, does not differ at all from the luminescence spectrum of Cu_2HgI_4 in the absence of a field. The absence of influence of the magnetic field on the emission lines of Cu_2HgI_4 is an interesting fact which requires explanation.***

It was of interest to obtain absorption spectra of crystals of Cu_2HgI_4 in order to compare them with the observed emission spectra. However, we have not succeeded in growing monocrystals of Cu_2HgI_4, and the preparation of transparent layers of Cu_2HgI_4 by evaporation from a melt was not possible because of the decomposition of the compound on heating. Therefore, it was necessary to limit ourselves to the study of the diffuse reflection of powdered Cu_2HgI_4. The reflection spectra were studied mainly at T = 4.2°K and, in addition at T = 77°K.

Fig. 2,c shows the spectrogram of light reflection of sample V, fig. 4 the microphotogram of the same spectrum. It can be seen that, on the long-wave side of the Cu_2HgI_4 absorption edge, against the background of the reflected light, there are weak narrow gaps ("lines") of reflection at 5507, 5533, 5578, 5582 and 5602 Å. Further, on the shortwave side there is a narrow portion of an extraordinarily strong reflection at 5423A, after which there is a narrow gap of reflection at 5411 Å, which gives a hint as to the structure of the latter intense band. The band at 5411-5423 Å also appears in the reflection spectra of all the other samples, while the longwave weak lines in the region of 5500-5600 Å begin to show a noticeable variation in the spectra of the different samples. Thus, for sample IV.

*** The spectra of Cu_2HgI_4 in the magnetic field were taken with the kind assistance of B. P. Zakharchenia to whom the author expresses his deep gratitude.

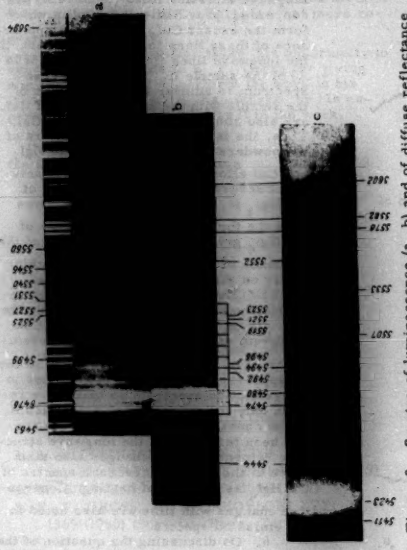

Figure 2. Spectra of luminescence (a, b) and of diffuse reflectance (c) of samples of Cu_2HgI_4, obtained with a spectograph of high dispersion. Samples: a -II; b, c - V

(fig. 1, d) the lines at 5507 and 5533 Å are nearly invisible, while, on the other hand, for sample II (fig. 1, e) these lines are strong; the lines at 5578, 5582 and 5602 Å, are weak and there is an additional line at 5683 Å.

On heating to 77°K, the structure of the reflection is displaced by approximately 20 Å towards the longwave region and becomes considerably less sharp, so that only the main intense line, whose center has been shifted to 5438 Å, can be seen distinctly in the spectrum; the weak longwave lines are considerably weaker.

The weak lines observed in the reflection spectra of powdered Cu_2HgI_4 are obviously connected with the corresponding absorption lines of Cu_2HgI_4, from which, according to the theory of diffuse reflection [18], one has to assume a small absorption coefficient for these lines. The character of the main intense band (5411-5423 Å) in the reflection spectrum points to a strong absorption for the corresponding line. This line introduces an essential contribution into the dispersion of the refractive index which also causes [18] a selective emission on its longwave side. Therefore, the reflectance spectra of Cu_2HgI_4 suggest the existence of a line structure in the region of the absorption edge of the crystal consisting of weak longwave lines, differing in different samples, and of an intense shortwave complex absorption line at 5411-5423 Å, present in all samples and apparently characteristic of Cu_2HgI_4.

Exposing the powder to white light for the study of reflection also causes photoluminescence, whose spectrum is superimposed on the reflection spectrum. To diminish the intensity of this emission, a yellow filter (OS-11), was used, cutting off the shortwave part of the continuous spectrum which excites the line luminescence. The use of the filter greatly weakens the luminescence lines; it is impossible, however, to exclude them completely. In the reflection spectrum of sample V (fig. 2, c), very intense luminescence lines at 5444, 5474, 5480 and 5494 Å are easily visible Also, one cannot obtain "pure" luminescence spectra, because a part of the emission (mainly in the continuous background) is reabsorbed in absorption lines. Thus, in fig. 2, b, longwave absorption lines at 5578, 5582 and 5602 Å, which usually appear in reflection, are visible in the luminescence spectrum of sample V.

The comparison of the luminescence and reflection spectra of Cu_2HgI_4 does not allow one to establish a correspondence between the absorption and emission lines with sufficient certainty. The known facts only allow an assumption to be made. In particular, studying the constancy of the main complex lines (at 5411-5423), in the reflection spectra of the different samples, and the group of intense lines (at 5474-5480) in their luminescence spectra, one cannot exclude the possibility of a resonance relation between these lines, although the Stokes shift in this case (of the order of 60 Å) exceeds by more than a factor of two the displacement usually observed for this kind of phenomenon.

Another fact which is notable is the extraordinary increase in the relative intensity of the emission line at 5444 Å on irradiation of the sample with a continuous spectrum as compared with its excitation by mercury lines (see fig. 2 b and 2 c). It is possible that the line at 5444 Å is coupled with the lines at 5411-5423 so that, on excitation with a continuous spectrum, the energy absorbed at 5411-5423 Å is emitted, through resonance, at 5444 Å.

4. In the present work Cu_2HgI_4 powders known to contain an excess of one of the components (CuI or HgI_2) were also investigated. They were prepared by melting together different proportions of powdered CuI and HgI_2 at 450°C in vacuo, followed by slow cooling and pulverization of the solid mass obtained. Three samples with an excess of HgI_2 (CuI:HgI_2 = 1:1, 1:2, 1:4) and one with an excess of CuI (CuI:HgI_2 = 4:1) were investigated.

The luminescence spectra of all three samples with an excess of HgI_2 are almost the same (fig. 1, f). Together with the most intense lines of the "pure" Cu_2HgI_4 (5474, 5480, 5494, 5521 Å; the line at 5444 Å is absent), a very strong line at 5306 Å and also a broad intense yellow line at 5577 Å appear in the spectrum. The last two bands at 5306 and 5577 are analogous with the ones previously observed in crystals of HgI_2

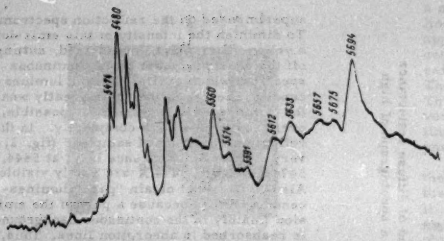

Figure 3. Microphotogram of the emission spectrum of Cu_2HgI_4 (sample II) at T=4.2°K.

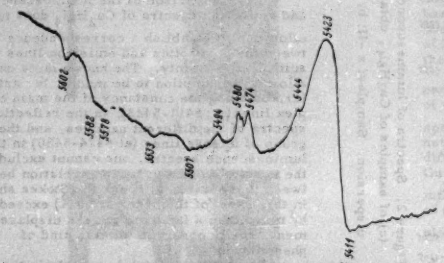

Figure 4. Microphotogram of the diffuse reflection spectrum of powdered Cu_2HgI_4 (sampleV.) at T=4.2°K.

[1,2] and they are, of course, connected with the excess of HgI_2 which does not enter into the lattice of Cu_2HgI_4. The existence of an excess of that kind is seen also in the reflection spectra of these samples, for, in addition to the main band at 5423-5411 and the weak lines at 5580 and 5602 Å, we noted the presence of an intense shortwave band with a region of selective reflection, at 5330 (at 77°K), which has appeared before in the reflection spectra of HgI_2 crystals. The appearance also of a weak emission line, at 5306 Å in the spectra of the series of samples of Cu_2HgI_4 prepared without measurable deviation from the stoichiometric amounts (fig. 1, a and 1 c) suggests the presence in this powder of a quantity of free HgI_2.

The luminescence spectrum of the sample with an excess of CuI (fig. 1, g) contains, in addition to the spectrum of the "pure" Cu_2HgI_4, a series of longwave lines, among them a line at 5694 Å and several of longer wavelengths and also a broad band at 6200 Å. The lines of the excess HgI_2 (e.g. at 5306 Å) are completely absent in this case. The band at 6200 Å is apparently identical with the band seen before [19] in the spectra of a film of CuI and is thus connected with the excess CuI not built into the Cu_2HgI_4 lattice. The presence of this kind of CuI excess also explains, in the reflection spectrum of the samples, the appearance, in addition to the main reflection band of Cu_2HgI_4 at 5411-5423 Å, of a line structure in the region of 4046 Å (at T = 77°K), where the absorption lines of CuI are found [11, 19]. As far as the narrow longwave emission lines ($\lambda \geq 5694$ Å) are concerned, it is difficult to say in which form the excess CuI, causing the appearance of these lines is present. Apparently, the longwave lines (in particular at 5694 Å) of the sample II, (fig. 1, b), whose spectrum is similar to the spectrum of the sample with the known excess of CuI, are also connected with the excess CuI. Thus, the investigation of the spectra of the powders with various ratios of HgI_2 and CuI allowed us to obtain some facts about several lines of the spectrum of Cu_2HgI_4 (e.g. λ= 5306 Å). At the same time the three component character of Cu_2HgI_4 greatly hampers the study of the influence of the deviation from stoichiometry on the spectrum of the crystal.

5. The above experiments also revealed the strong influence of heating the crystals on the emission and reflection spectrum of Cu_2HgI_4. Heating to a temperature of 100°C and higher leads to the disappearance of weak longwave lines in the reflection spectrum so that there remain only the main band at 5411-5423 Å. In the course of time, after the heating has been terminated, the longwave structure returns. Great changes also take place in the line luminescence spectra of Cu_2HgI_4 as a result of heating. Consecutive changes with time are also noted in the emission spectra.

6. On discussing the question of the nature of the observed line structure of the spectra of Cu_2HgI_4, it is first of all necessary to settle the problem of whether this structure is connected with the main lattice or with its distortions. In our opinion, it is very probable that the various lines of the spectra can have different origins: some, being connected with the main lattice, others with all kinds of defects. (One can apparently exclude foreign admixtures from consideration as a cause of the appearance of the lines in the spectra of Cu_2HgI_4. The consistency of the spectra of samples of different chemical history would speak in favor of this view.)

Undoubtedly distortion has a strong influence on the line structure of the spectra of Cu_2HgI_4. It is shown in the variation of some of the spectral lines from sample to sample (e.g. narrow lines in the reflection spectrum), in the observed influence of stoichiometry on certain emission and absorption lines, in the effect of heat treatment as shown by the change of the spectra with time, etc. At the same time, such phenomena as the great intensity of the main reflection band, reproducibility and constancy of the series of luminescence lines in the spectra of various samples, and other facts, point to the possibility of a connection of some lines with the main lattice of Cu_2HgI_4. The observations, however,

are not sufficient for an unambiguous solution of the question of the origin of these or other distinct lines in the spectra of Cu_2HgI_4; for that more research is necessary.

In closing the author takes this opportunity to express his gratitude to E. F. Gross for giving him the opportunity to perform the work in his laboratory, and to A. A. Kaplianskii for his experimental help and his interest in the work.

University of Peking and
the Institute of Applied Physics
AN CPR.

May 5, 1958

References

1. E. F. GROSS, A. A. KAPLIANSKII, B. V. NOVIKOV: ZTF, 26, 697 (1956) (See Sov. Phys. Tech. Phys.); DAN USSR, 110, 761 (1956) (See Sov. Phys., Doklady)
2. V. A. ARKHANGEL'SKAIA, P. P. FEOFILOV: DAN USSR, 108, 803 (1956) (see Sov. Phys. Doklady); OiS, 2, 107 (1957)
3. A. A. KAPLIANSKII: IAN USSR, Fiz. ser., 21, 531 (1957) (See CTT Bulletin, 21, 529)
4. M. SIESKIND: C.R., 245, 1006 (1957)
5. E. F. GROSS, M. A. IAKOBSON: ZTF, 26, 1369 (1956) (See Sov. Phys. Tech. Phys.)
6. E. GRILLOT, M. GRILLOT, P. PESTEIL, A. SMERLI: C.R., 242, 1794 (1956)
   E. GRILLOT: J. Phys. et rad., 17, 822 (1956)
7. V. V. EREMENKO: OiS, 4, 348 (1958)
8. E. F. GROSS, V. V. SOBOLEV: ZTF, 26, No. 7, 1622-24 (1956) (see Sov. Phys. Tech. Phys.)
9. G. PERNY, S. NIKITINE: C.R., 244, 878 (1957)
10. S. NIKITINE, G. PERNY: J. Phys. et rad., 17, 1017 (1956)
11. R. REISS: C.R., 243, 902 (1956)
    S. NIKITINE, R. REISS: C.R., 244, 2788 (1957); J. Phys. et rad., 17, (1956)
12. E. F. GROSS, A. A. KAPLIANSKII: OiS, 2, 204 (1957)
13. B. S. RAZBIRIN: Diploma thesis, Leningrad Univ., 1956
14. R. SHEKHMAMET'EV: Diploma thesis, Leningrad Univ., 1957
15. L. BERGMANN; J. HAENSLER: Z. Phys., 100, 50 (1936)
16. J. A. A. KETELAAR: Z. Kristal., 80, 190 (1931)
17. H. HAHN, G. FRANK, W. KLINGLER: Zs. anorg. u. allgem. Chem., 279, 271 (1955)
18. O. P. GIRIN, B. I. STEPANOV: ZETF, 27, 467 (1954)
19. K. V. SHALIMOVA, N. A. MENDAKOV: ZETF, 26, 248 (1954)

TOM VI, Vyp. 2 OPTIKA I SPEKTROSKOPIIA Fevral', 1959
VOL. VI, No. 2 OPTICS AND SPECTROSCOPY February, 1959

On the Electron Trapping Levels of the Activator in a NaCl-Ni Phosphor

I. A. PARFIANOVICH

Studies have been made of the spectrum of electron trapping levels of activators, and their properties, in an NaCl-Ni phosphor, activated by an electro-chemical method. It is found that not all the activators in the phosphor function as electron acceptors. Only a certain portion of the activators, under special circumstances, give rise to these levels. It is shown that this conclusion is correct for other activators. The question is discussed of the relation between the probabilities for localizing electrons at impurity levels and at trapping levels of the host material, as well as of the influence of the activator levels on the kinetics of afterglow.

More than ten years ago, Levshin [1] first propounded the hypothesis that an activator in a crystal phosphor was a site around which localizing of electrons could take place. Later this hypothesis found support in experiments on the spectra of impurity absorption in alkali-halide phosphors, excited by x-rays. In a number of works [2-11] it has been shown that an activator gives rise to electron acceptor levels. The free electrons produced in the alkali-halide phosphors by the action of the ionizing radiation can be localized not only at trapping centers of the host material but also at the activator centers. The result of electron trapping in activator levels is the formation of the so-called "atom-like" centers. The question of the mechanism of formation of these centers and of their structure has not yet been solved and is at present receiving much attention.

The capture of electrons in levels of the host material results in the formation of so-called "centers", e. g. F and M centers. These centers, as is well-known [12], play a large role in the storing of energy for the afterglow effect. The presence of activator acceptor levels has an effect both on the trapping of electrons and on the levels of the host material. Research on the distribution of electrons between levels of the various types is of considerable interest not only for studying the storage power of the phosphor but also for studying the kinetics of the afterglow. The question of the relative role of activator trapping centers and nonactivator trapping centers in the localization of electrons is currently receiving insufficient attention. There are several indications of the presence of two concurrent processes: 1) Electron capture at levels of the host material and 2) Localization of electrons at activator trapping centers. In references [3] and [7] it was observed that the concentration of F-centers in X-rayed NaCl-Ag and NaCl-Cu phosphors decreased with the increase of the activator concentration.

In the present work we give several results found by the author in research on the relative role of activator electron trapping levels in comparison with F-levels in a NaCl-Ni phosphor. The experiments were carried out on phosphors activated by electro-thermal diffusion. Natural crystals of NaCl served as host for the phosphors. The phosphors were excited by radiation from an x-ray tube with a tungsten anode (50kV, 18mA) at room temperature. The optical absorption spectra were measured with a SF-4 spectrophotometer.

The distribution of electrons among the trapping levels may be studied by means of the impurity absorption spectra, in which each band corresponds to a definite type of center. In Figure 1 we give the impurity absorption spectrum of a NaCl-Ni phosphor excited by x-rays. As can be seen from Figure 1, the spectrum has five major characteristic bands. Of these, two electron bands (F and M) and one hole V-band belong to the host material, whereas two bands, with λ_m = 276 and 308 mμ, are related to the presence of the activator. Both these bands have an electronic origin. This is obvious from the data found for the optical illumination of the F-band. The result of this illumination is shown in curve 2 of Figure 1. The decay of the F-bands leads to a strengthening of the bands at λ_m = 276 and 308 mμ, and shows directly that the latter are due to electronic centers. They are centers formed when the activator captures the electrons.

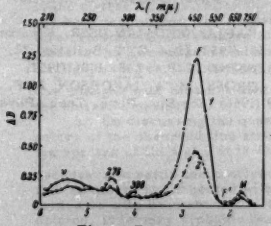

Photon Energy (eV)

Figure 1. Impurity absorption spectra for NaCl-Ni Phosphor

1. Right after x-irradiation; 2. Following subsequent exposure in F band.

The bands at λ_m = 276 and 308mμ are not as wide as the F-bands. On the basis of data reported in reference [7] for an NaCl-Ag phosphor we can assume that the oscillator strength of these bands is close to the oscillator strength of the F-center. In this way it becomes possible to draw a conclusion concerning the distribution of electrons between the host trapping levels and the activator levels by comparing the area of the absorption bands. Comparison of these areas shows that fewer than 5% of the total number of electrons localized in the process of x-irradiation, arrive at activator trapping levels. This nonuniform distribution of electrons points to a remarkable difference in the total effective capture cross-section at activator and non-activator centers. In order to explain the reasons for this difference let us try to estimate the concentrations of the two types of trapping centers.

The actual concentration of activators in the phosphor was determined by a polarimetric method. In a phosphor activated at 700° the concentration of nickel was $4 \cdot 10^{-4}$ mol. %. If all the activators are dispersed and appear as single ions then each cubic centimeter contains around $9 \cdot 10^{16}$ nickel ions.

The concentration of anion vacancies found in thermal equilibrium at the activation temperature of the phosphor may be found from the formula [13]

$$n = n_0 \gamma \exp(-w/2kT), \quad (1)$$

where n is the concentration of ion-vacancy pairs, n_0 is the concentration of ion pairs in the lattice, w is the energy necessary for formation of a single positive and negative ion vacancy pair, and γ is a constant. According to the results of reference [14] for the case of NaCl, w=2.02 eV and $\gamma = 5.4$. Hence it follows from formula (1) that the concentration of anion vacancies at the activation temperature (700°) should not be greater than $8.3 \cdot 10^{17}$ cm^{-3}. Upon cooling to room temperature, the concentration of single vacancies decreases. From measurements of the electrolytic conductivity and the mobility of positive vacancies it was found that near room temperature the concentration of these vacancies in NaCl was approximately 10^{16} cm^{-3}. Hence we arrive at the conclusion that the concentration of ion vacancies probably does not exceed the concentration of activator ions. It is doubtful that, even for equal concentrations of anion vacancies and activator ions, the reason for the different occupations of activator and host levels can be explained by different effective cross-sections for electron trapping between the activator ions and the anion vacancies. One might suppose that the reason for this difference of concentration of the "atom-like" and F-centers is due rather to the fact that not all of the activator ions take part in electron trapping.

This assumption is in agreement with results from experiments on the impurity absorption bands in alkali-halide phosphors activated by silver [7]. Reference [7] contains a series of convincing experimental results supporting the hypothesis of the participation of ion vacancies in the formation of "atom-like" centers. The results of our experiments may be explained by assuming that the centers which give rise to the bands at $\lambda_m = 276$ and 308 mμ are formed by electron capture, not at any random activator ion, but only at those which find themselves alongside an ion vacancy or in some other special site in the crystal. Naturally such structures, composed of an activator ion and a lattice defect, can account for only a certain fraction of the total number of activators. Hence it follows that not every activator in the phosphor will be active as an electron acceptor. This reasoning allows one to understand why, in the case of NaCl-Ni phosphor, the free electrons formed by x-ray irradiation are localized principally in levels of the host material and not at activator trapping centers.

More favorable conditions for localizing the electrons at activator trapping levels are produced by additive coloring of the phosphor. It is necessary to point out that on coloring NaCl-Ni in sodium vapor it is not possible to get distinct "atom-like" bands at λ_m=276 and 308 mμ. When coloring the phosphor by this method, the nickel goes into a colloidal state. The activators play a larger role as electron acceptors in additive coloring than they do during x-ray irradiation. The same is true for other activators. This may be seen especially clearly in phosphors activated by silver, which, under additive coloring, may be found in the form of "atom-like" centers without the formation of colloidal particles.

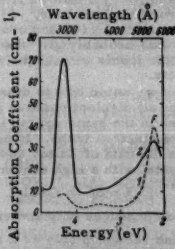

Figure 2. Impurity absorption spectra for CK-Ag(0.05 mol. % Ag) Phosphor.
1. After the effect of x-rays; 2. After added coloring.

In Figure 2, which is taken from reference [7], we give two curves which show the impurity absorption spectra of a KCl-Ag phosphor in which the activator concentration was 0.05 mol. %. Curve 1 was obtained after x-ray irradiation, and curve 2 after electrolytic coloring of the sample. As may be seen from the figure, an F-band as well as an "atom-like" band (λ_m = 283 mμ) is formed in both cases. However, the ratio of the intensity of these bands is dependent on the method used to color the crystal. X-ray irradiation causes development primarily of the F-bands. It is approximately five times stronger than the "atom-like" band. On the other hand, electrons going from the cathode into the conduction band during electrochemical coloring of the crystal are localized primarily at activator trapping levels. In a crystal colored by the two different methods, where the F-bands differed in strength by no more than 20%, the strength of the "atom-like" band in the additively colored crystal exceeds by approximately a factor of 10 the strength of the corresponding band in an x-ray irradiated crystal.

This result obviously shows that additive coloring creates more favorable conditions for the localization of electrons at activator levels. It is impossible to explain this result in terms of a simple competition between the activator levels and the levels of the host material. The overall number of activators is the same in both cases. The reason is probably to be found in the fact that during additive coloring, which takes place at elevated temperatures (when the equilibrium concentration of ion vacancies is increasing, and when these vacancies are becoming more mobile), there are created conditions favorable for the formation of electron trapping activator centers. Hence by this reasoning we are convinced that, as in the case of silver, not all the activators are effective in the formation of "atom-like"

centers during x-ray irradiation; rather only a certain portion of the activators in the crystal are effective.* It is probable that at room temperature, and even at high temperatures, stable "atom-like" centers are formed as the result of electron trapping by complexes containing activator ions and anion vacancies. This picture should be correct for activator ions with a single, elementary positive charge. For the divalent activator ions (Pb^{++}, Sn^{++}, and Ni^{++}) it follows from the researches of Andrianov and Kats, [4] Kats and Semenov, [5] Lushchik [10] and other authors, [2] that these ions probably give rise to deep electron acceptor levels without the co-operation of lattice defects.

In addition we would like to draw attention to the fact that not all divalent positive impurity ions lend themselves in the same degree to the formation of effective electron traps. Hence, for example, from the data of Zaitov and Kark, [15] in an NaCl crystal with a high content of divalent impurities Ca^{++} (0.5 mol. % $CaCl_2$), the process of x- irradiation produces only a very weak Z_1-band. This band shows up only as a result of optical ionization of the F-centers in the irradiated crystal. According to the model of Seitz, [16] a Z_1-center comprises an electron localized at a divalent alkaline-earth metal ion. Hence it follows that the alkaline-earth ions do not function as effective traps for free electrons arising under the action of x-rays. Regardless of the presence of a large number of Ca^{++} ions in greater concentration than the anion vacancies, electrons are localized primarily at anion vacancies during the process of x-irradiation. It is interesting to note that this circumstance cannot be attributed to a shielding of the effective charge of the Ca^{++} ions by the cation vacancies, since Ca^{++} ions and cation vacancies do not form stable complexes. Hence we are convinced that the presence of excess positive charge around an impurity ion is not a sufficient condition for the ion to behave as an effective center for electron trapping.

The divalent Cd^{++} ion behaves differently. From the research on the self-diffusion of Na^{+} ions in pure crystals of NaCl [17] and in crystals with excess Cd^{++} [18], it follows that Cd^{++} ions form stable complexes with cation vacant sites. Regardless of this fact, cadmium, as was established in reference [19], forms deep acceptor levels for electrons in NaCl.

In order to explain this result it is necessary to suppose that a certain fraction of the Cd^{++} ions do not unite with cation vacancies. It is possible also that Cd^{++} ions can unite not only with single cation vacancies but also with more complicated complexes formed from cation and anion vacancies. In any case we may assert that the question of impurity electron trapping levels in alkali-halide phosphors is very complicated and cannot be connected simply with the localization of electrons at isolated ions.

One may try to describe the general characteristics of impurity electron trapping centers independently of the structures of these centers. N. E. Lushchik and Ch. B. Luschchik [20] have divided all the well-known impurities in alkali-halide crystals into homologous groups according to their electronic configurations. They pointed out analogies in the electronic configuration of the Cd^{++}, Cu^{+}, and Ag^{+} ions, all of which are electron acceptors. In connection with this we would like to point out that the structure of the outer part of the electron shell of the ions may be used to make a qualitative determination of the effectiveness of the ions as electron traps. In analyzing the experimental data on impurity electron trapping centers, we have come to the following conclusion: effective electron trapping levels will be formed by those ions whose external electronic shell is characterized by the presence of d electrons (Cu^{+}, Ag^{+}, Cd^{++}), or by d and s electrons (Sn^{++}, Pb^{++}). On the other hand the Ca^{++}, Sr^{++}, and Ba^{++} ions, whose electron shells are similar in structure to the inert gases, function very weakly as electron traps. These ions take only a very small part in capturing free electrons produced by x-irradiation. In addition they markedly increase the rate of formation of F-centers, i. e. the capture of electrons at levels of the host atoms.

Now returning to the NaCl-Ni phosphor, one should note that the electronic structure of nickel ($1s^2 2s^2 2p^6 3s^2 3p^6 3d^8 4s^2$) predicts that nickel ions should be more effective in forming electron trapping centers than alkaline-earth ions. This is borne out by experiment. In addition, as we have seen, the effectiveness of the nickel centers as capture sites is markedly less than the effectiveness of anion vacancy clusters. As we have seen, more than 95% of the electrons localized in a NaCl-Ni phosphor (with an activator concentration of $4 \cdot 10^{-4}$ mol. %) accumulate in trapping levels of the host material.

Let us consider the role of the activator in an NaCl-Ni phosphor in the phenomenon of repeated electron capture. During optical emission of the F-band the electrons liberated from F-centers partly recombine with trapped holes and partly are localized both at activator and non-activator electron trapping levels. Curve 2 in Figure 1 shows the change in electron distribution among the trapping levels after ionization of the F-centers. By comparing that curve with curve 1 of Figure 1 it is seen that of the total number of electrons liberated from F-centers not more than 7% are localized at activator centers. A certain number of F-centers are transformed into M-centers, but the larger share of the liberated electrons recombines with captured holes. Hence we deduce the unimportant role of the activator electron trapping levels in the phenomenon of repeated electron capture. The recombination probability for electrons with captured holes in NaCl-Ni is considerably greater than the probability for localizing electrons at activator centers. By increasing the temperature one may exclude the possibility of electrons occupying M-levels and increase the cross-section at the hold centers. As a result of this fact it is possible to realize optical flashing with mono-molecular kinetics. This conclusion is supported by data found

* One of the factors influencing the filling of the activator trapping levels may be the emissive effect of the x-rays [22].

by the author during an investigation of the decay of optical flashes in NaCl-Ni phosphor [21].

Zaitov and Kark [15] investigated optical flashing and its non-isothermal relaxation in F- and Z_1 trapping centers in the following phosphors: $KCl.CaCl_2$ (0.5 mol.%), TlCl (0.1 mol.%) and $KCl.CaCl_2$ (0.5 mol.%). AgCl (0.3 mol.%). In spite of the large impurity content in the crystal, they found that for these phosphors the kinetics of flashing were monomolecular. This result shows that even in the presence of a high impurity content in the crystal, they found that for these phosphors the kinetics of flashing were monomolecular. This result shows that even in the presence of a high impurity content in a phosphor, the probability of recombination with trapped holes is many times larger than the probability of repeated electron capture at impurity centers.

March 3, 1958

References

1. V. L. LEVSHIN: IAN USSR, Fiz. ser., 5, No. 4-5, (1941)
2. J. H. SCHULMAN, R. J. GINTHER, C. C. KLICK: J. Appl. Phys., 22, 1479 (1951)
3. M. L. KATS: DAN USSR, 85, 539, 757 (1952); ZETF, 23, 720 (1952)
4. A. S. ANDRIANOV, M. L. KATS: DAN USSR, 96, 253 (1954)
5. M. L. KATS, B. Z. SEMEONOV: DAN USSR, 106, 415 (1956) (See Sov. Physics Doklady)
6. J. H. SCHULMAN: J. Phys. Chem., (1954) (1953)
7. H. W. ETZEL, J. H. SCHULMAN: J. Chem. Phys., 22, 1549 (1954)
8. CH. B. LUSHCHIK: Trudy, IFAAN ESSR, 3, 57 (1955)
9. CH. B. LUSHCHIK, N. B. ZAITOV: Trudy, IFAAN ESSR, 4, (1956)
10. CH. B. LUSHCHIK: OiS, 2, 220 (1957)
11. L. M. SHAMOVSKII, IU. N. ZHVANKO: IAN USSR, Fiz. ser., 21 (4), 557-559 (1957) (See CTT Bulletin, 21, 551)
12. I. A. PARFIANOVICH: IAN USSR, Fiz. ser., 13, 161 (1949) (See RT-632); ZETF, 19, 605 (1949)
13. N. F. MOTT, R. W. GURNEY: Electronic Processes in Ionic Crystals. Oxford, 2d ed., Clarendon Press, 1948
14. H. W. ETZEL, R. J. MAURER: J. Chem. Phys. 18, 1003 (1950)
15. F. N. ZAITOV, V. IA. KARP: Trudy, IFAAN ESSR, 6, 82 (1957)
16. F. SEITZ: Phys. Rev., 83, 134 (1951)
17. D. MAPOTHER, H. N. CROOKS, R. J. MAURE R. J. MAURER: J. Chem. Phys., 18, 1231 (1950)
18. F. SEITZ: Rev. Mod. Phys., 26, 7 (1954)
19. CH. B. LUSHCHIK, F. N. ZAITOV, V. IA. KARP, L. A. TEISS, I. V. IAEK: Materialy V Soveshch. po liuminestsentsii (Material of the V Conf. on Luminescence) 75, 1957, Tartu
20. N. E. LUSHCHIK, CH. B. LUSHCHIK: Trudy, IFAAN ESSR, 6, 5 (1957)
21. I. A. PARFIANOVICH: ZETF, 21, 314 (1951)
22. I. A. PARFIANOVICH: OiS, 5, 612 (1958)

TOM VI, Vyp. 2 OPTIKA I SPEKTROSKOPIIA Fevral' , 1959
VOL. VI. No. 2 OPTICS AND SPECTROSCOPY February , 1959

Investigation of the Scintillation Properties of Some 1,3,4 - Oxadiazole Derivatives

N. P. SHIMANSKAIA, A. P. KILIMOV, A. P. GREKOV

Abstract: We have synthesized 2- (naphthyl)-5-(4-biphenylyl)-1,3,4-oxadiazole (LNBD), 2-(4-metoxyphenyl)-5-phenyl-1,3,4-oxadiazole (MtPPD) and also 1-(1-naphthyl)-2-(4-biphenylyl)-hydrazine and 1-(4-methoxyphenyl)-2- phenylhydrazine, not previously described in the literature, which are the initial products in the production of the above-mentioned oxadiazoles. The spectral and scintillation characteristics of solutions of the substances LNBD, MtPPD and PBD in toluene and polystyrene have been studied

In the course of the past few years, numerous investigations have been made of various classes of organic compounds in order to clarify their suitability as scintillators. One such class of fluid scintillators, as has been shown by Hayes and his colleagues [1] is a series of derivatives of 1,3,4-oxadiazole, which have scarcely been studied except in the work [2] of the above-mentioned authors whose results are of a preliminary nature. Meanwhile the analysis of even these few experimental data permits some conclusions to be drawn as to the promise of such substances.

In this connection it was of considerable interest to synthesize and investigate a number of different derivatives of 1,3,4-oxadiazole in order to study the relation between the structures of such compounds and their effectiveness. as scintillators, as well as to search for the compond with the best scintillation properties among the number mentioned above.

In order to resolve these questions, we synthesized an extensive series of mono and diaryl substituted 1,3,4-oxadiazoles and studied their scintillation and luminescence properties with the result that we found the following new scintillators.* 2-(1-naphthyl)-5-(4-biphenylyl)-1,3,4-oxadiazole (LNBD) and 2-(4-methoxyphenyl)-5-phenyl-1,3,4-oxadiazole (MtPPD) are the best of all the liquid scintillators known at the present time. For comparison, we also investigated 2-phenyl-5-(4-biphenylyl)-1,3,4-oxadiazole (PBD), which is the best of the liquid scintillators in the 1,3,4 oxadiazole series described in the literature [1].

EXPERIMENTAL PART

1. Synthesis and Purification of the Original Materials. 2-(1-naphthyl)-5-(4-biphenylyl)-1,3,4-oxadiazole (LNBD) and 2-(4-methoxyphenyl)-5-phenyl-1,3,4-oxadiazole (MtPPD), as well as the corresponding hydrazines from which they are obtained, are not described in the literature. The following scheme was used for their production:

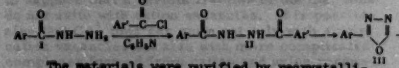

The materials were purified by recrystallization from appropriate solvents with subsequent chromatographic purification on aluminum oxide.

2. Measurement of the Scintillation and Spectral Properties of MtPPD, LNBD and PBD in Toluene and Polystyrene Solutions. The spectra, relative photo-luminescent intensity, and integrated scintillation light output in relative units were measured for all the materials in toluene and polystyrene solutions of different concentrations as was, finally, the absorption spectrum in heptane.

The plastic blocks were obtained by the method described in [3].

The spectra and the luminescence intensity were measured on an apparatus consisting of an SF-4 spectrophotometer, used as a monochromator, with a photoelectric adapter (which we prepared) and an FEU-18 photo-multiplier. An M-21 mirror galvanometer was used to record the photo-current.

The integrated scintillation light output was measured by the photo-current of the FEU-19, on whose aperture was mounted the sample bombarded by an Ag^{110} source of about 0.1 mC.

The absorption spectra were measured in the usual way on the SF-4 spectraphotometer

The results of the measurements are presented on Figures 1 - 11.

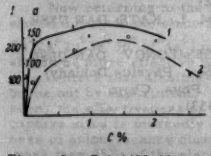

Figure 1. Scintillation (2) and photoluminescent (1) light output for solutions of MtPPD in polystyrene

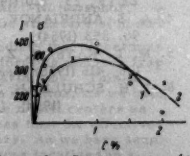

Figure 2. Scintillation (2) and photoluminescent (1) light output for solutions of LNBD in polystyrene

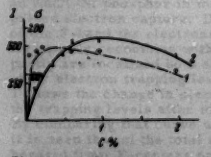

Figure 3. Scintillation (2) and photoluminescent (1) light output for solutions of PBD in polystyrene

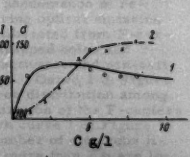

Figure 4. Scintillation (2) and photoluminescent (1) light output for solutions of MtPPD in toluene

DISCUSSION OF THE RESULTS

As in other cases we have investigated, a similar concentration dependence of the luminescence intensity and scintillation effectiveness is observed for all three materials in polystyrene (see Fig. 1-3). A more pronounced self-quenching is observed in toluene solutions of MtPPD in the case of luminescence (Fig. 4); the behavior of the

* The notation of [1,2] is used.

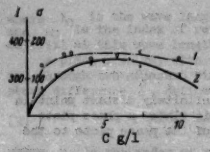

Figure 5. Scintillation (2) and photoluminescent (1) light output for solutions of LNBD in toluene

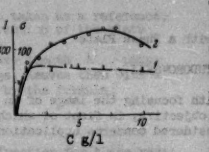

Figure 6. Scintillation (2) and photoluminescent (1) light output for solutions of PBD in toluene

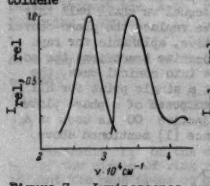

Figure 7. Luminescence and absorption spectra of MtPPD in heptane

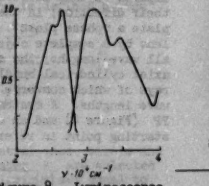

Figure 8. Luminescence and absorption spectra of LNBD in heptane

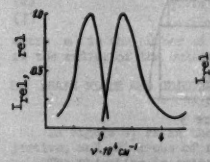

Figure 9. Luminescence and absorption spectra of PBD in heptane

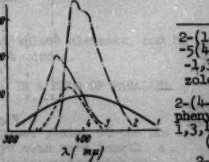

Figure 10. Luminescence spectra of oxadiazoles in polystyrene and spectral response of the FEU-19; 2 - luminescence spectrum of MtPPD; 3 - luminescence spectrum of LNBD; 4 - Luminescence spectrum of PBD

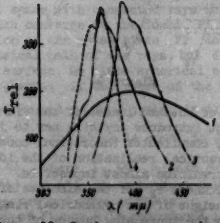

Figure 11. Luminescence spectra of oxadiazoles in toluene and spectral response of the FEU-19; 2-luminescence spectrum of MtPPD; 3-luminescence spectrum of LNBD; 4-luminescence spectrum of PBD.

curves is similar for the other two materials (Fig. 5 and 6).

The absorption spectra of the materials are shown on Figures 7 - 9. It should be noted that good agreement between the absorption maximum of the material and the maximum luminance of the polystyrene is observed for PBD and LNBD.

The luminescence spectra of the materials are located in the range of comparatively good response of the FEU-19 (see Fig. 10 and 11). However, improvement in the scintillation effectiveness could be expected for MtPPD upon the introduction of an additive having a POPOP-type spectrum (POPOP 1,4-di-[2-(5-phenyloxadiazole)]-benzene. The optimum concentrations and the scintillation effectiveness thus attainable for the materials described are presented in the table. Also presented there for comparison purposes are data for pTP (p-terphenyl) and pTP - POPOP scintillators. As is seen from a comparison of these results, the new scintillators obtained surpass the widely used pTP and pTP - POPOP solutions and are the best of those described up to the present time.

Scintillation and Luminescent Properties of 1,3,4-Oxadiazole Derivatives in Solutions

Material	Toluene				Polystyrene			
	λ_{abs}	λ_{lum}	c_{opt} (g/l)	$\sigma_{rel\ scint}$ eff.	λ_{lum}	c_{opt} (in %)	σ_{scint} (in % re ter-phenyl)	$\Delta\nu$ (cm^{-1}) in heptane
2-(1-naphthyl)-5(4-biphenylyl)-1,3,4-oxadiazole (LNBD)....	320	385	6	157	385	1	189*	5000
2-(4-methoxyphenyl)-5-phenyl-1,3,4-oxydiazole (MtPPD).....	293	370	10	150	370	1.6	134	6600
2-phenyl-5-(4-biphenylyl)-1,3,4-oxadiazole (PBD).....	320	365	7 10	130 128**	385 –	1 –	109 –	5500 –
p-terphenyl (pTP).....	279	345	3	100	365	2	100	–
pTP POPOP***	–	–	4+0.1	145	–	2+002	134	–

* In a freshly-polymerized sample
** According to the data of reference [1]
*** According to the data of references [3,4,5]

Compliance with the law of mirror symmetry is also shown in Figures 7 - 9 for solutions of the substances investigated in heptane. It should be noted that PBD solutions, which yield considerably less relative photo-luminescence energy output, also have a very low scintillation effectiveness.

February 17, 1958

References

1. F. N. HAYES, D. G. OTT, V. N. KERR, B. S. ROGERS: Nucleonics, 13, 38, Dec.(1955)
2. F. N. HAYES, B. S. ROGERS, D. G. OTT: J. Am. Chem. Soc. 77, 1850 (1955)
3. E. A. ANDREIBICHEV, E. E. BARONI, K. A. KOVYRZINA, I. E. PANI, I. M. ROZMAN V. M. SHONIIA: PiTE, No. 1, 32, (1956)
4. F. N. HAYES, D. G. OTT, V. N. KERR: Nucleonics, 14, 42, Jan.(1956)
5. N. A. ADROVA, M. M. KOTON, IU. N. PANOV, F. S. FLORINSKII: PiTE, No.3, 43(1957)

TOM VI, Vyp. 2 OPTIKA I SPEKTROSKOPIIA Fevral', 1959
VOL. VI. No. 2 OPTICS AND SPECTROSCOPY February, 1959

An Objective with a Phase Plate

A. I. TUDOROVSKII

Abstract: A theory is presented which deals with focusing the image of an infinitely distant point in light of different wave lengths by means of a given objective, in front of which is placed a phase plate (a circular diffraction grating). The question considered concerns application of the phase plate to the correction of chromatic aberration in the objective.

In the Doklady AN USSR there is a paper [1] by Sliusarev which contains a short presentation of work carried out in 1954-1955 and continued during the subsequent years. The work was directed toward physics and astronomy, since its object was to present a new method, termed the method of the "secondary spectrum", for correcting the objectives of telescope systems. The present work was carried out in order to re-examine the original situation and it differs from that investigation in the initial definitions, in the calculation methods and in some of the characteristics of the phase plate properties.

1. NOTCHED (OR STEPPED) LENS AND PHASE ZONE PLATE.

The essence of the new method of achromatizing objectives consists of the following. The beam of light, convergent at a point, is divided into several conical coaxial bundles; the phases of the oscillations of all rays in one bundle are the same at the point of convergence, but they (the phases) differ in magnitude, one bundle from the other being smaller than the phases of the preceding bundles and larger than the phases of the following. Such a result is achieved by modification of the objective lenses, whose spherical surfaces are replaced by complicated surfaces consisting of spherical zones with different radii of curvature.

Figure 1

Figure 2

It is possible to construct infinitely many such lenses with different cross-sectional profiles which behave identically. Figure 1 reproduces one of two examples taken from reference [1]; in Figure 2 is shown a variant of this lens, in which all of the rings which form the "stepped" lens of Figure 1 are displaced by joining their spherical surfaces with the spherical surface whose zone corresponds to the very last ring. In Figure 3 is presented a new variant, obtained from the preceding by adding together a sequence of cylindrical rings all having the same thickness (height). Cutting the complicated solid so constructed along the dotted line in a plane perpendicular to the axis, we obtain a system consisting of a plate with plane boundaries and a plano-convex lens. The plate formed by joining together cylindrical rings separates light rays parallel to the axis into cylindrical bundles and imparts to them different phases without changing their direction; in the sequel we shall call this plate a "phase plate". We replace the plano-convex lens by a complete objective, aplanatic for rays of all wave-lengths; the objective transforms the coaxial cylindrical bundles into conical ones, the rays of which converge at a single point for all wave lengths. A system composed of a phase plate PP (Figure 4) and an objective OO is used as a starting point in reference [1] mentioned above.

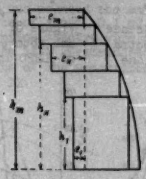

Figure 3

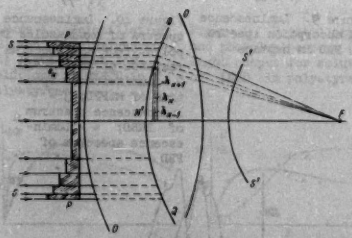

Figure 4

Application of notched lenses of the Fresnel variety does not introduce anything new to justify this system, complicates theoretical consideration and makes practical realization of the idea with sufficient precision almost impossible.

The thickness e_k of the elements of the phase plate (the height of the cylindrical rings) increases with the increasing number of the ring according to the formula:

$$e_k - e_{k-1} = \frac{\lambda_0}{n_0 - 1},$$

where λ_0 is the wave length taken as a reference, and n_0 is the index of refraction of the plate material at this wave length.

A plane-wave ray with wave length λ, passing through two adjacent rings, leaves them with a phase difference δ, defined by the formula:

$$\delta = \frac{2\pi (n-1)\lambda_0}{(n_0-1)\lambda}, \tag{2}$$

where n is the index of refraction for these rays; if $\lambda = \lambda_0$ then $\delta = 2\pi$.

If the phase lag of a ray with wave length λ after passing through the central part of the plate is called δ_1, then the lag δ_k of a ray, which passes through the k-th ring is defined by the following formula:

$$\delta_k = \delta_1 + \frac{2\pi (k-1)(n-1)\lambda_0}{(n_0-1)\lambda}.$$

As a simplification we assume that $\delta_1 = \frac{\lambda_0}{n_0-1}$; so that

$$\delta_1 = \frac{2\pi (n-1)\lambda_0}{(n_0-1)\lambda}, \tag{3}$$

$$\delta_k = k\delta_1. \tag{4}$$

The radii h_1 of the central inner circle and h_k of the circle of ring number k are selected so that the base areas of all rings are equal to the area of the central circle. In this case

$$h_k^2 - h_{k-1}^2 = h_1^2, \tag{5}$$

$$h_k^2 = k h_1^2, \tag{6}$$

$$h_m = \sqrt{m}\, h_1, \tag{7}$$

where m is the number of all plate elements, and h_m is the radius of the outermost circle.

2. PHASE PLATE AND OBJECTIVE IN A BEAM OF PARALLEL RAYS

In Figure 4, PP is the phase plate, OO the objective, and F' focus of rays with wave length λ.

The objective is entirely corrected with respect to spherical aberration and satisfies the law of sines. If the phase plate is removed, then each spherical surface S'S' centered at the focus F' of the objective is a wave surface, i. e. the geometrical locus of points of equal phase; this applies also to the spherical surface QQ, drawn through the second principal point H' of the objective (an imaginary wave surface). This surface at the same time according to the law of sines is the locus of the intersection of continued parallel rays in the object space with connected rays in the image space, which converge at the focus F'. The introduction of the phase plate PP does not change the geometrical path of the rays, but divides the spherical surface QQ into spherical zones with different phases: if the phase of the light at point H' is equal to $2\pi\frac{t}{T}$, then in all points of zone number k the phase is equal to $2\pi\frac{t}{T} - \delta_k$, or $2\pi\frac{t}{T} - k\delta_1$, where δ_k and δ_1 are defined by formulas (4) and (3); the spherical surfaces QQ and S'S' now are not wave surfaces.

A part of Figure 4 is reproduced in Figure 5 with the addition of the heights a_{k-1}, a, a_k of the segments of the sphere QQ which have base radii h_{k-1}, h, h_k. Using the Kirchhoff- Huygens principle, we calculate the perturbation dq at an arbitrarily chosen point n, situated on the axis at a distance $\bar{R}$ from the point H' and at a distance ΔR from the point F'. We assume that an imaginary point source, illuminating the surface QH', is situated at the focus of the objective F'. If the phase of the oscillation at this point is $2\pi\frac{t}{T}$, then the phase at the point K on the sphere is equal to $2\pi\left(\frac{t}{T} + \frac{R}{\lambda}\right) - \delta_k$, where δ_k, is the lag caused by the phase plate, and phase of the oscillation travelling from the point K to N, we have $2\pi\left(\frac{t}{T} + \frac{R-r}{\lambda}\right) - \delta_k$, where r is the distance KN.

The angles between normals to the sphere Q and rays from point F' are always equal to 180^0, and in the same way angles with the diffracted rays KN differ little from zero; therefore the difference of cosines in the Kirchhoff formula may be taken equal to 2, and for an elementary perturbation dq, caused at point N by diffracted rays from points in a zone element on the sphere, the following formula may be written

$$dq = \frac{A}{Rr\lambda}\sin\left[2\pi\left(\frac{t}{T} + \frac{R-r}{\lambda}\right) - \delta_k\right] dS, \tag{8}$$

where dS is the area of the zone element, given by

$$dS = 2\pi R\, da,$$

and A is the amplitude of oscillation at point F'

In order to find the light perturbation q_k, caused by the whole zone of number k at point N, we integrate (8) between the limits a_{k-1} and a_k. For this we use the relations

$$r^2 = R^2 - 2a\Delta R;$$

$$dS = -\frac{2\pi R\, dr}{\Delta R}; \quad r_k \cong R - \frac{a_k \Delta R}{R}, \quad a_k \cong \frac{h_k^2}{2R}.$$

After reducing the expression obtained for q_k to logarithmic form we expand it in a series in order to separate out the terms which do not contain k. In this way we arrive at the following formula:

$$q_k = \frac{2A}{\Delta R}\sin\frac{1}{2}\alpha_1\left[\sin\omega\cos k(\alpha_1 - \delta_1) + \cos\omega\sin k(\alpha_1 - \delta_1)\right],$$

in which for compactness we use the following notation

$$\alpha_1 = \frac{\pi h_1^2 \Delta R}{R\bar{R}\lambda}; \tag{9}$$

$$\omega = 2\pi\left(\frac{t}{T} - \frac{\Delta R}{\lambda}\right) - \frac{\pi h_1^2 \Delta R}{2R\bar{R}\lambda}.$$

We obtain the light disturbance q_m at point N, caused by the entire flux of radiant energy, by adding all values of q_k from k equal to 1, up to m, where m is the number of zones:

$$q_m = \frac{2A}{\Delta R}\sin\frac{1}{2}\alpha_1\left[\sin\omega\sum_{k=1}^{k=m}\cos k(\alpha_1 - \delta_1) + \cos\omega\sum_{k=1}^{k=m}\sin k(\alpha_1 - \delta_1)\right].$$

We calculate both sums according to formulas, in mathematical handbooks. Raising the coefficients of $\sin\omega$ and $\cos\omega$ to the 2nd power and adding the resulting expressions, we find a quantity proportional to the radiant power at point N; designating it as E_N we have

$$E_N = \frac{4A^2 \sin^2 \frac{1}{2} a_1 \sin^2 \frac{1}{2} m (a_1 - b_1)}{(\Delta R)^2 \sin^2 \frac{1}{2} (a_1 - b_1)} \tag{10}$$

The effective aperture of the phase plate may be calculated at the entrance pupil of the system; denoting its diameter by the letter D, and the relative aperture of the system by the letter P, we have

$$D = 2b_1 \sqrt{m}, \qquad P = \frac{D}{R} = \frac{2b_1 \sqrt{m}}{R}; \tag{11}$$

introducing this notation into Eq. (9) we get:

$$\alpha_1 = \frac{\pi D^2 \Delta R}{4mR^2\lambda}. \tag{12}$$

We may write Eq. (10) in the following form:

$$E_N = \frac{\pi^2 D^4 A^2}{16R^2\lambda^2 m^2} \cdot \frac{\sin^2 \frac{1}{2} a_1}{\left(\frac{1}{2} a_1\right)^2} \cdot \frac{\sin^2 \frac{1}{2} m (a_1 - b_1)}{m^2 \sin^2 \frac{1}{2} (a_1 - b_1)}. \tag{13}$$

From this formula we can obtain the well known formula for the intensity E_F at the focus of an objective without phase plate for a beam with wave length λ; for this it is necessary to take $\Delta R = 0$, and hence $\alpha_1 = 0$, $m = 1$, $R = R$; then

$$E_F = \frac{\pi^2 D^4 A^2}{16R^2\lambda^2}. \tag{14}$$

We shall denote the relative intensity of a beam with wave length λ at a point N by the ratio $E_N : E_F (= I_N)$:

$$I_N = \frac{R^2}{R_0^2} \cdot \frac{\sin^2 \frac{1}{2} a_1}{\left(\frac{1}{2} a_1\right)^2} \cdot \frac{\sin^2 \frac{1}{2} m (a_1 - b_1)}{m^2 \sin^2 \frac{1}{2} (a_1 - b_1)} \tag{15}$$

The function I_N is similar structurally to the distribution function for the spectral intensity of a plane diffraction grating, differing only in the first factor, which decreases monotonically with increasing R; this makes it possible to use the results of other studies of the grating formula, which can be found, e.g. in the book of Klemens Schaefer [2].

The function I_N has two sets of maximum values. The largest maxima occur at values of the variable α_1 which satisfy the condition

$$\frac{1}{2}(a_1 - b_1) = l\pi, \tag{16}$$

where l is an integer: $0, \pm 1, \pm 2 \ldots$

The values of the second set which are located among the first, are very small and may be neglected.

Replacing R in formula (9) by the sum $R + \Delta R$ and substituting in place of α_1 its value from Eq. (16), we find those values of $\Delta_m R$, for which the function I_N has a maximm in the first set:

$$\Delta_m R = \frac{8m R^2 \lambda \left(\frac{1}{2} b_1 + l\pi\right)}{\pi D^2 - 8m R\lambda \left(\frac{1}{2} b_1 + l\pi\right)}. \tag{17}$$

The corresponding maximm values of the relative intensity $I_{N\,max}$

$$I_{N.\,max.} = \frac{\sin^2 \frac{1}{2} b_1 \left[\pi D^2 - 8m R\lambda \left(\frac{1}{2} b_1 + l\pi\right)\right]^2}{\pi^2 D^4 \left(\frac{1}{2} b_1 + l\pi\right)^2}. \tag{18}$$

In the denominator of Eq. (17) and in the numerator of (18) the term $\left(\frac{1}{2} b_1 + l\pi\right)^2$ for small values of m from 10 to 30, amounts to only a few percent of the numerical value of the first term πD^2; neglecting this term, we obtain the following approximate formula:

$$I_{N.\,max.} = \frac{\sin^2 \frac{1}{2} b_1}{\left(\frac{1}{2} b_1 + l\pi\right)^2}. \tag{19}$$

$$\Delta_m R = \frac{8m R^2 \lambda \left(\frac{1}{2} b_1 + l\pi\right)}{\pi D^2} = \frac{8m\lambda \left(\frac{1}{2} b_1 + l\pi\right)}{\pi P^2}. \tag{20}$$

Moreover, in place of the exact formula (3) we may take

$$b_1 = \frac{2\pi l_0}{l}, \tag{21}$$

because the ratio $\frac{n-1}{n_0-1}$ differs little from unity.

3. THE RELATIVE INTENSITY AT THE FOCUS OF AN OBJECTIVE COMBINED WITH A PHASE PLATE

We apply formula (15) to calculate the relative intensity I_P at the focus of a beam with wave length λ, after a phase plate has been placed in front of the objective. In this case $R = R$, $\Delta R = 0$, $\alpha_1 = 0$ so that

$$I_P = \frac{\sin^2 \frac{1}{2} m b_1}{m^2 \sin^2 \frac{1}{2} b_1}. \tag{22}$$

Detailed investigation of the function I_P and a graph corresponding to it may be found in the book [3]. In the present case the argument of the function δ_1 varies between narrow limits corresponding to the wave lengths bounding the visible spectrum; therefore, instead of the usual investigation, it will be sufficient to cite the results of calculation according to formula (22) for two special cases, when the phase plates are made of KB glass, have 10 zones and are computed for wave lengths $589.3 \cdot 10^{-6}$ mm ($n_0 = 1.5163$) and $510.0 \cdot 10^{-6}$ mm ($n_0 = 1.5163$) (see Table 1.)

TABLE 1.

Relative Intensity at the Focus of An Objective Combined with a Phase Plate

m = 10	$\lambda_0 = 589.3 \cdot 10^{-6}$		$\lambda_0 = 510.0 \cdot 10^{-6}$	
$\lambda \cdot 10^6$	$\frac{1}{2}\delta_1$	$100\, I_P$	$\frac{1}{2}\delta_1$	$100\, I_P$
365.0	5.2639	0.7	4.5201	0.9
404.7	4.6944	0.03	4.0311	0.4
434.1	4.3486	0.3	3.7342	0.4
486.1	3.8503	1.2	3.3062	37.0
510.0	3.6586	3.3	3.1416	100.0
546.1	3.4032	3.8	2.9223	14.0
589.3	3.1416	100.0	2.6977	5.0
656.3	2.8078	0.4	2.4121	1.6
766.5	2.3807	1.9	2.0529	1.3
863.0	2.1156	0.8	1.8167	0.4
950.0	1.9166	0.1	1.6458	0.5

Adding a phase plate to the objective does not change the intensity at the focus of the beam at the wave length for which the plate is computed; at other wave lengths the intensity falls off sharply.

4. THE POINTS OF MAXIMUM RELATIVE INTENSITY AND THEIR DISTRIBUTION ALONG THE AXIS OF THE OBJECTIVE.

It was noted above, that the second term in brackets in the numerator of (18) and in the denominator of (17) is considerably smaller than the first term. Consequently the maximum relative intensity $I_{N'max}$ is almost independent of the number of zones m; this number does not appear in the approximate formula (19). At the same time the distance $\Delta_m R$, according to (17), is almost proportional to the number of zones m, and exactly proportional to it according to the approximate formula (20).

For sufficiently large values of m the denominator in Eq. (17) becomes zero, and the distance $\Delta_m R$ becomes infinitely large; hence $I_{N',\max}$ becomes zero.

For small values of m we may use the approximate formulas (19) and (20).

The largest (principal) value of the relative maximum intensity $I_{N'max}$ at the limiting value $\frac{1}{2}\delta_1$, shown in Table 1, according to (19), is obtained if $l = -1$; for this

$$I_{N,\max} = \frac{\sin^2 \frac{1}{2}\delta_1}{\left(\frac{1}{2}\delta_1 - \pi\right)^2}, \tag{23}$$

$$\frac{\Delta_m R}{m} = \frac{\sin\left(\frac{1}{2}\delta_1 - \pi\right)}{\pi^2}. \tag{24}$$

In Table 2 values of the largest relative maxima $100\, I_{N'max}$ are given in per cent and the ratio $\frac{\Delta_m R}{m}$ is calculated from Eqs. (23) and (24) for an objective with relative aperture 1:15.81 for various wave lengths at two values of λ_0: $589.3 \cdot 10^{-6}$ and $510.0 \cdot 10^{-6}$ mm.

Table 3 contains values of $\Delta_m R$ and $100\, I_{N'max}$, calculated from Eqs. (19) and (20) for five wave lengths and five integer values of l; the plate is computed for a wave length of $589.3 \cdot 10^{-6}$, the number of zones is 10.

TABLE 2

Principal Maximum Relative Intensities at Points on the Axis of an Objective with a Phase Plate and the Distance of these Points from the Foci.

m = 10	$\lambda_0 = 589.3 \cdot 10^{-6}$		$\lambda_0 = 510.0 \cdot 10^{-6}$	
$\lambda \cdot 10^6$	$100\, I_{N,\max}$	$\frac{\Delta_m R}{m}$	$100\, I_{N,\max}$	$\frac{\Delta_m R}{m}$
365.0	16	0.49	51	0.32
404.7	42	0.40	76	0.23
434.1	60	0.34	89	0.16
486.1	84	0.22	99	0.05
510.0	91	0.17	100	0.0
546.1	98	0.09	98	−0.08
589.3	100	0.00	94	−0.17
656.3	96	−0.14	86	−0.30
766.5	83	−0.37	68	−0.53
863.0	70	−0.56	54	−0.73
950.0	59	−0.74	44	−0.90

Examination of the formulae and results of calculation lead us to the following conclusions.

A phase plate, computed for a wave length λ_0 and located in front of the objective in a parallel beam of the same wave length λ_0, does not influence the image of an infinitely remote point at the focus of the objective, but destroys the images of those points produced by beams of other wave lengths at the corresponding foci of the objective; these images are replaced by a series of points along the axis with maximum values of intensity sharply decreasing with displacement in both directions from the point of largest maximum for the given wave length. The values of the largest maxima of the relative intensity are always smaller than unity (smaller than 100% in Table 2) and are smaller the more λ differs from λ_0; for beams with bounded wave lengths (see Table 2) these values are 15% and 60% if $\lambda_0 = 589.3 \cdot 10^{-6}$ mm, and 50% and 45% if $\lambda_0 = 510.0 \cdot 10^{-6}$ mm. Points with the largest maxima do not coincide with the foci of the corresponding beams.

The distances of the points of largest maximum value from the foci of the corresponding beams for objectives with relative aperture 1:15.81 and 10 zones in the first case are +5 and -7.5 mm, and in the second +3 and −9mm.

Table 3

Axial Positions of Points of Maximum Intensity and Values of the Intensities $P = 1{:}15.8$; $m = 10$; $\lambda_0 = 589.3 \cdot 10^{-6}$mm

$\lambda \cdot 10^6$	404.7		434.1		477.2		706.5		950.0	
l	$\Delta_m R$	$100\, I_{N,\max}$	$\Delta_m R$	$100\, I_{N,\max}$	$\Delta_m R$	$100\, I_{N,\max}$	$\Delta_m R$	$100\, I_{N,\max}$	$\Delta_m R$	$100\, I_{N,\max}$
−3	−12	5	−14	3	−17	2	−34	1	−45	2
−2	− 4	40	− 5	23	− 7	9	−19	3	−28	5
−1	+ 4	43	+ 3	80	+ 2	81	− 4	83	− 7	54
0	+12	5	+12	5	+12	3	+12	8	+12	24
+1	+20	2	+21	2	+22	1	+27	2	+31	4

The numbers in Table 3 show that the values of the principal maxima considerably exceed the others over almost the entire spectrum, but that at the edge of the violet region the maxima for l-1 and -2 are nearly equal.

5. INTENSITY AT POINTS IN A PLANE PERPENDICULAR TO THE AXIS THROUGH THE POINT OF LARGEST MAXIMUM

To resolve the question of how much the intensity at the point of maximum intensity on the axis differs from that at the focus of the objective without a phase plate, it is necessary to examine the distribution of intensity at neighboring points in a plane perpendicular to the axis, and to compare it with the distribution in the "Airy pattern"; derivations of the corresponding formulae are sufficiently complicated that for lack of space they will not be given here; only a general outline of the derivation is presented.

In Figure 6, analogous to Figure 5, P_1OP_2 is part of the "principal" sphere, passing through the second principal point O of the objective, with center at its focus; the intensity may be calculated at point N with coordinates $R + \Delta R(= \bar{R})$ and σ; point M lies on the sphere. A formula for calculating the intensity at an out-of-focus and off-axis point N for an objective without a phase plate was derived by Lommel [4], for which it was required to calculate the light disturbance at this point caused, according to Huygens-Fresnel, by oscillations arriving from all points of the partial sphere P_1OP_2 of base radius h. This formula was applied in the given case to calculate the disturbance at point N of zone number k formed after addition of the phase plate to the objective. It is evident that this disturbance is equal to other disturbances, caused in Lommel's case by those of the sphere with base radii h_k to h_{k-1}. It is necessary to pay attention to the phase lags δ_k, taking into account the phase plate as well as all points within zone number k. The disturbance q_N at the point N, caused by oscillations from all points of the sphere P_1OP_2, is obtained from the result of the sum of all differentials for values of the index k from 1 to m. The result may be presented in the following way:

$$q_N = \frac{A}{(\Delta R)}\left[S_N \sin\omega - C_N \cos\omega\right];$$

here $\omega = \frac{2\pi t}{T} - \Psi$; where Ψ depends on the given $\bar{R}$, σ, λ and does not depend upon time; S_N and C_N are complicated polynomials, containing special Lommel functions.

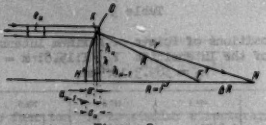

Figure 5

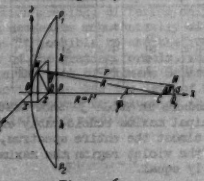

Figure 6

The desired intensity E_N at point N is given by the formula:

$$E_N = \frac{A^2}{(\Delta R)^2}\left[S_N^2 + C_N^2\right].$$

Let us suppose that a plane is drawn through point N perpendicular to the axis and passing through the point Q_1 of largest maximum intensity; the $E_{N,0}$ at point Q_1 may be obtained from formulas (10) and (16); we find

$$E_{N,0} = \frac{4A^2 m^2 \sin^2\frac{1}{2}\delta_1}{(\Delta_m R)^2}.$$

The relative magnitude $I_{N,0}$ at point N as a percentage of the intensity at point Q_1 is given by the formula

$$I_{N,0} = \frac{100 E_N}{E_{N,0}} = \frac{100\left[S_N^2 + C_N^2\right]}{4m^2 \sin^2\frac{1}{2}\delta_1}; \tag{25}$$

S_N and C_N are complicated functions of the argument z_1 defined by:

$$z_1 = \frac{\pi\sigma P}{\lambda\sqrt{m}}. \tag{26}$$

Calculations according to Eq. (25) have been carried out for an objective with relative aperture 1:15.81, and for a phase plate made of KS glass computed for a wave length $589.3 \cdot 10^{-6}$mm; the calculations of relative intensity were made for 14 points and for a single wave length $477.21 \cdot 10^{-6}$mm. In this case $\delta_1 = 2.5\pi$ and the largest value of maximum intensity at a point on the axis was 81.057% of the intensity for the same wave length at the focus of the objective without phase plate.

The corresponding ratio $I_{P,0}$, for points off the axis in the focal plane of an objective without phase plate in the Airy pattern, as is known, has the following value:

$$I_{P,0} = \frac{400 J^2(z)}{z^2}, \tag{27}$$

where J(z) is the Bessel function of the first kind and the first order with argument z, where

$$z = \frac{\pi\sigma P}{\lambda}. \tag{28}$$

From a comparison of Eqs. (26) and (28) it follows that the arguments z_1 and z, corresponding to one and the same value of σ (the distance of the point from the axis), satisfy the relation

$$z = z_1\sqrt{m}. \tag{29}$$

The functions S_N and C_N have a somewhat simpler appearance than for other values of λ namely

$$S_N = \sum_{1}^{k=m} U_{k,0} + \sum_{1}^{k=m} U_{N,0};$$

$$C_N = -\sum_{1}^{k=m} U_{k,0} + \sum_{1}^{k=m} U_{N,0}.$$

The functions $U_{I,k}$ and $U_{II,k}$ are Lommel functions, defined in the present case by the formulas:

$$U_{I,k} = \sum_{s=1}^{\infty} (-1)^s \left(\frac{z\sqrt{10}}{z_1}\right)^{2s+1} J_{2s+1}(\sqrt{z}\, z_1);$$

$$U_{II,k} = \sum_{s=1}^{\infty} (-1)^s \left(\frac{z\sqrt{10}}{z_1}\right)^{2s+2} J_{2s+2}(\sqrt{z}\, z_1);$$

J_{2n+1} and J_{2n+2} are Bessel functions of the first kind and order $2n+1$ and $2n+2$ respectively.

Values of the Lommel functions were calculated with the aid of eight-place tables of Bessel functions of integers; application of linear interpolation introduced error in the sixth place, sometimes in the fifth. In the results 3 or 4 decimal places may be taken as significant.

The results of the calculations are shown in Table 4. In the second column are given values of intensity at point N as a percentage of the intensity at a point on the axis, i.e. the value of the function I_{N0} according to Eq. (25); in the fourth column are values of the corresponding function $I_{F,0}$ for the Airy pattern at the focus of the objective without a phase plate. The first and third columns contain values of the arguments z_1 and z; the numbers located in a single row correspond to points equidistant from the axis, i. e. at a distance σ.

In order to obtain all values of relative intensity in identical units, taking 100 as the intensity at the center of the Airy pattern, it is necessary to multiply all numbers of the second column by 0.81057.

The numbers in the second and fourth columns are very close to each other; minimum values occur for the same value of the distance σ, and seemingly, in the diffraction pattern of the objective with a phase plate there are no points of zero intensity; but starting at a certain distance these values are approximately ten times larger than in the Airy pattern; in consequence of this it may be expected that the rings in the diffraction pattern differ from rings in the Airy pattern only by a small amount of contrast. This conclusion is based on a very scanty amount of material, but because calculation according to the above-mentioned equation requires much time and difficulty, it was considered practicable to present only limited results.

6. APPLICATION OF PHASE PLATES TO THE CORRECTION OF CHROMATIC ABERRATION OF THE OBJECTIVE.

The insertion of a phase plate into the bundle of parallel rays in front of a real objective changes the location of the objective's foci for rays of all wave lengths, except that for which the plate is computed. In Figure 7 the fine curve is the secondary spectrum of a double-lens achromatic objective with focus D 1000 mm; the distance ΔR of the focus from point D along the horizontal is plotted against wave length.

In Figure 7 the sloping straight line represents the dependence on wave length of $\Delta_m R$, the distance of the point of maximum intensity from the focus of rays with the same wave length in the absence of a phase plate; the distance $\Delta_m R$ is

Table 4

Intensities in a Plane, Perpendicular to the Axis and Passing through the Point of Largest Maximum and in the Focal Plane of an Objective without a Plate.

z_1	$I_{N,0}$	$z = z_1\sqrt{10}$	$I_{F,0}$
0.0	100.00	0	100.00
0.1	97.524	0.3162	97.526
0.5	51.273	1.5811	51.611
1.0	3.086	3.1623	3.056
1.21189	0.037	3.83171	0.000
2.0	0.429	6.3246	0.408
2.218523	0.0003	7.015587	0.000
3.0	0.147	9.4868	0.1196
3.83171	0.151	12.1189	0.1257
4.5	0.068	14.2302	0.0647
5.13563	0.0147	16.2403	0.0163
7.0156	0.0758	22.1852	0.0969
17.8598	0.0472	56.4853	0.0515
19.6158	0.0077	62.0308	0.0011

calculated from Eq. (24) for a plate made of K8 glass, with 5 zones and relative aperture 1:15.81 and for ray D.

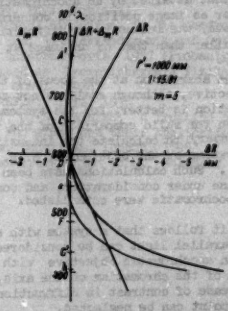

Figure 7

When the plate is inserted in front of the objective in a bundle of parallel rays of white light, instead of the image of an infinitely distant point appearing at the focus of rays with a particular wave length, a diffraction pattern is formed with a maximum intensity centered at a distance $\Delta R + \Delta_m R$ from the origin of co-ordinates; i. e., from focus D; the heavy curve shows the secondary spectrum of the system consisting of phase plate and achromatic objective

It is clear from the figure that the insertion of a phase plate improves the long-wave region of the curve. Because the dependence of $\Delta_m R$ on wave length λ is always represented by a straight line, the slope of which at a given P depends only on m, then for the best approximation of the entire curve of the secondary spectrum to the ordinate axis it is necessary to have an objective for which the secondary spectrum deviates least from the straight sloping line; i.e. it is necessary to design the objective for unusually large chromatic aberration. In order to avoid the necessity for such design calculations, a device used by Sliusarev [1] was applied, namely: to the double-lensed achromatic objective with focal distance 1000 mm

is attached a plano-convex lens of flint glass with focal distance 6000 mm, the system thus obtained constitutes an objective with focal distance calculated as 1000 mm. The chromatic aberration of this objective is represented by the fine curve of Figure 8, the main part of which is straight. To this objective is added a phase plate with 10 zones but it appears necessary to reduce the relative aperture of the objective to 1:16.33. The heavy curve represents the secondary spectrum of the system; the residual aberration for nearly all parts of the spectrum up to G' is very small, but in the short wave region it is significant.

For comparison, in the same figure a dotted curve shows the chromatic aberration of an apochromatic objective made of 4 lenses. The two curves are very close to each other.

The results presented have been obtained by rather casual examination of the system considered, but nevertheless they are sufficient to indicate the possibility of correcting chromatic aberration on the axis by applying a phase plate with a bundle of parallel rays. The result of the correction is close to that attained by an apochromatic objective as far as image position is concerned, but as was shown, the intensity at diffraction maxima is always smaller than that of an image at the foci of the ray.

If the aberration at the focus of the apochromatic objective, although small is not zero, and the correction is better, for the system with phase plate, then for valid comparison of the two systems it is necessary to calculate the intensity of rays in both systems at the best point, e. g. at the focus D . Such calculations have been carried out for the case under consideration, and some preferences for the apochromatic were established.

Thus, it follows that a system with a phase plate in parallel light can be considered equal in value to an apochromatic objective with respect to correction of the chromatism on the axis, if the small decrease of contrast in diffraction rings at the image point can be neglected.

Resolution of the question concerning the influence of a phase plate on the image at off-axis points presents more difficulty, because here it becomes necessary to take into account a series of complicated circumstances.

The center of the plate must be situated so as to intersect the main beam of incident rays, i.e. the plate has to be situated at the entrance pupil of the objective; the incident rays acquire phase differences not only as a consequence of passing through various zones of the plate, but also as a consequence of geometric path differences; the phase lag δ_1 depends on the angle of incidence; it is not easy to determine the kind of surface for which we must carry out the integration, or to indicate the phase distribution over it, etc. Still more complication presents itself in the theoretical examination of the properties of the plate in converging bundles of rays. Historical experience with zone plates does not furnish a basis for expecting better results from the application of phase plates in optical systems.

Naturally, these doubts and predictions may be disputed, but still it would be inappropriate to undertake a complicated theoretical investigation before the possibility of preparing phase plates with plane surfaces of the required precision has been demonstrated. An experimental investigation of the properties of such plates in optical systems would give definite answers to many questions. The possibility of preparing the phase plates with spherical surfaces ("notched lenses"), of satisfactory quality, appears very doubtful.

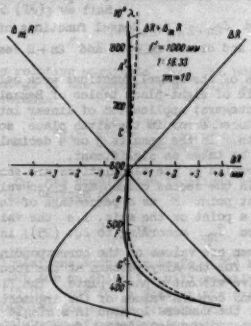

Figure 8

7. ADDITIONAL REMARKS

The largest difference between the work presented here and that in reference [1] appears in the replacement of the notched lens by a phase plate with plane surfaces in order to realize an interesting way of influencing the chromatism of ray bundles. This replacement offers the possibility of applying the theory of diffraction phenomena in parallel rays (Fraunhofer diffraction), simplifying the solution of the problem, and at the same time it makes the preparation of such phase plates with necessary precision more feasible.

In the results and calculations of the present work, the analogy between phase plate and lens known from the theory of zone plates has not been applied at all, because this analogy cannot be accounted as evident and must be justified first. It is easy to show that a phase plate for parallel rays is similar to a lens with focal distance f'_p, defined by the approximate formula

$$f'_p \cong \frac{h^2}{2(\lambda - \lambda_0)};$$

if $\lambda = \lambda_0$, then $f'_p = \infty$, i.e. a plate calculated for wave length λ_0, in rays of this wave length is equivalent to a plane parallel plate. In contradistinction to this formula the phase plate (notched lens) in reference [1] is assigned a focal distance given by the formula

$$f'_1 = \frac{h^2}{2\lambda},$$

which is defined as the "point on the abscissa , at which the maximum light energy is accumulated" in the case of plane waves, independent of the construction of notched lens.

In reference [1] Eq. (4) is used to calculate the ratio of intensities at the point of largest maximum at wave length λ to the focal intensity at λ_0 of an objective with phase plate designed for wave length λ_0; in the formula the factor $\left(\frac{A_\lambda}{A_{\lambda_0}}\right)^2$ the square of the ratio of the amplitudes is omitted. The complete formula is the following:

$$\frac{E(\lambda)}{E(\lambda_0)} = \left(\frac{A_\lambda}{A_{\lambda_0}}\right)^2 \cdot \left(\frac{\lambda_0}{\lambda}\right)^2 \cdot \left(\frac{\sin\frac{1}{2}B}{\frac{1}{2}B}\right)^2,$$

where $B = 2\pi - \delta_1$, and the first factor is a function defined by the spectral composition of the radiation and may take on values between zero and $+\infty$. This factor is equal to unity for radiation with a so-called "equal-energy spectrum". It may be noted that ratios of the intensities of various rays at various points on the axis cannot serve to characterize the influence of a phase plate on the spectral composition of the radiation.

Formulas for calculating the intensity at off-axis points in the plane passing through the point of principal maximum on the axis are obtained in the two papers by completely different methods and have different structures; it is possible that the method of integration applied in reference [1] is much more convenient than Lommel's method. For comparison, it would be necessary to have complete presentations of the two methods, to perform calculations on the same example and to estimate the precisions attained. Eq. (5) in reference [1] should reduce to the known distribution of intensity in the Airy pattern for q=1 zones and $B = 0$; $(B = 2\pi - \delta_1)$. With these substitutions the first term gives the required function, but it is not indicated that all of the expressions in brackets are equal to zero.

In order to draw conclusions concerning the aberration of lenses with phase plates it would be necessary to have a complete treatment of the problem with a precisely defined concept of aberration in the given case. It is appropriate to repeat that it would be expedient to postpone difficult theoretical investigations of the problem until phase plates with plane surfaces have been prepared, and until it appears possible to define experimentally the limiting relative aperture of a system, its field of view, etc. and until all possibilities of utilizing the original method of correcting chromatism at the objective have been explored.

April 29, 1958

References

1. G. G. SLIUSAREV: DAN USSR, 113, 780 (1957) (See Sov. Phys. Doklady)
2. C. SCHAEFER: Einfuhrung in die theoretische Physik. Bd. 3. Elektrodynamik und Optik, 1932. Quantentheorie, 1937 (Probably translated as Teoreticheskaia fizika. Optika, GONTI, 1938)
3. C. SCHAEFER: ibid, 1938
4. A. GRAY, G. B. MATHEWS: A Treatise on Bessel Functions and their Applications to Physics. Macmillan, London, 1895 (Russian translation used, published 1953)

TOM VI, Vyp. 2 OPTIKA I SPEKTROSKOPIIA Fevral', 1959
VOL. VI. No. 2 OPTICS AND SPECTROSCOPY February, 1959

The Influence of Temperature Gradient of Glass of Optical Systems on the Image Produced by the Latter

G. G. SLIUSAREV

Abstract: The influence of a non-uniform temperature distribution within optical components on the resultant images, is considered theoretically. The influence of thermal deformation of the shape of lens surfaces and the influence of the gradient of refractive index evoked by non-uniformity of temperature is also considered.

The question of the influence of temperature, or more accurately, changes of temperature, on the quality of images produced by optical systems, has become, in recent times, the topic of a number of investigations of both theoretical and experimental nature. Among works of theoretical nature should be noted articles by Krüger [1], Sonnefeld [2], Maksutov [3], and in particular papers by Perry [4] and Volosov [5], in which is considered the influence of temperature changes on representation coordinates of a point -- the object's temperature changes are supposed to be such that at each moment the temperature of all elements of the optical system (glass and casings) is identical. These calculations are performed for the paraxial region by means of procedures extremely close to those with which are determined chromatic aberrations of position and magnification.

In the particular case of a duo-lens objective, Maksutov derived a formula for the change in location of the focus, with change of temperature.

Volosov [5] extended Perry's work and brought into being a series of objectives corrected with respect to thermo-optical aberrations.

Let us denote by α the (linear) expansion coefficient of the lens material. This means that all its linear elements, l (thickness, radii of curvature), change according to the law $l=l_0[1+\alpha(t-t_0)]$, where l_0 is the size of the element at temperature t_0. Let us denote by β the coefficient of increase of the refractive index of glass, so that $n(t)=n_0+\beta(t-t_0)$. Upon change of t by Δt, l changes by $l\alpha\Delta t$, and n by $\beta\Delta t$. The change, $\Delta f'$, in the focal distance of an infinitely thin lens, defined by the equation $\frac{1}{f'}=(n-1)\left(\frac{1}{r_1}-\frac{1}{r_2}\right)$, is calculated from the formula

$$\frac{\Delta f'}{f'}=(n-1)\left(\frac{\Delta r_1}{r_1^2}-\frac{\Delta r_2}{r_2^2}\right)+\Delta n\left(\frac{1}{r_1}-\frac{1}{r_2}\right)-\left(\frac{\beta}{n-1}-\alpha\right)\frac{\Delta t}{f'};$$

$$\Delta f'=\left(\alpha-\frac{\beta}{n-1}\right)f'\Delta t. \quad (1)$$

The coefficient $\alpha-\frac{\beta}{n-1}$ plays an extremely important role in the calculation of the thermal change of the image position and Perry denoted it by the single letter θ. This quantity θ may, in a first approximation, be considered constant over a sufficiently wide range of temperature and wavelength changes. Just as the quantity D-- the dispersion coefficient of glass -- determines the chromatic aberration of optical systems as a result of dispersion, so the quantity θ determines the thermo-optic change of image location as a result of temperature change.

However the application of formula (1) and the greater generalities ensuing from it (see [1-5]), having a bearing on complex optical systems, in which also are taken into account the expansion of metallic tubes joining individual components of the optical system, is possible only with the indispensable stipulation that all lenses and all cases, at any instant should be at the same temperature in all their parts. This stipulation is not satisfied without special measures upon which there is no necessity to dwell here.

In optical systems of large dimensions, as astronomical refractors, reflectors, mirror-like lens systems it is impossible to attain the goal that the temperature of all parts--optics, cases and tubes--be one and the same. The temperature of the medium in which optical components of astronomic and other large instruments are submerged, is non-uniform. These non-uniformities set up a special temperature distribution within the material of lenses and mirrors at times radically different from a perfectly uniform distribution.

The question of the influence of a non-uniform temperature distribution within lenses is clarified very slightly in the literature and then only from the point of view of experiment.

A theoretical study of this question, based on the law of ray propagation in non-homogeneous media, taking into account surface deformations caused by the non-uniform temperature distribution, is the aim of the present article.

Non-uniform heating of an optical component leads to two consequences: 1. A change in the shape of the optical component, which causes deviation of ray through some angle ε; 2. The appearance of a gradient in the refractive index in the material of the component, which in turn causes bending of the ray trajectory as well as a deviation of the ray path. These two very small deviations are added in accordance with the law of addition of differentials.

1. CHANGE IN SHAPE OF AN OPTICAL COMPONENT UNDER THE INFLUENCE OF NON-UNIFORM HEATING

The following assumptions will be made to simplify the calculations:

1. A definite thermal regime, not varying with time, has been established in the optical component.

2. Upon achievement of the definite thermal regime there are no elastic stresses in the optical items. Therefore, the deformation of the optical piece is calculated solely on the basis of a linear expansion law.

This assumption cannot raise serious objections for the majority of optical components such as lenses and mirrors, the thickness of which is not large in comparison with the diameter, especially if measures are taken so that the expansion of the item takes place freely.

3. The temperature gradient is directed perpendicularly to the axis of symmetry of the optical item, if the latter possesses such a one.

If there is no axis of symmetry, the direction of the gradient will be specified in a special way every time.

4. The ray propagates in a manner such that the angle u formed with the axis is small, and the cosine of this angle may be taken equal to unity.

Let AB=e(h) (fig. 1) be the thickness of the item at a distance h from the axis (or from a chosen straight line which, upon heating, does not submit to a displacement). By convention, we will assume that the temperature equals zero on a level with the axis 00: At a height h the temperature equals t (h). The elongation, (de), of section AB will be de=αe(h) t (h).

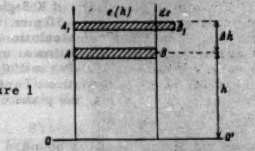

Figure 1

At the same time, section AB shifts in elevation. Each section, dh is elongated by α dht (h). The overall shift, Δh, equals: $\Delta h=\alpha\int_0^h t(h)\,dh$.

In this manner the element AB simultaneously expands by the quantity $de=\alpha e(h)\,t\,(h)$ and shifts upward by a quantity $\Delta h=\alpha\int_0^h t(h)dh$.

A ray, incident upon an optical detail at a specified elevation h, which upon absence of heating would have fallen on the element AB, in actuality will pass through element A_1B_1, located at a distance Δh below AB. Inasmuch as this element is lower, its thickness d is somewhat different from that of element AB. The difference in thickness, e (h), caused by the difference in elevations, Δh, equals $e(h)=\frac{de(h)}{dh}\Delta h$,

where $\Delta h=\alpha\int_0^h t(h)\,dh$. therefore the change of thickness, Δe, must be considered equal to:

$$\Delta e=\alpha e(h)t(h)-\alpha\frac{de}{dh}\int_0^h t(h)dh=\alpha\left[e(h)t(h)-\frac{de}{dh}\int_0^h t(h)dh\right].$$

The deviation of the ray from its initial direction may be calculated in the following manner.

Let e be the thickness of the optical element (fig. 2). The corresponding change in the position of the wave front, effected by this element, equals (n-1) e and is directed to the left. We will assume that upon passing from elevation h to elevation h + dh, the element thickness changes by de. Then the plane of the wave changes its slope by $(n-1)\frac{de}{dh}$, whereupon the ray deviates upward.

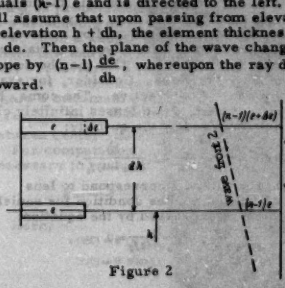

Figure 2

So, the deviation ε_1 of the ray upward is determined by the formula: $\varepsilon_1=(n-1)\frac{de}{dh}$.

Consequently ε_1 is determined by the equation:

$$\varepsilon_1=(n-1)\frac{d\varepsilon}{dh}=(n-1)\alpha\frac{d}{dh}\left[e(h)\,t(h)-\frac{de}{dh}\int_0^h t(h)\,dh\right].$$

Let us differentiate the expression within the square brackets:

$$\frac{d}{dh}\left[\ \right]=\frac{de}{dh}t(h)+\frac{dt}{dh}e(h)-\frac{d^2e}{dh^2}\int_0^h t(h)\,dh-\frac{de}{dh}t(h)=$$

$$=\frac{dt}{dh}e(h)-\frac{d^2e}{dh^2}\int_0^h t(h)\,dh.$$

and

$$\varepsilon_1=(n-1)\alpha\left[\frac{dt}{dh}e(h)-\frac{d^2e}{dh^2}\int_0^h t(h)\,dh\right].$$

2. EFFECT OF THE GRADIENT OF THE INDEX OF REFRACTION

We now consider a volume element of an isotropic, but non-homogeneous, medium the index of which changes from point to point. If the element is sufficiently small, it may be assumed that the variation of the index along the coordinates adheres to the linear law or, in other words, it may be assumed that the gradient of the index is constant. In the case considered in this paper, where the index varies slightly and smoothly, the gradient may be assumed to be constant even over large expanses of the volume of the medium, if the ray is propagated almost parallel to the axis and the gradient of the index is perpendicular to the axis.

Let ABCD (fig. 3) be a section of a small volume element of the meridian plane; GG' the gradient, which we will assume constant; i the angle that the incident ray, LM, makes with the gradient.

As is well known [6], the radius of curvature, R, of a ray trajectory is defined by the formula:

$$\frac{1}{R}=\frac{\sin i}{n}\operatorname{grad} n.$$

If the gradient is parallel to the h axis, $\operatorname{grad} n=\frac{dn}{dh}$, therefore $\frac{1}{R}=\frac{\sin i}{n}\operatorname{grad} n$.

As was pointed out above, we will be considering only such rays whose angle is small with respect to the axis. This means that the angles, i, will be close to $\pi/2$, and it is permissible to put $\sin i=1$.

Consequently $\frac{1}{R}=\frac{1}{n}\frac{dn}{dh}$.

If the ray traverses path e, then it is rotated through an angle δ (fig. 4), equal to $\frac{e}{R}$, i. e. $\frac{e}{n}\frac{dn}{dh}$.

This rotation occurs in the glass of the lens. Upon passage into the air, the angle of deviation, δ, increases n times, in accordance with the law of refraction and the deviation angle, ε_2, caused by the variation of the refractive index, is given by the formula: $\varepsilon_2=e\,(h)$.

The relation $\frac{dn}{dh}$ may be written in the form:

$$\frac{dn}{dh}=\frac{dn}{dt}\frac{dt}{dh}.$$

On the strength of the relationship $n=n_0+\beta(t-t_0)$, where β is a coefficient specifying the change of

refractive index with temperature, we have $\frac{dn}{dt}=\beta$, and therefore,

$$\varepsilon_2=\varepsilon(h)\beta\frac{dt}{dh}. \tag{2}$$

The deviation proceeds in the direction of large indices.

The overall ray deviation, ε, equals the sum $(\varepsilon_1+\varepsilon_2)$.

If the temperature gradient is directed upward, and the coefficients α and β are positive, which holds for conventional types of optical glass, both deviations have the same sign: the ray deviates upward. We will agree to consider such a deviation negative, inasmuch as in constructions of geometric optics it is customary to take clockwise rotation as positive (i.e. the deviation is directed downward, it is then assumed that light propagates from left to right).

Figure 3

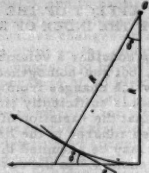

Figure 4

Therefore, for $\varepsilon=\varepsilon_1+\varepsilon_2$ we get

$$\varepsilon=-(n-1)\alpha\left[\varepsilon(h)\frac{dt}{dh}-\frac{d^2\varepsilon(h)}{dh^2}\int_0^h t(h)\,dh\right]-\varepsilon(h)\beta\frac{dt}{dh}.$$

For brevity we will denote $\frac{dt}{dh}$ by the letter g, remembering that this quantity is a function of h; in place of ε (h) and t (h) we write simply ε and t. Then we have:

$$\varepsilon=-(n-1)\alpha\left[\varepsilon g-g''\int_0^h t\,dh\right]-\varepsilon g\beta$$

or

$$\varepsilon=-\varepsilon g[(n-1)\alpha+\beta]+(n-1)\alpha g''\int_0^h t\,dh. \tag{3}$$

3. SOME PARTICULAR CASES

Case A-when the component is limited by plane surfaces--the parallel plate and prism with small refracting angle, positioned so that their edges form small angles with the gradient (cosine of which may be taken equal to unity).

In this case $\varepsilon''=0$ and formula (3) becomes:

$$\varepsilon=-\varepsilon g[(n-1)\alpha+\beta]. \tag{4}$$

If the component is made of a material for which $(n-1)\alpha+\beta=0$ (This relation, is fulfilled approximately by fluorite), the deviation ε equals zero, and the component may be called "non-perturbing", since the deviation is non-existent not only for a constant temperature gradient but even for any gradient.

If the quantity $(n-1)\alpha+\beta$ differs from zero, then the deviation ε is proportional to the product $\varepsilon g\gamma$, where $\gamma=(n-1)\alpha+\beta$ is written for brevity.

If we are dealing with a plane-parallel plate, e is constant and the deviation is proportional to the gradient; if the latter is constant the deviation is also constant, and the plane-parallel plate acts as a wedge.

If the optical item is a wedge, the deviation grows in proportion to the thickness. There occurs a defocusing of the beam: if it were parallel, it would become convergent when the gradient is directed upward.

a) Consider a plane-parallel plate of K8 glass, 100 mm thick. Assume the temperature gradient to be 1° per cm. For K8 glass, the coefficient α equals 70×10^{-7} reciprocal degrees; coefficient β equals 28×10^{-7} reciprocal degrees. We have, $\varepsilon=-100\times\frac{1}{10}\times65\times10^{-7}\times206{,}000=-13''$.

b) Wedge, 200 mm in diameter, of K 8 glass. Thickness of upper edge 0, of lower 50 mm. Gradient is 1° per cm. Benefiting by calculations of the previous example, we get: deviation at upper edge is zero, at the lower--$6.5''$. For a 200 mm diameter such a difference of deviations corresponds to a radius of curvature of the plane of the emerging wave of $\frac{200\text{ mm}}{\sin 6.5}=1$ km.

Case B-when the optical detail is bounded by non-planar surfaces. We consider the most important case in practice, the lens. Assume that the temperature of the axial portion of the bus does not change upon heating.

The dependence of thickness e on height h, for the case of a lens, has the form $\varepsilon=\varepsilon_0-\frac{h^2}{2(n-1)}\frac{1}{f'}$, where ε_0 is the thickness of lens at the center, f' is its focal length. Assume that the gradient, g, is constant.

In conformity with formula (3), we get:

$$\varepsilon=-\left[\varepsilon_0-\frac{h^2}{2(n-1)f'}\right][(n-1)\alpha+\beta]-(n-1)\alpha\frac{h^2}{2(n-1)f'}$$

After reductions, arising as a consequence of the fact that the deformation of the lens for a constant gradient reduces to zero, we obtain:

$$\varepsilon=-\varepsilon_0[(n-1)\alpha+\beta]+\beta\frac{h^2}{2(n-1)f'} \tag{5}$$

The first term is constant and very small. Practically, there remains only the second, depending only on β.

Since ε is proportional to h^2, the image is aggravated by a coma.

Assume a lens diameter of 500 mm, f'=5,000, K8 glass; difference in temperature along edges 10°, $g=\frac{1}{50}$; the transverse coma in the focal plane is equal to 0.004 mm, i.e. very small.

Even though the coma produced by a constant temperature gradient is small, yet in certain cases it is desirable to correct it. This may be done by a selection of type of glass. Consider, for example, the case of a dual-lens objective. The coma, K, produced by a system of two lenses infinitely close together is determined by the quantity:

$$K=\beta_1\frac{h_1^2}{2(n_1-1)f_1'}+\beta_2\frac{h_2^2}{2(n_2-1)f_2'},$$

where subscripts 1 and 2 correspond to lens numbers. If h_1 and h_2, the condition for vanishing of the coma is expressed by the equation:

$$\frac{\beta_1}{(n_1-1)f_1'}+\frac{\beta_2}{(n_2-1)f_2'}=0.$$

In view of the fact that in dual-lens objectives there exists also the achromatism condition:

$$\frac{1}{\nu_1 f_1} + \frac{1}{\nu_2 f_2} = 0,$$

where ν_1 and ν_2 are dispersion coefficients of the glasses, then there must be compliance with the condition: $\frac{\beta_1 \nu_1}{(n_1 - 1)} = \frac{\beta_2 \nu_2}{(n_2 - 1)}$

or,

$$\frac{\beta_1}{\Delta n_1} = \frac{\beta_2}{\Delta n_2},$$

where ΔN is the degree of dispersion of glass.

The glass types usually employed for astronomical objectives do conform to this requirement: The dispersion ratio for K8 and F1 glasses is about 0.5, and β is also almost 0.5. There results an automatic compensation for image distortion.

4. SYMMETRICAL DISTRIBUTION OF THE GRADIENT ABOUT THE OPTICAL AXIS

The large thermoconductivity of metallic housings in comparison with the thermoconductivity of glass, leads to the following: the housings quickly acquire the temperature of the surrounding air, generate near the edge of the glass lenses a definite, identical temperature for the whole configuration, different from the temperature of the glass. As a consequence of which, within the latter there forms a more or less symmetrical distribution of temperatures. It is possible, to a first approximation, to assign the formula, $t = Ah^2$ to this distribution where A is some constant and h is the distance of the considered element of the optical detail from the optical axis.

The gradient, $g = \frac{dt}{dh}$ is evaluated by the formula: $g = 2Ah$.

We consider first the case of components limited to plane surfaces (plane-parallel plates, wedges), the normal to which forms angles close to 90^0 with the gradient.

From the general formula (3), there follows:

$$(6) \qquad \varepsilon = -\alpha g [(n-1)\alpha + \beta] = -2Ahe[(n-1)\alpha + \beta].$$

1. For a plane-parallel plate e is constant and ε is proportional to h. This corresponds to a defocusing or to a shift of the image plane.

2. For a wedge, e (h) varies according to a linear law and ε varies according to a square law. Therefore, a coma appears on the axis. Consider a numerical example for a wedge, where e maximum equals 100 mm, h=250, $A = \frac{10^0}{(250)^2}$ (i.e. difference in temperatures between center and edge equals 10^0); K8 glass:

For computation of angular coma, it is necessary to evaluate the quantity:

$$K = \frac{\varepsilon(250) + \varepsilon(-250)}{2} - \varepsilon(0).$$

Here,

$\varepsilon(250) = 0$ since $e = 0$;

$\varepsilon(0) = 0$ since $h = 0$,

Whence, $K = \frac{\varepsilon(-250)}{2} = 6''$.

As was pointed out above, the use of a material for which $(n-1)\alpha + \beta = 0$ eliminates all consequences of non-uniform heating.

5. LENSES

For a lens,

$$\frac{d^2\varepsilon}{dh^2} = -\frac{1}{2(n-1)f'}; \quad g = 2Ah; \quad \int_0^h \varepsilon(h)\,dh = -\frac{Ah^3}{3}.$$

If the thickness of the lens at the center be neglected, we get a deviation, ε, proportional to h^3; consequently spherical aberration occurs as a result of non-uniform heating causing a parabolic temperature distribution symmetrical about the axis.

Assume (fig. 5) that the ray AB deviates by an angle ε at point A. If the ray form angle u' with the axis, the distance OB = s', distance OA = h, it is easy to obtain, for small ε:

$$\overline{BB_1} = \Delta s' = -\frac{\Delta s}{\sin^2 u'}.$$

So, the longitudinal spherical aberration, caused by a temperature distribution of parabolic type, is evaluated by the following formula:

$$(7) \qquad \Delta s' = -\frac{A\Delta t}{f' \sin^2 u'}\left[\frac{\beta}{\alpha - 1} + \frac{2}{3}\alpha\right].$$

We note that the longitudinal spherical aberration is proportional to the 4-th power of h, as was to be expected.

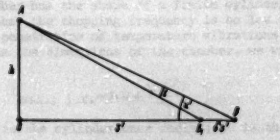

Figure 5

For a lens of 500 mm diameter, with a 5 m focal length, the difference in temperatures at the edge and at the axis is 10^0, K8 glass. The spherical aberration (longitudinal) at the edge, as evaluated from the formula, equals 0.5 mm.

Formula (7) may be written in a more concise form when the difference in temperatures, between the edge and axis, is specified. Let Δt be this difference. Then $A = \frac{\Delta t}{h^2}$, and in view of the fact that $\sin u' = \frac{h}{f'}$, formula (7) becomes:

$$(7*) \qquad \Delta s' = -f' \Delta t\left[\frac{\beta}{\alpha - 1} + \frac{2}{3}\alpha\right],$$

that is, the spherical longitudinal aberration at the edge of the aperture depends only on Δt and on the thermo-optic characteristics of the glass.

The simplest and the most interesting, in practice, cases of temperature distribution in optical items have been exhaustively studied by these several examples. The influence of more complex cases of temperature distribution may be evaluated with the aid of the general formula (3) derived in this paper.

March 4, 1958

References

1. A. KROEGER: Astr. Nachr., B60, No. 1421 (1863)
2. C. A. SONNEFELD: Zentr.- Ztg. Opt. u. Mech., 54, 3 (1933)
3. D. MAKSUTOV: Tsirkuliary, GAO in Pulkova, No. 20 (1936)
4. J. W. PERRY: Proc. Phys. Soc., 55, 257 (1943)
5. D. S. VOLOSOV: OiS, 4, 663, 772 (1958)
6. G. G. SLIUSAREV: Geometricheskaia Optika (Geometric Optics) Akad. Nauk USSR Press Moscow-Leningrad, 1946

TOM VI, Vyp. 2 OPTIKA I SPEKTROSKOPIIA Fevral', 1959
VOL. VI. No. 2 OPTICS AND SPECTROSCOPY February, 1959

On the Sensitivity Threshold of an Optic-Acoustic Receiver of Radiation

1. Low Chopper Frequency

A. O. SALL'

Abstract: The question of the sensitivity threshold is examined, of a selective optic-acoustic receiver of radiation (the spectraphone of M. L. Veingerov), which is based on the excitation of acoustic vibrations in a closed volume when an intermittent radiation flux is being absorbed by the gas, and the sensitivity threshold is also examined of a non-selective receiver with a thin radiation-absorbing film. Formulas for the determination of a numerical value of the sensitivity threshold are obtained, which are correct for a low chopper frequency of the radiation flux.

1. The sensitivity of an optic-acoustic radiation receiver [1-10] is limited by thermal fluctuating noises in the gas contained in the chamber of the radiation receiver, by electrical fluctuating noises of the microphone [11] and of the input stage of the amplifier, and by vibration interference also. In order to decrease the effects of these disturbances, it is essential to know at the design stage of building an optic-acoustic radiation receiver, the dependence of the numerical values of these disturbances on the type of microphone to be used, on the construction of the microphone and the chamber, and on the associated circuit of the microphone. The results of theoretical investigations and calculations to determine the threshold sensitivity of an optic-acoustic radiation receiver are given in this and in the following papers.

2. Let us examine the threshold sensitivity of a radiation receiver, limited by the fluctuations of the gas temperature in the receiver chamber. Let $(\Delta Q)_1$ be the amplitude of the periodic change in the thermal power liberated in the receiver chamber which causes the variations in the average gas temperature of the same magnitude as the temperature fluctuations.

The amplitude of the periodic change in the average volume temperature ϑ, caused by periodic harmonic heat emission in the volume of a solid, is given by a known expression.

$$\vartheta = \frac{(\Delta Q)_1}{|G + i\omega C|}.$$

where C is the lumped heat capacity of the heated body; ω is the circular chopping frequency; G is the heat conduction from the body to the surrounding medium.

The formula obtained may also be used for calculation of the average temperature in the chamber of an optic-acoustic receiver with absolutely rigid walls.

In order to use the cited formula, numerical values of G and C must be known in each particular case. When determining the numerical value of the heat conduction, one must take into account the fact that the heat is transmitted basically by means of the heat conduction of gas. The effect of convection may be neglected for the chamber sizes usually used. Accounting for radiation at normal pressure, room temperature, and sufficiently small dimensions of the ray-receiving camera, gives an insignificant correction.

To determine the heat conduction, the partial differential heat conduction equation must be solved in each particular case, and if the chopping frequency is so low that the chamber dimensions are smaller than the depth of penetration of temperature vibrations, the stationary Poisson equation may be used. In the calculation of the heat conduction for the case of the selective optic-acoustic effect, let us assume, in the first approximation, that heat is emitted with the same density over the total gas volume. For the simplest bodies (an infinitely long circular cylinder, an infinite flat slab, and a sphere), the heat conduction is given by

$$G = \frac{n(2+n)V\lambda}{a^2},$$

where λ is the heat conduction of the gas mixture filling the chamber; V is the chamber volume.

The numerical values of n for an infinite plate, an infinite cylinder and a sphere, assume the values of 1, 2, and 3, respectively. The values of a are equal to half the thickness of the plate, the radius of the cylinder, and the radius of the sphere, respectively. It may be shown that in the case of bodies of more complex shape (a finite cylinder, parallelopiped, etc) the heat conduction, to a first approximation, equals the sum of the heat conductions corresponding to orthogonal coordinates. For the selective radiation receiver, whose chamber has the shape of a finite cylinder, assuming that the chopping frequency is so low that the depth penetration of temperature vibrations is larger than the dimensions of the chamber, we will have

$$(2) \qquad G_{\text{sel.; l.f.}} = 8\lambda l + \frac{12\lambda r^2}{l},$$

where r is the cylinder-base radius; l is the cylinder height.

Let us, to a first approximation, consider that the thickness of the radiation-absorbing film in a non-selective optic-acoustic radiation receiver is so small that the heat conduction from the central portions of the film to the chamber frame may be neglected (as compared to the heat conduction of the gas). In this case, we have for the heat conduction of a cylindrical chamber because of the heat conductivity of the gas at a sufficiently low chopping frequency

$$(3) \qquad G_{\text{non-sel.; l.f.}} \simeq 8\lambda l + \frac{8\lambda r^2}{l}.$$

For the mean square of the gas temperature fluctuations in the chamber there exists the known expression [5]

$$\overline{\vartheta^2}_{\text{fl.}} = 4kT^2R^2\Delta f.$$

where k is the Boltzmann constant; Δf is the bandwidth of the recording device; T is the absolute temperature; R* is the thermal resistance of the heat conduction G and the heat capacity C, connected in parallel.

However, as we will see later, G and C only determine the size of the signal and not the level of the temperature fluctuations. In order to calculate the level of the fluctuations, it is necessary to introduce the concepts of heat conduction $G_{fl.}$ and heat capacity $C_{fl.}$. Then

$$R^* = \frac{1}{G_{fl.}\left[1+\left(\frac{\omega C_{fl.}}{G_{fl.}}\right)^2\right]} \quad \text{and} \quad R^*_{fl.} = \frac{1}{G_{fl.}\left[1+\left(\frac{\omega C_{fl.}}{G_{fl.}}\right)^2\right]}. \tag{4}$$

The necessity of replacing G by $G_{fl.}$ and C by $C_{fl.}$ is explained by the following.

The heat conduction $G_{fl.}$ and heat capacity $C_{fl.}$, which determine the level of gas-temperature fluctuations, in the general case are not equal to the corresponding values of the conductivity G and the heat capacity C, which determine the amplitude of the variations of the average gas temperature with periodic heat emission in the gas volume. For example, comparing (2) and (3), valid at sufficiently low modulation frequencies ($\omega C \ll G$), we see that the magnitude of the heat conduction depends on where the heat emission occurs in the chamber: uniformly over all of the chamber space or in the thin film at the center of the chamber ($G_{non\text{-}sel.;\ l.f.} < G_{sel.;\ l.f.}$). The heat conduction $G_{fl.}$, for given chamber dimensions and contents, does not depend on where the heat emission occurs in the chamber. Consequently, $G_{fl.} \neq G$, in the general case

Solving the generalized equation of heat transfer [9], it may be shown that the heat capacities, determining the magnitudes of the signals in the selective and non-selective receivers are not equal in the general case. (i.e. $C_{sel} \neq C_{non\text{-}sel}$). In other words, the magnitude of the heat capacity (just as the magnitude of the heat conduction) depends on where the heat emission occurs in the chamber: uniformly over all of the chamber space or in the thin film at the center of the chamber. At the same time the heat capacity C, determining the level of the gas-temperature fluctuations in the chamber, does not depend on where the heat emission occurs in the chamber. Consequently, in a general case $C_{fl.} \neq C$.

This follows also from the fact that the quantities $G_{sel.}$ and $C_{sel.}$ for the selective radiation receiver (as we will see later) depend on the degree of nonuniformity of radiation absorption over the gas volume, while quantities $G_{fl.}$ and $C_{fl.}$ do not.

Using (1) and (4) we obtain

$$(\Delta Q_1) = \sqrt{\frac{G^2 + (\omega C)^2}{G^2_{fl.} + (\omega C_{fl.})^2}} \sqrt{4kT \cdot G_{fl.} \Delta f}. \tag{5}$$

In approximate calculations for uniform heat emission over the gas volume of a selective receiver, one may consider that

$$G_{sel.;\ l.f.} \simeq G_{non\text{-}sel.;\ l.f.} \simeq 8\varkappa l + \frac{12\varkappa l \cdot a}{l}. \tag{6}$$

If in the first approximation it is considered that $C_{fl.} \simeq C_{sel.} \simeq C_{non\text{-}sel.} \simeq C$, then we will have for the selective optic-acoustic radiation receiver

$$(\Delta Q)_1 \simeq \sqrt{4kT\, G_{sel.;\ l.\ f.}\, \Delta f}, \tag{7}$$

and for the non-selective

$$(\Delta Q)_1 \simeq \sqrt{\frac{G^2_{sel.;\ l.f.} + (\omega C)^2}{G^2_{fl.;\ l.f.} + (\omega C)^2}} \sqrt{4kT \cdot G_{fl.;\ l.f.}\, \Delta f}. \tag{8}$$

If the chopping frequency is so small that the depth of penetration of the temperature vibrations is significantly larger than the chamber dimensions, then for $l < r$ the threshold value $(\Delta Q)_1$ for the non-selective chamber will be somewhat lower than for the selective chamber, the non-selective receiver will be more sensitive than the selective. This is explained by the fact that equal thermal powers cause unequal rises in the average gas temperature in the case of the selective and non-selective receivers: the temperature rise for the non-selective receiver is larger because the heat source is located further from the chamber walls. Solving the generalized heat-transfer equation for the case of a chamber with non-rigid walls, the amplitude of the periodic change in the average volume-temperature will be

$$\vartheta = \frac{(\Delta Q)}{\left|G + i\omega C_v + \frac{i\omega (C'_p - C_v)}{(1 + i\omega z V \cdot P^{-1})}\right|}, \tag{9}$$

where z is the acoustic resistance of the microphone; C_v and C_p are the specific heats of the gas at constant volume and constant pressure; P is the gas pressure in the chamber.

In the general case of a non-rigid-wall chamber, instead of the heat conductions G, $G_{fl.}$ and the heat capacities C, $C_{fl.}$, the conductivities G', $G'_{fl.}$ and the capacities C' and $C'_{fl.}$ must be used in formulas (5), (7), and (8) to determine the values of $(\Delta Q)_1$. The primed values take into account the mechanical resistance of the movable microphone system. In order to determine these quantities let us replace G and C by G' and C', respectively, in the denominator of the right hand side of (1), and let us equate the new expression to the right-hand side of (9). Then, considering that the movable system of the microphone is governed by elasticity, we will get

$$C' = C_v + (C_p - C_v)\left(1 + \frac{V}{PC_m}\right) \cdot \left[\left(1 + \frac{V}{PC_m}\right)^2 + \left(\frac{\omega r_m V}{P}\right)^2\right]^{-1}. \tag{10}$$

$$G' = G + \left(\frac{\omega^2 r_m V^2}{P}\right) \cdot \left[\left(\frac{\omega r_m V}{P}\right)^2 + \left(1 + \frac{V}{PC_m}\right)^2\right]^{-1}. \tag{11}$$

where C_m is the resultant flexibility of the membrane and of the surrounding space; r_m is the active acoustic resistance.

Thus, in order to account for the influence of the acoustic resistance of the microphone it is necessary to add quantities which depend on r_m and C_m to the values of the conductivities. This concerns both the heat conductions $G_{sel.}$ and $G_{non\text{-}sel.}$, which determine the magnitude of the signal, as well as the heat conduction $G_{fl.}$ which determines the temperature fluctuation level. As the chopping frequency increases, the sensitivity of the radiation receiver drops. This may be shown by substituting corresponding expressions,

which account for the mechanical resistance of the moving system of the microphone (10) and (11), instead of $G_{sel.}$, l.f. $G_{non\text{-}sel.}$, l.f. $G_{fl.}$ l.f., and C, in (7) and (8). If the moving system of the microphone is governed by elasticity ($\omega C_m \cdot r_m \ll 1$) and the elastic acoustic resistance of the space is greater than the elastic resistance of the membrane ($V < C_m P$), and if the depth of penetration of the temperature vibrations is greater than the dimensions of the chamber ($\omega C < G$), then the numerical value of $(\Delta Q)_1$ will be the same as that for a chamber with absolutely rigid walls. Let the chamber of a selective radiation receiver be cylindrical and filled with carbon monoxide. Also, let the chamber volume and the chopping frequency be so small, that the chamber walls may approximately be considered absolutely rigid when computing $(\Delta Q)_1$. Then, letting $r = 1$ cm, $l = 0.5$ cm, $\Delta F = 1$ cps, $T = 300^\circ$ K, we will get

$$(\Delta Q)_1 \simeq \sqrt{4kT^2\Delta f\left[\frac{8\pi l}{l} + \frac{12\pi l^2}{l}\right]} \simeq 3 \cdot 10^{-20}\ \text{W}. \tag{12}$$

As we pointed out earlier, the formulas obtained for the determination of $(\Delta Q)_1$ are absolutely correct for such low chopping frequencies that the depth of penetration of the temperature vibrations is greater than the chamber dimensions. This is correct for a cylindrical ray-receiver of $r = 1$ cm and $l = 0.5$ cm, if the chopping frequency is less than 1 cps. However, for approximate computations the given formulas are correct for higher frequencies also. For instance, calculations for a chamber with the dimensions given above show that the numerical value of $(\Delta Q)_1$ increases only to $5 \cdot 10^{-10}$ watts as the chopping frequency rises to 50 cps.

3. Electrical noises at the input of the amplifier also may limit the sensitivity of the radiation receiver. Let $(\Delta Q)_2$ be the amplitude of a periodic change in the thermal power emitted in the receiver chamber which causes an AC signal at the microphone output equivalent to the noise voltage at the amplifier input.

Let us find an expression for $(\Delta Q)_2$. For that purpose we will set the voltage in the microphone due to $(\Delta Q)_2$ equal to the mean-square voltage of the noise of the input resistance of the amplifier R and the shot-noise of the input tube of the amplifier (the latter may be quantitatively determined by means of an equivalent resistance R),

$$\frac{P(\Delta Q)_2 E_0}{\tau\left|G + i\omega C\right|\left|1 + \frac{\left(\frac{G + i\omega C_e}{G + i\omega C_e}\right)\frac{P}{i\omega V}}{}\right|} = \sqrt{4kT\Delta f\left[R + \frac{R}{1 + (\omega R C_{el.})^2}\right]}, \tag{13}$$

where E_0 is the microphone seasitivity in a free field; $C_{el.}$ is the electrical capacitance of the microphone. If the chopping frequency is considerably lower than the resonant frequency of the moving system of the microphone and if the chamber dimensions are considerably larger than the depth of penetration of the temperature vibrations, then the threshold value of $(\Delta Q)_2$ is

$$(\Delta Q)_2 \simeq \frac{\omega C_e T}{P E_0}\left[1 + \frac{\gamma P S_m^2}{\omega_0^2 m_m V}\right]\sqrt{4kT\Delta f\left[R + \frac{R}{1 + (\omega R C_{el.})^2}\right]},$$

where ω_0 is the resonant frequency of the moving system of the microphone; m_m is the mass of the moving system of the microphone; S_m is the effective surface area of the microphone; γ is the ratio of the specific heats.

The formula obtained is correct for the selective radiation receiver, and also for the non-selective receiver if the specific heat of the radiation-absorbing film of the latter is considerably less than the specific heat of the gas layer surrounding the film, whose thickness is equal to the depth of penetration of the temperature vibrations [9].

Taking into account that $\omega R C_{el} \ll 1$ for an electrodynamic microphone and that, usually, the acoustic resistance of the microphone is considerably larger than the acoustic resistance of the chamber space ($\gamma P S_m^2 \ll \omega^2 m_m V$), then setting $\gamma = 1.4$, $V = 3$ cm^3, $R + R' \simeq 10^4$ ohms, $\Delta f = 1$cps, $E_0 \simeq 10^{-4}$ volt/bar, we will have

$$(\Delta Q)_2 \simeq \frac{\omega V}{(\gamma - 1)E_0}\sqrt{4kT(R + R')\Delta f} \simeq 3 \cdot 10^{-9}\ \text{W}.$$

Taking into account that the acoustic resistance of a condenser microphone is considerably larger than the acoustic resistance of the volume, then substituting the numerical values $\gamma \simeq 1.4$, $f = 50$ cps, $P = 10^6$ bar, $S_m \simeq 5$ cm^2, the polarizing voltage $V \simeq 100$ volts, $\Delta f = 1$ cps, $R = 10^8$ ohms $\gg R'$, the electrode separation $d = 0.1$ mm, $C_{el.} \simeq 4.10^{-11}$ farad [8] we will have

$$(\Delta Q)_2 \simeq \left(\frac{\gamma}{\gamma - 1}\right)\left(\frac{\omega P S_m d}{V}\right)\sqrt{4kT\Delta f\left[R + \frac{(R + R')}{(\omega R C_{el.})^2}\right]} \simeq 5 \cdot 10^{-9}\ \text{W}.$$

In order to increase the sensitivity of a microphone chamber with a condenser microphone with a given microphone capacitance $C_{el.}$ and a given input amplifier resistance R, the chopping frequency must be decreased down to values where $R(\omega R C_{el.}) \leqslant R + R'$. For values of $R \simeq 10^8$ ohms and $C_{el.} = 50.10^{-12}$ farad, the inequality is satisfied at frequencies of several tens of cycles per second. As follows from the formula obtained the sensitivity of the microphone chamber increases as R is increased.

The noise level of the grid resistance of the amplifier input may be made lower than the shot-noise effect of the tube, by using the method of amplitude modulation for instance. In this case one may achieve that $(\Delta Q)_2 < (\Delta Q)_1$, i. e. that the threshold sensitivity of a radiation receiver, related to these quantities in the general case, will be limited by the magnitude of the temperature fluctuations of the gas in the chamber.

Using the results of [9], we will get for the threshold sensitivity of a selective receiver (the minimum flux of radiant energy which may be detected with a given degree of accuracy)

$$(\Delta J) \simeq N\beta^{-1}(p\tau)^{-1}\sqrt{1 + (\omega\tau)^2} \cdot \sqrt{(\Delta Q)_1^2 + (\Delta Q)_2^2}, \tag{14}$$

where β is the transmission coefficient of radiation through the chamber window; ω is the circular chopping frequency; τ is the lifetime of the excited state of the molecules; p is the probability of transition of a molecule from an excited state to the normal state with emission of heat; N is a numerical coefficient.

If, for example, it is considered that the amplitude of the signal in the receiver due to a flux (ΔJ), must be two-three times the amplitude of the receiver noise, N will be on the order of magnitude of ten [5].

Restricting the radiation measurements to just the spectrum interval where practically total absorption of the radiation by the gas of the ray-

receiving chamber takes place, the setting $r = 1$ cm, $l = 0.5$ cm, $T = 300°$ K, $\Delta f = 1$cps, $f \leq 1$-10cps, $\beta \simeq 1$, $p_T \simeq 1$, $\omega \leq 1$, $(\Delta Q)_1 > (\Delta Q)_2$, $N \simeq 10$ and taking (12) into account, we will get a quantity on the order of $3 \cdot 10^{-9}$ watts for the value of the threshold sensitivity of the receiver. Actually, the receiver sensitivity may be lower due to the passive volume and other sources of noise.

For a non-selective receiver we will get

$$(\Delta Q)_1 \simeq N\beta^{-1}\gamma^{-1}\sqrt{(\Delta Q)_1^2 + (\Delta Q)_2^2}, \tag{15}$$

where γ is the absorption coefficient of radiation by the absorbing film.

4. The rotation of the chopper may cause vibrations of the radiation-receiver frame of the same frequency as the chopping frequency. These vibrations start vibrations of the moving system of the microphone with respect to the frame of the radiation receiver. The equivalent amplitude of the change in thermal power, causing as large a signal as the frame vibration (of amplitude x) is

$$(\Delta Q)_3 \simeq P^{-1}S_m^{-1}T\sqrt{C^2 + (\omega C)^2}\, m_m \omega^2 x \simeq (\gamma - 1)^{-1} S_m^{-1} m_m \omega^2 V x.$$

Setting $\gamma = 1.4$, $m_m / S_m = 2.10^{-3}$ g/cm^2, $V = 3$ cm^3, $\omega = 314$ sec.$^{-1}$, $x \simeq .1$mm for a condenser microphone, we will get $(\Delta Q)_3 \simeq 5 \cdot 10^{-4}$ watts. Using an electrodynamic microphone, which has a much larger mass, the effect of vibration will be greater. A more exact calculation of the effect of vibrations, taking into account the mass of the gas mixture which is vibrating together with the moving system of the microphone, gives the same order of magnitude. The threshold sensitivity, limited by vibrations, may be evaluated using eqs. (14) and (15) if $(\Delta Q)_3$ is substituted for the factor $\sqrt{(\Delta Q)_1^2 + (\Delta Q)_2^2}$. Assuming that radiation enters the receiver in the form of rectangular pulses of magnitude (ΔJ) ("rectangular modulation") and that the amplitude of the harmonic of the heat emitted in the chamber is $(\Delta Q)_3$ (the signal on the level of interference), we will have $N \simeq 1.6$.

5. Let us examine the question of determining the optimum length for the ray-receiving cylinder of an optic-acoustic radiation receiver. Consider the case when the threshold sensitivity is determined by the level of fluctuations of the gas temperature and of the fluctuations of the moving system of the microphone. Let us assume that the chopping frequency is so low that the threshold sensitivity is determined by the heat conductivity. Then, for a given numerical value of the chamber diameter, the optimum length of the cylinder, as follows from an examination of (2) and (7), will be 1.2 r. Using equations (3) and (8), it may be shown that the optimum length of the cylinder of a non-selective optic-acoustic radiation receiver, equals 0.8 r at a sufficiently low chopping frequency.

When the noise level of the microphone and of the input circuit of the recording device determines the threshold sensitivity of the selective radiation receiver, then, for the ideal case in the absence of passive volume and rigid chamber walls (the acoustic microphone resistance is considerably greater than the acoustic resistance of the chamber space), the optimum length of the ray-receiving cylinder will be, using (1) and (2):

$$l_0 \simeq 1.2r\left[1 + \left(\frac{c_v \rho r^2}{4\lambda}\right)^6\right]^{-\frac{1}{12}},$$

where c_v is the specific heat of per unit volume of gas.

If the cylinder radius is considerably greater than the penetration of the temperature vibrations, then

$$l_0 \simeq 1.4\sqrt{\frac{\lambda}{c_v f}}.$$

As the passive pre-membrane volume is increased and the acoustic resistance of the microphone is decreased, the optimum length of the ray-receiving cylinder increases. For a microphone chamber with a condenser microphone [8], the optimum ray-receiving cylinder length, which corresponds to a maximum signal-to-noise ratio, reaches a value of 2 – 3 mm for methane at 50 cps and a loosely stretched microphone membrane. If the optic-acoustic receiver is used in a gas analyzer in order to decrease the error of the latter [12], it is desirable in many cases to increase the length of the ray-receiving cylinder to 5 – 10 mm.

6. The given formulas enable one to determine, in each particular case, the optimum radius of the ray-receiving cylinder of an optic-acoustic radiation receiver. As an example, let us examine the case where at a sufficiently low chopping frequency, the threshold sensitivity of the radiation receiver is limited by temperature fluctuations of the gas in the chamber. If, at the same time the radius is varied, the cylinder length is varied proportionally, the quantity $(\Delta Q)_1$ will change proportionally with $\sqrt{r}$.

Usually, only some portion of the total radiation flux which is to be measured can be focused on the receiver window. Let ξ be the ratio of the fraction of flux, which enters the ray-receiving window, to the total flux. The magnitude of that ratio increases with increasing r. Then, the maximum sensitivity to the flux to be measured will be achieved for a window radius which makes the ratio $\sqrt{r} \cdot \xi^{-1}$ a minimum.

7. The fluctuations of radiation flux in infrared gas analyzers give rise to an additional signal in the receiver. To avoid a drop in the gas-analyzer's sensitivity, the radiation absorbed in the receiver must be limited so that the fluctuations of the thermal power emitted in the camera, caused by fluctuations in the radiation flux, would not exceed $(\Delta Q)_1$. Let, for example, the spectrum region used in the analysis be at the wavelength of 4μ, and let $(\Delta Q)_1 \simeq 3.10^{-10}$w, (for $\Delta f = 1$ cps). Then, the radiation flux absorbed in the receiver should not exceed $0.5\,(\Delta Q)_1^2\,(h\nu)^{-1}\,(\Delta f)^{-1} \simeq 1$ watt.

This condition is fulfilled when a selective optic-acoustic radiation receiver is used in an infrared gas analyzer. If a non-selective receiver is used and the magnitude of the radiation absorbed exceeds the given value, additional filtration of the radiation flux is necessary.

At a sufficiently low chopping frequency, the spectral sensitivity of an ideal non-selective radiation receiver, whose film absorbs almost all of the radiation incident on it, will be greater than the spectral sensitivity of a selective radiation receiver, referred to a narrow spectral band in the most intense region of gas absorption. However, if the noise level of the radiation receiver determines the threshold sensitivity of the infrared gas analyzer, the gas analyzer with a selective radiation receiver will be more sensitive than the one with a non-selective receiver and a monochromator. This is explained by the fact that, in order to achieve

maximum selectivity of a gas analyzer with a monochromator, the spectral slit width of the latter must be of the order of the line-width of the component to be determined [13], so that only one absorption line is used. Using the selective receiver, the signal, which appears as a result of a variation in concentration of the component in the mixture under analysis, depends on absorption of radiation in all the absorption lines of the component which is being determined, and not in just one line.

September 6, 1957

References

1. M. L. VEINGEROV, DAN-USSR, 19, 687 (1938); (In German) 46, 200 (1945); (In English) Zav. Lab. 4, 426 (1947)
2. S. M. LUCHIN: ZTF, 16, 1115 (1946)
3. A. N. TERENIN, N. G. LAROSLAVSKII: IAN USSR, Fiz. ser., 9 (1945)
4. P. E. WEBER: Optik, 152, 1950
5. M. GOLAY: Rev. Sci. Instr., 18, 367, 357 (1947); 20, 816 (1949)
6. P.V. SLOBODSKAIA: IAN USSR, Ser. fiz., 12, 656 (1948)
7. B. I. STEPANOV, O. I. GIRIN: ZETF, 20, 10 (1950)
8. V. A. PAVLENKO: Sovremennye Gazoanalizatory. (Modern gas analyzers) In Sbornik Lonitopribor: Novye Teploenergeticheskie Proizvodstvennye pribory i regulatory (New heat engineering production instruments and regulators) Mashgiz, 1953; ZAV. LAB, No 7, 868(1954)
9. O. A. SALI: ZTF, 25, No. 1, 157 (1956)(See Sov Phys. Tech. Phys.)
10. N. A. PANKRATOV: O.S., 2, 662 (1957)
11. V. K. IOFE: Trudy, NIIRPA, No. 1, Lenizdat, 51-57, 1954
12. A. O. SALI: Priborstr., No. 6, 14 (1956)
13. A. O. SALI: Priborstr, No. 9, 12 (1956)

TOM VI, Vyp. 2 OPTIKA I SPEKTROSKOPIIA Fevral', 1959
VOL. VI. No. 2 OPTICS AND SPECTROSCOPY February, 1959

BRIEF REPORTS

The Law of Phosphorescence Decay for Trypaflavine in Formic Acid

G. M. KISLIAK

As is well known, fluorescence lifetimes are independent of the wavelength of the exciting light, and on excitation in the anti-Stokes region, only the quantum yield is changed [1].

During a study of the influence of the wavelength of the exciting light on phosphorescence lifetime, it was shown by the author that the lifetime of the excited state of organic dyes (trypaflavine, fluorescein, rivanol) in various solvents depends on the wavelength of the exciting light when the wavelength of excitation is in the anti-Stokes region but remains constant during long wavelength irradiation in the Stokes region [2]. For all solutions with the exception of trypaflavine in formic acid the decay follows an exponential law. However for trypaflavine in formic acid, the decay follows a more complicated law in which the rate of extinction of luminescence depends on the wavelength of the exciting light in both Stokes and anti-Stokes regions.

The decay curve for the quenching of phosphorescence of trypaflavine in an 85% aqueous solution of formic acid may be decomposed into two exponential parts. The presence of two excited state lifetimes obviously indicates the presence of two different kinds of excited molecules--trypaflavine in water and trypaflavine in formic acid.

The apparatus used to measure the decay curves was similar to that described earlier [2].

The solutions investigated were trypaflavine in 85, 50, 25, 10, and 5% aqueous solutions of formic acid. The absorption spectrum was measured only for the solution in 85% formic acid.

INFLUENCE OF FORMIC ACID ON THE ABSORPTION OF TRYPAFLAVINE

Aqueous solutions of trypaflavine phosphoresce only weakly, but the addition of formic acid leads to the appearance of a bright phosphorence at low temperature, when the molecule is irradiated with either ultraviolet or visible light of wavelength up to 400-500 mμ. The addition of formic acid to aqueous solutions of trypaflavine also results in a marked change in the absorption spectrum of the latter.

As may be seen from Fig. 1 the absorption spectrum shifts to short wavelengths, with a maximum appearing at 400-405 mμ. In the long wavelength region the steep drop characteristic of all dyes is completely absent, and a secondary maximum occurs at 448-450 mμ, corresponding to the peak found in aqueous trypaflavine solutions. The effect of formic acid on the absorption spectrum in the wavelength region from 400 mμ downward to shorter wavelengths was not studied. The presence of two maxima may be explained by the presence of two different forms of the dye in solution: trypaflavine in water and trypaflavine in formic acid. Obviously in 100% formic acid the subsidiary peak around 450 mμ must disappear.

The marked change in the absorption spectrum of the dye may be attributed either to a perturbation of the electronic levels of the dye molecule by formic acid, or to the formation of a new substance with different properties as a result of a chemical reaction. If the absorption changes only because of the perturbing effect of the formic acid on the energy levels of the dye, and no chemical reaction forming a new molecule is involved, then all the chemical and physical properties of the trypaflavine should be restored on removal of the formic acid.

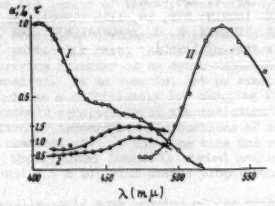

Figure 1. Absorption spectrum (I) and luminescence spectrum (II) of trypaflavine in 85% aqueous formic acid. Curves 1 and 2 show the dependence of lifetime of the excited state on the wavelength of the exciting light. Conc. of dye 10^{-4} g/cc; a (absorption) and I_0 (emission) intensities in arbitrary units. 1 - secondary lifetime; 2 - sum of both decay curves.

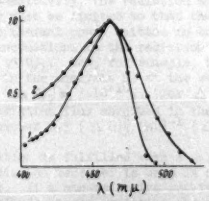

Figure 2. Absorption spectrum of trypaflavine in ethanol. 1 - pure trypaflavine; 2 after solution in formic acid. Conc. 10^{-5} g/cc. Absorption in arbitrary units.

To test this proposal the following experiment was performed: pure trypaflavine was dissolved in 85% formic acid, and the formic acid evaporated off. The absorption spectrum of the residue was then determined after dissolving it in ethyl alcohol. The absorption spectrum of pure trypaflavine in ethanol was also determined. The results obtained are reproduced in Fig. 2., from which it may be seen that the absorption maxima of the two spectra are coincident.

However the absorption spectrum of the trypaflavine which was first dissolved in formic acid is broadened both on the long wave and on the short wave side.

The experiment does not unequivocally answer our question. It is possible that the trypaflavine reacts partly or completely with formic acid and forms a new chemical substance, the molecules of which have physical properties close to those of pure trypaflavine.

THE PHOSPHORESCENCE DECAY LAW

The decay in the phosphorescence of organic dyes in various solvents usually follows an exponential law. In [3] it was shown that for trypaflavine the lifetime of the metastable state at low temperatures is relatively insensitive to a change in the solvent. For this reason the authors assume that this value is characteristic of the activated molecule itself.

When the phosphorescence lifetime for trypaflavine in formic acid is measured, it turns out that the decay follows a complex law, and the decay curve may be decomposed into two exponentials with excited state lifetimes of 0.2 and 0.95 sec. According to [3] the lifetime in various solvents changes only from 2.2 to 2.6 secs, and is ~ 2.55 secs. in pure water. The complex decay law for phosphorescence is observed all the way down to 5% formic acid solutions when the excitation is by ultraviolet light, and the decay constants retain almost exactly the same values. However the presence of two decay times still does not indicate the presence of two long lived states in the same trypaflavine molecule. On going from 85% to 50% formic acid and also exciting with monochromatic light in the visible region, one of the luminescent centres gradually disappears, and in the 25 and 10% solutions has vanished completely, the decay now following an exponential law. Obviously in 100% formic acid the phosphorescence decay law would again be exponential.

Thus the presence of two values for the excited state lifetimes for trypaflavine in formic acid solutions must be explained by the existence of two modifications of the dye: trypaflavine in water and trypaflavine in formic acid. Which luminescence belongs to which modification is unknown, since the spectral distribution of the luminescences was not investigated.

In the Stokes region the phosphorescence lifetime (τ) of trypaflavine in formic acid increases with increasing wavelength of the exciting light λ_{ex}, up to a limiting maximum value. Further increase in exciting wavelength, and shifting to anti-Stokes excitation both result in a τ decreasing again.

Thus formic acid influences not only the absorption of the trypaflavine molecule, but also the probability of the transition from the metastable to the normal state.

We also investigated the effect of formic acid on the relationship between τ and λ at various formic acid concentrations in aqueous trypaflavine solutions.

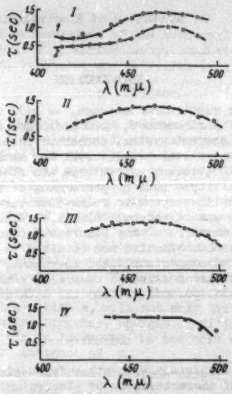

Figure 3. Depencence of excited state lifetime of trypaflavine in formic acid on wavelength of exciting light.
I - 85% formic acid I- τ_2 2- τ_c ; II - 50% soln.; III - 25% soln.; IV - 10% soln.
Conc. 10^{-4} g/cc.

The results are reproduced in Figure 3, from which it may be seen that on going from 85% to 10% formic acid the curve of τ vs. λ is markedly changed. In the 10% solutions the curve is of the same form as that found for trypaflavine in other solvents, and the decay law is an exponential one--i.e. one of the two kinds of luminescent centres has disappeared. From this it follows that the trypaflavine molecule itself does not possess two centres of long lived luminescence.

This work was carried out under the direction of N. A. Lebedev, to whom the heartiest thanks are offered.

February 22, 1958

References

1. B. IA. SVESHNIKOV: Tr. GOI, 12, 108 (1938)
L. A. TUMERMAN: Tr. FIAN USSR, 1, No. 4 (1938)
B. S. NEPORENT, N. A. BORISEVICH: DAN, USSR, 44, 447 (1945) (In English)
2. G. M. KISLIAK: OiS, 5, 297 (1958)
3. B. IA. SVESHNIKOV, A. A. PETROV: DAN USSR, 71, 461 (1950)

TOM VI, Vyp. 2 OPTIKA I SPEKTROSKOPIIA Fevral', 1959
VOL. VI. No. 2 OPTICS AND SPECTROSCOPY February , 1959

On Relaxation of Electroluminescence for Small Departures from the Stationary State

V. V. ANTONOV - ROMANOVSKII

INTRODUCTION

For electroluminescence, as well as for other forms of luminescence, upon prolonged excitation, the luminescent system, sooner or later, approaches a stationary state (relaxes). For small departures of the luminescent system from its stationary state a possibility exists of performing certain calculations with respect to relaxation curves and moreover, in a most general form, i.e. without detailed consideration of any concrete mechanism of luminescence. Results are obtained in a form permitting comparison with experiment, moreover, there is also possible a numerical evaluation of theoretical parameters from the data of the experiment.

THEORY

In comparison with other forms of luminescense the chief characteristic of electroluminescence is that the electrons participating in the recombination simultaneously also take part in the excitation process. Therefore, the absorption of electric field energy depends critically on the state of the electrons in the luminophor.

Since under stationary conditions the number of acts of recombination is balanced by the number of acts of ionization, then this implies that under these conditions each electron, displaced from its initially stable state and until disappearance as a result of recombination (return to a stable state) must, on the average, produce 1 electron. If the stationary conditions are somewhat upset by the fact that there exists a small excess (or deficiency) of electron concentration, Δn, above the stationary n_∞, then the coefficient of electron multiplication ρ will differ somewhat from 1.*

In the first approximation it may be assumed that under quasi-stationary conditions

$$\rho = 1 - \frac{1}{\mu}\frac{\Delta n}{n_\infty} \tag{1}$$

where μ is some positive dimensionless constant, and

$$\Delta n = n - n_\infty, \quad |\Delta n| \ll n_\infty \tag{2}$$

where n is the non-stationary electron concentration. Formula (1) qualitatively agrees with experiment since

Within a small interval of variation of n, the intensity of luminescence may be approximated by the following power function

$$J = qpn^\alpha \tag{3}$$

where α is the order of the luminescence recombination process; q is the probability of radiation upon recombination and p is some constant.

*Stationary quantities are those averaged over the period of the applied voltage. Nonstationary quantities (also average) vary slowly within the period. For more details, see [1].

The quantity pn^α in (3) denotes the rate of decrease of n due to recombination, and the quantity $pn^\alpha\rho$ is the rate of its reproduction, therefore

$$\frac{dn}{dt} = -pn^\alpha(1-\rho). \tag{4}$$

From (1), (2) and (4), neglecting the quantity of order $\frac{\Delta n}{n_\infty}$ in comparison with unity, we get

$$\frac{d\Delta n}{dt} = \frac{1}{\mu\tau}\Delta n \tag{5}$$

where

$$\frac{1}{\tau} = pn_\infty^{\alpha-1} \tag{6}$$

The quantity τ has the meaning of the average lifetime of an electron from the moment of its escape from the stable state, until recombination. From (2), (3) and (6) it follows that τ may be considered a constant quantity to the same accuracy with which (5) was obtained.

Integrating (5), we get

$$\Delta n = \Delta n_o e^{-\frac{t}{\mu\tau}} \tag{7}$$

From (2), (3) and (7) it follows that the rise (or diminution) in intensity, ΔJ, relative to the stationary value, equals

$$\Delta J = J - J_\infty = \Delta J_o e^{-\frac{t}{\mu\tau}} \tag{8}$$

where

$$\frac{\Delta J_o}{J_\infty} = \alpha\frac{\Delta n_o}{n_\infty} \tag{9}$$

According to (9), the relative rise (diminution) in the intensity of luminescence is equal to the relative rise (drop) in the electron concentration, multiplied by the order of the reaction, α.

From (3), (6), (8) and (9) it follows that the excess (deficiency) of the light sum, ΔS, relative to the stationary value during the relaxation time of the J up to the stationary value J_∞, is

$$\Delta S_o = \int_0^\infty \Delta J\,dt = q\alpha\mu\Delta n_o \tag{10}$$

If Δn_o be measured by the excess (deficiency) of light sum, ΔS_o, during natural decay (due to removal of the electric field), then

$$\Delta s_o = q'\Delta n_o \tag{11}$$

where q is the probability of radiation for recombination during the natural decay.

From (10) and (11) we then get

$$\alpha\mu = \frac{q}{q}\,\frac{\Delta s_o}{\Delta s_o} \tag{12}$$

The right side of (12) has a simple physical meaning. The total light Δs_o, divided by q, according to (11), is equal to the initial excess (deficiency) of electrons, Δn_o. Correspondingly, the total light ΔS_o, divided by q, is the excess (deficiency) in the number of acts of recombination, ΔN_o during the total relaxation time. Then, from (12) we find that:

$$\alpha\mu = \frac{\Delta N_o}{\Delta n_o} \tag{13}$$

Since ΔN_o was obtained as a result of production (annihilation), of ΔN_o electrons and ionized centers at first, then the ratio $\frac{\Delta N_o}{\Delta n_o}$ may be termed the gain, M(it is obvious that $M \geq 1$). According to (13), M is equal to the product of μ and the order of the reaction, α, i.e.

$$M = \alpha\mu \tag{14}$$

From (14) there follows an important result -- for Δn small, the gain is independent of the quantity Δn.

EXPERIMENTAL EVALUATION OF RELAXATION PARAMETERS μ and τ

In reference [1], in Figure 3, are drawn data of electroluminescence relaxation of a ZnS-Cu, Cl phosphor which was previously non-uniformly excited. Precisely the ratio $\frac{\Delta S_o}{\Delta s_o}$ was measured by the authors. Then, to within the accuracy of the ratio of the yields $\frac{q}{q}$, with the aid of (12) and (13), from their data, it follows that

$$M \approx 150 \text{ --- } 320. \tag{15}$$

If one were to take advantage of the relaxation curves themselves, then for $\Delta J \sim J_\infty$, both for positive, as well as negative ΔJ, it appeared that ΔJ relaxes approximately according to the exponential law (8), with

$$\mu\tau \approx 1200 \text{ sec.} \tag{16}$$

Then from (14) - (16), assuming a reaction order $\alpha = 2$, we get

$$\tau \approx 7 \text{ --- } 16 \text{ sec.} \tag{17}$$

and

$$\mu \sim 160 \text{ --- } 75. \tag{18}$$

Direct measurements of the average lifetime of an electron, τ, during decay, conducted specially by L. A. Vinokurov and M. V. Fok [1], showed that

$$\tau \sim 0.5 \text{ sec.} \tag{19}$$

From (17) and (19) it follows that the average lifetime of an electron in the presence of an electric field is greater than in its absence. At first glance this appears to be hardly likely. A possible error of several times does not help the situation inasmuch as τ and τ will differ somewhat than an order of magnitude. To all appearances such growth of τ may be explained by two causes.

First of all, the electric field drives apart unlike charges as they escape, which obviously must hinder recombinations. However, this effect is greatly weakened by the fact that the electric field, being variable, will not only drive apart, but even bring together, charges of different signs. Therefore the following may be the more effective cause of an increase of τ.

Obviously the free electrons dispersed by the field are capable of gaining an energy of several eV's, since otherwise there would be no electroluminescence. This energy exceeds by far the average kinetic energy, $\frac{3kT}{2}$ of thermal electrons. A marked rise in the energy of electrons, as pointed out by Hsui Hsui Yun [2], diminishes the ratio of effective cross-sections of recombination and capture by ~ 100 times. This implies that the number of repeated captures increases correspondingly, and consequently also, the average lifetime of an electron until its recombination. The field, as it were, drives the freed electrons back into the trap.

If the above is true then one may expect an increase in total light upon photoexcitation in conjunction with the additional influence of a weak electric field which by itself is incapable of contributing an observable quantity of total light. In reference [3] are conducted certain tests which seem to affirm this.

The electric field at the same time acts also in the opposite direction, i. e. it decreases τ by reducing the depth of electron traps and also by the fact that the free electrons, thereby dispersed, may set free the localized ones (impact freeing). However, these effects can apparently play an appreciable role at low temperatures only.

If, as follows from the above, the quantity τ which plays the part of a parameter in relaxation kinetics, has an explicit physical meaning, then the clarification of the physical meaning of μ will demand, obviously, a special investigation.

In conclusion I wish to express deep thanks to M. V. Fok for his consideration of the obtained results.

April 15, 1958

References

1. E. E. Bukke, L. A. Vinokurov, M. V. Fok; Hsui Hsui-Yun; DAN USSR, 103,585 (1955); 106,818 (1956) (See Sov. Phys. Doklady)
2. E. E. Bukke, L. A. Vinokurov, V. E. Oranovskii, Z. A. Trapeznikova, V. S. Trofimov; Izv. AN, USSR ser., 21,716 (1957)

TOM VI, Vyp. 2 OPTIKA I SPEKTROSKOPIIA Fevral', 1959
VOL. VI. No. 2 OPTICS AND SPECTROSCOPY February , 1959

The Mutual Influence of Certain 9-Monosubstituted Anthracenes on the Quantum Yield of their Photochemical Transformations and on the Quantum Yield of Fluorescence

T. M. VEMBER and A. S. CHERKASOV

It has been previously established that mono mesosubstituted anthracenes in solution undergo photochemical changes under the action of light, forming in the presence of oxygen two stable products, a photo-oxide, and a photo dimer. It has also been shown [1,2] that as the concentration of the substance under investigation is increased there is an increased quantum yield for the photo-oxidation and photo-dimerisation reactions, and a fall in the quantum yield of fluorescence.

It appeared interesting to investigate how the chemical reactions would go when two or more of the above mentioned class of compounds are present simultaneously. Would the role of all other substances, with respect to each given one, be simply that of absorbing impurities, or would there be any interaction between them?

Obviously in the first case the total quantum yield of the photo-oxidation (φ_f) or photodimerisation reaction (φ_d) will be given by the expression

$$(1) \qquad \varphi = \frac{\varphi'_{c_1}\varepsilon_1 c_1 + \varphi''_{c_2}\varepsilon_2 c_2 + \ldots + \varphi^i_{c_i}\varepsilon_i c_i}{\varepsilon_1 c_1 + \varepsilon_2 c_2 + \ldots + \varepsilon_i c_i},$$

where φ'_{c_1}, φ''_{c_2} and $\varphi^i_{c_i}$ are the quantum yields of the photo-oxidation or photo-dimerisation reactions of the 1st, 2nd and i-th substances at concentrations c_1, c_2 and c_i, and ε_1, ε_2 and ε_i are the corresponding molar absorption coefficients for the monochromatic light falling on the solution.

In the other limiting case, we may assume that the addition of a second substance to the solution of a given substance has the same effect on the system as would increasing the concentration of the first substance, (and vice versa). The expression for the quantum yields of the photo-oxidation and photo-dimerisation reactions will take the form

$$(2) \qquad \varphi = \frac{\varphi'_{c_1}\varepsilon_1 c_1 + \varphi''_{c_1+c_2}\varepsilon_2 c_2 + \ldots + \varphi^i_{c_1+c_2+\ldots+c_i}\varepsilon_i c_i}{\varepsilon_1 c_1 + \varepsilon_2 c_2 + \ldots + \varepsilon_i c_i},$$

where $\varphi'_{c_1+c_2+\ldots c_i}$, $\varphi''_{c_1+c_2+\ldots+c_i}$ and $\varphi^i_{c_1+c_2+\ldots+c_i}$ are the quantum yields for photo-oxidation and photo-dimerisation for the 1st, 2nd, and ith substances at a concentration equal to the sum of the concentrations of all of the dissolved substances.

We have determined the quantum yields for photo-oxidiation and photo-dimerisation and the quantum yields of fluorescence for alcohol solutions of mixtures of the following substances:

1.) 3×10^{-3} molar 9-methylanthracene (MeA) and 3×10^{-3} M. 9-ethylanthracene(EtA);
2.) 6×10^{-3} M. MeA and 6×10^{-3} M. EtA;
3.) 3×10^{-3} M. MeA and 3×10^{-3} M. EtA, 3×10^{-3} M. propylanthracene (PrA)
4.) 6×10^{-3} M. MeA and 6×10^{-3} M. EtA,
5.) 3×10^{-3} M. MeA and 9×10^{-3} M. 9-acetoxyanthracene (AcA).
6.) 6×10^{-3} M. MeA and 6×10^{-3} M. AcA
7.) $9\cdot10^{-3}$ M. MeA and 3×10^{-3} M. AcA

The solutions were irradiated with light of wavelength about 365 mμ. At the concentrations used, all the incident light was absorbed. The experiments were conducted[1] at 20°.

The experimentally found values of the quantum yield for the photo-oxidation and photo-dimerisation reactions and for fluorescence[2] are given in the table. In the same table are shown the quantum yields computed[3] from equations (1) and (2).

Experimentally found and calculated quantum yields for the photo-oxidation (φ_f) and photo-dimerisation (φ_d) reactions, and for fluorescence (B) of alcohol solutions of mixtures of substituted anthracenes.

Mixture No.	φ_f			φ_d			B		
	Found	Computed From (1)	Computed From (2)	Found	Computed From (1)	Computed From (2)	Found	Computed From (1)	Computed From (2)
1	0.089	0.051	0.091	0.031	0.020	0.030	0.22	0.26	0.23
2	0.120	0.091	0.148	0.053	0.030	0.045	0.19	0.23	0.19
3	0.097	0.043	0.105	0.034	0.018	0.033	0.21	0.28	0.21
4	0.142	0.081	0.153	0.072	0.028	0.054	0.16	0.25	0.17
5	0.060	0.037	0.063	0.031	0.013	0.024	0.13	0.15	0.13
6	0.120	0.052	0.088	0.034	0.017	0.034	0.16	0.17	0.14
7	0.127	0.091	0.114	0.065	0.046	0.056	0.17	0.18	0.16

As the data in the table show, the experimental values of the quantum yields of the processes being considered are very close to the values computed from expression (2), and differ markedly from those given using (1). This is especially well shown in the cases of the trimolecular mixtures 3 and 4, and in the mixtures containing methylanthracene and acetoxyanthracene 5, 6, and 7. This shows that in the simultaneous presence of several substances, the quantum yields of the photo-oxidation and photo-dimerisation reactions of each of them is increased, and the fluorescence yield diminished; i. e. addition of one of these substances to the solution of another has an effect analogous to that produced by a corresponding increase in the concentration of the first substance

1. The experimental methods are described in more detail in [1].
2. Reabsorption of fluorescence in the case of the above mixtures is almost identical with that in the case of a one-component solution at a concentration equal to the sum of the concentrations of the substances in solution, since the absorption and fluorescence of all the substances investigated do not differ appreciably from each other.
3. The quantum yields of fluorescence were computed from expressions analogous to (1) and (2). Since the differences in the values of ε at λ=365 mμ for the substances investigated are negligible, ε may be eliminated from expressions (1) and (2).

(and vice versa). It is interesting that the addition to a solution of 9-methylanthracene of 9-acetoxyanthracene, which by itself has a very low quantum yield for the photoreactions, also results in an increase in the overall quantum yield for the photoreactions.

The fact that the simultaneous presence of several alkyl substituted anthracenes in the same solution leads to an increased quantum yield in the dimerisation reaction can obviously only be explained by the fact that under these conditions not only dimers formed from two molecules of the same substance are formed, but also dimers formed by the pairing of two different molecules.

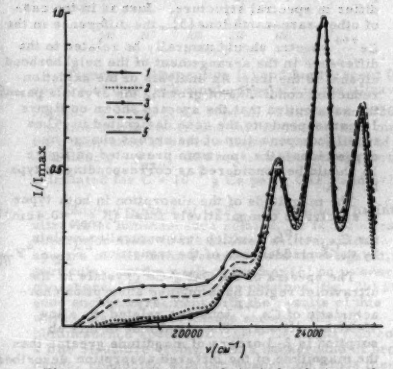

Fluorescence spectra of alcohol solutions of alkyl substituted anthracenes.

1. MeA (2×10^{-2} Mol./liter) 2. PrA (2×10^{-2} M.). 3. PrA (6×10^{-2} M.) 4. Mixture of MeA (2×10^{-2} M.), EtA (2×10^{-2} M. and PrA (2×10^{-2}M.). 5. Mixture of MeA (3×10^{-3} M.), EtA (3×10^{-3} M and PrA (3×10^{-3} M.).

The similarity of the interaction between molecules of two different species (among the molecules investigated in this work) and between a pair of identical molecules is shown by the fact that in the fluorescence spectrum of a concentrated mixture of substances, a new fluorescence band appears in the long wave region, just as is the case for a concentrated solution of a pure substance (see figure)*, and its appearance is determined not by the concentration of each individual substance, but by the sum of the concentrations of all dissolved substances.

May 12, 1958

References

1. A. S. CHERKASOV, T. M. VEMBER: OiS, 4, 203 (1958)
2. A. S. CHERKASOV, T. M. VEMBER: OiS, (in press)
3. T. FOERSTER, K. KASPER: Z. Elektrochem., 59, 976 (1955)
4. G. A. TISHCHENKO, B. IA. SVESHNIKOV, A. S. CHERKASOV: OiS, 4, 631 (1958)

* The appearance of an analogous band was detected earlier in the fluorescence spectra of single component concentrated solutions of pyrene [3] and monoalkyl substitutes of anthracene [4] and it has been explained by the luminescence of unstable dimers, formed by the union of excited and unexcited molecules of substance.

TOM VI, Vyp 2 OPTIKA I SPEKTROSKOPIIA Fevral', 1959
VOL. VI. No. 2 OPTICS AND SPECTROSCOPY February', 1959

On Absorption and Luminescence Spectra of Ce^{+++} Ions

P. P. FEOFILOV

In the 4f electron shell of the Ce^{+++} ion, enclosed by the populated $5s^2 5p^6$ shell, there is just one electron which can be in the $^2F_{5/2}$ (ground) and $^2F_{7/2}$ states [1]. The energy spacing between these states, determined from the spectra of the free ion, is 2253 cm^{-1}. Repeated attempts to detect the corresponding optical transitions for ions in crystals and solutions have not yielded positive results [1,2]. This led to the conclusion that "Cerium does not display spectra which are characteristic for transitions between f-shell levels". Gobrecht [2] related this circumstance to the low probability of transitions within the limits of the ground term which are accompanied by an increase in the magnetic quantum number. However, it could be imagined that the absence of results on the 4f - spectra of Ce^{+++} is occasioned by matters, not of principle, but of technique. Actually, the enclosed nature of the 4f-shell affords reason to presume that the position of the ion levels in the condensed phase should not differ radically from the position of the free ion levels, i.e., the corresponding absorption should be sought in the infrared region around 4 - 5 μ. As is known, in this region there are water absorption bands, which excludes the possibility of detecting absorption bands of Ce^{+++} in aqueous solutions and crystal hydrates with which investigations are commonly performed.

The introduction of the Ce^{+++} ions into an artificial fluorite crystal, which is a transparent medium to approximately 9 μ, would permit us to investigate the infrared spectrum of ions and to detect the absorption band which could uniquely be identified with the forbidden transitions $^2F_{5/2} - {}^2F_{7/2}$. Fluorite single crystals (CaF_2) with admixtures of 10^{-4} - 10^{-2} g Ce per gram CaF_2 (the Ce was introduced as CeF_3 or CeO_2) were grown at our request by M. A. Vasil'eva and I. V. Stepanov [3]. Graphite powder is added to the mixture in order to produce the reducing conditions needed to produce Ce^{+++} ions in the crystals.

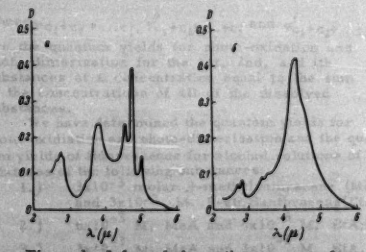

Figure 1. Infrared absorption spectra of CaF_2-Ce single crystals
a-type I; b - type II, C = 10^{-2} g Ce per g CaF_2; d=10mm, temperature 20° C.

The infrared absorption spectra were obtained on a UR-10 recording spectrophotometer [4] with a lithium fluoride prism.* An absorption band with a clearly defined structure even at room temperature which was different for the various samples was detected in the 3 - 6 μ range for all the crystal samples investigated. As an example, presented on figure 1 are the processed spectrograms of two samples which differ in spectral structure. Just as in the case of other rare-earth ions [5], the difference in the Ce^{+++} spectra should naturally be related to the difference in the arrangement of the neighborhood closest to the ion. An analysis of the oxidation-reduction conditions of growing the crystals permits the assumption that the spectra shown on figure 1a corresponds to the case designated in [5] as type I (compensation of the excess charge by oxygen ions); the spectrum presented on figure 1b should be considered as corresponding to type II.

The magnitude of the absorption in both types of spectra is comparatively small ($K_{max} \approx 0.4\ cm^{-1}$ for $C_{Ce} = 1\%$), which it is natural to explain by the forbiddenness of the transition $^2F_{5/2} - {}^2F_{7/2}$.

The spectra of the CaF_2-Ce crystals in the ultraviolet region have intense absorption characteristic of Ce^{+++} ions are related to allow 4f-5d transitions. The magnitude of this absorption is 2-3 orders of magnitude greater than the magnitude of the infrared absorption described above. Investigating the spectra of ultraviolet absorption, we detected their differences in individual crystals, which apparently should also be related to the difference in the structure of the centers. Presented on figure 2 are two typical absorption spectra whose maxima are located around 330 and 306 mμ. The absence of photochemical response in the crystals with an absorption maximum around 306 mμ requires the assumption that the structure of the centers in these crystals corresponds to the structure of centers displaying a type II infrared spectrum. Both absorption bands are observed in many of the crystals investigated.

A clear-cut line structure occurs in the ultraviolet absorption spectra when the crystals are cooled to a liquid nitrogen temperature. Lines with λ313.1 and 308.6 mμ appear in the shortwave range of the absorption band for all the crystals; moreover, intense λλ309.3, 304.9 mμ lines and a number of weaker lines are observed in certain crystals. On the low frequency tail of the band with a maximum around 330 mμ, there is a sharp intense line with λ338 mμ.

* The author is grateful to A. N. Sidorov for having made the recording of these spectra possible.

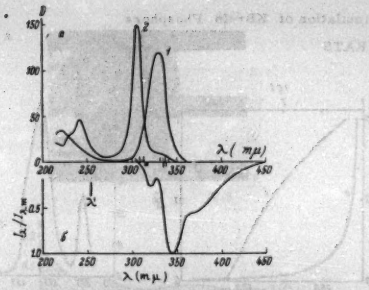

Figure 2. Absorption (a) and luminescent (b) spectra of CaF_2-Ce single crystals in the ultraviolet region. 1 - type I; 2 - type II. Temperature 20°. The line segments around the horizontal axis mark the appearance of narrow lines in the cooling of the samples; $\lambda' = \lambda_{exc} = 254$ mμ. Absorption spectra calculated for $C = 10^{-2}$ g Ce per g CaF_2 and d=10 mm.

Single crystals of CaF_2 - Ce disclose an intense ultraviolet luminescence related, as is the ultraviolet absorption also, to the allowed d-f transitions. The spectra of this luminescence were investigated, in particular, in the work of Ginther [6] on powdered phosphors. The spectra we obtained (fig. 2b) are in good enough agreement with the results of this work. As our experiments showed, the d-f luminescence spectra of CaF - Ce display on cooling, a line structure rising from a background of broad bands, connected with two absorption bands mentioned. The position of certain of these lines has been on figure 2.

The appearance of structure in broad absorption and luminescence bands related to allowed f-d transitions seems to us to be of considerable interest and to merit a special study.

The term scheme of the Ce^{+++} ion with one 4f-electron is in many ways analogous to the scheme of the Yb^{+++} ion with thirteen 4f-electrons [1]. The essential difference between the Yb^{+++} and the Ce^{+++} ions is the presence of intense d-f luminescence in the latter. In the luminescence spectra of fluorite crystals containing Yb^{+++}, we successfully observed just f-f luminescence [7]. Searches for the corresponding f-f luminescence of Ce^{+++} are fraught with great technical difficulties since it can be expected that its spectrum is located around 5 - 6μ. The duration of this luminescence must be very significant. To look for it is of great interest since, firstly, the Ce^{+++} ion remains the only rare-earth ion (without considering prometheum) for which f-f-luminescence is unknown and secondly, we would be dealing with a fact of great importance, in principle, a two-quantum optical transition in a condensed phase, in this case.

I am deeply grateful to M. A. Vasil'eva and I. V. Stepanov for growing the single crystals investigated and also to O. V. Sokolova for taking part in the measurement of the ultraviolet spectra.

June 10, 1958

References

1. M. A. EL'IASHEVICH: Spektry redkikh zemel' (Spectra of the rare earths) GITTL, Moscow 1953
2. H. GOBRECHT: Ann. Phys., 5 Folge, Band 31, 755 (1938)
3. I. V. STEPANOV, P. P. FEOFILOV: Iskusstvennyi fliurit (Artificial fluorite) in "Rost Kristallov" (Growth of Crystals), Akad. Nauk Press, Moscow, 1957 (Translated by CB)
4. H. M. BOLZ: Jenaer Rundschau, 2, No. 1, 4 (1957)
5. I. V. STEPANOV, P. P. FEOFILOV: DAN USSR, 108, 615 (1956) (See Sov. Phys. Doklady)
6. R. J. GINTHER: J. Electrochem. Soc., 101, 248 (1954)
7. P. P. FEOFILOV: OiS, 5, 216 (1958)

TOM VI, Vyp. 2 OPTIKA I SPEKTROSKOPIIA Fevral', 1959
VOL. VI. No. 2 OPTICS AND SPECTROSCOPY February, 1959

Phosphorescence and Thermal Stimulation of KBr-In Phosphors

M. L. KATS

In the paper of the author and of V. K. Nikol'skii [1] we gave results of a study of absorption and fluorescence spectra of KBr-In phosphors. Under the conditions of the experiment of the cited work (thin crystals and an exciting source of weak intensity), prolonged afterglow of the above phosphors has not been found. However, if the excitation of the KBr-In phosphor is produced by the undispersed light of a mercury arc, then a comparatively bright phosphorescence can be observed, whose decay curve (fig. 1) points to the recombination character of the luminescence. This is also indicated by the thermal stimulation of these phosphors (fig. 2) previously irradiated with x-rays. The thermal stimulation curve consists of two peaks of which the high temperature one is caused by electrons localized in F-centers, as is easily established by parallel optical measurements of changes in the absorption spectrum in the process of heating. Various arguments are also given in the paper [2] in favor of a recombination mechanism for the luminescence of indium-activated alkali-halide phosphors.

It is important to stress that the fluorescence and thermoluminescence spectra of the KBr-In phosphors which we measured with an illuminating ISP-66 spectrograph were essentially identical. Consequently, in both cases the luminescence is caused by identical electron transitions in the same centers.

July 13, 1958

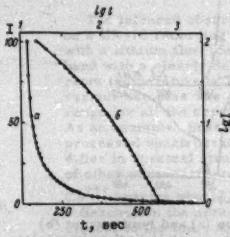

Figure 1
a - I as a function of t;
b - log I as a function of log t.

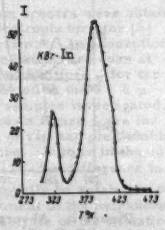

Figure 2. Thermal excitation of the KBr-In phosphor.

References

1. M. L. KATS, V. K. NIKOL'SKII: OiS, 4, 354 (1958)
2. N. E. LUSHCHIK: Trudy, IFAAN ESSR, 6, 149 (1957)
L. M. SHAMOVSKII, IU. N. ZHVANKO: IAN USSR, Fiz. ser., 21, 557 (1957) (See CTT Bulletin, 21, 551)
CH. B. LUSHCHIK, V. I. VOLIN: Trudy, IFAAN ESSR, 7, 311 (1958)

TOM VI, Vyp. 2 OPTIKA I SPEKTROSKOPIIA Fevral', 1959
VOL. VI. No. 2 OPTICS AND SPECTROSCOPY February, 1959

Absorption Spectra of Vanadium - Colored Corundum at Low Temperatures (down to 1.7° K)

S. V. GRUM-GRZHIMAILO, N. A. BRILLIANTOV, AND R. K. SVIRIDOVA

We have studied specimens of vanadium-colored corundum, resembling alexandrite in color, at low temperatures (down to 1.7° K).

The plane-parallel plates, cut paralled to the optic axis, had thicknesses up to 28 mm. Their colors were not very intense.

Previous studies [1] at 100° K showed a vibrational structure on the long-wave side of the absorption in the visable spectrum. This structure appears in both the ordinary and the extraordinary spectra at 100° K, at 1.7° K it becomes more distinct; the structure bands become narrower. As the temperature is lowered from 100° to 1.7° K the number of bands grows from 5 or 6 to 8 or 9, going towards shorter wave lengths from the first and narrowest structure band.

From our spectrograms (see Fig. a)* it is plain that practically the whole region of absorption consists of a series of vibrational bands spaced approximately equally from each other. This structure in the absorption spectra and its character agree completely with the theory of Krivoglaz and Pekar [2].

At 1.7° K the first band of the ordinary spectrum falls at $\lambda_o = 6291$ Å (see Fig. b, I), that of the extraordinary spectrum at $\lambda_e = 6298$Å (Fig. c, II). The greater the distance of a given structure band from the first one, the broader and less distinct it appears. The separation of adjacent bands is about 200 cm^{-1}.

* The four-digit numbers on the figures denote wavelengths in Augstroms.

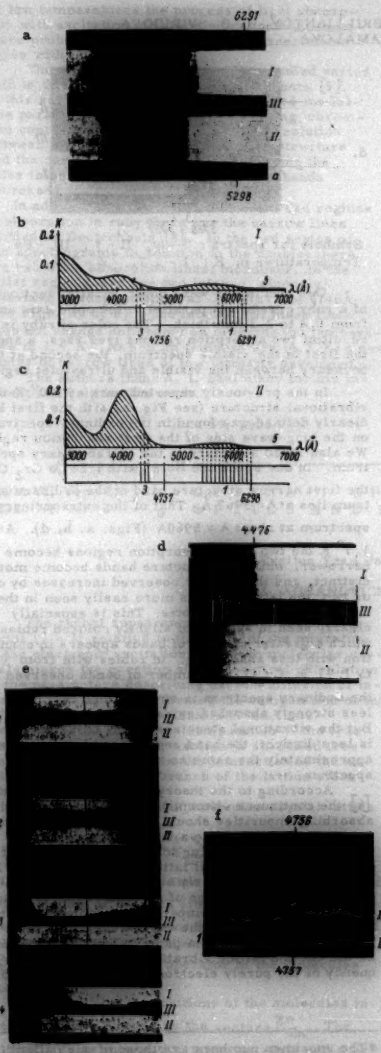

Symbols for spectra: I - ω, II - ε, III - Fe
Temperatures in °K: 1 - 1.7, 2 - 4.2, 3 - 77, 4 - 290, 5 - 293°.

On the longwave side of the broad absorption region of vanadium-corundum, situated at the boundary between the visible and the ultraviolet, there are some more diffuse absorption bands. The first of these is found at about $\lambda_\omega = 4476$Å and $\lambda_\varepsilon = 4480$Å. Here also the separation of adjacent bands is about 200 cm^{-1}. These bands apparently represent a second vibrational structure of the vanadium corundum spectrum and belonging to the broad absorption region in question (Fig. d) They are observed in both the ordinary and the extraordinary spectra.

For vanadium-corundum at 77° K we found narrow absorption lines in the blue region which had about the same intensity in the ordinary and extraordinary spectra ($\lambda_\omega = 4756$Å, $\lambda_\varepsilon = 4757$Å, see Figs. b, c). At room temperatures thses lines become indistinct. At 4.2° K their relative intensities change, the line in the extraordinary spectrum becoming markedly weaker than that in the ordinary spectrum. At 1.7°K the line in the extraordinary spectrum has practically disappeared (Figs. e, f).

The weakening of the extraordinary absorption line $\lambda_\varepsilon = 4757$Å in vanadium-corundum at low temperatures finds a possible explanation in the splitting of the ground state of the trivalent vanadium ion into two sub-levels under the action of the crystalline field. The temperature dependence of the lines corresponding to different sub-levels is different. At 1.7°K the intensity of the line corresponding to the transition from the higher sub-level of the ground state becomes markedly weaker. These remain the line corresponding to the transition from the lowest sub-level; an analogy is observed in crystals containing ions of the rare earths [3].

The authors thank A. I. Shal'nikov for his interest and help in connection with the present work.

June 14, 1958

References

1. S. V. GRUM-GRZHIMAILO, B. N. GRECHUSHNIKOV, R. A. KRAVCHENKO-BEREZHNOI: Materialy X Vsesoiuznogo soveshchaniia po spektroskopii (Proceedings of the X-th All-Union conference on spectroscopy) vol. 1, No. 3(8) L'vov Univ. Press, Minsk, 1957
2. M. A. KRIVOGLAZ, S. I. PEKAR: Trudy, IFAN Ukr. SSR, No. 4, 37 (1953)
3. M. A. EL'IASHEVICH: Spektry redkikh zemel' (Spectra of the rare earths) GITTL, 1953

On the Absorption Spectra of Rubies at Low Temperatures (down to 1.7° K)

S. V. GRUM-GRZHIMAILO, N. A. BRILLIANTOV, R. D. SVIRIDOVA
and A. S. DZHAMALOVA

In a study of ruby at the temperature of liquid nitrogen Feofilov found a vibrational structure in the absorption spectrum of the ordinary name. Feofilov and Grechushnikov [1] later showed that the separation between these structure bands is about 200 cm^{-1}, which is comparable to the corundum lattice frequency of 194 cm^{-1} observed in the infrared spectrum of ruby [2].

In a continuation of this research at the Institute of Crystallography of the U. S. S. R. Academy of Sciences a vibrational structure was also observed in the spectra of corundum colored with vanadium [3, 4]. All these observations were made at 100° K.

We have set up apparatus for recording absorption spectra of crystals at the temperatures of liquid nitrogen, hydrogen and helium. This comprises an ISP-51 prism spectrograph with a camera of F = 270 [sic] and glass Dewars with unsilvered strips on both sides.

The investigations were conducted in polarized light. By using a crystal of Iceland spar 10 cm thick as a polarizer we could simultaneously record the ordinary and extraordinary absorption spectra of the crystal under investigation. The polarizer and the specimen were so oriented that the planes of polarization of the two beams emerging from the crystal were inclined at 45° to the slit of the spectrograph; in this way we made sure that the intensities of the two beams were equal in those spectral regions where the crystal did not absorb light.

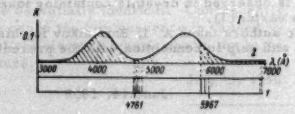

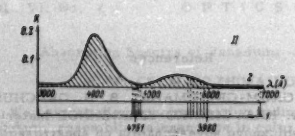

Symbols for spectra : I - ω, II - ε, III - Fe.
Temperatures in K : 1 - 1.7, 2 - 293.

Our specimens were plane-parallel sections of a ruby crystal cut parallel to the optic axis and from 0.4 to 2.3 mm thick. The color of ruby is a result of two absorption regions (see Figs. a and b), the first in the visible spectrum, the second at the boundary between the visible and ultraviolet regions.

In the previously reported work at 100° K the vibrational structure (see Fig. a) with the first band clearly defined was found in the ordinary spectrum on the long-wave side of the first absorption region. We also found structure in the extraordinary spectrum. In our specimen No. 88 with 1.24 % Cr_2O_3* the first narrow structure band of the ordinary spectrum lies at λ = 5967 Å. That of the extraordinary spectrum at about λ = 5960A (Figs. a, b, d). At 1.7° K the two broad absorption regions become narrower, while the structure bands become more distinct, and the number observed increases by one or two; the latter point is more easily seen in the more weakly colored rubies. This is especially clearly seen in spectra of slightly colored rubies in which a greater number of bands appears in connection with less absorption. In rubies with from 0.66 to 1.97 % Cr_2O_3 the number of bands observed in the ordinary spectrum is smaller than that in the less strongly absorbed extraordinary spectrum. But the vibrational structure of the latter spectrum is less distinct; the band separation, however, is approximately the same as that of the ordinary spectrum.

According to the theory of Krivoglaz and Pekar [6] the continuous absorption of crystals containing absorbing impurities should, on lowering the temperature, resolve itself into a series of bands with a separation corresponding to a characteristic vibration frequency of the crystal lattice. The absorption lines corresponding to a purely electronic transition start from the long-wave edge of a broad region of absorption; on lowering the temperature a vibrational structure should develop in the short wave direction from a line corresponding to a purely electronic transition as the excited lattice vibrations combine with the frequency of the purely electronic transition and add to it.

*The specimen numbers are those of our collection [5]. The chromium content was determined by chemical analysis.

At low temperatures the process of light absorption with excitation of lattice vibrations becomes more probable. The results of our experiments agree with this theory.

The series of ruby sections we studied varied both in thickness and in chromium contents [5]. In this series both the color intensity and the lattice parameters increase with increasing chromium content [7]. But we did not find a relation between the position of the vibrational structure and the chromium content. On increasing the color intensity the number of observed bands decreases.

In addition to the structure of the broad regions of absorption in ruby there are the narrow lines studied by Deutschbein [8]. In the red region of our spectrograms in addition to the daublet there are two weak absorption lines; moreover, in the violet region there are two intense, strongly polarized absorption lines at λλ 4761 and 4746Å (See Figs. a, b, c). The intensity of these lines does not change noticeably on lowering the temperature to 1.7°K. At helium temperature (4.2°K) a new series of narrow lines of low intensity developed.

The authors thank A. I. Shal'nikov for his interest and help in this work.

June 14, 1958

References

1. B. N. GRECHUSHNIKOV, P. P. FEOFILOV: ZETF, 29, 384 (1955) (See Sov. Phys. JETP)
2. R. S. KRISHNAN: Proc. Ind. Acad. Sci., 26A, 450 (1947)
3. S. V. GRUM-GRZHIMAILO, B. N. GRECHUSHNIKOV, R. A. KRAVCHENKO-BEREZHNOI: Materialy X Vsesoiuznogo Soveshchaniia po Spektroskopiia (Proceedings of the X All-Union Conf. on Spectr.) 1, #3(8), 144. L'vov Univ. Press, 1957
4. S. V. GRUM-GRZHMAILO, M. G. ENIKEEVA: Kristallografiia, 2, 186 (1957) (See Sov. Phys. Crystallography)
5. S. V. GRUM-GRZHMAILO, E. I. UTKINA: Tr. Inst. Krist., AN USSR, 8, 99 (1953)
6. M. A. KRIVOGLAZ, S. I. PEKAR: Trudy, IFAN Ukr. SSR, 4, 37 (1953)
7. N. A. SHAL'NIKOVA, I. A. IAKOVLEV: Kristallografiia, 1, 531 (1956)
8. O. DEUTSCHBEIN: Ann. Physik, 5 Folge, B. 14, 712 (1932); 5 Folge, B. 14, 729 (1932)

TOM VI, Vyp. 2 O P T I K A I S P E K T R O S K O P I I A Fevral', 1959
VOL. VI. No. 2 O P T I C S A N D S P E C T R O S C O P Y February, 1959

On the Exciton Free Path in a Molecular Crystal

V. M. AGRANOVICH, IU. V. KONOBEEV

The recent appearance of experimental material [1 - 3] relative to the study of the migration of the electronic excitation energy in molecular crystals makes the question of a theoretical calculation of the parameters describing exciton diffusion of interest. Trlifaj [4] performed the computation of the diffusion coefficient for 'localized' excitons.

Presented below is a computation of the free path of a 'non-localized' exciton (a so-called free exciton) determined from the interaction of the exciton with the acoustic branch of the lattice vibrations.

The Hamiltonian of a molecular crystal lattice is the following:

$$\hat{H} = \sum_{\vec{n}\alpha} \hat{H}_{\vec{n}\alpha} + \hat{T}_R + \frac{1}{2} \sum_{\vec{n}\alpha, \vec{m}\beta} \hat{V}^0_{\vec{n}\alpha, \vec{m}\beta}(\vec{R}_{\vec{n}\alpha} - \vec{R}_{\vec{m}\beta}). \quad (1)$$

Here $\hat{H}_{\vec{n}\alpha}$ is the Hamiltonian operator of the isolated α-th molecule at the n-th site ($\alpha = 0, 1, \ldots, g-1$), $\hat{T}_R$ the kinetic energy operator for the translational and rotational motion of all the molecules in the crystal, $\hat{V}^0_{\vec{n}\alpha, \vec{m}\beta}$ the interaction operator of the molecules $(\vec{n}\alpha)$ and $(\vec{m}\beta)$.

The equilibrium positions of the molecules in the crystal are defined by the vectors $\vec{R}^0_{\vec{n}\alpha}$. The intermolecular interaction operator varies as a result of the lattice vibrations. Let us expand the operator $\hat{V}^0_{\vec{n}\alpha, \vec{m}\beta}$ in a power series of the molecular displacement $\vec{u}_{\vec{n}\alpha}$ from the equilibrium position and let us be limited to terms of the expansion linear in $\vec{u}_{\vec{n}\alpha}$:

$$\hat{V}^0_{\vec{n}\alpha, \vec{m}\beta}(\vec{R}_{\vec{n}\alpha} - \vec{R}_{\vec{m}\beta}) = \hat{V}^0_{\vec{n}\alpha, \vec{m}\beta}(\vec{R}^0_{\vec{n}\alpha} - \vec{R}^0_{\vec{m}\beta}) + \hat{V}'_{\vec{n}\alpha, \vec{m}\beta}(u_{\vec{n}\alpha} - u_{\vec{m}\beta}). \quad (2)$$

The molecular displacement $(\vec{n}\alpha)$ in normal coordinates can be written as follows:

$$u_{\vec{n}\alpha} = (Ns)^{-\frac{1}{2}} \sum_{\vec{q}} e^{\alpha}(qs)\left(A_{qs} e^{i\vec{q}\vec{R}^0_{\vec{n}\alpha}} + A^{*}_{-qs} e^{-i\vec{q}\vec{R}^0_{\vec{n}\alpha}}\right), \quad (3)$$

where s is the subscript of the frequency branch, $\vec{q}$ the wave vector, $\vec{e}^{\alpha}$ the wave polarization vector, $N = N_1 N_2 N_3$ the total number of elementary cells in the crystal. According to [5], the wave function of a molecular crystal in which an exciton is propagated with the wave vector $\vec{k}$ can be represented as

$$\Phi_{f,\vec{k}}(u) = (Ns)^{-\frac{1}{2}} \sum_{\vec{n}\alpha} B_{\vec{n}\alpha} \chi^f_{\vec{n}\alpha} e^{i\vec{k}\vec{R}^0_{\vec{n}\alpha}} \prod_{\vec{q},s} \varphi_{N_{\vec{q}s}}, \quad (4)$$

$$\chi^f_{\vec{n}\alpha} = (Ns)^{-\frac{1}{2}} \sum_{\vec{m}\beta} (-1)^{\alpha} P_{\alpha\beta} \varphi^f_{\vec{m}\beta} \prod_{\vec{n}\alpha \neq \vec{m}\beta} \varphi^0_{\vec{n}\alpha}, \quad (5)$$

where $\varphi^f_{\vec{n}\alpha}$ is the wave function describing the f-th

electronic excitation of the nα-th molecule, $\varphi^{0}_{m\beta}$ the wave function of the unexcited mβ-th molecule, P_ν the permutation operator for the ν-th electron pair, $\psi_{N_{qs}}$ the wave function of an harmonic oscillator.

For the sake of simplicity, let us analyze a crystal with 1 molecule in the elementary cell. The probability of an exciton being scattered by a phonon (q, s) per unit time is calculated from

$$w_{k,k'} = \frac{2}{\hbar} |M_{k,k'}|^2 \delta [\varepsilon(k') - \varepsilon(k) \pm \hbar\Omega_{qs}], \tag{6}$$

where $\varepsilon(\vec{k})$, $\varepsilon(\vec{k}')$ are the exciton energy before and after production (annihilation) of the phonon, Ω_{qs} the frequency of the appropriate branch of the lattice vibrations

$$M_{k,k'} = \frac{1}{\sqrt{Ns}} \int \sum_{n} \chi^{*}_{k'} e^{-ik'n} \prod_{m\beta} \varphi^{*}_{m\beta} \left[\frac{1}{2} \sum_{n,m} V_{n,m}(u_n - u_m) \right] \times \times \sum_{n} \chi_{k} e^{ikn} \prod_{m\beta} \varphi_{m\beta}\, d\tau\, dA_{qs}. \tag{7}$$

If we are limited to dipole-dipole interaction for a molecule, then

$$\hat{V}^{0}_{n,m} = -\frac{e^2}{R^{(0)3}_{n,m}} \sum_{ij} (2x^{i}_{n}x^{j}_{m} - y^{i}_{n}y^{j}_{m} - z^{i}_{n}z^{j}_{m}). \tag{8}$$

Here, the summation is over all electrons i and j of the molecules $\vec{n}$ and $\vec{m}$, $R^{(0)}_{\vec{n},\vec{m}} = |\vec{n} - \vec{m}|$.

After simple manipulation, we find that the probability of a phonon $(\vec{q}s)$ being emitted is given by the expression

$$P^{k,k'}_{n} = \frac{\pi c^4}{MN} \cdot \frac{N_{qs}+1}{\omega_{qs}} F_s(k,k') \delta [\varepsilon(k') - \varepsilon(k) + \hbar\Omega_{qs}]|_{k'=k-q}, \tag{9}$$

and the probability of a phonon being absorbed, by the expression

$$P^{k,k'}_{n} = \frac{\pi c^4}{MN} \cdot \frac{N_{qs}}{\omega_{qs}} F_s(k,k') \delta [\varepsilon(k') - \varepsilon(k) - \hbar\Omega_{qs}]|_{k'=k+q}, \tag{10}$$

where the function $F_s(\vec{k}, \vec{k}')$ is *

$$F_s(k,k') = \frac{9}{16} \cdot \frac{F^{2}_{0i} k^2}{S^{3}\omega_{if}} |e(qs)\, S|^2 (3\cos^2\psi - 1)^2. \tag{11}$$

Here $F_{of} = \frac{2m\omega_{of}}{\hbar} \left| \int \varphi^{f}_{n} \vec{r} \varphi^{0}_{n}\, d\tau \right|^2$ is the oscillator strength of the transition in an isolated molecule, ω_{of} the appropriate frequency of the optical transition, μ the electron mass, θ^z the angle which the dipole transition vector forms with the z axis. The vector $\vec{S}$ is defined thus:

$$S = \sum_{\vec{l}} \frac{1}{|\vec{l}|^2} (e^{i\vec{q}\vec{l}} - 1) e^{-i\vec{k}\vec{l}}. \tag{12}$$

Here the vector $\vec{l} = l_1\vec{a}_1 + l_2\vec{a}_2 + l_3\vec{a}_3$; l_1, l_2, l_3 are integers; $\vec{a}_1, \vec{a}_2, \vec{a}_3$ are basis vectors of the lattice.

The relaxation time τ for not too low temperatures can be calculated by using the formula [8]

$$\frac{1}{\tau} = -\sum_{q} \frac{\Delta k_x}{k_x} (P^{k,k'}_{n} + P^{k,k'}_{n}), \tag{13}$$

where $\Delta k_x = k'_x - k_x$ is the change in the quasi-momentum component of the exciton with scattering:

Taking into account that $N_{qs} \approx N_{qs} + 1 \approx \frac{k_\delta T}{\hbar\Omega_{qs}}$ at high temperatures $(k_\delta T \gg \hbar\Omega_{qs})$, replacing the summation over $\vec{q}$ in (13) by integration and summing over all phonon polarization vectors, we find

$$\frac{1}{\tau} = -\frac{1}{8\pi^2} \cdot \frac{k_\delta T c^4 V_0}{kMc^2} \int \frac{\Delta k_x}{kx} \sum_{s} F_s(k,k') \{\delta[\varepsilon(k') - \varepsilon(k) + \hbar\Omega_{qs}]|_{k'=k-q} + + \delta[\varepsilon(k') - \varepsilon(k) - \hbar\Omega_{qs}]|_{k'=k+q}\} dq \sin\theta d\theta d\varphi. \tag{14}$$

Here k_δ is the Boltzmann constant, V_0 the volume of the elementary cell, M the mass of a molecule, c the velocity of sound in the crystal, θ the angle between the vectors $\vec{k}$ and $\vec{q}$.

For the sake of simplicity, let us analyze the case of a cubic lattice and let us take into account the interaction between nearest neighbors only. Moveover, let us use the effective mass approximation for the exciton. Then, the exciton energy can be represented as $\varepsilon(\vec{k}) = A + \frac{\hbar^2 k^2}{2m_e}$ where A is a constant, m_e is the exciton effective mass. The approximation used is valid if $ka \ll 1$, where a is the lattice constant. In the thermal equilibrium state for the majority of excitons, $k \approx k_T$, where $k_T = \frac{\sqrt{3m_e k_\delta T}}{\hbar}$. Hence, the effective mass approximation will be justified if $\frac{\sqrt{3m_e k_\delta T}}{\hbar} a \ll 1$.

This condition imposes a limitation on the exciton effective mass at high enough temperatures.

The expression for the vector $\vec{S}$ is simplified substantially in the approximation used: $\vec{S} = 2i\frac{\vec{q}}{a^3}$.

Integrating over the angles φ and θ in (14) and over $|\vec{q}|$ within the limits found from the law of conservation of quasi-momentum and energy (from $q_{min} = 0$ to $q_{max} = 2k_T$), we obtain the exciton free path as

$$\langle l \rangle_{fr} = \frac{\pi}{8} a \left(\frac{\hbar\omega_{of}}{c^2} \right)^2 \left(\frac{\mu}{m_e F_{of}} \right)^2 \frac{Mc^2}{k_\delta T}. \tag{15}$$

According to estimates made in [6], the exciton effective mass can be determined from the relation

$$m_e \approx \frac{\mu}{F_{of}} \left(\frac{a\hbar\omega_{of}}{c^2} \right).$$

Using this relation, we find that $\langle l \rangle_{fr} \approx \frac{\pi}{8} \frac{Mc^2}{k_\delta T} a$. Putting $M = 150 m_H$, where m_H is the mass of the hydrogen atom, $c = 10^5$ cm/sec, $T = 300^\circ$ K, we obtain $\langle l \rangle_{fr} \approx 20$ A.

Using the relations obtained, we find that the exciton diffusion coefficient is $D = \frac{\langle l \rangle_{fr} v}{3} = \frac{\pi}{9} \frac{Mc^2 a}{\sqrt{3kTm_e}}$.

If it is assumed that $m_e \approx 10\mu$, $a \approx 5 \times 10^{-8}$ cm, we find $D \approx 1$ cm^2/ sec. The value of the free exciton diffusion coefficient obtained exceeds the values found as a result of direct measurements [1 - 3] by more than an order of magnitude. Such a discrepancy between the observed and the calculated

*The function $F(\vec{k}, \vec{k}')$ has recently been calculated incorrectly in the paper [6] published recently. In this connection, the results of [6, 7] are not correct

values of the diffusion coefficient can be caused either by the substantial role of the 'localized' excitons or by the presence of lattice defects, the average distance between which should be less than the computed value $\langle l \rangle_{fr}$ in this case. Certainly, the very approximate character of the computations made should also be kept in mind. In order to explain the scattering mechanism during exciton migration, it would be very useful to make an experimental study of the temperature dependence of the exciton diffusion coefficient, which differs substantially for different scattering mechanisms. Actually, the scattering of free excitons by phonons leads to the dependence $D_{fr} \sim 1/\sqrt{T}$, while the diffusion coefficient of the localized excitons, according to [4], is given by the relation $D_{loc} \sim \exp(-U/kT)$.

If the free path of the free exciton is determined by the presence of lattice defects, the diffusion coefficient must drop exponentially, as the temperature increases, in proportion to $\exp(-U/kT)$ (here U is the activation energy for the formation of defects).

June 25, 1958

References

1. M. D. GALANIN, Z. A. CHIZHIKOVA: OiS, 1, 175 (1956)
2. O. SIMPSON: Proc. Roy. Soc., A238, 402 (1957)
3. V. M. AGRANOVICH, I. IA. KUCHEROV, O. M. FAIDYSH: Ukr. Fiz. Zh., 2, No. 1, (1957)
4. M. TRIFLAJ: Czech. Phys. Jnl, 6, No. 6 (1956) (In Russian with English summary)
5. A. S. DAVYDOV: Teoriia pogloshcheniia sveta v molekuliarnykh kristallakh (Theory of light absorption in molecular crystals) Akad. Nauk Ukr. SSR Press, Kiev, 1951
6. A. S. SELIVANENKO: OiS, 4, 92 (1958)
7. A. S. SELIVANENKO: OiS, 4, 122 (1958)
8. H. FROEHLICH: Proc. Roy. Soc., A160, 230 (1957)

TOM VI, Vyp. 2 O P T I K A I S P E K T R O S K O P I I A Fevral', 1959
VOL. VI. No. 2 O P T I C S A N D S P E C T R O S C O P Y February, 1959

Improved Analytic Single-Electron Wave Functions

S. D. BUDRITE, L. L. KUZMITSKITE, V. K. SHUGUROV

INTRODUCTION

The accuracy of computations of various physical quantities depends to a large degree on the accuracy of the wave functions being used. The best of the single-electron functions are the Fock self-consistent-field solutions [1]. However, the difficulty of numerical integration and the inconvenience of presenting the functions in tables complicate and limit their application. On the other hand, the analytic functions of Morse [2] are free of these inadequacies. Moreover, their parameters may be found easily by utilizing electronic computers. But the accuracy of the results obtained in this case is considerably lower.

The purpose of the present work is to find analytic functions which would give the same or almost the same results as do the numerical Fock functions. We start from the fact that the inaccuracy of the Morse functions [2], which are only a particular modification of the hydrogen functions, follows from the approximate character of the analytic representation, and not from the corresponding Fock equations.

In order to make them more accurate, let us proceed as follows. Let us write the Fock equations in momentum space and let us solve them by successive approximations. The hydrogen functions can be taken as the initial functions. Since the functions [2] are close enough to the exact solution, it will be sufficient to limit ourselves to the first approximation. The functions thus obtained which describe different terms will generally be different not only in their parameters but also in the analytic form. The parameters should be established from the minimum energy condition. This program is performed herein for helium-like atoms in the ground configuration.

1. WAVE FUNCTION OF THE GROUND CONFIGURATION OF THE HELIUM ATOM

Let us consider the single-electron wave function

$$\psi(r) = R(r)\, Y\left(\frac{r}{r}\right), \tag{1}$$

where R is the radial part, Y the spherical harmonic. Making use of the Fourier transform

$$\psi(r) = \int \psi(k)\, e^{i(kr)}\, dk, \tag{2}$$

we find

$$\psi(k) = R(k)\, Y\left(\frac{k}{k}\right), \tag{3}$$

where

$$R_{nl}(r) = \int_0^\infty R_{nl}(k)\, g_l(kr)\, k^2 dk, \tag{4}$$

$$g_l(x) = (2x)^{\frac{1}{2}}\, i^l\, \frac{J_{l+\frac{1}{2}}(x)}{\sqrt{x}}. \tag{5}$$

J is a Bessel function.

Then using the expansion

$$\frac{1}{r} = \frac{1}{2\pi^2}\int e^{i(kr)}\frac{1}{k^2}\,dk$$

and summing over the spins, we obtain the expression for the energy of a helium-like atom with the nuclear charge N in an s^2 configuration

$$E = \int \psi^*(k)\,k^2\psi(k)\,dk - \frac{N}{\pi^2}\iint \psi^*(k_1)\frac{1}{|k_1-k_2|^2}\psi(k_2)\,dk_1dk_2 + \tag{6}$$
$$+ 4\pi\iiint \psi^*(k_1)\psi^*(k_2)\frac{1}{|k_1-k_2|^2}\psi(k_2)\psi(k_1+k_2-k_2)\,dk_1dk_2dk_2.$$

The first integral in (6) yields the kinetic energy of the electrons, the second, the interaction energy of the electrons with the nucleus, the third (we denote it by F) is the interaction energy between the electrons.

Let us transform F to another form. To do this, let us write the series expansion

$$\psi(k_1+k_2-k_2) = e^{i(k_1-k_2,\,r_{12})}\psi(k_2) \equiv \psi(k_2) + \dots \tag{7}$$

Taking into account the relation

$$(2\pi)^3\int \psi^*(k)\,e^{i(kr_{12})}\psi(k)\,dk = \int \psi^*(r)\,e^{i(kr)}\psi(r)\,dr,$$

we have

$$F = \frac{1}{(2\pi)^3}\iint \psi(k_1)\frac{1}{|k_1-k_2|^2}\psi(k_2)\,dk_1dk_2\int \psi(r)\,e^{i(k_1-k_2,\,r)}\psi(r)\,dr. \tag{8}$$

Here the exponential, as in (7), is an abbreviated notation of the series

$$e^{i(kr)} \equiv 1 + i(kr) + \dots \tag{9}$$

If the last term in (6) is discarded, then the remaining expression equals twice the energy of the hydrogen atom. The equations obtained by the variational method have hydrogen function solutions (for the lowest configuration)

$$R(r) \sim e^{-\frac{r}{N}} \tag{10}$$

with the parameter $Z = N$. Retaining just the first term in the expansion (9) and keeping in mind the normalization of $\Psi(r)$ to unity, we again obtain hydrogen functions but with the parameter $Z = N - \frac{1}{Z}$. The parameter which yields a minimum of the energy of the $1s^2$ configuration is $N - \frac{5}{16}$.

In order to write the Fock equation, let us take a variation of the following expression with respect to R(k)

$$E' = E + \varepsilon N,$$

where

$$N = (2\pi)^3\int \psi^*(k)\psi(k)\,dk = 1,$$

ε is the undefined Lagrange multiplier which provides for normalization. Hence, it should be taken into account that, after the variation of F, the term corresponding to the first in (9) is multiplied by the factor 2 and the rest, the factor 4. Finally the equation becomes

$$(11)\left(k^2 + \varepsilon^2\right)R(k_1) - \frac{1}{\pi^2}\left(N + \frac{1}{2}\right)\iint V\left(\frac{k_1}{k_1}\right)\frac{1}{|k_1-k_2|^2}\psi(k_2)\,dk_2dk_2 +$$
$$+ \frac{1}{\pi^2}\iint V^*\left(\frac{k_1}{k_1}\right)\frac{1}{|k_1-k_2|^2}\psi(k_2)\,dk_2dk_2\int \psi^*(r)\,e^{i(k_1-k_2,\,r)}\psi(r)\,dr = 0.$$

In contrast to the Fock integro-differential equation, it is convenient to solve this nonlinear integral equation by successive approximations. As the initial approximation, let us take the hydrogren functions (10), whose Fourier transforms are Gegenbauer polynomials [3]. As a result of integration in (11), transforming into ordinary space, we obtain in the first approximation

$$(12)\quad \left(R_{1s}(r) = \frac{2\sqrt{4Z^3}}{r}\left[\frac{Z-\frac{1}{2}}{Z^2-\varepsilon^2}\left(e^{-\varepsilon r} - e^{-2Zr}\right) + \right.\right.$$
$$\left.\left. + \frac{15Z^2-\varepsilon^2}{(9Z^2-\varepsilon^2)^2}\left(e^{-\varepsilon r} - e^{-3Zr}\right) - \frac{Z}{9Z^2-\varepsilon^2}re^{-3Zr}\right].$$

where we write the parameter Z again instead of N.

The wave function of the $2s^2$ configuration would have 1 parameter and 2 undetermined factors, one of which provides for normalization and the other orthogonality to the 1s function.

2. NUMERICAL RESULTS

The energy of an atom calculated by using (12) is a particular function of the parameter Z and the factor ε, which are determined from the extremum and normalization conditions. The appropriate computations appear to be simpler than the establishment of the parameters of the Morse functions P(2s), for example. The results of our computations are in the table, where are also presented, for comparison, the values of the energy computed by using the hydrogen functions with parameters [2] and by using numerical Fock functions in the single-configuration approximation with complete separation of variables [4]. Our results are very close to the latter.

Values of the Parameters and Energy of Helium-like Atoms in the $1s^2$ Configuration

Atom	Z	ε	Energy of the atom (in atomic units)		
			Calculated by using hydrogen functions [2]	Calculated by using function (12)	Calculated by using numerical Fock functions [4]
He	1.613	1.441	- 2.848	- 2.860	- 2.862
Li+	2.600	2.432	- 7.223	- 7.234	- 7.236
Be++	3.619	3.452	-13.598	-13.61	-13.611
$B^{3}+$	4.634	4.468	-21.973	-21.99	-21.986

The authors are grateful to Prof. A. P. Iutsis and the participants of his seminar for discussion of the work and for critical remarks.

July 7, 1958

References

1. V. FOCK: Z. Phys., 61, 126 (1930)
2. P. M. MORSE, L. A. YOUNG, E. S. HAURWITZ: Phys. Rev., 48, 948 (1935)
3. B. PODOLSKY, L. PAULING: Phys. Rev., 34, 109 (1929)
   E. A. HYLLERAAS: Z. Phys., 74, 216 (1932)
   I. N. SNEDDON: Fourier Transforms, New York, McGraw-Hill, 1951 (IL, Moscow, 1955)
4. G. K. TSIUNAITIS, V. V. KIBARTAS, A. P. IUTSIS: OiS, 1, 5 (1956)

TOM VI, Vyp. 2 OPTIKA I SPEKTROSKOPIIA Fevral', 1959
VOL. VI. No. 2 OPTICS AND SPECTROSCOPY February, 1959

Application of Kravets' Method to Determine Optical Constants of Metals

G. P. SKORNIAKOV and M. M. KIRILLOVA

The revival of research in metal optics in recent years has brought out a series of new methods for determining the optical constants of metals n and k. Since mostly these methods require special optical apparatus, any simpler methods deserve notice.

Kravets and collaborators [1-3] proposed to determine optical constants of dyes with strong absorption from measurements of specular reflection at normal incidence, of these substances in contact with transparent supports in the form of wedges with different refractive indices.

This method requires a proper selection of properties for the contact medium with a view to the greatest possible difference between the refractive indices n_1 and n_2, as well as the absence of selective absorption over the spectral region in question.

We applied Kravets method to some metals and report our results here.

For the case of metal films on transparent supports the conditions in most respects follow those adopted for dye films [2]. But the method can also be applied to the measurement of massive metal specimens. The problem of contact media is solved simply by the use of liquids.

In the present work the polished specimen is immersed in a liquid to a depth of several millimeters and is so positioned that the liquid above its surface forms a wedge (see Figure). The reflectance is measured at angles near normal incidence.

1--exit slit of monochromator;
2--lens; 3--cell with specimen;
4--photocell.

A UM-2 furnished the light, and the detector was a silver sulfide photocell connected to a sensitive galvanometer. Between immersions in different liquids the sample was thoroughly cleaned. For immersion, organic liquids are preferred which are inert with respect to the metals investigated, and are transparent over a wide spectral range. Refractive indices of many organic liquids are known [4]; we chose methanol, benzene and toluene, the latter serving to duplicate the measurements made with benzene. To calculate the absolute values of the reflection coefficient R_1 and R_2 of the metal immersed in the two liquids, we corrected for reflection losses at the air/liquid and liquid/air boundaries.

The final expressions take the forms

$$(1) \qquad R_1 = \frac{I_2 R_0}{I_1\left[1 - 2\left(\frac{1 - n_1}{1 + n_1}\right)^2\right]}$$

$$(2) \qquad R_2 = \frac{I_2 R_0}{I_1\left[1 - 2\left(\frac{1 - n_2}{1 + n_2}\right)^2\right]},$$

where n_1 and n_2 are refractive indices of the contact liquids; I_1 and I_2 are galvanometer readings when the light beam is reflected from the unimmersed and the immersed specimen, respectively; and R is the reflection coefficient of the metal in air. The refraction and absorption indices are calculated from the expressions

$$(3) \qquad n = \frac{1}{2}\,\frac{(1 - R_1)(1 - R_2)}{\frac{R_1 - R_2}{n_1 - n_2} + \frac{1 + R_1 R_2}{n_2 + n_1}},$$

$$(4) \qquad k = \sqrt{\frac{R_1 (n + n_1)^2 - (n - n_1)^2}{1 - R_1}}.$$

In this way we measured the optical constants of specimens of Ni, Co, Cu, Ag, Al; the latter was a film, while the others were polished plates.

λ (in Å)	Co			Ni			Cu			Ag			Al		
	R_0	n	k	R_0	n	k	R_0	n	k	R_0	n	k	R_0	n	k
5330	0.548	1.90	2.50	0.580	1.68	2.5	—	—	—	—	—	—	0.875	0.96	5.01
5700	0.582	1.91	2.66	—	—	—	0.703	0.82	2.33	0.890	0.20	2.11	—	—	—
5950	0.592	2.00	2.92	—	—	—	0.715	0.77	2.40	0.895	0.23	2.26	0.870	1.02	4.84
6200	—	—	—	0.602	1.82	2.82	0.720	0.58	2.36	0.900	0.24	2.30	—	—	—
6800	0.615	1.97	2.8	0.618	1.87	2.98	—	—	—	0.900	0.24	2.32	0.868	1.20	5.30
6730	0.622	2.32	3.51	0.627	1.99	3.17	0.810	0.62	2.95	0.910	0.21	2.12	0.866	1.30	5.45
7150	—	—	—	0.637	2.10	3.32	0.810	0.69	3.31	—	—	—	0.858	1.41	5.48
7400	0.650	2.38	3.55	0.655	2.15	3.44	0.815	0.91	3.80	0.920	0.26	2.62	0.845	1.53	5.63
8500	0.724	2.5	4.15	0.684	2.34	3.8	—	—	—	—	—	—	0.865	1.28	5.40

Our results are set out in the accompanying table. The uncertainty in the measurement of n and k does not exceed 5 to 7%. A comparison with the same constants found in the literature [5-7] shows satisfactory agreement.

Thus our work demonstrates the suitability of Kravets' method for the measurement of the optical constants of metals.

Evidently the application of this method in the ultraviolet and infrared spectral regions, where polarimetric methods encounter considerable difficulties, should not run into objections of a fundamental nature.

July 8, 1958

References

1. T. P. KRAVETS, KH. L. PES KINA, N. N. PRIBYTKOVA: IAN USSR, Ser. fiz., 12, 504 (1948)
2. N. N. PRIBYTKOVA: OiS, 2, 623 (1957)
3. N. N. PRIBYTKOVA, L. S. AGROSKIN: OiS, 2, 628 (1957)
4. B. V. IOFFE: Rukovodstvo po refractometrii dlia khimikov (Handbook on refractometry for chemists) Leningrad Univ. Press, 1956
5. M. BORN: Optik. Berlin, Springer, 1933 (ONTI, 1937)
6. LANDOLT-BORNSTEIN: Physikalisch-chemische Tabellen, 5 Auflage, 2, 907, 1923
7. L. G. SCHULZ, F. R. TANGHERLINI: JOSA, 44, No. 5, 362 (1954)

TOM VI, Vyp. 2 OPTIKA I SPEKTROSKOPIIA Fevral', 1959
VOL. VI. No. 2 OPTICS AND SPECTROSCOPY February , 1959

On Temperature Dependence of Line Intensities of the Raman Effect in Gaseous CO_2 and N_2

V. M. PIVOVAROV, IA. S. BOBOVICH

1. The results of numerous investigations have shown that the Raman line intensities of liquids, contrary to theoretical predictions, more or less significantly decrease with an increase in temperature [1]. The study of the temperature dependence of Raman spectrum lines in gases can be useful for interpretation of the above mentioned anomaly.

Indeed, if the anomaly in liquids is dependent on molecular interaction, then for gases the temperature behavior of intensity must be normal; that is, the Raman line intensities must increase as the temperature rises, and must increase in a greater degree the smaller is the Raman frequency.

A direct answer to the above question could be obtained by a study of line intensities in the low frequency region. With such lines a notable increase in intensity with a relatively moderate increase of temperature could be expected. The vapors of some volatile organic liquids satisfy the above requirements. However, the study of such liquids is connected with some specific difficulties. It is much easier to conduct quantitative measurements of the Raman effects in gases. Even though the spectrum lines of common simple gases have extremely high frequencies, it is still possible to obtain some information on the question we are interested in.

2. We have investigated carbon dioxide and nitrogen, which have sufficiently intense lines at 1289 and 1388, and 2330/cm respectively. For the excitation and recording of lines by photoelectric means, the equipment developed previously and described in references 2, 3 was used. A container was filled from a gas bottle. The heating was provided by the coil mounted on the container. The line intensities were measured for two temperature points: 40-50 and 110-120 degrees centigrade. The gas pressure inside the container was 4.9 and 5.8 atmospheres respectively. The spectral slit width of the monochromator was approximately 50 cm^{-1}. The results evaluated from five to nine measurements are summerized in the following table.

Gas	Line frequency in cm^{-1}	Average intensity (in relative units) ($t°$ = 40-50°) I_1	($t°$ = 110-120°) I_2	I_2/I_1
CO_2	1285	52	53	1.02 ± 0.07
	1388	77	78	1.01 ± 0.02
N_2	2330	35.5	35	0.98 ± 0.07

The results show that within the accuracy of measurements, from 2 to 7%, no noticeable changes in intensities of investigated lines were observed during the heating of the gases. This fact is probably evidence for the absence of a temperature anomaly in the gas phase, because during the increase of gas temperature from 40-50 to 110-120 degrees, only a negligible increase in intensity in this case can be expected for the lines corresponding to high frequencies. Hence, the obtained results do not contradict the assumption that the temperature anomaly in the intensity of Raman spectrum in liquid substances is caused by molecular interaction.

July 16, 1958

References

1. IA. S. BOBOVICH, V. M. PIVOVAROV: OiS, 3, 227 (1957)
2. V. M. PIVOVAROV, IA. S. BOBOVICH: ZTF, 26, 649 (1956) (See Soviet Physics, Technical Physics)
3. B. A. KISELEV: OiS, 1, 597 (1956)

TOM VI, Vyp. 2 OPTIKA I SPEKTROSKOPIIA Fevral', 1959
VOL. VI. No. 2 OPTICS AND SPECTROSCOPY February, 1959

The Shape of Absorption and Emission Bands of Complex Molecules

N. G. BAKHSHIEV

A great deal of work has already been devoted to the shape of continuous absorption and emission bands. References [1 - 6] occupy a special place among these investigations. These papers showed that it is in principle both possible and fruitful to construct one-dimensional models of potential curves, especially for the case of the electronic-vibrational spectra of complex organic molecules. This approach - starting from the most general physical considerations - led to intensity distribution formulas for absorption and fluorescence spectra which conformed well with the experiment. In this connection, Neporent introduced generalized parameters describing average properties of all vibrational systems (potential curves of higher and lower electronic states approximating parabolas). Stepanov, developing the question further, also took the distribution of the vibrational energy levels of the molecules into consideration. He came to the conclusion that in calculating the shape of an absorption band it is necessary to consider two basic factors - the distribution of the molecules in coordinate-momentum phase space, and the probability distribution for motion of the nuclei during electronic vibrational transitions (i.e., degree of violation of the Franck-Condon principle).

It seems to us that in considering the question of the shape of the absorption band it is necessary to consider another essential factor - the great anharmonicity of the potential function of complex molecules. We have therefore attempted to allow for the anharmonic potential function in the simplest manner, by calculating the shape of an absorption band within the framework of a one-dimensional model. The calculation of anharmonicity by means of such a model consists, of course, in replacing potential curves of the parabolic type by curves such as those described, e. g., by Morse's function (fig. 1), characterised by the parameters α and D.

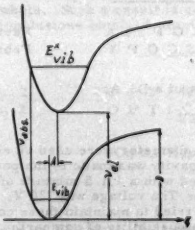

Figure 1.

$$E_{vib} = D\,(1 - e^{-\alpha q})^2 .$$

Following Stepanov [4, 5], we shall assume for simplicity that the probability of an electron transition does not depend on the coordinates (q) and momentum (p) of the nuclei, and that the vibrational energy distribution of the molecules is given by the simple expression $\rho\,(E_{vib}) = C \exp\left(-\frac{E_{vib}}{kT}\right)$.

Besides, let us assume that transitions between electronic levels occur without violation of the Franck-Condon principle (only vertical transitions take place). Then the vibrational energy of a molecule at the point qp of phase space is determined by the expression

$$E_{vib} = D\,(1 - e^{-\alpha q})^2 + \frac{1}{2\mu}\,p^2,$$

in which μ is the mass of the molecule.

If the parameters of the upper and lower potential curves are identical, and the curves themselves are displaced relative to each other by an amount A, then the quantity of vibrational energy after the transition into the excited state is equal to

$$E^*_{vib} = D\,(1 - e^{-\alpha(q-A)})^2 + \frac{1}{2\mu}\,p^2.$$

The total change of energy in the process of electron transition can be written as

$$\nu_{abs} = \nu_{el} + E^*_{vib} - E_{vib} = \nu_{el} - 2De^{-\alpha A}\,(e^{\alpha A} - 1) + De^{-2\alpha A}\,(e^{2\alpha A} - 1).$$

By simple transformations (analogous to [4, 5]) we obtain the following expression for the distribution of intensity within the absorption band (for $\nu > \nu_{el}$)

$$(1) \qquad a(\nu) = a_0\,\frac{e^{-\frac{a}{kT}\left[1 - \frac{a}{b} - b(\nu)\right]^2}}{b(\nu)\left[\frac{a}{b} + b(\nu)\right]},$$

where

$$b(\nu) = \sqrt{\frac{a^2}{b^2} + \frac{\nu - \nu_{el}}{bD}}, \quad a = (e^{\alpha A} - 1), \quad b = (e^{2\alpha A} - 1).$$

It is easily seen that formula (1) is very close to the formula suggested by Neporent [1], and differs only by the presence of a denominator depending on frequency. The formula includes two parameters determined by the properties of the molecule: D and $e^{\alpha A}$. The spectrum also depends on the temperature and on the frequency of the electron transition ν_{el}, which, obviously, does not influence the shape, but just determines the position of the absorption band on the frequency scale. By analogy an expression can be obtained which will give the distribution of intensity in fluorescence bands (for $\nu < \nu_{el}$). This expression will differ from formula (1) by having different values for the parameters. On analyzing expression (1) it is not difficult to relate the quantities D and $e^{\alpha A}$ to the experimentally determined halfwidths of the absorption band ($\Delta\nu_{1/2}$) and the difference $\Delta\nu = \nu_m - \nu_{el}$, in which ν_m is the frequency corresponding to the peak of the band. Accordingly

$$(2) \qquad \Delta\nu_{1/2} \approx 4e^{\alpha A}\,(e^{\alpha A} - 1)\sqrt{kTD\ln 2},$$

$$(3) \qquad \Delta\nu = \nu_m - \nu_{el} \approx D\,(e^{\alpha A} - 1)^2.$$

Utilization of relations (2) and (3) makes it possible to subject formula (1) to experimental verification. Such a test was carried out on the absorption spectra of vapors and solutions of several derivatives of phthalimide. The results showed that formula (1) agrees very well with experiment.

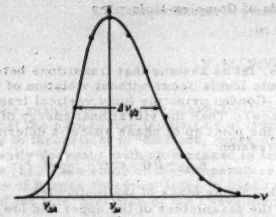

Figure 2.

Thus, for example, the continuous line of fig. 2. shows the longwave absorption band of 3-aminophthalimide in water (the band is characterized by the fact that $\nu > \nu_{el}$ for almost the entire band). The points marked by small circles, were calculated according to formula (1), assuming that $\Delta\nu_{1/2} = 4800\ cm^{-1}$ and $\Delta\nu = \nu_m - \nu_{el} = 3500\ cm^{-1}$. The agreement with experiment is good. As for the dependence of the shape of the absorption band on temperature, it would seem that such a dependence, can be not only explicit, as e. g. in formula (2) but also implicit. In particular, there is reason to assume that the shift of the potential surfaces of the higher and lower electronic states relative to each other (A) decreases with increasing temperature. It should also be mentioned that in the most general case, the parameters of the upper and lower potential curves can be different. This leads to a complication of the expressions describing the shapes of the absorption and emission bands, but also makes it possible to explain some of the peculiarities appearing in the spectra. Unfortunately, lack of space prevents us from going into detail.

Our derivation thus shows that in the case of a one dimensional model, calculation of the anharmonic potential function allows us to obtain a comparatively simple expression which satisfactorily describes the form of the continuous absorption and emission bands of complex molecules. At the same time, it proves possible to do without the questionable assumption based on the violation of the Franck-Condon principle which has been used in the literature [5] to explain the form of these bands. It turns out that the form of the continuous absorption and emission bands of complex molecules, within the framework of the foregoing proposals, is apparently determined by the vibrational energy distribution of the particles, and by the form and anharmonicity of the potential curves.

In conclusion I take this opportunity to express my gratitude to B. S. Neporent for his consideration and his interest in this work.

July 25, 1958

References

1. B. S. NEPORENT: ZETF, 21, No. 2, 172 - 188 (1951) (See TT-559)
2. B. S. NEPORENT: IAN USSR, Ser. fiz., 15, No. 5, 533-541 (1951) (See TT-440)
3. B. S. NEPORENT: Trudy, GOI, Sessiia pamiati S. I. Vavilova (Session in memory of S. I. Vavilov) Oboronizdat, 1953
4. B. I. STEPANOV, L. P. KAZACHENKO: IAN BSSR, No. 3, 53 (1955)
5. B. I. STEPANOV: Liuminestsentsiia slozhnykh molekul (Luminescence of complex molecules) Minsk, 1955
6. V. V. ZELINSKII, V. P. KOLOBKOV, L. G. PIKULIK: OiS, 2, 405 (1957)

TOM VI, Vyp. 2 OPTIKA I SPEKTROSKOPIIA Fevral', 1959
VOL. VI, No. 2 OPTICS AND SPECTROSCOPY February, 1959

The Distribution of Neutral Atoms in the Plasma of a DC Arc

E. I. NIKONOVA, V. K. PROKOF'EV

In [1], we investigated the radial distribution of neutral sodium atoms over a central section of a dc arc plasma by the anomalous dispersion method. These investigations have been continued, and the distribution of neutral sodium atoms investigated over sections of the arc located at various distances from the cathode.

It is well known from experimental work in spectrochemical analysis that the concentration of neutral atoms is considerably greater near the cathode than in the middle sections of the electrode gas. The "cathode layer" method of spectrochemical analysis is based on this phenomenon. An increase (up to 10 times) in the concentration of atoms in the layer near the cathode has also been detected by Eberhagen [2].

The procedure used in our present investigations is similar to that explained in [1]. Carbon rods 7 mm in diameter were used as electrodes. A 1 mm diam. cavity was made in the positive electrode and filled with a 1:1.5 mixture of NaCl and carbon powder. The voltage was 120 V, the current 3.5 - 4.0 A. We tried to maintain these conditions so as to have the possibility of comparing the new results with those obtained earlier.

The investigation was carried out as follows: A very narrow beam of light was passed through the discharge axis at various distances from the cathode (greater than 1 mm), and the "hooks" characteristic of the method of anomalous dispersion were photographed. Taking into account the fact that the discharge diameter was practically the same (about 9-10 mm), in all sections, we used the quantity $\int_0^l N\,dl$, obtained directly from measurements of

the "hook" photographs, as the characteristic of the change in concentration along the discharge axis. The total electrode gap was 9 mm. Five series of such photographs were taken. The average results are presented in Figure a, where the distribution of atoms is shown with respect to a certain maximum value ($\int_0^l N\,dl = 10^{15}$), observed at a distance of 1 mm from the cathode. The diameter of the light beam traversing the arc was about 1 mm: consequently, we could not sucessfully approach the cathode to within less than 1 mm. However, even at a distance of 2 mm from the cathode (1/5 the total length of the electrode gap), the concentration of sodium atoms begins to increase considerably (as much as threefold). A similar growth in the concentration around the cathode was found by Alekseev [3] by the emission method for a sample tamped into the anode.

After having obtained the results cited, we investigated the radial distribution of atoms over a discharge section located 2mm from the cathode. The method of computing the radial distribution was similar to that used previously [1].

The distribution in this section, obtained as the average of 8 photographs, is shown in sketch b. The maximum sodium atom concentration was 1.4×10^{15} cm^{-3} at a distance of 1.5 mm from the axis of the discharge. Starting from this concentration, we can, on the basis of measurements of the vertical distribution (see sketch a) estimate the maximum concentration in the middle section as being equal to approximately 0.5×10^{15} cm^{-3}. For this concentration, the radial distribution of atoms over the middle section of the arc is shown by a curve taken from [1] (see sketch c). We consider such borrowing to be completely legitimate since the arc conditions in the previous and present works are sufficiently identical. Comparing the two distributions (sketches b and c), we see that if there is a characteristic reduction in the concentration of atoms toward the discharge axis for the middle section, then the distribution near the cathode is considerably more homogeneous over the section as a whole. Such a result is conceivable on the basis of conclusions obtained previously [1]: as the total concentration of atoms increased, their radial distribution becomes more homogeneous.

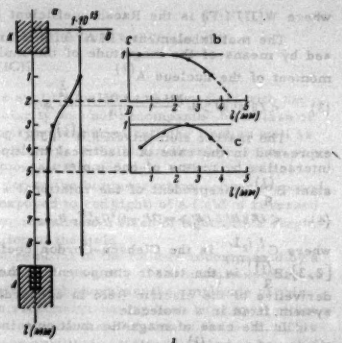

A - anode; K - cathode $B\int_0^l N\,dl$, $C = \frac{N(r)}{N(r=1.5)}$

$D = \frac{N(r)}{N(r=2.5)}$

a. Distribution of concentration along axis of discharge

b. $N(r=1.5) \approx 1.4 \times 10^{15}$ cm^{-3}; c: $N(r=2.5) \approx 0.5 \times 10^{15}$ cm^{-3}.

V. P. Sigov took part in the experimental work.

July 25, 1958

References

1. E. I. NIKONOVA, V. K. PROKOF'EV: OiS, 4, 144 (1958)
2. A. EBERHAGEN: Z. Phys., 143, 312 (1955)
3. M. A. ALEKSEEV: Uch. Zap. Iakutsk. Univ., No. 1, 17 (1957)

TOM VI, Vyp. 2 OPTIKA I SPEKTROSKOPIIA Fevral', 1959
VOL. VI, No. 2 OPTICS AND SPECTROSCOPY February, 1959

On the Hyperfine Structure of the Rotational Spectra of Molecules of the Symmetric Rotor Type

K. K. SVIDZINSKII

In order to calculate the hyperfine structure of rotational spectra of molecules, it is expedient to represent the interaction energy of the nucleus with the electric and magnetic fields of the molecules as the scalar product of the so-called irreducible tensor operators.

$$(1) \qquad \mathcal{H}_1(IJ) = [A^{(l)}(I) \cdot B^{(l)}(J)] = \sum_m (-1)^m A^{(l)}_m B^{(l)}_{-m}$$

The components of the irreducible tensor of the l-th rank A^l_m or B^l_m are transformed according to the irreducible representation of the rotation group of three dimensional space, i.e., have the same angular dependence as do the spherical functions $Y_{lm}(\theta, \phi)$ [1].

Using the formula of Racah and Eckart-Wigner [1], the general matrix element $\mathcal{H}_l$ calculated in terms of rotational wave functions of the molecules of symmetric rotor type can be represented as

$$(2) \qquad \langle JKIF|\mathcal{H}_l|J'K'IF\rangle = (-1)^{I+J-F} W(JIJ'I; Fl) \times \langle I\|A^{(l)}\|I\rangle \langle JK\|B^{(l)}\|J'K'\rangle,$$

where W(JIJ'I:Fl) is the Racah coefficient [1,2].

The matrix element $\langle I \| A^{(l)} \| I \rangle$ is expressed by means of the magnitude of the multipole moment of the nucleus $A^{(l)}$

$$\langle I \| A^{(l)} \| I \rangle = \frac{\|(2I+1+1)!\,(2I-l)!\|^{\frac{1}{2}}}{(2I)!}\, A^{(l)}. \quad (3)$$

The matrix element $\langle JK \| B^{(l)} \| J'K' \rangle$ is expressed in the case of electrical multipole interaction by means of one molecular constant $B_q^{(l)}$ independent of the rotational state

$$\langle JK \| B^{(l)} \| J'K' \rangle = (2J'+1)^{\frac{1}{2}} C^{J'l}_{K'q-K'}\, B_{q-K'}^{(l)}, \quad (4)$$

where $C^{l_1 l_2 L}_{m_1 m_2}$ is the Clebsch-Gordon coefficient [2,3]; $B_q^{(l)}$ is the tensor component of the l-th derivative of the electric field in a coordinate system fixed in a molecule.

In the case of magnetic multipole interaction, $\langle JK \| B^{(l)} \| J'K' \rangle$ is expressed by means of two molecular constants $D^{(l+1)}$ and $D^{(l-1)}$ which characterize the magnetic field in a fixed molecule.

$$\langle JK \| B^{(l)} \| J'K' \rangle = [J(J+1)(2J+1)(2J'+1)(2l+1)]^{\frac{1}{2}} \times$$
$$\times [W(J'l+1J1;\, Jl)\, C^{J'l+1J}_{K'q-K'} D^{(l+1)}_{q-K'} + W(J'l-1J1;\, Jl)\, C^{J'l-1J}_{K'q-K'} D^{(l-1)}_{q-K'}] \quad (5)$$

A result is obtained for a magnetic dipole interaction ($l=1$) which is rather different from the Henderson result [4]. A comparison of these results shows that the quantities a and b, introduced by the author mentioned as molecular constants, actually depend on J as follows:

$$a = 3\left(\frac{J+1}{2J-1}\right)^{\frac{1}{2}} D_0^{(1)};$$
$$b = D^{(0)} - \left(\frac{J+1}{2J-1}\right)^{\frac{1}{2}} D_0^{(1)}, \quad (6)$$

which, apparently, should explain the dependence of these constants on the rotational state, noted in [5,6].

The matrix element for spin-spin interaction of nuclei with spins I_1 and I_2 in the addition scheme $J+I_1=F_1$, $F_1+I_2=F$ is

$$\langle JKI_1F_1I_2F \| \mathcal{H}(I_1I_2) \| J'K'I_1F_1'I_2F \rangle = (-1)^{F_1+I_1-F+1} W(F_1I_2F_1'I_2;\, F_1) \times$$
$$\times [I_1(I_1+1)(2I_1+1)I_2(I_2+1)(2I_2+1)(2F_1+1)(2F_1'+1)5]^{\frac{1}{2}} U \begin{pmatrix} I_1I_1 & 1 \\ JJ & 2 \\ F_1F_1' & 1 \end{pmatrix} \times$$
$$\times (2J'+1)^{\frac{1}{2}} C^{J'2}_{K'q-K'} R^{(2)}_{q-K'}(I_1I_2), \quad (7)$$

where g_1 and g_2 are the g-factors of the nuclei 1 and 2. The irreducible tensors $R_q^{(2)}$ consists of the tensor component

$$R_{rs} = -3r^{-5}\left(r_r r_s - \frac{1}{3} r^2 \delta_{rs}\right),$$

where $\vec{r}$ is the difference of the vectors of the first and second nuclei ($\vec{r}=\vec{r}_1-\vec{r}_2$). The quantity U is an algebraic function of 9 of its arguments and is a generalization of the Racah coefficient to the case of "over-coupling" of four moments [7].

When the nucleus is on the axis of symmetry of the molecules, all the tensor components of the molecular constants of type $D_q^{(l)}$ are zero with the exception of those components for which q=0. In conformance with this, the interaction energy of such a nucleus must be diagonal in K. The interaction energy of a nucleus not on the axis, has matrix elements which are not diagonal in K, consequently, reduction of the degeneracy in K can occur in a first approximation of perturbation theory (over the rotational states). Thus, for example, the degeneracy for |K|=1 in the NH_3 case is reduced not only because of the spin-spin interaction of protons with the nitrogen and the spin-orbital interaction of the protons, as has been shown in [5], but also because of the spin-spin interaction of the protons.

The magnitude of the splitting for |K|=1 for the spin-orbital interaction is

$$\Delta E_{|K|=1} = 2E \frac{3J(J+1)\,|D_0^{(1)}|}{|3-J(J+1)|\sqrt{6}\,D_0^{(1)} + J\sqrt{2}\,(J+1)(2J-1)D^{(0)}|}, \quad (8)$$

where E is the shift of the level JK=1IF, specified by the interaction under consideration. In ordinary tensor notation

$$|D_0^{(1)}| = \frac{1}{2}\sqrt{(D_{xz}-D_{yy})^2 + 4D_{xy}^2}; \quad D_0^{(1)} = \frac{1}{\sqrt{6}} D_{zz}. \quad (9)$$

In the case of quadrupole and spin-spin interaction $\Delta E_{K=1}$ is also described by (8) in which there are the energy E and the constants for the appropriate interaction (where $D^{(0)}=0$).

July 28, 1958

References

1. G. RACAH: Phys. Rev., 62, 438 (1942)
2. A. SIMON, J. H. VANDERSLUIS, L. C. BIEDENHARN: Tables of the Racah Coefficients. USAEC Report ORNL 1679, 1954
3. E. U. CONDON, G. H. SHORTLEY: The Theory of Atomic Spectra, N.Y. Macmillan, 1935 (IL, Moscow, 1949)
4. R. S. HENDERSON: Phys. Rev., 74, 107 (1948)
5. G. R. GUNTHER-MOHR, R. L. WHITE, A. L. SCHAWLOW, W. E. GOOD, D. K. COLES: Phys. Rev., 94, 1184 (1954)
   G. R. GUNTHER-MOHR, C. H. TOWNES, J. H. VAN VLECK: Phys. Rev., 94, 1191 (1954)
6. J. P. GORDON: Phys. Rev., 99, 1253 (1955)
7. A. ARIMA, H. HORIE, Y. TANABE: Progr. Theor. Phys., 11, 143 (1954)

TOM VI, Vyp. 2 OPTIKA I SPEKTROSKOPIIA Fevral', 1959
VOL. VI. No. 2 OPTICS AND SPECTROSCOPY February, 1959

On Electroluminescent Phenomena When a Electric Field is Switched On and Off

A. M. BONCH-BRUEVICH

1. An investigation of the electroluminescence which arises from a nonsinusoidal voltage gives important information about the mechanism of the phenomenon [1-3]. Usually a periodic sequence of rectangular, sawtooth, trapezoidal or exponential pulses is used and the investigations are conducted in the steady state. As observed by several authors, a change in the frequency of pulse alternation, in their length or in the parameters of the wave front is accompanied by a change in the form of the observed luminescence pulses [3-7]. Of special interest to us were observations of pulses of electroluminescence corresponding to a single application and removal of the electric field [8]. For this purpose a thyratron circuit was used which allowed the field on the electroluminescent cells (flat condensers with thicknesses of the order of 0.01 mm filled with the luminous phosphor ZnS-CuA1 in cable oil) to increase or decrease rapidly or to change polarity suddenly. * The rise time did not exceed one microsecond and the length of the step could be varied within broad limits. For observation of the luminescence pulses and the current pulses, ENO-1, SI-1 and OK-17M oscilloscopes were used (depending on the lengths of the pulses).

2. The flash of luminescence which is observed when a field is applied depends substantially on the state of the electroluminescent phosphor. Preliminary exposure to red light (200 watt incandescent lamp, KS-14 light filter) leads to the absence of a flash (in every case, in our experiments, its amplitude did not exceed 0.001 times the amplitude of the flash upon application of the field in the steady state). As the time interval increased between the moment of cutting off the illumination and of application of the field (for this, the luminous phosphor was placed in the dark), the amplitude of the flash increased slightly; the amplitude of the flash was about 0.01 times the steady state value for a time interval of about 5 minutes at $T = 300^\circ$ K. Successive applications were accompanied by an increase in the amplitude of the flashes of luminescence and the steady state was built up after 3 - 5 cycles of the field. If, after the steady state had been built up, the sample was held without a field for several minutes, the flash which is observed with a single application of the field, again was shown to be somewhat smaller than the steady state value.

The application of a two-step field with the same polarity was not accompanied by a flash of light upon application of both the first as well as the second step, if the luminescent phosphor was initially exposed to red light. Finally, initial application to the luminescent condenser (exposed or not exposed to red light) of a field of reversed polarity, stimulated a flash of light with a single application of the field.

The removal of the field is accompanied by a light flash independently of the initial exposure of the luminescent phosphor; the amplitude of this flash is stationary, having been built up at either the first or second application of the field. This stationary amplitude or steady state has been built up much faster than the steady state amplitude of the light flashes which occur upon application of the field. The duration of the pulses in our experiments was not less than several tenths of a second, and an increase was not accompanied by a noticeable change in the character of the build up of the amplitude of the flash of light. The processes which were observed proceeded equally well in the blue as well as in the green band of radiation of the luminescent phosphor.

3. We attempted to compare the duration of the flash of light with the duration of the current pulses in the supply circuit of the electroluminescent condenser. The duration of the current pulses which we observed did not exceed 10^{-6} sec., and we did not succeed in observing any current pulse processes with durations of the same order of magnitude as the duration of the luminescence pulses. If such processes also took place, then their level was less than several tenths of a percent of the level of the high-speed process. It is possible that the essential difference between the duration of current pulses proceeding in the supply circuit of the electroluminescent condenser and the length of the light pulses may be interpreted as an indication that the kinetics of the light corresponds to the rate of the recombination processes in luminescent phosphors. (In contrast to this, several authors connect the kinetics of the luminescence with the kinetics of the build up of the space charge and estimate the build up of the polarization field to be 700 μsec [4]). However, in order to make such an important conclusion, it is necessary to increase the accuracy of observation of the possible relatively slow processes in the current pulses.

4. The described effect of the preliminary exposure of the luminescent phosphor confirms the important role of the electrons (holes) stored in local levels in the mechanism of electroluminescence [9]. The differences in the characters of the growth of the amplitude of the pulses corresponding to when the electric field was applied and removed, can be explained

* The basic measurements were made by O. S. Marenkov.

qualitatively as follows. Upon a single application of the electric field to the initially luminescent phosphor, centers of luminescence are ionized and the liberated electrons are retained in a region far from the ionized centers where they are distributed in bound states. After removing the external potential difference, part of the electrons, localized on relatively shallow bound states, is rapidly returned by the polarization field to the region of the ionized luminescent centers. Also, at the same time a number of luminescent centers is ionized in the region of the first concentration of electrons. As a result a large flash occurs upon removal of the field and conditions are prepared for a light flash with the next application of the field. Successive applications and removals are accompanied by a rise in the number of ionized luminescent centers in the region of the first concentration of electrons although the steady state distribution of electrons and holes is not built up. It does not correspond to the steady state distribution at a given temperature in the absence of the ionizing agent, the field. This is indicated by the decrease we observed in the amplitude of the flash of luminescence corresponding to a single application of the field after the steady states had been attained and then the luminescent phosphor was held without the field for several minutes. The state established under the action of the field relaxes for a comparatively long time and apparently connected with this is the comparatively large amplitude of the light pulse upon application of the field after a preliminary supply of the opposite field to the condenser.

The qualitative reasoning presented here is wanting in accuracy. One may think that the development of the investigation of the kinetics of luminescence for a single excitation, the character of the build up of the steady state and the detailed elucidation of the conditions under which luminescence is observed at the first application of the field would be useful to the elucidation of the mechanism of electroluminescence.

July 28, 1958

References

1. G. DESTRIAN, H. F. IVEY: Proc. IRE, 43, 1911 (1955)
2. P. ZALM, G. DIEMER, H. A. KLASENS: Phillips Res. Rep., 9, 81 (1954)
3. I. N. ORLOV, I. IA. LIAMICHEV: Trudy, NII MRTP (edited by Deviatkov), No. 9, 3 (1957)
4. S. NUDELMAN, F. MATOSSI: J. Electrochem. Soc., 101, 546 (1954)
5. J. F. WAYMOUTH, F. BITTER: Phys. Rev., 95, 941 (1954)
6. D. HAHN, F. W. SEEMAN: Zs. Phys., 149, 486 (1957)
7. A. N. GEORGOBIANI, M. V. FOK: Doklad na VII Soveshchanii po liuminestsentsii (Report to the VII Conference on luminescence) Moscow, 1958
8. I. IA. LIAMICHEV: Trudy, VII Soveshchaniia po liuminestsentsii (Transactions, VII Conf. on luminescence) Moscow, 1958 (in press)
9. C. H. HAAKE: JOSA, 47, 881 (1957)

TOM VI, Vyp. 2 OPTIKA I SPEKTROSKOPIIA Fevral', 1959
VOL. VI. No. 2 OPTICS AND SPECTROSCOPY February, 1959

Influence of an Additional Impurity on Impurity Absorption and Luminescence Spectra of Molecular Crystals

A. V. SOLOV'EV

The recently detected variability of the luminescence spectra of molecular crystals [1], and some other peculiarities of the absorption and luminescence of impurities in molecular crystals [2] have been connected with defects of various kinds in crystal lattices. Considering the fact that distortions of the crystal lattice arise from introduction of impurities, we introduced into the crystal under investigation an additional impurity in order to effect an additional distortion of the crystal lattice. With the increase of the concentration of the impurity one expects an increase of distortion in the lattice which manifests itself in the spectrum of the impurity dissolved in the crystal.

We studied the change in the absorption and luminescence spectra of naphthacene dissolved in a crystal of dibenzyl [3] resulting from the introduction of an additional impurity of stilbene. The concentration of stilbene in the impure naphthacene-dibenzyl crystal was gradually increased. The concentration of naphthacene in the dibenzyl crystal remained unchanged.

Fig. 1. Absorption spectra of naphthacene in a crystal of dibenzyl (a) and of naphthacene in a crystal of dibenzyl with added stilbene (b, c, d, e) The concentration of stilbene increases from b to d. The broad bands which appear are marked by arrows. The spectra were obtained using light polarized parallel to ong axis of the dibenzyl crystals, which were cooled to 20° K.

As is known, the absorption regions of stilbene, naphthacene and dibenzyl occur in different parts of the spectrum [2,3].

It has been found that with small concentrations of stilbene the strong lines in the absorption spectrum of naphthacene become broad and diffuse with increasing concentration of stilbene, while the weak lines disappear (fig. 1, b,c). The lines lying close to the strong lines on the low frequency side gain in intensity, while those on the high frequency side get weaker. With high concentrations of stilbene (not less than 5-10^{-2}/o) a series of broad bands (fig. 1, d,e) appears between the spectral bands of naphthacene. At the same time the intensity of the naphthacene bands is decreasing. The wide bands are similar in appearance and polarization to the bands of the absorption spectrum of naphthacene in stilbene [3] displaced by 400 cm^{-1} toward higher frequencies. Apparently the broad bands appearing in the spectrum correspond to the absorption spectrum of those molecules of naphthacene whose close neighbours are stilbene rather than dibenzyl molecules.

The luminescence spectra in all cases mirror the changes which occur in absorption spectra. (see fig. 2).

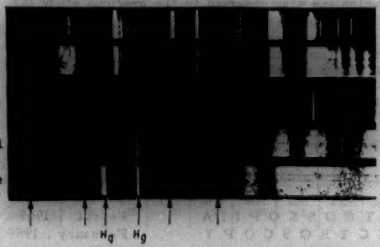

Fig. 2. Luminescence spectra of naphthacene in a dibenzyl crystal (a) and of naphthacene in a dibenzyl crystal with stilbene impurity (b,c,d,e). The concentration of stilbene increases from b to d. The broad bands which appear are marked by arrows. The spectra were obtained with crystals cooled to 20°K. The Hg-radiation used for the excitation of luminescence was produced by SVD Sh-1000 lamps.

Thus the influence of an additional impurity on the absorption and luminescence spectra of naphthacene in dibenzyl is different for small than for large concentrations of stilbene. The influence of small concentrations of stilbene on the naphthacene molecule is due to the fact that the position of the dibenzyl molecule in the crystal lattice is disturbed by the intrusion of foreign molecules of stilbene. In larger concentrations of stilbene, there is probably a direct interaction of the molecules of the impurity on each other. With this assumption one can explain the pecularities in the absorption spectrum of stilbene in a dibenzyl crystal [4], since at larger concentrations of stilbene (5°/o) its spectrum is similar to the absorption spectrum of pure stilbene. The reason could be that the molecules of stilbene are not uniformly distributed in the dibenzyl crystals but lie in groups. Thus some of the stilbene molecules are surrounded not by dibenzyl, but by stilbene molecules, and this causes a change in the spectrum. X-ray investigations [5] have confirmed the non-uniformity of distribution of the stilbene impurity in the lattice of dibenzyl.

Detailed data about these studies and similar studies of other molecular crystals will be published later.

July 29, 1958

References

1. A. F. PRIKHOT'KO, I. IA. FUGOL': OiS, 4, 335 (1958)
2. A. F. PRIKHOT'KO, M. T. SHPAK: OiS, 4, 17, 30 (1958)
3. A. F. PRIKHOT'KO, A. V. SOLOV'EV: Ukr. Fiz. Zh. (in press)
4. A. F. PRIKHOT'KO, M. T. SHPAK: Materialy X Vsesoiuznogo Soveshchaniia po Spektroskopiia (Proceedings of the X All-Union Conf. on Spectr.) L'vov Univ. Press, 1957
5. A. I. KITAIGORODSKII: Kristallografiia, 2, 456 (1957) (See Sov. Phys. Crystallography)

TOM VI, Vyp. 2 OPTIKA I SPEKTROSKOPIIA Fevral', 1959
VOL. VI. No. 2 OPTICS AND SPECTROSCOPY February, 1959

Microwave Spectrum of the $FH_2C\text{-}CH_2Cl^{37}$ Molecule

I. A. MUKHTAROV

The microwave spectrum of the $FH_2C\text{-}CH_2Cl^{35}$ molecule has been described in previous papers [1]. It is also of interest to study the microwave spectrum of the molecule $FH_2C\text{-}CH_2Cl^{37}$, whose absorption line for a natural mixture of chlorine isotopes is weaker in intensity than that for molecules with the Cl^{35} isotope.

Absorption lines of the rotational transitions $1_{01} - 1_{10}$, $2_{02} - 2_{11}$, $3_{03} - 3_{12}$, $4_{04} - 4_{13}$ and $5_{05} - 5_{14}$ of the $FH_2C\text{-}CH_2Cl^{37}$ molecule have been observed and identified. These lines correspond to the gauche-isomer with the azimuthal angle $\alpha = 70^0$ (α is the angle between the projections of the C-F and C-U bonds on a plane perpendicular to the C-C axis).

Values of the quadrupole bond constant have been determined from the hyperfine structure of the rotational transition of the $1_{01} - 1_{10}$ line in the directions of the principal axes of the $FH_2C\text{-}CH_2Cl^{37}$ molecule, namely: $\chi_a = -17.6$ mc, $\chi_b = -6.1$ mc and $\chi_c = 23.7$ mc. The magnitudes of A-C and χ (the asymmetry index) have been determined from the observed rotational transitions $1_{01} - 1_{10}$ and $2_{02} - 2_{11}$: A-C = 10744.55 mc, $\chi = -0.9262$.

Starting from the values found for A-C and, values of the absorption line frequencies were calculated for other transitions of the Q-branches.

The following table lists both the experimental values of the Q-branch line frequencies and the values calculated from the A-C and χ figures given above.

Transition	Frequency (in mc) Experimental	Calculated
$1_{01}-1_{10}$	10744.55	-
$2_{02}-2_{11}$	11152.15	-
$3_{03}-3_{12}$	11784.5	11784.7
$4_{04}-4_{13}$	12665.0	12666.3
$5_{05}-5_{14}$	13825.4	13828.1

There is a noticeable disagreement between the experimental and calculated values of the absorption line frequencies. This difference is related to the influence of a centrifugal perturbation, which was also observed in the previous study [1].

August 1, 1958

References

1. I.A. MUKHTAROV: DAN USSR, 115, 486 (1957) (See Soviet Physics, Doklady) IAN USSR, Ser. fiz., 22, 1154 (1958) (See CTT Bulletin, 22,)

TOM VI, Vyp. 2 OPTIKA I SPEKTROSKOPIIA Fevral', 1959
VOL. VI. No. 2 OPTICS AND SPECTROSCOPY February, 1959

Microwave Excitation of Spectra of Gaseous Mixtures

A. A. VASHMAN, L. V. LIPIS and N. A. TETERINA

In the spectroscopic analysis of gases, the high frequency electrodeless gaseous discharge is widely employed. Usually the high frequency generators employed do not have frequency regulation; the range of frequencies of the applied sources lies between 5 and 30 megacycles. In spite of the undisputed advantages of the electrodeless discharge, the chief of which is the absence of internal electrodes, it does not avoid, in this range of frequencies, noticeable absorption and emission of gases by the wall of the discharge tube. This deficiency fundamentally is linked with the strong and nonuniform heating of the discharge tube. Moreover, only an insignificant part of the power of the generator, working in the above-mentioned frequency range is spent in the excitation of the gas to be analyzed.

Regrettably, the question of the influence of the generator frequency on the excitation of the analytical lines and on the character of the gaseous discharge still is insufficiently studied. The application of generators operating in the centimeter region is of great promise as shown in references [1] - [6].

In the present communication some data are given on the use of a magnetron generating oscillations at a frequency of 3000 megacycles for the excitation of spectra of gaseous mixtures. The diagram of the generator is shown in Figure 1. The magnetron, operating continuously, has the following parameters: $U_a = 4150$ V, $I_a = 50$-70 mA, $U_H = 6.3$ V, B = 1200 gauss.

For the protection of personnel from microwave radiation, the terminations of the waveguide and the cathode outlets of the magnetron are screened by means of metal netting. The gas to be analyzed is excited in a quartz discharge tube, inserted into the waveguide at the place of an antinode of the electromagnetic wave. In the side wall of the wave guide a slot is cut out for the passage of light into the spectroscopic apparatus.

With the help of this generator, the argon-helium gaseous mixtures in the discharge tube were investigated at pressures from 20 to 0.3 tor. The experiments showed that intensities of the spectral lines of the gas are increased for excitation by a frequency of 3000 megacycles as compared to excitation by a frequency of 6 megacycles.

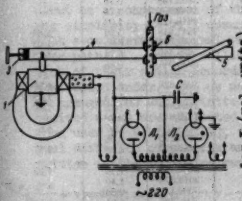

Fig. 1 Diagram of the Microwave Generator

(1) Magnetron; (2) magnet (B = 1200 gauss (3) insulated piston; (4) waveguide; (5) non-reflecting load; (6) discharge tube with the gas to be analyzed; capacity of the filter C = 4μF voltage (V = 6 k V); L_1 and L_2 are gas rectifiers VG-129.

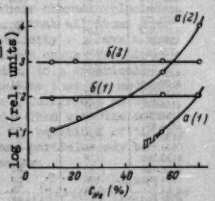

Fig. 2 Graph showing the logarithm of the intensity of helium lines (a) and argon lines (b) versus the helium concentration.
(1) Excitation of the gas by a generator with a frequency of 6 mc.; (2) excitation of the gas by a 300 mc generator.

In the table are listed the intensities of various lines of the spectra of pure helium, pure argon, and a 50% helium-50% argon mixture excited by means of the generator with a frequency of 3000 megacycles (I_m), referred to the intensities of the corresponding lines with the excitation of spectra by the generator VG-2 with a frequency of 6 megacycles (I_v). Spectra were excited at the optimal pressure of the gas in the discharge tube, which corresponds for pure helium to 6 tor, for pure argon to 0.5 tor and for a 50% helium-50% argon mixture to 0.5 tor.

Finally, the temperature of the wall of the quartz discharge tube during work with the generator VG-2 (f = 6 mc.) attains 300-400°, while during work with the magnetron generator (f = 3000 mc.) its temperature does not exceed 40-50°. On analysis of the argon-helium mixture in a discharge tube with 4 mm. diameter, the λ = 5875 A° line of helium attains noticeable intensity only for concentrations of helium not less than 50% for excitations at 6 megacycles; and for excitation at 3000 megacycles its intensity is considerable, beginning with a helium concentration on the order of 10%.

In Figure 2 is shown the change of the logarithm of intensity of the λ = 5875 A° line of helium and of the λ = 5888 A° line of argon versus the helium concentration in the mixture for excitation of the gas mixture. Thus, by exciting the gas mixture with the help of the 3000 megacycle generator, it is possible to raise significantly the concentration sensitivity of the analysis of helium in a mixture with argon. Results from investigations of the excitation of spectra of binary and ternary gas mixtures with the help of a high frequency generator and analytical applications will be presented in subsequent communications.

August 10, 1958

Pure He, p = 6 tor

λ (in Å) ..	5875	5015	4920	4713	4471	4387	4020	3888
I_M/I_V ..	20	25	20	10	20	20	20	10

Pure A, p = 0.5 tor

λ (in Å) ..	5912	5888	4702	4628	4598	4522	4510
I_M/I_V ..	3	3	4	4	3	4	4

50% He and 50% A mixture, p = 0.5 tor

λ (in Å) ..	5875	5888	4702	4620	4594	4522	4510	4471
I_M/I_V ..	10	4	5	5	5	5	9	4

References

1. E. JACOBSEN, G. R. HARRISON: JOSA, 39, 1054 (1949)
2. W. F. MEGGERS, F. O. WESTFALL: J. Res. Bur. Stand., 44, 447 (1950)
3. A. T. FORRESTER, R. A. GUDMUNDSEN, P. O. JOHNSON: JOSA, 46, 339 (1956)
4. M. ZELIKOFF, P. H. WYCKOFF: L. M. ASCHENBRAND, R. S. LOOMIS: JOSA, 42, 818 (1952)
5. F. S. TOMKINS, M. FRED: JOSA, 47, 1087 (1957)
6. L. ROVEY: Spectrochim. Acta, 432 (1958) 10,

TOM VI, Vyp. 2 OPTIKA I SPEKTROSKOPIIA Fevral', 1959
VOL. VI. No. 2 OPTICS AND SPECTROSCOPY February, 1959

Isotopic Shift in the Spectrum of Thorium Th^{232} - Th^{229}

E. A. VERNYI AND V. N. EGOROV

Isotopic shifts in the spectrum of thorium were measured with the aid of a sample containing the isotopes Th^{229} and Th^{232} in a 1:1 ratio. Thorium chloride in the form of 50 - 60 μg of solution was deposited on the end of a carbon electrode of 4 mm diameter and sealed in with paraffin. The thorium spectrum was excited in an ac arc operated at a current of 5 amp. The excitation was carried out in a carbon monoxide gas atmosphere in order to suppress the cyanogen bands.

The spectra were recorded on a two-meter spectrograph with a diffraction grating, in a Paschen mounting. The linear dispersion of the instrument was 3.4 Å/mm in the first order, at which a light maximum occurred. The sample spectra were photographed several times with 20 sec. exposures until the thorium lines vanished completely. This permitted spectra to be obtained which had different intensities, and the isotopic shifts could be measured for both the weak and the strong lines.

The isotopic shifts were detected for a significant number of lines (more than 250) in the 2600-4400 Å range. The results of measurements for 76 lines, for which the shifts were more clearly observed, are presented in the table. Given in the same table are the ratios of the shifts $\Delta\sigma(232-229)/\Delta\sigma(232-230)$ which characterize the even-odd effect. The values of the isotopic shifts between the Th^{232} and Th^{230} lines are taken from Stukenbroeker and McNally [1]. As is seen from the tabular data, this ratio is within 1.6 - 1.8 limits for the majority of lines, which is in agreement with the general character of the even-odd shifts for heavy elements [2-4]. This quantity is somewhat larger for certain lines, where the deviation exceeds the measurement error. The reasons for this have not yet been clarified.

λ(in Å)	Δσ (232–229) (in cm⁻¹)	Δσ (232–229) / Δσ (232–230)	λ (in Å)	Δσ (232–229) (in cm⁻¹)	Δσ (232–229) / Δσ (232–230)
4391.114	0.80	1.54	3852.168	0.76	—
4382.044	0.50	1.51	3849.251	0.76	—
4381.859	0.44	—	3848.422	1.02	—
4277.322	0.89	1.62	3847.648	0.86	1.83
4276.814	0.58	—	3842.249	0.80	1.80
4273.363	0.80	1.58	3839.449	0.76	1.85
4270.332	0.75	—	3835.944	0.68	—
4250.339	0.85	—	3834.584	0.86	—
4229.459	0.85	1.44	3832.626	0.79	1.55
4178.084	0.57	1.46	3435.979	1.13	1.82
4159.667	0.61	1.61	3184.898	1.12	1.58
4156.523	0.63	1.54	3179.047	0.98	—
4149.991	0.54	1.63	3174.166	1.17	1.67
4132.751	0.60	—	3169.279	1.06	—
4131.433	0.93	—	3049.053	1.30	1.67
4123.569	0.78	—	3045.568	0.91	—
4108.428	0.75	1.87	3034.069	1.10	1.69
4104.392	0.98	1.58	3019.378	1.40	—
4094.751	0.84	1.79	3009.725	0.94	—
4086.520	1.14	1.61	3002.390	1.04	1.51
4085.036	0.70	1.67	3001.264	1.28	1.58
4036.567	0.84	1.47	2988.234	1.27	1.82
4025.158	0.75	1.44	2974.013	1.06	1.63
4019.137	0.61	1.49	2972.224	0.82	—
3988.015	0.78	1.56	2971.482	1.21	—
3981.110	0.76	1.52	2968.585	1.05	1.68
3978.418	0.72	1.80	2957.591	1.33	1.75
3945.825	0.95	1.76	2928.256	1.20	1.71
3937.043	0.65	1.67	2919.842	1.16	1.97
3932.230	0.67	1.56	2917.390	1.18	1.84
3927.425	0.66	1.53	2898.359	1.42	—
3927.181	0.80	1.82	2895.143	1.09	—
3905.190	0.67	1.81	2891.254	1.36	—
3904.089	0.98	1.78	2885.045	0.97	1.70
3734.801	1.14	1.48	2884.295	1.17	1.72
3730.753	0.81	1.76	2737.418	1.33	—
3723.291	0.77	1.71			
3711.309	0.69	1.82			
3706.769	0.80	1.68			
3659.513	0.85	1.98			

The values of the isotopic shifts between the Th^{232} and Th^{230} lines are taken from Stukenbroeker and McNally [1]. As is seen from the tabular data, this ratio is within 1.6 - 1.8 limits for the majority of lines, which is in agreement with the general character of the even-odd shifts for heavy elements [2-4]. This quantity is somewhat larger for certain lines, where the deviation exceeds the measurement error. The reasons for this have not yet been clarified.

The spectra of samples with a 1:1 and 1:20 ratio of Th^{229} and Th^{232} were also photographed on an auto-collimation diffraction grating spectrograph (DAS) in the fifth order. The linear dispersion was 0.92 A/mm for λ 4019.137 Å and 0.815 A/mm for λλ 4381.859 and 4391.114 Å. Broadening of the Th^{229} lines was observed at the λλ 4019.137, 4273.363, 4382.044 and 4391.114 Å lines because of the hyperfine structure (HFS). The instrument did not provide complete resolution of the HFS component. The HFS width for these lines is approximately 0.3 - 0.4 cm^{-1}.

The investigation of isotopic shifts and of HFS in Th^{229} is continuing.

The authors are grateful to V. K. Markov and M. F. Koringskii for separation and purification of the Th^{229} compound.

August 30, 1958

References

1. G. L. STUKENBROEKER, J. R. MC NALLY, Jr. JOSA, 43, 36 (1953)
2. J. G. CONWAY, M. FRED: JOSA, 43, 216 (1953)
3. T. E. MANNING, C. E. ANDERSON, W. W. WATSON: Phys. Rev., 78, 417 (1950)
4. D. D. SMITH, G. L. STUKENBROEKER, J. R. MC NALLY, Jr.: Phys. Rev., 84, 383 (1951)

TOM VI, Vyp. 2 OPTIKA I SPEKTROSKOPIIA Fevral', 1959
VOL. VI. No. 2 OPTICS AND SPECTROSCOPY February, 1959

On the Question of Mutual Diffusion of Photons and Particles

B. A. VEKLENKO

We have found previously [1] a Green's function of the integral equation, which describes the distribution of atoms radiating in an infinite space. At the time, in accord with other work [2,3] it was supposed that the intrinsic velocity of the radiating particles is zero. On the other hand, upon study of the distribution of the metastable atoms, it is assumed [4] that the optical lifetime of the metastable state is infinite. In nature, strictly speaking, an intermediate case is always

present. Therefore it seemed to us expedient to study the mutual diffusion of photons and particles and to ascertain its basic regularities. At the same time, we succeeded in obtaining criteria which allow one to determine the physical conditions under which one or the other of the mechanisms of transfer may be neglected.

Let the intrinsic motion of the atoms be brought about as a consequence of their thermal velocities. For simplicity we will assume that all atoms move with some average thermal velocity v, have a mean free path λ, and on collision change the direction of their motion according to a spherical scattering index. Let us assume that the medium is homogeneous and infinite. Collisions between excited atoms are neglected. Then with the notation used by Veklenko [1], the equations of the mutual diffusion of photons and particles may be written in the following manner:

$$\frac{\partial f(r;\,t);\,v}{\partial t} = v\,\mathrm{grad}\,f(r;\,t);\,v + kf(r;\,t);\,v - \frac{1}{(4\pi)^2 k_\nu}\int_0^\infty k_\nu k_{\nu'} f(r';\,t)\,\frac{e^{-k_\nu|r-r'|}}{|r-r'|^2}\,dv'dV$$

$$-\frac{v}{4\pi\lambda_\nu^2} f(r;\,t) = 0. \tag{1}$$

Here $k = \frac{1}{\tau} + \varepsilon + \frac{v}{\lambda}$, $f(r;\,t) = \int f(r;\,t,\,v)\,dv$. The initial conditions are: $f(r;\,t) = \varphi(r)$ when $t = 0$.

The transformation of Ambartsumian [1,5] allows the solution of equation (1) to be obtained in the form:

$$f(r;\,t) = -\frac{e^{-\alpha t}}{(2\pi)^{3/2}}\cdot\frac{\partial}{\partial r}\int_{-\infty}^{\infty} e^{-\frac{1}{2}\rho^2}\exp\left\{-\frac{t}{\tau}|1 - J_{(\rho)}| - D_\tau\rho^2 + \frac{t}{\lambda\tau}\left(\frac{r\rho}{t}\right)^3|1 - J_{(\rho)}|\right\}d\rho, \tag{2}$$

where

$$J_{(\rho)} = \frac{1}{\rho}\int_0^\rho k_\nu\lambda,\ \text{are tg}\,\frac{\rho}{k_\nu}\,dv;\quad D_\tau = \frac{1}{3}\left(\frac{1}{\tau} + \frac{v}{\lambda}\right)\left(\frac{r}{t}\right)^2,$$

r is the modulus of the vector $\vec{r}$.

The solution (2) is not exact: the particle motion considered by us was asymptotic. For $v = 0$, the solution (2) coincides with the expression obtained by Biberman [2]; as $t \to \infty$ it describes the particle motion, the asymptote of which is governed by the normal distribution law.

Let the form of the spectral lines be disperse. If the time τ is sufficiently long, then the asymptotic value of the function $f(r;t)$ may be represented in the following form:

$$f(r;\,t) = \frac{1}{(4\pi D_\tau t)^{3/2}}\exp(-\varepsilon t - 2\gamma^2) + \frac{\lambda e^{-\varepsilon t}}{3\pi r\sqrt{2k_0}\,(8D_\tau t)^{1/4}}\cdot\frac{\partial^3}{\partial r^3}\,\gamma^{\frac{1}{2}} e^{-\gamma^2} I_{\frac{1}{4}}(\gamma^2)$$

$$= f^M(r;\,t) + \Delta f^M(r;\,t). \tag{3}$$

Here $f^M(r;t)$ and $\Delta f^M(r;t)$ are appropriate components

$$\gamma^2 = \frac{r^2}{8D_\tau t};$$

and $I_{\frac{1}{4}}(\gamma^2)$ is the Bessel function with pure imaginary argument of order $1/4$.

The behavior of the functions $f^M(r;\,t)$ and $\Delta f^M(r;\,t)$ may be seen in the figure.

Thus, if the time τ is long, that is, if the photon transport mechanism plays a subordinate role, then the mutual diffusion of photons and particles is governed by the normal distribution law with increment $\Delta f^M(r;\,t)$.

We introduce the integral measure of the deviation of the function $f(r;\,t)$ from $f^M(r;t)$. The quantity

$$\int_0^\infty 4\pi r^2 f(r;\,t)\,dr$$

is the probability of the excited atom being in the region $r > \zeta$;

$$\int_\zeta^\infty 4\pi r^2 f^M(r;\,t)\,dr$$

is the analogous probability for diffusion, determined by the function $f^M(r;t)$. Consequently, the measure of the deviation being sought may be represented in the form

$$\delta = \frac{\int_\zeta^\infty 4\pi r^2\Delta f^M(r;\,t)\,dr}{\int_0^\infty 4\pi r^2 f(r;\,t)\,dr} \tag{4}$$

The point ζ is determined from the equation

$$\Delta f^M(\zeta;\,t) = 0,$$

which leads to the relation

$$\zeta = t\sqrt{8D_\tau t}, \tag{5}$$

where $\xi = 1.25$.

Substituting (5) into (4) taking (3) into account we find

$$\delta = 0.3\frac{\lambda}{\tau\sqrt{k_0 D_\tau^3}}\cdot\frac{1}{t^{\frac{3}{4}}} \tag{6}$$

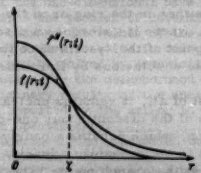

Hence, it follows that the role of diffusion of photons increases with time. For the case of the equality $S \ll 1$, the photon mechanism of transport plays a subordinate role. It should be remembered, however, that as a consequence of the slow character of the decrease of the kernel of (1) there are always distances so large that the distribution function $f(r;\,t)$ will be determined only by photon diffusion.

In a similar manner, one can study also the case of mutual diffusion when the subordinate role is played by particle diffusion.

In conclusion I express my gratitude to L. M. Biberman, who guided the present work to completion.

September 16, 1958

References

1) B. A. Veklenko, ZETF, 33, 817 (1957) (See Sov. Phys. JETP)
2) L. M. Biberman, ZETF, 17, 416 (1947)
3) T. Holstein, Phys. Rev. 72, 1212 (1947)
4) V. A. Fabrikant; DAN SSSR, 19, 385 (1938) (Probably in English)
5) V. A. Ambartsumian: Biull. Erevan Actr. Observ., 6, 3 (1945)

TOM VI, Vyp. 2 OPTIKA I SPEKTROSKOPIIA Fevral', 1959
VOL. VI. No. 2 OPTICS AND SPECTROSCOPY February, 1959

DISCUSSIONS

Apropos the Article by L. A. Borovinskii, "On Conditions for Joining Functions in the One-Dimensional Metal Model of a Molecule"

T. K. REBANE

In his article [1] Borovinskii subjects to criticism the requirement of continuity imposed on a wave function in a branched one-dimensional metal model of a molecule at the nodes of a network of conjugate bonds. He arrives at the conclusion that in a one-dimensional metal model there is no basis to consider the wave function to be continuous at the branch point, as has been done up to now. Without solving the problem of the general form of new conditions for joining the functions at the branch points, Borovinskii proposes these conditions for two particular cases ("a ring with a side piece" and "two rings with a connector"). It must be assumed in both cases that the one-dimensional wave function equals 0 identically either in the ring or on the side piece (connector), where it undergoes a discontinuity at the branch point of the system of conjugate bonds.

These conclusions by Borovinskii call forth objections.

First of all, it remains unclear what is the significance of the discontinuous one-dimensional wave function, which denotes a poorly-defined definiteness in the probability density of finding an electron at the branch point. The single example, cited by Borovinskii to explain the possibility of the occurrence of a discontinuity in the one-dimensional wave function during the passage to the limit from the two-dimensional to the one-dimensional model, causes confusion. Actually, the solution given by Borovinskii of the wave equation for the "ring with the side piece" (see fig. 2 of [1]) is incorrect. It is easy to see that the shape of the contour of the region under consideration does not allow separation of the variables ρ and φ, and consequently, the solution of the wave equation [formulas (8), (9a) and (9b)], constructed under the assumption that the variables are separable, does not satisfy the first of equations (7) on the arc, which is conceived as separating the "side piece" from the ring. Consequently, the Borovinskii conclusion that the two-dimensional wave function "either equals 0 identically on the side piece or equals 0 identically in the ring" is incorrect since it is based on an incorrect solution of the wave equation for the region he considered.

Secondly, the conditions proposed by Borovinskii for joining wave functions of molecules of the biphenyl and benzene radical types simply correspond to the dissociation of the network of conjugate bonds into separate, isolated sections (rings, side pieces and connectors). Borovinskii proposes to construct wave functions for each section independently. Consequently, the conditions he proposed for the joining are certainly not capable of taking into account effects related to the presence of a single system of conjugated π electrons in molecules of the type mentioned.

Thirdly, it should be noted that Borovinskii makes an erroneous deduction from his analysis of the example of the "ring with a side piece" on the basis of the one-dimensional metal model (see fig. 1 of [1]). Passing to the limit, during which the side-piece length approaches 0 and a node of the one-dimensional wave function appears on the ring, the author finds that the result obtained indicates the unsuitability of the continuity condition for the one-dimensional wave function at the branch point. Meanwhile, the appearance of a node of the one-dimensional wave function on the ring is completely unrelated to the condition for joining the functions: it depends solely on the requirement that the one-dimensional wave function vanish at the end of the side piece, where (from the viewpoint of the one-dimensional model) there is an infinite potential barrier. It is natural that this potential barrier appears on the ring as a result of the abovementioned passage to the limit and that it affects the behavior of the wave functions. Consequently, the example being considered has no relation to the question of the conditions for joining functions at the branch point.

It is seen from the above that the requirement to reject the continuity of the one-dimensional wave function at the branch point, proposed by Borovinskii, has not sufficient foundation. Although the problem he formulated of eliminating the inadequacies of the branched one-dimensional metal model of a molecule is unquestionably of interest, the question of means to solve this problem remains open.

May 16, 1958

Reference

1. L. A. BOROVINSKII: OiS, 4, 526 (1958)

TOM VI, Vyp. 2 OPTIKA I SPEKTROSKOPIIA Fevral', 1959
VOL. VI. No. 2 OPTICS AND SPECTROSCOPY February, 1959

More on the Conditions of Joining Functions in the One-dimensional Metal Model of a Molecule

(In Reply to T.K. Rebane[1])

L.A. BOROVINSKII

1. T. K. Rebane regards as incorrect the solution of the wave equation for the "ring with side piece" region in our article [2] on the basis that separation of the variables ρ and φ is not permissible in the problem studied. Separation of variables, however, stems directly from the second equation of the system (7), expressing the conservation of the square of the moment of momentum. Actually, the general solution of the equation shown is as follows:

$$\psi(\rho, \varphi) = Q_1(\rho)\cos\lambda\varphi + Q_2(\rho)\sin\lambda\varphi.$$

On the strength of the boundary conditions imposed upon $\psi(\rho, \varphi)$ on the side walls of the side piece, $Q_1(\rho)$ and $Q_2(\rho)$ differ only by a factor; if the polar axis coincides with the axis of symmetry of the side piece, then either $Q_1(\rho)$ or $Q_2(\rho)$ reduce to 0. This leads to the conclusion regarding separation of the variables. The solutions of the system (7) are inevitably such, that on the line separating the side piece from the ring $\frac{\partial\psi(\rho, \varphi)}{\partial\rho}$ undergoes a discontinuity of the first kind. This actually appears to be a defect in the accepted approximation of the wave function, as was previously noted by the author in a report to the 11th Spectroscopy Conference. The reason for this defect appears to be the utilization of the second of the equations (7). The conclusion regarding the conservation of the square of the moment of momentum is carried over from classical mechanics on the hypothesis that it is approximately valid in the quantum treatment of the problem also. Regardless of the cited assumption, we regard the conclusion about the localization of an electron either in the ring or in the side piece to be approximately correct. We noted that our conclusions have a simple physical meaning. It seems quite impossible that the wave of a π-electron, being propagated, for instance, into the side piece, could also be propagated into the ring. This makes it necessary for the longitudinal wavelength in the side piece to correspond to the transverse dimensions of the ring. This would correspond to very high energy of a π-electron and such states are of no interest. Apparently the wave function of an electron localized, for instance, in the side piece, quickly diminishes upon transition into the ring.

In connection with Rebane's notes regarding the obscurity of the significance of the discontinuous one-dimensional function, it is expedient to dwell in more detail on this problem. The introduction of a one-dimensional wave function to describe the movement of an electron, which actually always is three-dimensional, stems from the hypothesis of the possibility of separating the variables into longitudinal and lateral ones with respect to the direction of the chain of conjugate bonds. It may be assumed that the longitudinal part of the wave function changes relatively slowly in comparison with the lateral part. In the region of the branch point separation of the variables into longitudinal and lateral ones loses its meaning, and therefore the introduction of a one-dimensional wave function also loses its meaning. The representation of a wave function as the product of a longitudinal and lateral function in case of branching of the molecules should be considered as the asymptotic expression of a wave function for portions of the potential well, removed from the branch point. Let the longitudinal part of this asymptotic expression be extrapolated to the region of the branch point, where this expression yields results radically different from the actual values of the wave function. It is clear that at the branch point asymptotic expressions of a wave function in converging branches of conjugate bonds, generally take on different values. It is precisely in this sense that we understand the discontinuity of the one-dimensional wave function.

There arises the problem of determining the relationship between the values of the asymptotic expressions of a wave function in converging branches. This problem may be solved by numerically solving the wave equation for the neighborhood of the branch point. Preliminary results of the analysis of this problem were reported by the author to the XIth Conference on Spectroscopy.

2. Rebane objects to the conclusion emanating from our studies regarding the dissociation of the system of π-electrons of molecules of the biphenyl type into sub-systems, localized on separate parts of the molecules (ring's connectors). In this connection let us mention that experimental data pertaining to biphenyl indicate weak conjugation of the benzene rings and therefore confirm our conclusion. It is known that the central C-C bond in a biphenyl molecule is considerably longer than the C-C bonds in rings, that the absorption frequencies are close to the benzene frequencies and that the anisotropy of the diamagnetic susceptibility differs slightly from the twofold value of benzene anisotropy. Interpretation of a vibrational spectrum of biphenyl [3] also shows that the conjugation of rings in the molecule is weak and that the central bond is an ordinary bond. Hence, the proposed model basically explains the experimental data. At the same time calculations of the spectrum and the distribution of the electron density in biphenyl, performed on the basis of a one-dimensional network model, yield results which disagree with experimental data. As Rebane's calculations indicate [4], the calculated value of the anistropy of diamagnetic susceptibility also appears to be lowered. It stands to reason that examples may be shown of the manifestation of the interaction of π-electrons of one biphenyl ring with π-electrons of another ring: the band shift in comparison with the bands of benzene, reduction in the prohibition of the transaction corresponding to the transition $^1A_{1g} \rightarrow {}^1B_{2u}$ in benzene; the considerable rise in the intensity of this transition, and the deflection of the anisotropy of the diamagnetic susceptibility from the doubled value of

the anisotropy of benzene. More exact theory should take this interaction into account.

3. In Rebane's opinion, the paradoxical result obtained in the "ring with side piece" example studied by us, does not indicate the unsuitability of the conditions for joining the wave functions and appears to be inherent in the one-dimensional model. From the example studied by us, it follows that in a network model with the addition of an infinitely short side piece, the inherent requirement of a continuous change in the state of the electrons is broken. As previously shown by Rebane [5], in the case of molecules without free ends this requirement is also broken when the constant K in the work formula (3) of [2] differs from 0. We cannot agree that a model having the mentioned defect may be considered adequate. By making considerations expressed in [2], more precise, let us mention that this defect is connected not only with conditions for joining wave functions, but generally with the impossibility of describing the movement of π-electrons in branched molecules on the basis of a one-dimensional model. In our opinion, a modified one-dimensional model may be utilized for branched molecules only in order to define the above-mentioned asymptotic expressions of wave functions in two- or three-dimensional models.

July 17, 1958

References

[1] T. K. Rebane, OIB, 6, 266 (1959)
[2] L. A. Borovinskii, OIB, 4, 526 (1958)
[3] M. A. Kovner, OIB, 1, 742 (1956)
[4] T. K. Rebane, Doctoral Thesis, Leningrad Univ., 1958
[5] T. K. Rebane, Vestnik, Leningrad Univ. No. 10, 11 (1958)

REVIEW

Works on Luminescence Published in 1955-1958 in the Collections, "Trudy Instituta Fiziki i Astronomii Akademii Nauk Estonskoi SSR", No. 1, 3, 4, 6, 7 (Transactions of the Physics and Astronomy Institute of the Esthonian Academy of Sciences)

V. V. ANTONOV-ROMANOVSKII

The "Trudy Instituta Fiziki i Astronomii Akademii Nauk Estonskoi SSR", the majority of which are devoted entirely on research on luminescence, began publication in 1955 in Tartu.

The research published in the "Trudy" concern, basically, questions of the kinetics of phosphorescence, the nature of coloring and capture centers, the structure of phosphors, mainly alkali-halides, and also research methods.

The works on kinetics and capture centers are very new and interesting. A great deal of attention is paid to the relation between additional absorption, which occurs in the excitation of phosphors, and luminescence. A new method of investigating this question, the method of thermal bleaching, is described, which has the great advantage over the thermal coloring method in that it permits the change (with time) in the concentration of the localized charges to be traced directly. Sufficient attention is also paid to improving and making more precise the classical thermal coloring method, the method of combined effect of heat and illumination (thermal-optic coloring) on excited phosphors and the method of "impulse" heating. Also investigated are parameters which are important for kinetics, such as the ratio of the recombination to the capture probabilities, the energy of charge localization, the thermal dissociation energy of excited centers, etc. Use of various methods permits reliable results to be obtained with the aid of theory.

In other works, the center of gravity is transported to research on the structure of luminous centers themselves (here, both theoretical computations are presented as well as a definition of certain parameters of the luminous center on the basis of investigations on the shape of the luminescence and absorption spectra, etc. in a specially selected series of phosphors with variations in both the host substance and the activator), the excitation mechanism where a large part is attributed to excitons as well as to such complicating factors as ionic processes.

A broad circle of investigations concerns the structure of phosphors and their formation. A great deal of attention is paid to questions of activation of phosphors (the influence of lattice parameters and the kind of activator, its concentration, the part of the temperature, etc.). This permits certain general laws to be established.

Individual works are devoted to the influence of lattcce deformation and hydrostatic pressure on the luminescent characteristics of phosphors and to the effect of infrared light.

In all this kind of investigation, they did not neglect also such phosphors as, for example, zinc-sulfides, the alkaline-earths, ammonia-halides, etc.

In conclusion, it can be said that the Tartu collections are of great interest especially for specialists in crystal phosphors. The published works are on a high scientific level. Regrettably, the small printing of the collections, only 800 copies, could not satisfy all those working in luminescence.

TOM VI, Vyp. 2 OPTIKA I SPEKTROSKOPIIA Fevral', 1959
VOL. VI. No. 2 OPTICS AND SPECTROSCOPY February, 1959

CHRONICLE

First All-China Conference on Spectroscopy

The First All-China Conference on Spectroscopy occurred in Peking on 2-6 November, 1958. There were 280 participants in the work of the conference, delegates from 144 different organizations. The delegation from the Academy of Science of the USSR consisted of Corr. Memb. S.E. Frish of the Academy of Science and V. I. Malyshev, Senior Scientific Worker of the Physical Institute of the Academy of Science. Moreover, the Soviet specialists A. A. Demidov and A. G. Krest'ianinov, who had been in China, also participated.

The conference was opened by a plenary session in which the vice-president of the Academy of Science of the Chinese peoples Republic, Prof. Woo Yiu Hsun presented a long report on the organization of the scientific research in China and on the prospects for the development of spectroscopy. The subsequent meetings were divided into the following four sections, running simultaneously: 1) The Molecular Spectroscopy Section; 2) The Section to Determine Impurities by Using Light Sources and Instruments; 3) The Section on the Spectrum Analysis of Mineral Ores; 4) The Section on the Spectrum Analysis of Alloys and Steels. Primarily research of applied nature was reported at the sections. There were 124 reports in all. The following subjects can be mentioned as typical: Infrared spectrum analysis of hydrocarbons; determination of the degree of crystallization of polystyrol by means of infrared absorption spectra; electronic spectrum of compounds of molecules of the aromatic series and oxygen; spectral determination of germanium in coal and coal cinders; spectral determination of impurities in rare-earth elements; determination of helium in natural gas; spectral analysis of ores and rock for potassium, magnesium, aluminum, iron and titanium; express method of determining vanadium in cast iron and steel, etc.

The Soviet participants presented the following reports: 1) A. A. Demidov, "Use of an evaporation method to determine impurities in infusible elements" ; 2)V. I. Malyshev, " Infrared ray absorption in fog" ; 3) A. G. Krest'ianinov, "Photo-electric method of recording spectra" ; 4) S. E. Frish, " Quantitative spectrum analysis of gases " . All these reports were heard with great attention and aroused numerous questions. The Soviet representatives also participated actively in the discussion on the other reports.

The conferees expressed a desire to organize a spectroscopic commission on the order of the Soviet Commission on Spectroscopy and to publish a Chinese Spectroscopy Journal.

After the conference ended, the delegation was first introduced to the spectroscopy laboratories of the institutes of the Chinese Academy of Science, located in Peking to Peking University and a number of other scientific research organizations and then it completed a long trip around China. Shanghai, Hankov, Canton, Changchun and Shen Yang (Mukden). In these cities, the scientists of the delegation also visited scientific organizations, universities and factories.

All the research in the CPR proceeds under the slogan High Jump , and is subject completely to the purpose of acquiring a substantial development in the economics and engineering of the nation in a very short time. Acquaintance with the research organizations, universities and factory laboratories showed that research on spectroscopy in the CPR is growing extremely intensively and rapidly on a very wide range of applied problems. Spectrum analysis methods have been introduced into ferrous and non-ferrous metallurgy, into geology, into chemical production. The newest methods of analyzing ultra-pure materials used in nuclear power and in semiconductor physics have been developed. A significant amount of research is devoted to the spectrum analysis of rare earths and the spectrum analysis of gases (gases in metals and natural gases). Infrared and ultra-violet absorption and combination light scattering methods are used in molecular spectroscopy; molecular analysis of various organic compounds (mainly oil) is carried out; research is proceeding on studying the properties of polymers by spectral methods, etc. Energetic attempts are being made to set up the domestic production of optical and spectral apparatus. Less attention is paid to research of a generally theoretical and exploratory character.

The majority of laboratories is well equipped and has a complete set of the required spectral apparatus, to a great extent of Soviet production (ISP-22, ISP-51 spectrographs, MF-2 microphotometers or microdensitometers, etc.). There are also instruments produced in the GDR, Czechoslovakia, Hungary, England, Italy and the German Federal Republic. In passing, the members of the delegation had an opportunity to see the newest automatic Zeiss (GDR) infrared spectrometer UR-10 in operation in several Chinese laboratories. As is known, this instrument is available only to very few Soviet research laboratories.

There are very good libraries in all the scientific organizations and a large number of scientific journals from all nations are acquired regularly. The Soviet periodical literature is represented very well, many Soviet books have been translated into Chinese or photo-copies have been produced.

In the majority of laboratories, the collaborators are youths working with enormous enthusiasm who will have the courage to solve very diverse and difficult scientific problems.

The following separate organizations should be mentioned.

PHYSICAL INSTITUTE of the Academy of Science of the CNR in Peking (Prof. ShihJu-Wei, director). There is a spectrum analysis laboratory with thirteen coworkers, studying hot plasmas by optical methods, doing spectrum analysis of gases in metals, studying oils and high-molecular-weight compounds by combination light scattering and infrared spectroscopy methods. A large luminescence laboratory (50 people) operates within the Institute. Electroluminescence, cathode luminescence, excitation of luminosity by high-speed particles are studied in this laboratory. Semiconducting materials are analyzed spectrally as to purity also.

INSTITUTE of PRECISION MECHANICS AND OPTICS in Chanchun (Van DaKai, director). The Institute carries out a great amount of research on producing Chinese optical apparatus. Copies of Soviet instruments in the spectral apparatus branch are constructed: The quartz spectrograph ISP-28; the large auto-collimation spectrograph with interchangeable optics KSA-1. Research is carried out

on engraving machines to rule diffraction gratings. The construction of an automatic infrared spectrometer has been worked out. Interference light filters are produced. Single crystals of NaCl, KBr, LiF are grown for infrared instruments. The production of optical glass in the CNR is supervised by the Institute. Steeloscopes are produced in the factory at Nanachan. The serial manufacture of portable steeloscopes is set for the optical factory at Shanghai. A number of universities is also developing spectral apparatus.

INSTITUTE of APPLIED CHEMISTRY of the Academy of Science of the CNR in Changchun (Prof. Woo Hsue Chow, director). There are well equipped laboratories of atomic and molecular spectroscopy in the Institute. Pure rare earths are produced by a semi-factory installation. The degree of purity is verified by spectroscopic methods.

SPECTROSCOPY LABORATORY in the AUTOMOBILE FACTORY in Changchun. There is a well organized and equipped central laboratory and two laboratories with steeloscopes in the casting departments. Moreover, there are checking posts with portable steeloscopes.

During the visit to the CPR, the delegation received the most cordial and warm regards from the Chinese comrades. The numerous meeting and social engagements were undoubtedly most friendly. The Academy of Science of the CPR did everything possible to make the visit of the delegation interesting, useful and pleasant.

S. Frish

Academy of Sciences of the USSR Section of Physical-Mathematical Seciences

ON A COMPETITION FOR THE S. I. VAVILOV GOLD MEDAL

The Section of Physical-Mathematical Sciences of the Academy of Sciences of the USSR announces that the competition for the S. I. Vavilov Gold Medal has been transferred from 1958 to 1959.

The S. I. Vavilov Gold Medal is awarded once every three years for outstanding work in physics.

Soviet scientists have the right to compete for the Vavilov medal. Only individuals, personally, can participate in the competition.

Candidates for the competition can be proposed by scientific establishments of the USSR and the union republics (scientific-research institutes and laboratories); constructor-bureaus; higher educational institutions, scientific and engineering societies; honorary members, members and corresponding members of the Academy of Sciences of the USSR.

The organizations and the individuals proposing the canditates to the competition for the gold medal must present the following material to the examining commission:

1) Published scientific work, material of scientific discovery or invention in 3 copies;
2) Discussion material on the work being presented by the scientific community;
3) A short summary not longer than one-quarter page;
4) Brief biographical information on the candidate with a list of his basic scientific works.

Works awarded prizes earlier are not admissible.

The work inscribed "For the competition for the S. I. Vavilov Gold Medal" should be directed to the Examining Commission on the Vavilov Gold Medal, Moscow, Leninskii prospekt, D. 53, Fizicheskii Institute AN USSR.

Last day for filing is Sept. 15, 1959.

AFFILIATIONS OF AUTHORS FROM ISSUES 1 and 2

IU. P. DONTSOV - LABORATORIIA IZMERITEL'NYKH PRIBOROV AN USSR (Laboratory of Measuring Instruments)
G. V. VEINBERG - NAUCHNO-ISSLEDOVATEL'SKII FIZICHESKII INSTITUT LENINGRADSKOGO GOSUDARSTVENNOGO UNIVERSITETA (Scientific Research Physics Institute of Leningrad State University)
M. P. VANIUKOV
A. A. MAK - GOSUDARSTVENNYI OPTICHESKOI INSTITUT im. S. I. VAVILOVA, LENINGRAD (S. I. VAVILOV State Optical Institute)
V. R. MURATOV
T. K. REBANE - LENINGRADSKII GOSUDARSTVENNYI UNIVERSITET (Leningrad State University)
M. S. BRODIN
A. F. PRIKHOT'KO - INSTITUT FIZIKI AN UkrSSR, KIEV (Physics Institute AN Ukr SSR)
M. S. SOSKIN
A. I. FINKEL'SHTEIN - DZHERZHINSKII FILIAL NAUCHNO-ISSLEDOVATEL'SKOGO I PROEKTNOGO INSTITUTA AZOTNOI PROMYSHLENNOSTI (Dzherzhinskii Branch of the Scientific-Research and Planning Institute of the Nitrogen Industry)
N. A. CHUMAEVSKII
V. M. TATEVSKII - MOSKOVSKII GOSUDARSTVENNYI UNIVERSITET (Moscow State University)
IU. K IUR IEV
V. L. LEVSHIN - FIZICHESKII INSTITUT im. P. N. LEBEDEVA AN USSR (P. N. Lebedev Physics Institute)
E. G. BARANOVA
I. N. SHKLIAREVSKII - KHAR KOVSKII GOSUDARSTVENNYI UNIVERSITET (Khar'kov University)
V. G. PADALKA
F. I. FEDOROV - BELORUSSKII GOSUDARSTVENNYI UNIVERSITET, MINSK (Belorussian State University)
A. N. FAIDYSH - KIEVSKII GOSUDARSTVENNYI UNIVERSITET (Kiev State University)
V. L. ZIMA
V. M. PIVOVAROV - GOSUDARSTVENNYI OPTICHESKOI INSTITUT im. S. I. VAVILOVA
IA. I. RYSKIN - INSTITUT KHIMII SILIKATOV AN USSR (Institute of Silicate Chemistry)
E. F. GROSS
L. G. SUSLINA - LENINGRADSKII GOSUDARSTVENNYI UNIVERSITET
T. P. BELIAKOVA - FIZICHESKII INSTITUT im. P. N. LEBEDEVA
M. T. SHPAK - INSTITUT FIZIKI AN Ukr SSR
N. G. PREOBRAZHENSKII - SIBIRSKII FIZIKO-TEKHNICHESKII INSTITUT, TOMSK (Siberia Physical-Technical Institute)
CH. B. LUSHCHIK - INSTITUT FIZIKI I ASTRONOMII AN ESSR, TARTU (Institute of Physics and Astronomy)
N. A. TOLSTOI - GOSUDARSTVENNYI OPTICHESKOI INSTITUT im. S. I. VAVILOVA
M. A. EL'IASHEVICH - LABORATORIIA IZMERITEL'NYKH PRIBOROV AN USSR
R. GRIGOROVICI - K. PARKHON UNIVERSITY, BUCHAREST
G. CRISTESCU
R. B. TAGIROV - KAZANSKII GOSUDARSTVENNYI UNIVERSITET (Kazan State University)
E. E. NIKITIN - GOSUDARSTVENNYI OPTICHESKOI INSTITUT
R. I. PODLOVCHENKO
L. M. SVERDLOV - SARATOVSKII AVTODOROZHNYI INSTITUT (Saratov Auto Highway Institute)
M. M. SUSHCHINSKII
R. S. LEBEDEV - KEMEROVSKII PEDAGOGICHESKII INSTITUT (Kemerov Pedagogic Institute)
N. I. ZHIRNOV - MOSKOVSKII GOSUDARSTVENNYI PEDAGOGICHESKII INSTITUT (Moscow State Pedagogic Institute)
L. A. LYZINA - GOSUDARSTVENNYI OPTICHESKOI INSTITUT
A. T. VARTANIAN
CHAO HUANG-TSEN - INSTITUT PRIKLADNOI FIZIKI AN KNR & PEKINSKII UNIVERSITET (Applied Physics Institute of the Academy of Science , CPR and Pekin University)
I. A. PARFIANOVICH:-IRKUTSKII GOSUDARSTVENNYI UNIVERSITET (Irkutsk University)
G. G. SLIUSAREV - GOSUDARSTVENNYI OPTICHESKII INSTITUT
A. O. SALL' - GOSUDARSTVENNOE SOIUZNOE KONSTRUKTORSKOE BIURO ANALITICHESKOGO PRIBOROSTROENIIA (State Union Structural Bureau of Analytic Instrumentation)
G. M. KISLIAK - POLTAVSKII PEDAGOGICHESKII INSTITUT (Poltava Pedagogic Institute)
V. V. ANTONOV-ROMANOVSKII - FIZICHESKII INSTITUT AN USSR
T. M. VEMBER
A. S. CHERKASOV - GOSUDARSTVENNYI OPTICHESKOI INSTITUT
P. P. FEOFILOV
M. L. KATS - SARATOVSKII GOSUDARSTVENNYI UNIVERSITET (Saratov University)
G. P. SKORNIAKOV - INSTITUT FIZIKI METALLOV URAL'SKOGO FILIAL AN USSR (Metal Physics Institute of the Ural Branch AN USSR)
M. M. KIRILLOVA -
IA. S. BOROVICH - GOSUDARSTVENNYI OPTICHESKII INSTITUT
E. I. NIKONOVA
V. K. PROKOF'EV -
A. M. BONCH-BRUEVICH
A. A. VASHMAN
L. V. LIPIS - MOSKOVSKII KHIMIKO-TEKHNOLOGICHESKII INSTITUT im. D. I. MENDELEEVA (D. I. Mendeleev Moscow Chemical Technology Institute)
N. A. TETERINA
L. A. BOROVINSKII - INSTITUTA VYSOKOMOLEKULIARNYKH SOEDINENII AN USSR (Institute of High Molecular Compounds)

ABBREVIATIONS OFTEN ENCOUNTERED AND USED HEREIN

Journals and Institutions

DAN USSR	Doklady Akademii Nauk USSR (Reports of the Academy of Sciences of the USSR)
DAN UkrSSR	Dopovidi Akademii Nauk UkrSSR (Reports of the Academy of Sciences of the Ukraine SSR)
DAN ArmSSR	Doklady Akademii Nauk ArmSSS (Reports of the Academy of Sciences of the Armenia SSR)
IAN USSR	Izvestiia Akademii Nauk USSR (Bulletin of the Academy of Sciences of the USSR)
	Seriia fizika (Physics series)
	Seriia matematika (Mathematics series)
	Otdelenie khimicheskikh nauk (Section of chemical sciences)
OiS	Optika i Spektroskopiia (Optics and Spectroscopy)
PiTE	Pribory i Tekhnika Eksperimenta (Instruments and Techniques of Experiment)
AE	Atomnaia Energiia (Atomic Energy)
AZ	Astronomicheskii Zhurnal (Astronomy Journal)
FMM	Fizika Metallov i Metallovedenie (Physics of Metals and Metallography)
Radiotekh.	Radiotekhnika (Radio Engineering)
RiE	Radiotekhnika i Elektronika (Radio Engineering and Electronics)
UK	Uspekhi Khimii (Progress in Chemistry)
UFN	Uspekhi Fizicheskikh Nauk (Progress in Physical Sciences)
UFZ	Ukrainskii Fizichni Zhurnal (Ukraine Physical Journal)
ZETF	Zhurnal Eksperimental'noi Teoreticheskoi Fiziki (Journal of Experimental Theoretical Physics - JETP)
ZTF	Zhurnal Tekhnicheskoi Fiziki (Journal of Technical Physics)
FTT	Fizika Tverdogo Tel (Solid State Physics)
ZFKh	Zhurnal Fizicheskoi Khimii (Journal of Physical Chemistry)
ZOKh	Zhurnal Organicheskoi Khimii (Journal of Organic Chemistry)
ZNKh	Zhurnal Neorganicheskoi Khimii (Journal of Inorganic Chemistry)
Tr.	Trudy (Transactions, as for instance, Tr. FIAN)
FIAN	Fizicheskii Institut Akademii Nauk (S. N. Lebedev Physical Institute of the Academy of Sciences USSR)
Sb.	Sbornik (Collection, as for instance, Fizich. sb. L'vovskogo universitet)
Fizich. sb.	Fizicheskaia sbornik (Physics Collection)
Uch. Zap.	Uchenye Zapiskii (Scientific Records)
Vestn.	Vestnik (Herald or Messenger)
FTIAN	Fiziko-Tekhnicheskii Institut Akademii Nauk (Physical-Technical Institute of the Academy of Sciences)
GITTL	Gostekhizdat - Gosudarstvennoe Izdatel'stvo Tekhniko-Teoreticheskoi Literatury (State Publishers of Technical-Theoretical Literature)
GIFML	Fizmatgizdat - Gosudarstvennoe Izdatel'stvo Fiziko-Matematicheskoi Literatury (State Publishers of Physical-Mathematical Literature), formerly Gostekhizdat
IL or IIL	Izdatel'stvo Inostrannoi Literatury (Publishers of Foreign Literature)
Izd. AN USSR	Izdatel'stvo Akademiia Nauk USSR (Academy of Sciences Press)
ZL	Zavodskaia Laboratoriia (Factory Laboratory)
GOST	Gosudarstvennyi Obshchesoiuznyi Standart (All-Union State Standard)

Apparatus

IKS-11	Infrakrasnyi spektrofotometer (Infrared spectro-photometer)
VIKSM-3	Vakuumnoe Infrakrasnyi spektrometer (Vacuum Infrared Spectrometer)
SF-4	Spektrofotometer (spectro-photometer)
DFS-2	Difraktsionnyi Spektrograf (Grating Spectrograph)
DG-1	Generator dygi peremennogo toka (AC Arc Generator)
FEU	Fotoelektronnyi Umozhnitel' (Photo-electron Multiplier)

S. V. GRUM-GRZHIMAILO, N. A. BRILLIANTOV, R. K. SVIRIDOVA, A. S. DZHAMALOVA
O spektry pogloshcheniia rubinov pri nizkikh temperaturakh (do 1.7° K) 240
V. M. AGRANOVICH, IU. V. KONOBEEV
O dline svobodnogo probega eksitona v molekuliarnom kristalle 242
S. D. BUDRITE, L. L. KUZMITSKITE, V. K. SHUGUROV
Utochnennye analiticheskie odnoelektronnye funktsii 245
G. P. SKORNIAKOV, M. M. KIRILLOVA
Primenenie metoda Kravtsa dlia opredeleniia opticheskikh kharakteristik metallov 248
V. M. FIVOVAROV, IA. S. BOBOVICH
O temperaturnom khode intensivnosti linii kombinatsionnogo rasseianiia gazo-obraznykh CO_2 i N_2 249
N. G. BAKHSHIEV
K voprosu o konture polos pogloshcheniia i ispuskaniia slozhnykh molekul 250
E. I. NIKONOVA, V. K. PROKOF'EV
K voprosu o raspredelenii neitral'nykh atomov v plazme dugi postoiannogo toka 253
K. K. SVIDZINSKII
K teorii sverkhtonkoi struktury vrashchatel'nykh spektrov molekul tipa simmetrichnogo volchka 254
A. M. BONCH-BRUEVICH
Ob elektroliuminestsentnykh iavleniiakh pri vkliuchenii i vykliuchenii elektricheskogo polia 256
A. V. SOLOV'EV
Vliianie dopolnitel noi primesi na spektry primesnogo pogloshcheniia i liuminestsentsiiu molekuliarnykh kristallov 258
I. A. MUKHTAROV
Mikrovolnovyi spektr molekuly $FH_2C-CH_2Cl^{37}$ 260
A. A. VASHMAN, L. V. LIPIB, N. A. TETERINA
Sverkhvysoko-chastotnyi istochnik vozbuzhdeniia spektrov smesei gazov 260
E. A. VERNYI, V. N. EGOROV
Izotopicheskoe sdvigi v spektre toriia $Th^{232} - Th^{229}$ 262
B. A. VEKLENKO
K voprosu o sovmestnoi diffuzii fotonov i chastits 263
DISKUSSII
T. K. REBANE
Po povody stat'i L. A. Borovinskogo "Ob usloviiak sshivaniia funktsii v odno-mernoi metallicheskoi modeli molekuly" 266
L. A. BOROVINSKII
Eshche raz ob usloviiakh sshivaniia funktsii v odnomernoi metallicheskoi modeli molekuly (Otvet T. K. Rebane) 267
RETSENZII
V. V. ANTONOV-ROMANOVSKII
Retsenziia na raboty po liuminestsentsii, opublikovannye v 1955-1958 gg. v sbornikakh Trudy Instituta fiziki i astronomii Akademii nauk Estonskoi SSR (No. 1, 3, 4, 6 i 7) 269
KHRONIKA
Pervaia vsesoiuznaia konferentsiia po spektroskopii S. FRISH 270
Izveshchenie o konkurse na soiskanie zolotoi medali imeni S. I. Vavilova 272
On the absorption spectra of rubies at low temperatures (down to 1.7° K) 154
On the exciton free path in a molecular crystal 155
Improved analytic single-electron wave functions 157
Application of Kravets method to determine optical constants of metals 159
On temperature dependence of line intensities of the Raman effect in gaseous CO_2 and N_2 160
The shape of absorption and emission bands of complex molecules 161
The distribution of neutral atoms in the plasma of a DC arc 162
On the hyperfine structure of the rotational spectra of molecules of the symmetric rotor type 163
On electroluminescent phenomena when an electric field is switched on and off 165
Influence of an additional impurity on impurity absorption and luminescence spectra of molecular crystals 166
Microwave spectrum of the $FH_2C-CH_2Cl^{37}$ molecule 168
Microwave excitation of spectra of gaseous mixtures 168
Isotopic shift in the spectrum of thorium $Th^{232} - Th^{229}$ 170
On the question of mutual diffusion of photons and particles 170
DISCUSSION
Apropos the article by L. A. Borovinskii "On conditions for joining functions in the one-dimensional metal model of a molecule" 172
More on the conditions of joining functions in the one-dimensional model of a molecule (In reply to T. K. Rebane) 173
REVIEW
Works on luminescence published in 1955-1958 in the collections, Trudy Instituta Fiziki i Astronomii Akademii Nauk Estonskoi SSR, No. 1, 3, 4, 6, 7 (Transactions of the Physics and Astronomy Institute) 174
CHRONICLE
First All-China conference on spectroscopy S. FRISH 175
Competition for the S. A. Vavilov gold medal 176
Affiliations of Authors from Issues 1 and 2 177
Abbreviations often encountered and used herein 178

Printed by Blackburn Printing Company, Concord, Mass.

TOM VI, Vyp. 2 OPTIKA I SPEKTROSKOPIIA Fevral' 1959
VOL. VI, No. 2 OPTICS AND SPECTROSCOPY February, 1959

SODERZHANIE

R. GRIGOROVICI, G. CRISTESCU
K teorii vysokochastotnogo fakel'nogo razriada 129

R. B. TAGIROV
K voprosu o prirode smeshcheniia infrakrasnykh polos ispuskaniia v spektrakh plamen 137

E. E. NIKITIN
O vychislenii veroiatnosti kolebatel'nogo vozbuzhdeniia molekul pri stolknoveniiakh 141

R. I. PODLOVCHENKO, L. M. SVERDLOV, M. M. SUSHCHINSKII
Kolebatel'nye spektry i povorotnaia izomeriia 2,3-dimetilbutana 146

R. S. LEBEDEV
Raschet kolebatel'nykh spektrov molekul tsikloe pentana i deterotsiklopentana 154

M. I. ZELENOV
K voprosu ob interpretatsii kolebatel'nogo spektra koronena 162

CH. K. MUKHTAROV
Ob odnovremennom pogloshchenii sveta v binarnykh smesiakh 168

L. A. LYUBIMA, A. T. VARTANIAN
Spektry pogloshcheniia sloev krasitelei v vakuume 172

CHAO HUAN-TSEN
Linezichatye spektry liuminestsentsii i otrazheniia kristallov iodomerkurata medi pri nizkikh temperaturakh 181

I. A. PARFIANOVICH
Ob aktivatornykh urovniakh zakhvata elektronov v NaCl-Ni-fosfore 189

N. P. SHIMANSKAIA, A. P. KILDOV, A. P. GRSKOV
Issledovanie stsintilliatsionnykh svoistv nekotorykh proizvodnykh 1,3,4-oksadiazola 194

A. I. TUDOROVSKII
Ob'ektiv s fazovoi plastinkoi 198

G. G. SLIUSAREV
Vliianie temperaturnogo gradienta stekla opticheskikh sistem na izobrazhenie, davaemoe poslednimi 211

A. O. SALL'
O poroge chuvstvitel'nosti optiko-akusticheskogo priemnika radiatsii. 1. Nizkaia chastota obtiuratsii 219

KRATKIE SOOBSHCHENIIA

G. M. KISLIAK
O zakone zatukhaniia fosforestsentsii tripaflavina v murav'inoi kislote 226

V. V. ANTONOV-ROMANOVSKII
O relaksatsii elektroliuminestsentsii pri malykh otkloneniiakh ot statsionarnogo sostoianiia 229

T. M. VENGER, A. S. CHERKASOV
O vzaimnom vliianii nekotorykh 9-mono-proizvodnykh antratsena na kvantovye vykhoda ikh fotokhimicheskikh prevrashchenii i kvantovye vykhody fluorestsentsii 232

P. P. PROFILOV
O spektrakh pogloshcheniia i liuminestsentsii ionov Ce^{+++} 234

M. L. KATS
Fosforestsentsiia i termovysvechivanie fosforov KBr-In 237

S. V. GRUM-GRZHIMAILO, N. A. KRILLIANTOV, R. K. SVIRIDOVA
Spektry pogloshcheniia korunda, okrashennogo vanadiem, pri nizkikh temperaturakh (do 1.7° K) 238

CONTENTS

The theory of the high frequency brush discharge 85

On the question of the nature of the infrared emission band displacement in flame spectra 90

On the calculation of the probability for vibrational excitation of molecules during collisions 93

Vibrational spectra and rotational isomerization of 2,3-dimethylbutane 96

Calculation of the vibrational spectra of the cyclopentane and deuterocyclopentane molecules 101

Interpretation of the vibration spectrum of coronene 105

On the simultaneous absorption of light in binary mixtures 108

Absorption spectra of dye films in vacuo 110

Line luminescence and reflection spectra of copper-iodo-mercurate crystals at low temperatures 115

On the electron trapping levels of the activator in a NaCl-Ni phosphor 120

Investigation of the scintillation properties of some 1,3,4-oxadiazole derivatives 124

An objective with a phase plate 126

The influence of temperature gradient of glass of optical systems on the image produced by the latter 134

On the sensitivity threshold of an optic-acoustic receiver of radiation. 1. Low chopper frequency 139

BRIEF REPORTS

The law of phosphorescence decay for trypaflavine in formic acid 144

On relaxation of electroluminescence for small departures from the stationary state 146

The mutual influence of certain 9-mono-substituted anthracenes on the quantum yield of their photochemical transformations and on the quantum yield of fluorescence 148

On absorption and luminescence spectra of Ce^{+++} ions 150

Phosphorescence and thermal stimulation of KBr-In phosphors 152

Absorption spectrum of vanadium-colored corundum at low temperatures (down to 1.7°) 152